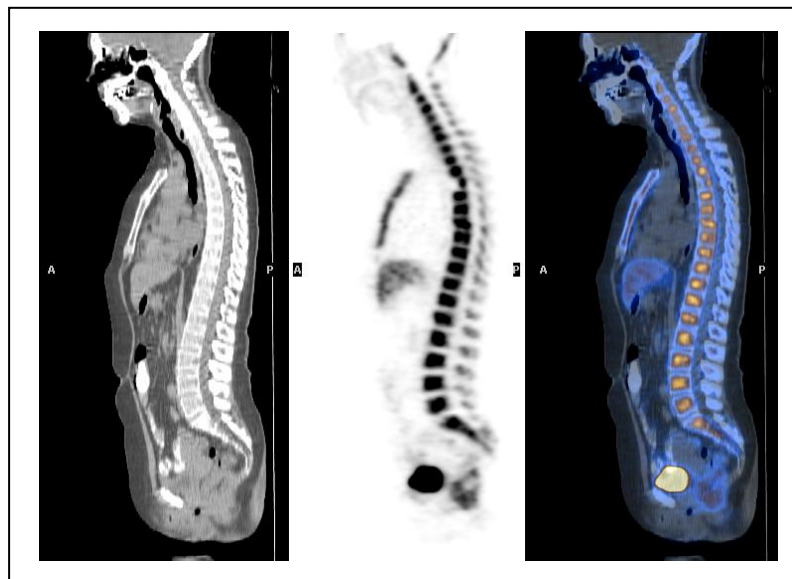


Molecular Imaging using Positron Emission Tomography in Gastrointestinal Malignancy

A thesis submitted to the University College London
for the Degree of Doctor of Medicine

by
Farrokh Pakzad BSc(Hons) MBBS MRCS



**The Institute of Nuclear Medicine and
The Department of Surgery**
Royal Free and University College Medical School
University College London

2008

STATEMENT OF ORIGINALITY

The studies described and presented in this thesis are the original work of the author. Data collection and analysis relating to the clinical part of this thesis are the sole work of the author. Image analysis was however carried out by senior grade nuclear medicine physicians and/or radiologists.

All PET, CT scans and PET image/data reconstruction were performed by qualified radiographers in accordance with local protocol and clinical guidelines. Radioactive tracers were synthesised at the MRC Cyclotron Unit, Hammersmith Hospital, London. These were then transported to the Institute of Nuclear Medicine on the day of PET scanning. Radiochemical analysis was performed by a radiochemist at the Institute of Nuclear Medicine.

No part of this work has been submitted to any other university for consideration for a higher degree.

Immunohistochemistry for Ki-67 was carried out in collaboration with the histopathology department at University College London. Histological analysis was performed in conjunction with a senior histopathologist.

All *in vitro* experiments including cell culture work, gel electrophoresis, western blot analyses and flowcytometry results were the sole work of the author.

CONTENTS	Page
Title page	1
Statement of Originality	2
Table of Contents	3-12
Abstract	13
Acknowledgements	14
Figures and tables	15-19
Abbreviations	20

Chapter 1

Introduction

1.1 Molecular imaging and cancer	22
1.2 Approaches to <i>in vivo</i> molecular imaging	24
1.2.1 Nuclear imaging	24
1.2.2 Optical imaging	25
1.2.3 Magnetic Resonance Imaging (MRI)	26
1.2.4 Ultrasound	
1.3 Molecular imaging of cancer with Positron Emission Tomography (PET)	28
1.3.1 Imaging with PET – the basic principles	29
1.3.2 The PET detector unit	29
1.3.3 Annihilation coincidence detection	29
1.3.4 Attenuation correction	30
1.3.5 Quantitative imaging	31
1.3.6 Multimodality imaging with PET/CT	32
1.3.7 Imaging protocols with PET and PET/CT	33
1.4 Molecular and cellular targets for PET imaging	35

1.4.1	Aerobic glycolysis, cancer and imaging with PET	37
1.4.2	[18F]-fluoro-2-deoxy-D-glucose (18F-FDG)	38
1.5	Cellular proliferation	41
1.5.1	The cell cycle	41
1.5.2	Proliferation and tumour growth	43
1.5.3	Assessment of proliferation	44
1.5.3.1	Mitotic index	45
1.5.3.2	Incorporation techniques using nucleotide analogues	45
1.5.3.3	DNA cytometry and percentage S-phase determination	45
1.5.3.4	Proliferation associated antigens	46
1.5.4	Tumour heterogeneity – a problem of assessing proliferation	47
1.5.5	Thymidine analogue PET tracers for imaging cell proliferation	48
1.6	[18F]-3'-deoxy-3'-fluorothymidine (18F-FLT)	50
1.6.1	The development of 18F-FLT	50
1.6.2	The molecular kinetics of 18F-FLT	50
1.6.3	Cellular trapping of 18F-FLT	51
1.6.4	18F-FLT as a proliferation PET tracer	52
1.6.5	Clinical applications of 18F-FLT	53
1.7	The role of PET in diagnosis and staging of pancreatic cancer	59
1.7.1	Background	59
1.7.2	Clinical features of pancreatic cancer	59
1.7.3	Routine management of algorithm of patients with suspected pancreatic cancer	61
1.7.3.1	Basic investigations	62
1.7.3.2	Conventional imaging of the pancreas	63

1.7.4	18F-FDG PET in diagnosis of primary pancreatic cancer	68
1.7.5	Staging of pancreatic carcinoma with 18F-FDG PET	71
1.7.6	The prognostic significance of 18F-FDG uptake in pancreatic cancer	74
1.7.7	18F-FDG PET in the detection of recurrent pancreatic cancer	75
1.7.8	The pitfalls of imaging pancreatobiliary disease with 18F-FDG PET	76
1.7.9	Pancreatic cancer and image fusion with PET/CT	77
1.8	The role of PET in diagnosis and staging of colorectal cancer	80
1.8.1	Background	80
1.8.2	Detection of pre-malignant colonic lesions	81
1.8.3	Screening for colorectal cancer with PET	82
1.8.4	The role of 18F-FDG PET in the diagnosis of primary colorectal cancer	82
1.8.5	Detection of recurrent and metastatic disease	84
1.8.5.1	Locoregional recurrence	84
1.8.5.2	Metastatic disease	87
1.8.6	The impact of dual modality imaging with PET/CT on the management of colorectal cancer	89
1.8.7	Therapy response monitoring with PET	91
1.8.7.1	Response to radiotherapy	91
1.8.7.2	Response to chemotherapy	92
1.8.7.3	Monitoring local ablative therapy	93
1.8.8	Limitation of imaging colorectal cancer with 18F-FDG PET	94
1.9	Chapter overview and aims of thesis	95

Chapter 2

Materials and methods

2.1	Patient recruitment	98
2.2	Whole body FDG-PET/CT scans	99
2.2.1	18F-FDG	99
2.2.2	Patient preparation	99
2.2.3	Acquisition of whole body FDG PET/CT scans	100
2.3	Whole body FLT-PET/CT scans	101
2.3.1	Radiosynthesis of 18F-FLT	101
2.3.2	Dose calibration	102
2.3.3	Patient preparation and dose administration	102
2.3.4	Acquisition of whole body 18F-FLT PET/CT images	103
2.4	Image analysis	104
2.4.1	Visual analysis	104
2.4.2	Quantitative analysis	105
2.5	Computed tomography imaging protocols	108
2.5.1	Patient preparation	108
2.5.2	Image acquisition	108
2.5.3	Image reconstruction and analysis	110
2.6	Confirmation of diagnosis and follow up	110

Chapter 3

Does 18F-FDG PET/CT play a role in the routine management of pancreatic cancer?

3.1	Background	112
3.2	Aims	113
3.3	Methods	114
3.3.1	Patient recruitment	114
3.3.2	Imaging protocols	114
3.3.3	Data presentation	115
3.4	Results	116
3.4.1	Patient demographics	116
3.4.2	Diagnosis of primary pancreatic lesions	117
3.4.3	Staging accuracy of 18F-FDG PET/CT in pancreatic cancer	119
3.4.3.1	Local (T) and nodal (N) staging	119
3.4.3.2	Distant metastases	120
3.4.4	Additional findings	123
3.4.5	The impact of 18F-FDG PET/CT on clinical management	124
3.5	Discussion	125
3.6	Conclusion	131

Chapter 4

Does 18F-FDG PET/CT provide additional information to conventional imaging in the management of colorectal liver metastases?

4.1	Background	133
4.2	Aims	136
4.3	Methods	137
4.3.1	Patient group	137
4.3.2	Imaging protocols	137
4.3.3	Image analysis	137
4.3.4	Clinical Risk Score (CRS)	139
4.3.5	Data presentation and statistical analysis	139
4.4	Results	140
4.4.1	Patient demographics	140
4.4.2	18F-FDG PET/CT versus routine ceCT	140
4.4.3	The impact 18F-FDG PET/CT on management	144
4.4.4	The impact of CRS on the clinical yield of 18F-FDG PET/CT	146
4.4.5	The incremental value of PET/CT over that of imaging with PET alone	147
4.5	Discussion	150
4.6	Conclusions	156

Chapter 5
Targeting proliferation in pancreatic cancer using 18F-FLT PET –
A comparative study with 18F-FDG.

5.1	Background	158
5.2	Aims	159
5.3	Methods	160
5.3.1	Patient recruitment	160
5.3.2	Imaging protocols	160
5.3.3	Image analysis	160
5.3.4	Histological analysis	162
5.3.4.1	Specimen preparation	162
5.3.4.2	Examination of histological sections	162
5.3.5	Statistical analysis	163
5.4	Results	164
5.4.1	Patient demographics and tumour characteristics	165
5.4.2	Detection of primary pancreatic disease – comparison between 18F-FDG and 18F-FLT PET imaging	166
5.4.3	Correlation between tracer uptake and proliferative activity	168
5.4.4	Correlation between tumour SUV's and patient survival	172
5.5	Discussion	174
5.6	Conclusions	179

Chapter 6
Staging of advanced colorectal cancer using 18F-FLT PET –
A comparative study with 18F-FDG

6.1	Background	181
6.2	Aims	183
6.3	Methods	184
6.3.1	Patient recruitment	184
6.3.2	Imaging protocols	184
6.3.3	Image analysis	185
6.3.4	Statistical analysis	185
6.4	Results	186
6.4.1	Patient demographics	186
6.4.2	Comparison of imaging with 18F-FDG and 18F-FLT PET in detecting malignant lesions	186
6.4.3	Comparison between lesion tracer SUVs (18F-FDG vs 18F-FLT)	191
6.5	Discussion	194
6.6	Conclusions	199

Chapter 7
**Measuring early adaptive response to 5-flurouracil with 18F-FLT –
an *in vitro* study**

7.1	Background	201
7.2	Aims	204
7.3	Material and methods	205
7.3.1	Materials and cell lines	205
7.3.2	Routine cell line maintenance	205
7.3.3	Basic experimental protocol	206
7.3.4	Defining drug dose parameters	207
7.3.5	Tracer uptake experiments	208
7.3.6	Cell cycle phase determination	209
7.3.7	TK-1 protein expression	210
7.3.7.1	Protein extraction	210
7.3.7.2	Protein assay	210
7.3.7.3	Gel electrophoresis and Western Blot	211
7.3.8	Statistical analysis	212
7.4	Results	213
7.4.1	Cytotoxic effect of 5-FU and Cisplatin	213
7.4.2	18F-FLT vs 18F-FDG uptake following 5-FU treatment	215
7.4.3	Cell cycle changes in 5-FU treated cells	218
7.4.4	Changes in TK-1 expression	221
7.5	Discussion	223
7.6	Conclusions	228

Chapter 8

Summary of findings and overall conclusions

8.1	Summary of results	230
8.2	Conclusions	236
	References	237-259
	Appendices	260-288
	List of publications	289
	List of presentations	290-291

ABSTRACT

Positron Emission Tomography (PET) with 18F-FDG has emerged as a powerful tool in oncology. Furthermore, recent advent of PET/CT and novel tracers are continually expanding its role. This thesis investigates its application in two solid cancer models.

In the diagnosing of primary pancreatic cancer, 18F-FDG PET/CT was shown to be more accurate than conventional CT. It did not add information to locoregional staging of disease but impacted management of patients with potentially operable tumours, by accurately confirming the presence / absence of metastases. In the pre-operative staging of patients with colorectal liver metastases (CLM), 18F-FDG PET/CT was also superior to CT in assessing extrahepatic disease, where it again impacted management. The accuracy of detecting hepatic disease was similar for both. Compared to PET alone, PET/CT improved the accuracy of lesions localization and interpretation.

Next, the feasibility of imaging with the novel thymidine analogue tracer 18F-FLT was investigated. Overall, 18F-FLT PET was less accurate than 18F-FDG in detecting lesions in both cancer types, thus suggesting it to be an unsuitable tracer for routine diagnosis and staging. In the cohort of pancreatic cancer patients, 18F-FLT uptake (SUVs) were found to strongly correlate with the immunohistochemical proliferation marker, Ki-67 antigen. This supported 18F-FLT's potential role as a surrogate marker of proliferation. The prognostic implications of these require further investigation.

Finally, an *in vitro* model was used to examine **early** changes in 18F-FLT uptake in response to treatment with cytotoxics. At 2 hours following pulse treatment with 5-fluorouracil, (and before changes in cell numbers and cell cycle phase were seen), a dose dependent increase in 18F-FLT uptake was seen. No change was observed with 18F-FDG nor following Cisplatin treatment. This adaptive response may have a role as an early predictor of response to 5-FU (and potentially other antimetabolites), which requires further investigation.

ACKNOWLEDGEMENTS

I would like to thank every single person that gave a helping hand in this work by name, unfortunately limited space makes this impossible. My first thanks must go to the patients who despite suffering from terminal cancer, were bravely willing to put themselves forward in the interest of science and that of the greater good.

I am eternally grateful to Dr. Marilena Loizidou, the one person that has relentlessly egged me on through times where there seemed not to be a light at the end of the tunnel. She believed in me when others lost interest. Without her advice, support and guidance this thesis could not exist.

My thanks go to Professor Irving Taylor and Professor Peter Ell for allowing me to partake in this project and for their invaluable advice and support.

My time at the Institute of Nuclear Medicine was often a humbling one, as I was surrounded by great clinical and scientific minds. I am grateful to Dr. Jamshed Bomanji for showing me the power of lateral thinking and Dr Ashley Groves for showing me the art of perseverance in academic medicine. My thanks also goes to Caroline Townsend for her continued support of my research work, amidst a busy timetable of routine clinical scans. I am indebted to Dr's Wendy Waddington and Ian Callum for their expertise in the chasm that is medical physics.

The completion of this thesis is in no small part due to the encouragement and help of my family. I thank my wife Mahreen for putting up with my endless week-ends away in the laboratory, for her unflinching support through the dark times and for her continued selflessness in all aspects of my career. I thank my mother and father without whom I would never have reached this stage in my life.

Finally I would like to dedicate this thesis to my son Sirius. Although he's only been in this world a short time, he has done more to focus my mind than any other event in my life. With every smile he invigorates me and with every look he puts my life into perspective. Thank you son.

LIST OF FIGURES	Page
1.1 The three main classes of imaging probes used in molecular imaging.	23
1.2 Image demonstrating the difference between non-attenuated and attenuated corrected PET images.	30
1.3 Dedicated dual modality PET/CT scanner.	33
1.4 Phosphorylation pathway of ¹⁸ F-FDG.	39
1.5 The cell cycle.	42
1.6 Mechanism of cellular trapping of ¹⁸ F-FLT compared to Thymidine (dTh).	51
1.7 Comparative ¹⁸ F-FDG (top row) and ¹⁸ F-FLT (bottom row) PET images in the same patient with a locally advanced rectal carcinoma.	55
1.8 The management algorithm of suspected pancreatic cancer.	61
2.1 Tracerlab FFX-N (GE Healthcare) automated fluorination kit used in the synthesis of ¹⁸ F-FLT.	101
2.2 Comparison between methodologies for determining tumour SUV.	106
3.1 ceCT and ¹⁸ F-FDG PET/CT images of a mass in the uncinate process of pancreas.	118
3.2 ¹⁸ F-FDG PET/CT images demonstrating the primary lesion in the head of the pancreas. PET/CT also confirmed the presence of liver and lung metastases, where the lesions were deemed equivocal on ceCT.	122

3.3	18F-FDG PET/CT images of primary pancreatic lesion and incidental colonic lesion found to be an adenomatous polyp.	123
4.1	The distribution of discordant findings between PET/CT and ceCT.	142
4.2	18F-FDG PET/CT images of a large liver metastasis and 18F-FDG uptake in mediastinal lymph nodes due to tuberculosis.	143
5.1	Graphs representing the relationship between tumour SUVs for the two tracers (18F-FDG vs 18F-FLT).	167
5.2	Graphs illustrating the correlation between 18F-FDG and 18F-FLT SUVs and MIB-1 LI (%).	168-170
5.3	Comparative 18F-FDG and 18F-FLT PET images for three patients with pancreatic cancer.	171
5.4	Kaplan-Meier survival graphs of patients with high and low tracer SUVs.	172-173
6.1	Rectal primary showing 18F-FDG and 18F-FLT avidity.	188
6.2	Coronal slices of 18F-FDG and 18F-FLT PET scans demonstrating a tracer avid solitary metastasis in the right lobe of the liver.	189
6.3	Graph demonstrating the difference between the <u>average</u> SUV_{Mean} and SUV_{Max} figures for 18F-FDG and 18F-FLT.	192
6.4	Correlation between 18F-FDG 18F-FLT SUVs for all detected lesion.	193
7.1	Graphs representing the cytotoxic effect of 5-FU and Cisplatin on cell numbers.	213-214

7.2	Changes in uptake of 18F-FDG and 18F-FLT in response to treatment with 5-FU and Cisplatin.	215-216
7.3	Dose dependent increase in 18F-FLT uptake in 5-FU treated cells.	217
7.4	Flowcytograms representing the distribution of S-phase cells on day 0 following 5-FU treatment.	219
7.5	Fold change in S-phase fraction (SPF) in cells treated with 5-FU.	220
7.6	Western blot analysis for TK-1 (24 kDa) expression (representative result of 3 independent experiments).	222

LIST OF TABLES	Page
1.1 Non-FDG tracers and biochemical targets.	36
1.2 Summary of studies examining the role of 18F-FLT PET imaging in a range of cancers.	56
1.3 Tabulated summary of the staging system for pancreatic cancer.	67
1.4 Summary of studies examining the role of 18F-FDG PET in diagnosing and staging of primary and recurrent pancreatic cancer.	73
1.5 Summary of published studies looking at the role of 18F-FDG PET in recurrent and metastatic colorectal cancer.	85
3.1 Summary of patient demographics with suspected pancreatic cancer.	116
3.2 Comparison of detection rates between 18F-FDG PET/CT and ceCT in pancreatic cancer.	117
3.3 Comparison of the distribution of metastatic deposits detected by ceCT and PET/CT.	121
4.1 Comparison of detection rates between 18F-FDG PET/CT and ceCT in patients with CLM.	141
4.2 The impact of 18F-FDG PET/CT on management of patients with CLM.	145
4.3 The distribution of Clinical Risk Scores (CRS) in patients with CLM.	146
4.4 Comparison of high and low Clinical Risk Scores (CRS).	147
4.5 Tabulated summary of the difference in the certainty of lesion interpretation with PET only imaging compared to that with PET/CT .	148

4.6	The difference in inter-observer variability between PET only scans and PET/CT.	149
5.1	The demographics and tumour characteristics of pancreatic cancer patients imaged with 18F-FDG and 18F-FLT PET.	165
6.1	Number of PET positive lesions detected with 18F-FDG compared to 18F-FLT scans.	187
6.2	Tabulated summary of SUVs measured for 18F-FDG and 18F-FLT avid lesions.	191
7.1	The distribution of S-phase cells at different time points in the 5-FU treated and untreated groups.	218

LIST OF ABBREVIATIONS

18F-FDG	[18F]-fluoro-2-deoxy-2 glucose
18F-FLT	18F-3'-deoxy-3'-fluorothymidine
18F-FMAU	18F-1-(2'-deoxy-2'-fluoro-beta-D-arabinofuranosyl)-thymidine,
5-FU	5-fluorouracil
ARSAC	Administration of Radioactive Substances Advisory Committee
ATP	Adenosine triphosphate
ceCT	contrast enhanced CT
CRC	Colorectal Cancer
CT	Computed Tomography
DMEM	Dulbecco's Modified Eagle's Medium
dNTP	Deoxyribonucleotide triphosphate
DoH	Department of Health
dTMP	Deoxy-thymidine-5'-monophosphate
dUMP	Deoxyuridine-5'-monophosphate
EDTA	Ethylenediamine tetracetate
FCS	Fetal calf serum
GTV	Gross Tumour Volume
H&E	Hamatoxyline and Eosin
HIV	Human immunodeficiency virus
iv	Intravenous
KeV	Kiloelectron Volts
MBq	Megabequerels
MDT	Multidisciplinary Team
OSEM	Ordered Subsets Expectation Maximization
PBS	Phosphate Buffered Saline
RECIST	Response Evaluation Criteria in Solid Tumours
SOP	Standard Operating Procedure
SPF	S-phase fraction
SUV	Standardised Uptake Value
TBS	Tris-Buffered Saline
TK-1	Thymidine Kinase-1
TS	Thymidylate synthase
UCLH	University College London Hospitals
VEGF	Vascular Endothelial Growth Factor
WHO	World Health Organisation

CHAPTER 1

Introduction

1.1 Molecular imaging and cancer

The modern management of cancer relies heavily on cross-sectional imaging, a role routinely played by anatomical imaging modalities such as ultrasound, Computed Tomography (CT) or Magnetic Resonance Imaging (MRI). These imaging techniques detect pathology based on anatomical distortion of normal structures. Such changes in morphology however are the defined end-products of a complex series of molecular events, which derive oncogenesis. Consequently, since biochemical aberrations precede anatomical changes, there has been a tremendous amount of interest in developing techniques for detecting cancers earlier in the disease process. This paradigm shift has been spurred on by advances in genomics and proteomics, which has in turn paved the way for the emergence of a novel imaging discipline coined “molecular imaging”.

The term molecular imaging (MI) represents the convergence of several biomedical disciplines that include image capture techniques, cellular and molecular biology, chemistry, medical physics, biomathematics and bioinformatics. Its principal aim is to interrogate the biochemical processes of disease without breaching the integrity of the living subject. Although several different approaches to molecular imaging have been developed, the core principles of probe labelling and signal amplification have emerged from techniques used in nuclear imaging.

The key component of MI is the molecular probe, which ideally not only has a high affinity for its target, it can also overcome biological delivery barriers to produce high resolution images. Broadly, there are 3 types of molecular probes (figure 1.1):

- a) The compartmental probe: These non-specific probes may be used in measuring changes in blood volume and perfusion. As the compartmental distribution of these probes changes over time, a fast image acquisition is required.
- b) Targeted probes: These more specific probes are targeted against a specific molecule, enzyme or receptor. They may represent labelled small molecules, peptides, enzyme substrates or antibodies.
- c) “Smart” probes: The most specific of probes, they are designed to be detected only after they have interacted with their substrate. This results in reducing the signal-to-noise ratio often encountered with other probes. More recent addition to this group are the paramagnetic nanosensors that can be used to detect oligonucleotides sequences in DNA or RNA.

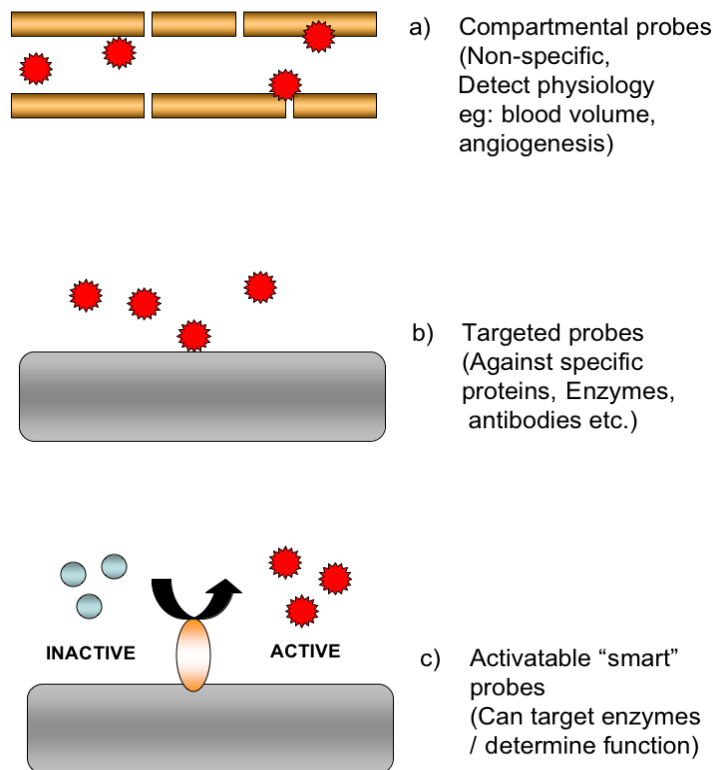


Figure 1.1: Three main classes of imaging probe used in molecular imaging (Adapted from Jaffer and Weissleder 2005).

On reaching the target, the signal from the probe is amplified in order for it to be detected outside the living system. In this respect, signal amplification defines the molecular imaging technique. For example, in nuclear imaging such as Positron Emission Tomography (PET), signal amplification is achieved with the use of positron emitting radiopharmaceuticals that emit high energy photons, whereas optical imaging employs emitted light from the targeted biological source.

1.2 Approaches to *in vivo* molecular imaging

In developing a molecular imaging strategy for a specific disease, the key question to be answered is ;

“What is the most appropriate molecular imaging system that would provide the required spatial resolution, sensitivity and the depth of penetration?”

(Jaffer and Weissleder 2005).

So far, four broad category of imaging techniques have emerged as forerunners in the molecular imaging race. Each technique bears inherent advantages and limitations, which are briefly outlined below.

1.2.1 Nuclear Imaging

Nuclear imaging techniques include Single Photon Emission Computed Tomography (SPECT) and Positron Emission Tomography (PET). The main advantages of these techniques are their intrinsic high sensitivity and unlimited depth of penetration. The versatility of nuclear imaging techniques also lie in their ability to target potentially any biochemical or molecular event, through the incorporation of radioactive isotopes

with naturally occurring biochemical agents. PET in particular can also be quantitative and produces higher resolution tomographic images compared to SPECT. The main limitations of nuclear imaging techniques are their spatial resolution and the risk of radiation exposure to the patient and the health care professionals. Furthermore, the preparation of PET radiopharmaceuticals requires a cyclotron, which is costly and may not be readily available.

1.2.2 Optical Imaging

Optical imaging is still in its relative infancy. Advances in this field have resulted from developments in mathematical modelling of tissue light properties and the development of near infrared probes. Compared to other molecular imaging modalities, optical imaging is cheap and can achieve a spatial resolution of 1-2 mm. However, its application can be limited by the poor tissue penetration properties of light, thus making it unsuitable for imaging solid visceral organs.

Optical imaging technology can be broadly divided into 2 groups:

- a) Fluorescence imaging: This is based on the absorbance of light at one wavelength (thus requiring a light source) and emission at a lower wavelength.
- b) Luminescence imaging: This process is analogous to the luciferin/luciferase reaction that results in bioluminescence in a male firefly (*Photinus pyralis*). It therefore does not require an external light source.

Near infra red (NIR) light is best suited to imaging *in vivo* as it maximizes tissue penetration and minimizes autofluorescence from non-targeted tissue. An application of this in the pre-clinical setting has been with the use of “smart” NIR fluorochromes

have been developed for quantifying specific enzyme activities such as the cathepsin B family (Weissleder et al. 1999) .

1.2.3 Magnetic Resonance Imaging (MRI)

The fundamental principle behind imaging with MRI is that unpaired nuclear spins align themselves when placed in a strong magnetic field. A temporary radiofrequency pulse then results in a change in alignment of the spin, which on return to the baseline is recorded as an electromagnetic flux.

The main advantage of MRI as a molecular imaging technique is its ability to provide molecular and anatomical information within a single imaging mode. It also produces high-resolution images (<1mm) and has a good depth of penetration (>10cm). However it suffers from an inherently lower sensitivity than other molecular imaging techniques, a feature that can be overcome by specific signal amplification to create a higher target to background contrast. Several paramagnetic (eg: gadolinium) and supramagnetic (eg: iron oxide) agents have been developed that can help overcome this.

1.2.4 Ultrasound

Imaging with ultrasound (US) uses the echogenic properties of high frequency sound waves to create images of different density tissue at different depths. Similar to MRI, US offers high resolution (<1mm) images that can be co-registered with the molecular data in the same sitting. A number of imaging agents have been developed that use microbubbles, liposomes or perfluorocarbon emulsions as scaffolds. The limitation of

these is the relative large size of the imaging particles, which can restrict tissue penetration and limits their application to imaging vascular organs.

As the main focus of this thesis is the role of PET as a molecular imaging tool, other emerging technologies will not be reviewed in any more detail than that already covered in this chapter.

1.3 Molecular imaging of cancer with Positron Emission Tomography (PET)

1.3.1 Imaging with PET - The basic principles

PET can be thought of as a camera that can take images of high energy γ -rays that are emitted from inside the subject (Gambhir 2002). The principal component of imaging with PET is the radiopharmaceutical agent (also known as a ligand or tracer). The tracer molecule is formed by incorporating a positron emitting isotope (radionuclide) into a metabolically active molecule. ^{15}O , ^{13}N , ^{11}C , ^{64}Ga and ^{18}F are some commonly available isotopes with varying radioactive half-lives. ^{18}F in particular has a half-life of 110 minutes and has proved the most practical isotope for routine clinical use to date.

The radionuclide has an unstable nucleus. It decays to reach a stable state by emitting positrons (an antimatter counterpart of an electron). Once expelled from the nucleus, a positron travels a short distance ($\sim 1\text{mm}$) and collides with an electron in the surrounding tissues. This mutual annihilation results in production of two high energy (511 KeV) photons or γ - rays, which are emitted at almost 180° to each other. The detection of two simultaneous photons by the PET scanner by a process called coincidence detection, is subsequently used to reconstruct tomographic PET images.

1.3.2 The PET detector unit

The core components of the PET detector unit consists of:

- a ring of scintillation crystals to detect “coincidence events”
- an external radiation source used for attenuation correction of the emission data
- a computer system to reconstruct the raw data into 3 dimensional tomographic images.

Most dedicated PET cameras in use today use Bismuth Germinate Oxide (BGO) crystals, which are best suited for high energy photons of 511 KeV. Although the quoted spatial resolution of 3rd generation PET scanners is approximately 6-8 mm³, there are several newer detector units emerging in the market with improved resolution. A more detailed description of this aspect of PET technology would be beyond the scope of this thesis.

1.3.3 Annihilation coincidence detection

As outlined earlier, the two γ -rays released following the annihilation event are emitted at almost 180^o to each other. If these two photons are detected within a certain time of each other (known as the coincidence time window), it is then assumed that they both originated from the same point source. The position of the annihilation event can then be estimated along a line joining the two detection positions. Images acquired by the PET scanner are therefore a collection of these 'coincidence events', which are reconstructed using a set of mathematical algorithms to produce three-dimensional images of the subject. The images from a PET camera are often shown in colour, which represent γ -ray events of the same energy. The colour scale is thus used to reflect the concentration of the isotope.

1.3.4 Attenuation correction

Attenuation is the loss of detection of true coincidence events as a result of tissue absorption of energy or random scattering of photons outside the field of view of the detector. Despite higher energy photons used in PET, attenuation is a bigger problem with PET compared to SPECT imaging. With PET, coincidence detection means that the average photon path distance from emission to detection is greater than for SPECT. Loss of counts due to attenuation increase image noise, image artefacts, and image distortion (figure 1.2). Therefore attenuation correction of data is required for accurate qualitative (visual) and quantitative measurement of PET tracer activity.

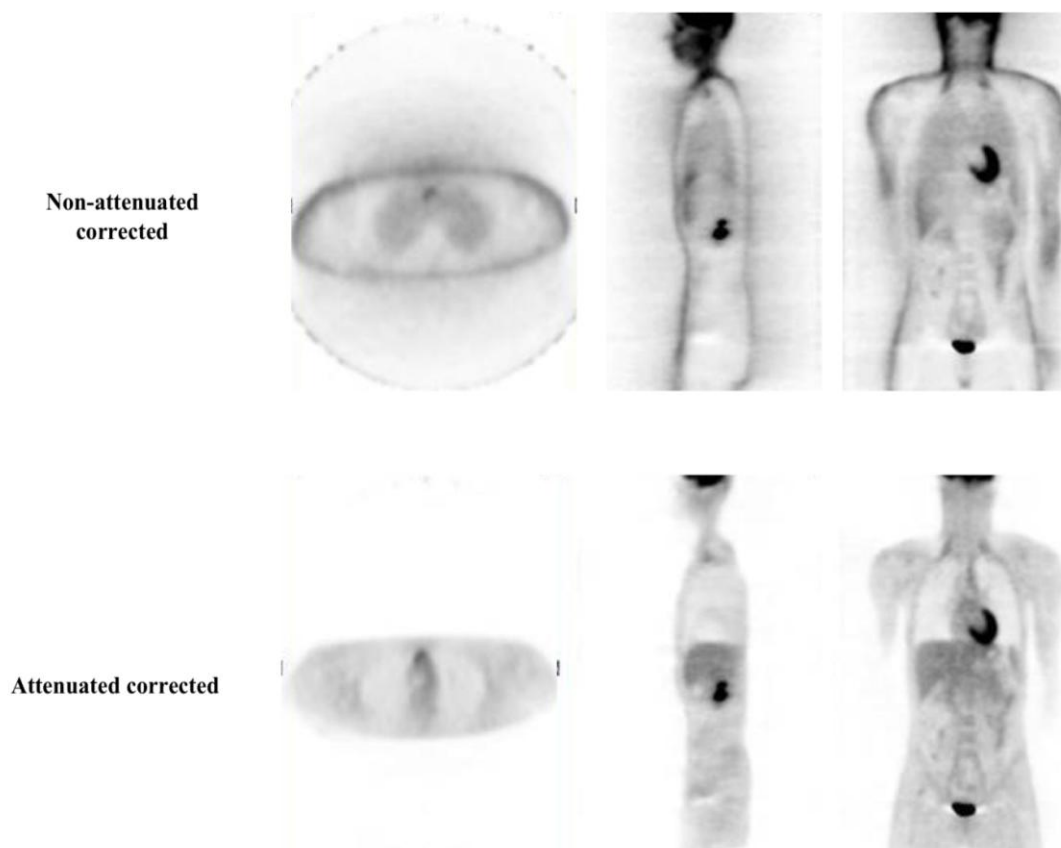


Figure 1.2: Images demonstrating the difference between non-attenuated and attenuated corrected PET images. Note sharper, less noisy image in the latter.

In order to address the above, an attenuation map of the subject is obtained, which is used as mathematical template for attenuation correction. Early generation PET scanners commonly used an external γ -ray source to acquire an attenuation map. The major disadvantage of this was the length of time it took for obtaining transmission scans (in excess of 30 minutes). The recent introduction of dual modality PET/CT scanners have been principally aimed at producing CT attenuation maps that can be acquired much more quickly (over 30 seconds) and produce less noisy images. PET/CT is explained further in later sections.

1.3.5 Quantitative imaging

Imaging with PET has above all the advantage of being quantitative. As the amount of tracer uptake mirrors the relative activity of the targeted biochemical process, measurement of emitted radioactivity allows “quantification” of the biochemical process in question.

The most common means of tracer semi-quantification is with the use of Standardised Uptake Values (SUV). These calculated units relate to the activity concentration per tissue volume and are corrected for the amount of injected tracer and the body habitus (weight, surface area) of the patient. The latter allows differences between individuals and the amount of injected tracer activity to be taken into account. It must however be noted that tracer activity in a region of interest is not static, and SUVs do not account for tissue / tracer dynamics over time. This can be addressed with the use of dynamically acquired data and application of compartmental models that give a better assessment of tracer biodistribution. SUVs provide a ready measure of the amount of tracer uptake at a specific time point, making it a more suitable technique for use in

routine clinical practice. Although compartmental modelling provide more specific means of quantifying tissue dynamics of tracer uptake *in vivo*, they require serial arterio-venous blood samples that are not only invasive for the patient, but are time consuming. This technique is therefore solely reserved for tracer analysis in the pre-clinical (research) setting and not the routine clinical practice.

1.3.6 Multimodality imaging with PET/CT

One of the disadvantages of imaging with PET has been its lack of anatomical resolution, which can limit the accuracy of lesion localization and lesion characterization. This limitation of PET has now been addressed with the introduction of dual modality PET/CT scanners. In 2001, the first dual modality (hybrid) PET/CT scanner was developed primarily as a proof of concept that concurrent image acquisition with PET and CT was possible. Today's dedicated PET/CT scanners essentially consist of a multidetector spiral CT, attached to the front of a standard PET detector unit (Figure 1.3).

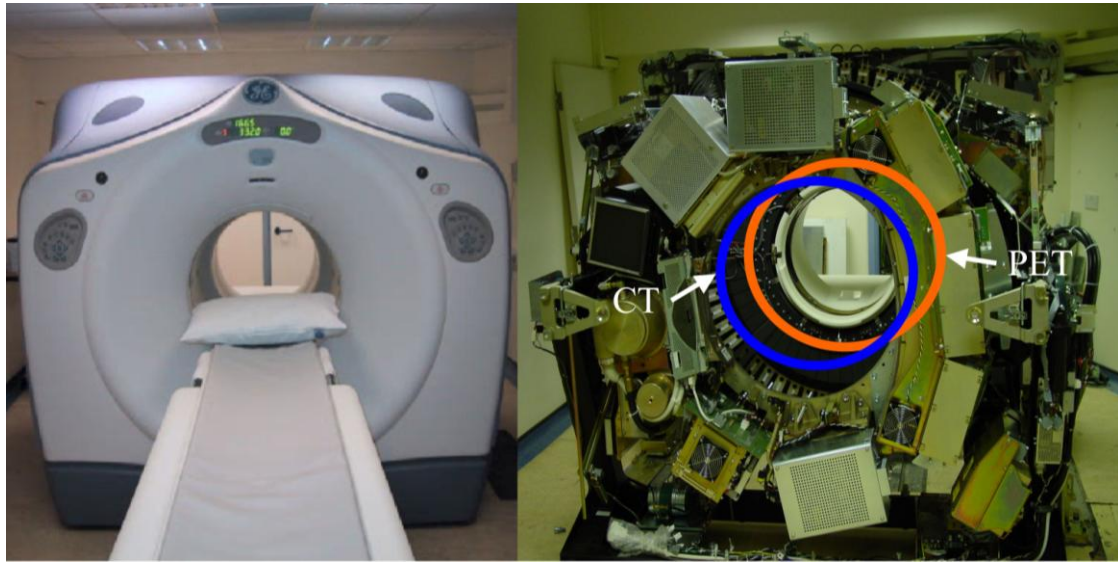


Figure 1.3: Dedicated dual modality PET/CT scanner used at our institution. The detector unit is shown with the outer casing removed, demonstrating the relative position of the CT and PET component of the scanner.

The PET and the CT images are acquired sequentially and in the same sitting. This allows for minimal patient movement between the two scans, which in turn allows accurate co-registration of the biological and anatomical data. The CT component is also used for attenuation correction of PET images. This has not only helped produce sharper and clearer images, it has also reduced PET acquisition times by approximately 25 minutes. Consequently, this has resulted in better patient compliance and increase in scanner throughput.

1.3.7 Imaging protocols for PET and PET/CT

Patient preparation prior to imaging with PET (and PET/CT) is dependant on the tracer being used. With ^{18}F -FDG, the patient is routinely fasted for at least 4 hours and measures are taken to ensure normo-glycaemia. This is important as for two reasons: abundance of serum glucose can compete with ^{18}F -FDG and result in

incidence of false negative findings; activity of the GI tract after eating can result in non-specific ^{18}F -FDG and diagnostic uncertainty. As active muscle tissue also metabolise significant amounts of glucose, a muscle relaxant (diazepam) is also routinely administered to reduce high levels of non-specific uptake. In using an alternative tracer such ^{18}F -FLT, such measures are often not required. This will be discussed further in later chapters.

1.4 Molecular and cellular targets for PET imaging

One of the key advantages of imaging with PET is the ability to quantify potentially any biochemical event *in vivo*. In targeting specific cellular and molecular pathways of cancer with PET, several assumptions are often made. These assumptions stem from the fact that although under specific conditions labelled analogues mimic their natural counterpart, there may be notable exceptions. For a tracer to be a successful imaging probe for PET, it must fulfil the following criteria (Gambhir 2002):

- 1) The positron emitting isotope must not dissociate easily from the molecule of interest as this may result in the free isotope being imaged and not the labelled tracer.
- 2) The isotope labelling must not alter the biological properties (such as transport, elimination or affinity for the target) of the parent molecule.
- 3) The tracer must clear rapidly from non-target sites, without which it would be impossible to image sites of specific targeting.

To date, a number of labelled analogues have been developed that target cellular properties ranging from glucose metabolism to apoptosis. Some of the commonly investigated tracers other than ^{18}F -FDG and their targets are listed in table 1.1. The focus of this thesis is to investigate the role of imaging with two PET tracers; the routine glucose analogue [^{18}F]-fluoro-2-deoxy-D-glucose (^{18}F -FDG) and the thymidine analogue [^{18}F]-3'-deoxy-3'-fluorothymidine (^{18}F -FLT). The latter in particular has emerged as a potential PET tracer for measuring cellular proliferation. In the following sections, the above two tracers will be described in more detail.

Target	Tracer
Blood Flow	[15O]- water
Tumour Hypoxia	[18F] misonidazole
Amino acid synthesis	[11C] methionine
DNA synthesis	[11C] thymidine
DNA synthesis	[18F] FLT
Tumour receptors	[68Ga] SMS
Oestrogen receptor	[18F]-16 α -Fluoroestrodial
Apoptosis	[18F] annexin V
Chemotherapy drugs	[18F] fluorouracil

Table 1.1: Non 18F-FDG tracers and biochemical targets

1.4.1 Aerobic glycolysis, cancer and imaging with PET

One of the properties common to all invasive cancers is that of altered glucose metabolism. In normal untransformed cells, glucose is converted to glucose-6-phosphate by hexokinase and then to pyruvate, generating 2 ATP molecules per glucose. In the presence of oxygen, pyruvate is oxidized in mitochondria to produce 36 additional ATP molecules per glucose. In the absence of oxygen, pyruvate is reduced to lactate, which is exported out of the cell without energy production. This latter step known as glycolysis is inhibited by mitochondria (Pasteur effect), where pyruvate is oxidized to CO₂ and H₂O. In cancer cells however, the conversion of glucose to lactic acid occurs despite the presence of oxygen. This phenomenon is known as aerobic glycolysis and has been coined the “Warburg effect”, named after the German biochemist Otto Warburg. In investigating the metabolic properties unique to cancer cells, Warburg set out to answer one fundamental question:

“If the carcinoma problem is attacked in its relation to the physiology of metabolism, the first question is: In what way does the metabolism of growing tissue differ from the metabolism of resting tissue?” Otto Warburg (1924).

Following a series of observations in a rat model and later in human cancer cell lines, Warburg concluded that the predominant metabolic pathway in cancer cells is that of glucose metabolism by aerobic glycolysis (Warburg 1931). Although his initial hypothesis that cancer resulted from impaired mitochondrial metabolism has been disproved, observations of enhanced glycolysis in cancer cells has been repeatedly verified. Initial interest in tumour glycolysis was overshadowed by the widespread application of molecular and genetic techniques in investigating cancer biology.

However, the subject of glycolysis was once again re-kindled with the emergence of PET and the glucose analogue tracer ^{18}F -FDG.

Although the rate of glycolysis can be controlled at several steps, most studies to date have indicated the predominant role of glucose transport and phosphorylation in controlling the glycolytic flux. The resultant demand of malignant cells for glucose has been shown to be met by an activation of the glucose reliant hexose monophosphate pathway, which provides the backbone for DNA and RNA synthesis, (Webber 1977a, 1977b), and an increased expression of glucose transporters (Flier et al. 1987; Hatanaka 1974), of which GLUT 1 has been shown to be the predominant element (Hiraki et al. 1981).

1.4.2 [^{18}F]-fluoro-2-deoxy-D-glucose (^{18}F -FDG)

The simple rationale for blocking accelerated glycolysis and thus tumour growth, initially lead to the development of the drug 2-deoxy-D-glucose (DG). However, as DG also blocked brain glycolysis, it could not be routinely used. Later however, Sokoloff et al. (1977) used ^{14}C -labelled DG for imaging local cerebral glucose metabolism. Substitution of hydroxyl group in the 2-position with ^{18}F later lead to the development of [^{18}F]-fluoro-2-deoxy-D-glucose (^{18}F -FDG).

The first application of FDG was in the 1980's where it was used in the assessment of the degree of malignancy in cerebral tumours (Di Chiro 1987). By the 1990's, FDG labelled with ^{18}F had swiftly become the mainstay of imaging with PET, where its application extended beyond neuro-oncology to the detection of a wide variety of solid cancers.

Following intravascular injection and passive diffusion into the interstitial space, ^{18}F -FDG is transported into cells by specific glucose transporters (GLUT-1). It is then phosphorylated by hexokinase to form FDG-6-phosphate. As ^{18}F -FDG lacks the hydroxyl group at position 2, FDG-6-phosphate cannot undergo further glycolysis. It therefore becomes metabolically redundant and subsequently intracellularly trapped (Figure 1.4).

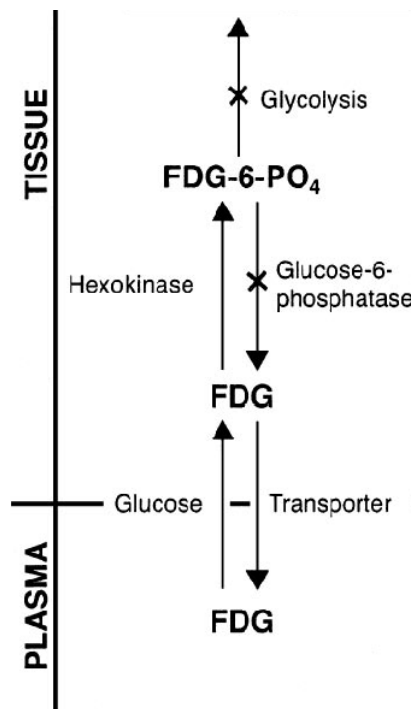


Figure 1.4: Phosphorylation pathway of ^{18}F -FDG (Czernin and Phelps 2002)

When interpreting ^{18}F -FDG PET images, normal uptake of tracer within the body also needs to be considered. The brain has a high physiological glycolytic index and often exhibits extremely high ^{18}F -FDG accumulation. Such high background levels limit the use of this tracer for detecting cerebral metastases. The uptake of ^{18}F -FDG by the myocardium is driven by the abundance of insulin sensitive glucose transporters (mainly GLUT-4). This uptake is generally variable, decreasing in the fasting state and increasing in the presence of insulin. This pattern is also seen in skeletal muscle. As for this, imaging protocols such as those used in this thesis ensure

a state of euglycaemia in the patient and during the uptake phase of the tracer, the patients are required to limit their movement and to remain undisturbed in a darkened room. Finally the renal excretion of ^{18}F -FDG also limits its use in imaging renal tract tumours and the intense accumulation of the tracer within the bladder can at times obscure the detection of adjacent ^{18}F -FDG avid disease within the pelvis.

1.5 Cellular proliferation

One of the hallmarks of cancer is uncontrolled proliferation. Over the last few decades, significant effort has been focused on understanding this process as it is a key determinant of how a cancer behaves clinically. Through advances in molecular and genetic analysis of cancer we now have a better understanding of the various regulatory mechanisms that control cellular proliferation. These have and are being exploited for use as diagnostic, prognostic and therapeutic tools in cancer management. Efforts at quantifying proliferative activity have also extended to the field of molecular imaging with PET where novel tracers have been developed to target various steps of the proliferative activity. The development of “proliferation” PET tracers have been essentially borne out of the *in vitro* use of thymidine for determining DNA turnover. One such PET tracer is the thymidine analogue 18F-3'-deoxy-3'-fluorothymidine (18F-FLT). 18F-FLT potentially brings quantitative imaging of tumour proliferation from the bench to the routine clinical practice. In order to understand the kinetics of 18F-FLT in targeting proliferation, some of the key concepts such as cellular growth and the cell cycle need to be reviewed.

1.5.1 The cell cycle

The concept of cellular proliferation has evolved from early days of light microscopy where mitotic figures were observed in eukaryotic cells. From this, it was postulated that cells exist in one of two states; either in a state of cellular division during mitosis or remain in an inactive state (interphase). Later breakthrough work by (Howard and Pelc 1951) lead to the concept of the cell cycle. They concluded that the cell cycle consisted of four stages during which DNA synthesis (S phase) and cell division

(mitosis, M phase) were separated by two gap phases, G1 and G2 respectively (figure 1.5).

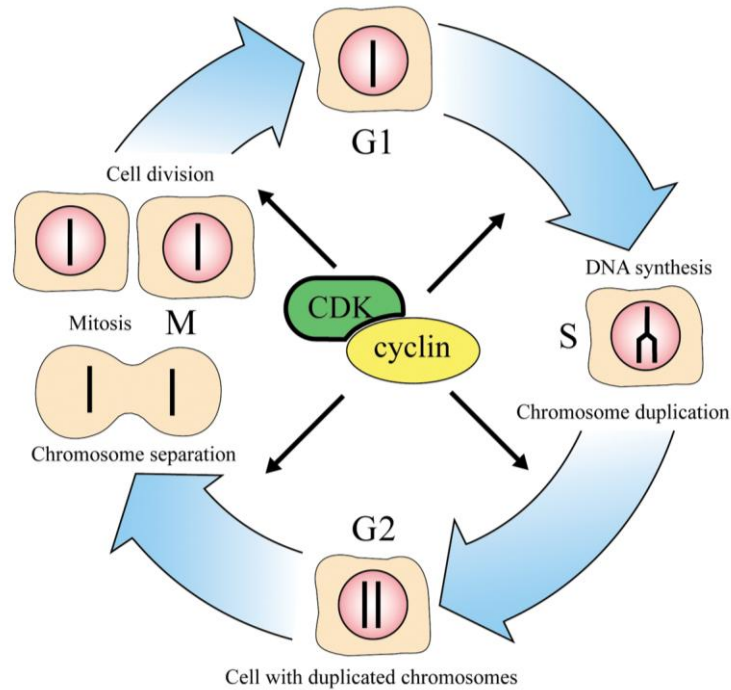


Figure 1.5: *The cell cycle*

The cell cycle is a highly conserved and ordered set of events, tightly controlled by a series of positive (cyclins) and negative (tumour suppressor genes such as P53 or retinoblastoma (Rb)) effectors. Collectively, these regulatory proteins are responsible for the timely transition of cells through the cell cycle, while arresting propagation of DNA mutations through their communication with the cells' fail safe mechanisms such as DNA mismatch repair proteins and the apoptotic pathway.

1.5.2 Proliferation and tumour growth

Understanding the growth rate of a tumour is an important step in understanding the spectrum of cancer behaviour observed clinically. It has been shown that tumours with rapidly proliferating cells are associated with a poorer long term survival (Tubiana et al. 1984; Murray and Kirschner 1989; Pardee 1989; Tubiana and Courdi 1989). Furthermore, the rate of proliferation can be indicative of the sensitivity of a tumour to cycle-dependent cytotoxics, which may in turn direct clinicians in adjusting adjuvant strategies. In order to quantify proliferative activity of a tumour, one must understand its temporal relationship with the cell cycle and its resultant effect on tumour growth.

Growth is the overall increase in cell number, which is the net effect of cell gain by proliferative activity and cell loss by apoptosis or necrosis (van Diest et al. 1998).

Proliferative activity (P) on the one hand is the result of cell cycle activity, which in turn consists of the speed of the cell cycle (which is inversely proportional to the generation time (T)), and the growth fraction (G). Mathematically, the relationship between proliferative activity and the growth fraction can be summarised as;

$$P=G/T.$$

In other word, a high proliferative activity can be the result of either a high growth fraction or short generation time, or both. This is an important consideration as many of the methods used in assessing proliferative activity are in fact quantifying growth fraction, whereas owing to its complexity, cell cycle time is often ignored.

1.5.3 Assessment of proliferation

To date, several *in vitro* and *in vivo* techniques have been investigated for the assessment of proliferative activity. Each technique carries an inherent advantage and disadvantage, which will be briefly outlined below.

1.5.3.1 Mitotic index

Interphase, which consists of G1, S and G2 phases, is the longest part of the cell cycle. However, cells during this phase cannot be morphologically recognised whereas those in mitotic phase (M phase) can be identified by the presence of chromosomal sets that are known as mitotic figures. Counting mitotic figures is one of the oldest ways of assessing proliferation. It can easily be used in the routine clinical setting, requiring only an adequate microscope and a well-stained H&E slide. The most commonly used technique for counting mitotic figures is by expressing the number of mitoses seen within a pre-defined number of high power fields (eg: 10) or per unit area (eg: 2 mm²), thus giving rise to a mitotic index.

Despite its popularity, quantifying the mitotic index of a specimen has its limitations. The M phase of cell cycle can be widely varied in duration, particularly in an aneuploid population of cells. Therefore, number of mitoses observed do not necessarily correlate with the rate of cell proliferation in a linear fashion. This may also explain the partial correlation observed between other proliferation indices such as the Ki67 labelling index (Isola et al. 1990; Di Stefano et al. 1991) and Bromodeoxyuridine (BrdU) incorporation assays (Weidner et al. 1993). Furthermore, mitosis counting is subject to reproducibility errors unless strict tissue fixing, staining and counting protocols are used.

1.5.3.2 Incorporation techniques using nucleotide analogues

Incorporation techniques use radiolabeled nucleotide analogues to measure the rate of DNA synthesis and thus cellular growth. Thymidine labelled with tritium has often been considered as the gold standard marker of S-phase cells, as thymidine is the only nucleotide that is exclusively incorporated into DNA and not RNA. More recently other nucleotide analogues have been employed of which bromodeoxyuridine (BrdU) is the most widely used. Such incorporation techniques have been applied to autoradiography (³H-thymidine) and immunohistochemistry (BrdU). *In vitro*, pulse labelling of cancer cells can also be used to determine the proportion of cells entering the S-phase over a period of time, thus giving a measure of cell cycle time. In the clinical setting, the use of ³H-thymidine is not popular as it involves handling of a radioactive substance. Autoradiography can also be a cumbersome and lengthy procedure (it may take up to a week to develop the images). Use of immunohistochemistry with BrdU is also subject to limitation and errors of tissue sampling.

1.5.3.3 DNA cytometry and percentage S-phase determination

In DNA cytometry, nuclei are stained with a stoichiometric DNA binding stain, which allows the amount of DNA present to be measured. The two applications of this are with the use of a flow-cytometry, which uses a fluorescence dye on a suspension of cells and static cytometry where the optical density of stained cells fixed on a slide, are measured. Both techniques produce DNA histograms, which are representations of the cells within different phases of the cell cycle (G₀/G₁, S and G₂/M phase). Although strictly speaking, the proliferative fraction includes cells in both the S and G₂/M phase, the most commonly used proliferation variable is the S-phase fraction.

Historically, estimation of S-phase fraction by flow cytometry has been regarded as being more reliable due to its higher resolution DNA histograms. However, recent sophisticated hardware and software solutions have made % S-phase estimates from static cytometric histograms a valid alternative. Overall, the reliability of % S-phase determination by cytometry is dependent on software variables that determine different cycle phases and the inter-observer variability in interpreting them. Several large studies have therefore been carried out in order to provide a consensus on what parameters are used for cytometric analysis (Bergers et al. 1997a; Bergers et al. 1997c). Notably however, factors such as cell fixation delays do not interfere with % S-phase measurements (Donhuijsen et al. 1990; Bergers et al. 1997b).

1.5.3.4 Proliferation associated antigens

Identification of cellular antigens that are upregulated in proliferating cells has provided yet another relatively easy means of quantifying proliferative activity. The proliferating cell nuclear antigen (PCNA) is one such protein, expression of which is upregulated during active proliferation. Although several studies have shown a correlation between PCNA and other proliferation markers such as S-phase fraction (Visscher et al. 1992; Siitonen et al. 1993), mitotic index (Siitonen et al. 1993) and Ki67 staining, this has not been consistently seen. This may be due to the fact that PCNA is also involved in DNA repair (Masih et al. 2008). Malignant cells are often undergoing active DNA repair, which has led to the observation that in some tumours 100% staining of cells with PCNA is seen. As for this, the routine use of PCNA as a routine marker of proliferation in cancer cells has fallen out of favour.

The Ki67 antigen is another nuclear antigen, coded by a gene on chromosome 10. It is expressed in the G1, S and G2 phases of the cell cycle but not G0. Initial work with

the Ki67 antigen was carried out on frozen sections, but recently a number of antibodies, namely MIB-1, have been developed that allow the antigen to be detected on paraffin embedded sections and archived material (Cattoretti et al. 1992; McCormick et al. 1993). As with most immunohistochemical techniques, adequate staining methodology is required to obtain reproducible results. A number of automated scanning techniques are also employed to produce quick and reliable results. To date, a number of studies have shown Ki67 labelling score (index) to correlate with % S-phase fraction (Isola et al. 1990; Lee et al. 1992) and mitotic index (Barnard et al. 1987; Isola et al. 1990; Marchetti et al. 1990; Di Stefano et al. 1991; Sahin et al. 1991).

1.5.4 Tumour heterogeneity – a problem of assessing proliferation

One of the limiting factors of assessing tumour proliferation with the above techniques is the inherent heterogeneity of a tumour mass. This has been reported for several tumour types, which may be one of the reasons for the apparent contradictory results seen in the literature. Generally it is considered that the highest proliferative part of a tumour determines its clinical behaviour. Therefore in order to obtain clinically meaningful results, the most active part of the tumour mass needs to be sought.

With morphological methods of analysis, the problem of heterogeneity can be overcome by examining the tumour mass for the most proliferative area. However, in the routine clinical setting this may also not be feasible, as surgery and thus whole tumour resection may not be indicated in all patients. Where sampling of a tumour by way of percutaneous biopsy can yield diagnostic information, targeting the biopsy to

the most proliferative area of the tumour is near impossible with current localization / imaging techniques. This highlights the advantage of molecular imaging with PET, whereby the focal abnormality being targeted is localized and tracer uptake quantified accord to its differential tracer uptake kinetics compared to surrounding tissues. The “hot spot” seen on the PET scan therefore theoretically represents the focus of tumour with the highest proliferative activity.

1.5.5 Thymidine analogues PET tracers for imaging cell proliferation

The understanding that emerged from the use of labelled thymidine eventually led to the development of the first proliferation PET tracer, ¹¹C-Thymidine. The advantage conferred by radiolabelling thymidine is that as the native compound, it is readily taken up by cells and incorporated into DNA. Several pilot studies in patients have demonstrated the feasibility of using ¹¹C-thymidine PET in imaging tumours and their response to treatment. Eary et al. (1999) demonstrated the use of ¹¹C-thymidine for imaging proliferation in primary and recurrent brain tumours. van Eijkeren et al. (1992) investigated the role of ¹¹C-thymidine in monitoring response to therapy in 13 patients with head and neck cancers. In a small study of 4 patients with small cell lung carcinoma and 2 with high grade sarcoma, Shields et al. (1998b) also showed that a persistence of ¹¹C-thymidine uptake one week post treatment can be predictive of progressive disease. More recently, Wells et al. (2002) showed that PET derived parameters of ¹¹C-thymidine uptake in patients with advanced intra-abdominal malignancy correlated with Ki67 labelling, thus supporting its role as a surrogate marker of proliferation.

Despite early promising results, ¹¹C labelled thymidine has been deemed impractical for routine clinical use. This has been due to the fact that thymidine can only be labelled with ¹¹C, which has a short half-life (approximately 20 minutes) and its synthesis is complex and expensive. Furthermore, ¹¹C is rapidly metabolised *in vivo* to carbon dioxide and a series of complex metabolites, quantification of which requires the use of complex kinetic models (Mankoff et al. 1998; Eary et al. 1999). This process of kinetic modelling is time consuming and requires extensive work by the imaging team, which again makes its routine clinical use impractical.

The above however lead the search for other more suitable labelled nucleotides for imaging proliferation with PET. Two of the more extensively studied agents are ¹⁸F-3'-doxy-3'-fluorothymidine (18F-FLT) and ¹⁸F-1-(2'-doxy-2'-fluoro-beta-D-arabinofuranosyl)-thymidine. In both 18F-FLT and 18F-FMAU, placing fluorine in the 2' or 3' position of the deoxyribose sugar, stabilises the molecules' glycosidic bonds, thus preventing degradation (Shields 2006). However, both agents undergo glucuronidation, which can further complicate the dynamic distribution of these tracers (Shields et al. 2005).

As the focus of this thesis is the comparison of imaging with 18F-FLT and 18F-FGD PET, there will not be any further review of the role of 18F-FMAU in imaging proliferation will not be covered further.

1.6 [18F]-3'-doxy-3'-fluorothymidine (18F-FLT)

1.6.1 The development of 18F-FLT

FLT (Alovudine) was initially developed as an anti-retroviral agent for the treatment of patients with human immunodeficiency virus (HIV) (Flexner et al. 1994). However, it was soon withdrawn from phase II clinical trials due to its high levels of myelotoxicity. As mentioned previously, radiolabeled FLT was found to be more stable to cellular degradation than its native counterpart thymidine, and therefore, its use as a potential PET tracer quickly generated a large body of interest. Wilson et al. (1991) were the first to describe the 18F labelling of FLT. Later, modifications of its radiosynthesis by Grierson and Shields (2000) lead to the development of a more simplified, reproducible and clinically feasible approach to synthesising 18F-FLT (Machulla et al. 2000).

1.6.2 The molecular kinetics of 18F-FLT

It is believed that 18F-FLT enters cells by a complex mechanism of facilitated transport, similar to that observed *in vitro* from studies with labelled thymidine. There are two transport mechanisms involved; equilibrative transporters that mediate both the influx and efflux of nucleosides (Belt et al. 1993) and concentrative Na⁺-dependent carriers which have been described to mediate only influx (Vijayalakshmi and Belt 1988). While concentrative transporters are mostly expressed in normal tissues, equilibrative transporters have been found in large numbers in tumour cells (Belt et al. 1993).

It is yet unclear which equilibrative transporters play a dominant role in 18F-FLT uptake. However, transport of 18F-FLT into cells seems to follow a biphasic kinetic

pattern, with a rapid initial accumulation that correlates with the rate of FLT phosphorylation by the enzyme thymidine kinase (TK). This is followed by a slower rate of accumulation, which may be due to competing efflux mechanisms (Scwartz et al. 2001).

1.6.3 Cellular trapping of 18F-FLT

The initial rapid accumulation of 18F-FLT within cells is thought to be associated with its rate of phosphorylation that is controlled by the enzyme thymidine kinase (TK). Thymidine kinase is present in cells in two isomeric forms; cytosolic TK known as TK-1 and its ribosomal counter-part, TK-2. TK-1 has a higher affinity for thymidine than TK-2. It is the rate limiting enzyme of the salvage pathway of pyrimidine synthesis and exhibits a complex cell cycle regulated expression. It is virtually undetectable in quiescent cells (G0) but its levels peaks at the end of the G1/S-phase and finally return to background levels by the end of the M-phase of the cell cycle (Sherley and Kelly 1988; Munch-Petersen et al. 1995; Grierson et al. 2004). *In vitro*, TK-1 activity has been reported to be 3-4 times higher in cancers cells compared to their benign counterparts (Boothman et al. 1994). The phosphorylation of 18F-FLT by TK-1 results in formation of negatively charged 18F-FLT monophosphate. In a way analogous to the cellular trapping of 18F-FDG by hexokinase, 18F-FLT monophosphate is intracellularly trapped (Figure 1.6). The accumulated radioactivity can then be detected with PET.

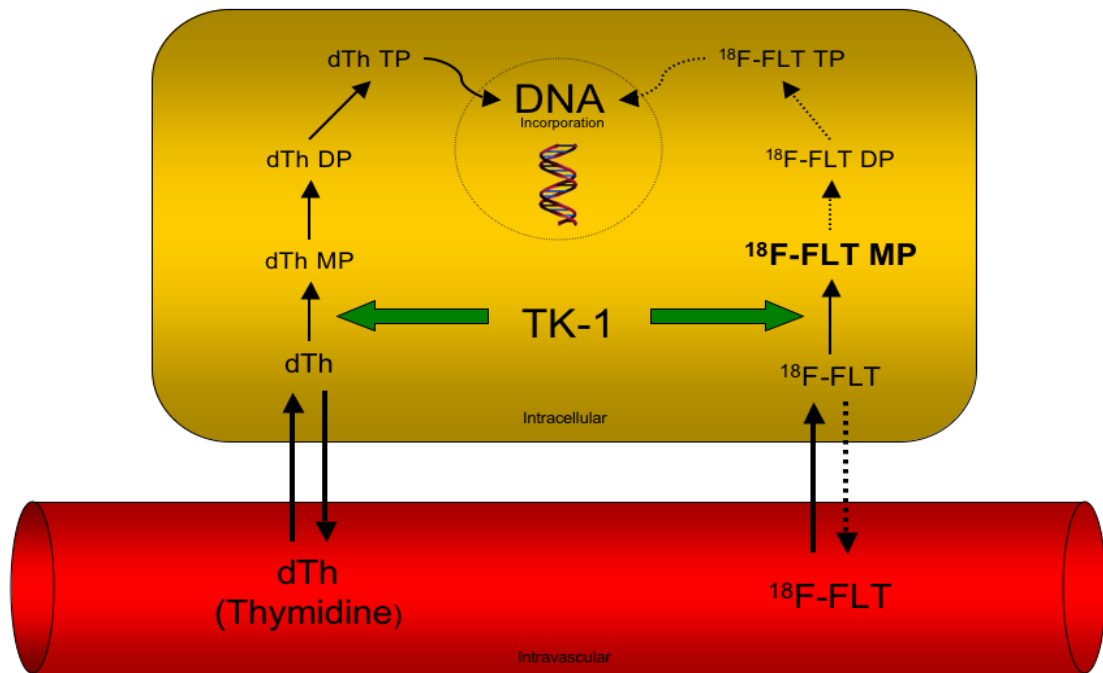


Figure 1.6: The mechanism of cellular trapping of ^{18}F -FLT compared to that of Thymidine (dTh) – [Abbreviations: MP=monophosphate; DP=diphosphate, TP=triphosphate]

1.6.4 ^{18}F -FLT as a proliferation PET tracer

The link between ^{18}F -FLT uptake and thymidine kinase is the fundamental basis that supports its role as a surrogate marker of proliferation. *In vitro*, a strong association between the rate of ^{18}F -FLT uptake and TK-1 activity has been demonstrated. In a human lung carcinoma cell lines, Rasey and colleagues showed a strong correlation between ^{18}F -FLT uptake, cell growth, S-phase fraction (SPF) and TK-1 activity (Rasey et al. 2002). Similarly, Barthel et al. (2005) showed a significantly lower ^{18}F -FLT uptake in TK deficient mouse lymphoma tumours as compared to their TK proficient variants. In a panel of 22 asynchronously growing cancer cell lines, Toyohara et al. (2002) also showed ^3H -FLT uptake to strongly correlate with both

SPF ($r=0.76$) and 3H-thymidine uptake ($r=0.88$, $P<0.0001$), thus supporting the role of FLT as a proliferation PET tracer. This group also found that over 90% of 3H-thymidine was incorporated into DNA compared to negligible levels (0.2%) of [3H]-FLT. The reason for this is the fact that FLT acts as a chain terminator of DNA due to its lack of 3'-hydroxyl side group.

Unlike thymidine, which represents the totality of DNA turnover, FLT seems to target the first step of the DNA salvage pathway. This has raised the question of whether TK-1 activity accurately reflects cellular proliferation. So far it is understood that the relative contribution of the salvage and the *de novo* pathways of DNA synthesis vary in different tumour types. In a study on a panel of 6 malignant cell lines, Schwartz et al. (2003) showed the uptake of labelled FLT and thymidine to correlate with TK-1 activity, only in cells with TK-1 dependent proliferative activity. In two of the cell lines, proliferation seemed to be less TK-1 dependent and thus the correlation was poor. Furthermore, other studies have shown that antimetabolite chemotherapeutic agents such as 5-fluorouracil and methotrexate result in a paradoxically increase in TK-1 activity possibly as a result of their effect on the pyrimidine salvage pathway (Dittmann et al. 2002). This paradigm will be further investigated in later chapters but as it stands, there are indications that in certain situations, 18F-FLT uptake may not reflect proliferative activity.

1.6.5 Clinical applications of 18F-FLT

To date, several studies have examined the feasibility of imaging with 18F-FLT PET in the routine clinical setting. Much of the published data so far are from studies with relatively small patient numbers. Although 18F-FLT has been shown to be a feasible

tracer for visualising a range of solid and haematological cancers, it has been consistently found show a lower degree of cellular accumulation compared to 18F-FDG. In organs such as the lungs and the brain where background 18F-FLT uptake is low, this appears to be less of a problem. However in the liver or bone marrow where background 18F-FLT uptake is high (the former being due to the glucuronidation of 18F-FLT in hepatocytes), this can result in under-detection and staging inaccuracy (Dittmann et al. 2003; Francis et al. 2003b). The above is demonstrated in figure 1.7 where the whole body distribution of 18F-FDG and 18F-FLT can be seen in within normal organs and that of a primary rectal cancer.

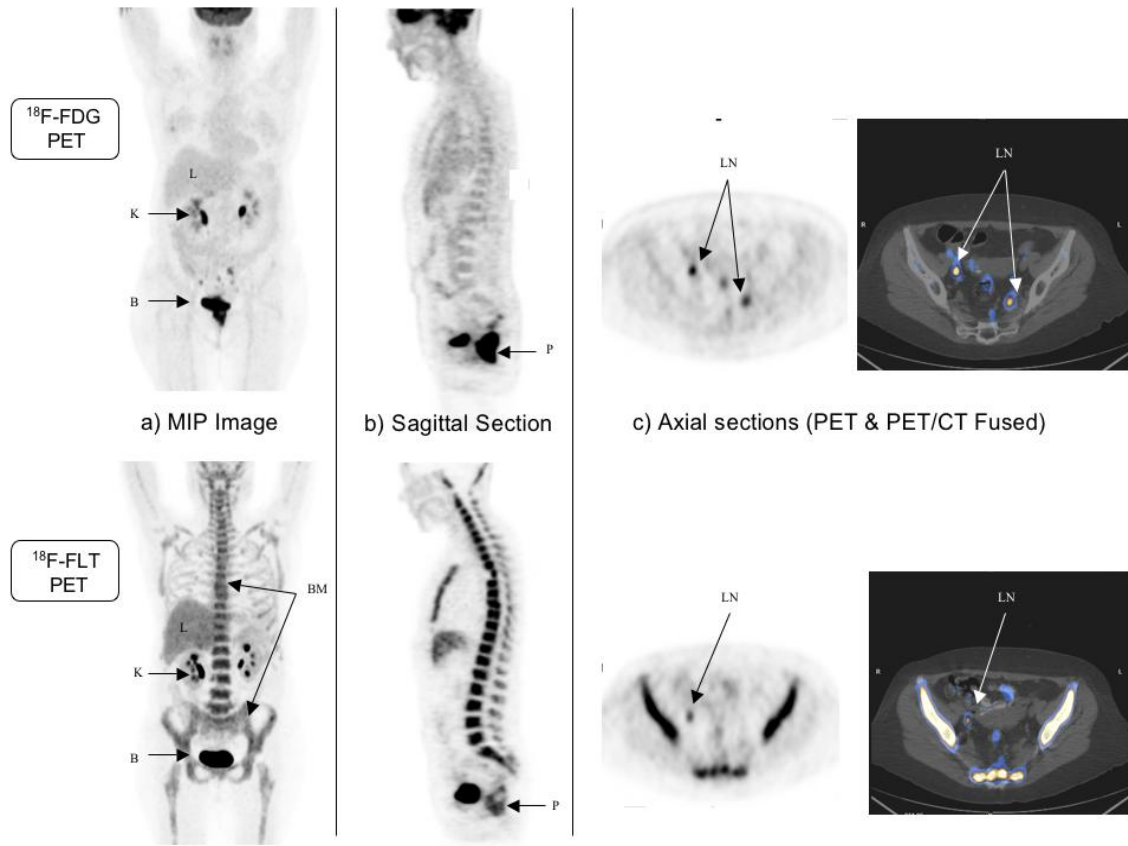


Figure 1.7: Comparative ^{18}F -FDG (top row) and ^{18}F -FLT (bottom row) PET images in the same patient with a locally advanced rectal carcinoma.

a) Maximum intensity projections (MIP) demonstrating the difference in whole body distribution between ^{18}F -FDG and ^{18}F -FLT. Note high background uptake in the liver (L) and the bone marrow (BM) on ^{18}F -FLT PET (K = Kidney; B = Bladder)

b) Sagittal sections showing uptake of tracers at the primary rectal site (P)

c) Axial PET and PET/CT fused slices demonstrating ^{18}F -FDG and ^{18}F -FLT avid pelvic lymph nodes (LN). Note, only one nodal site was positive on ^{18}F -FLT PET.

Several studies have also aimed at validating ^{18}F -FLT PET as a means of quantifying proliferative activity of a tumour. There are two potential applications of this in oncology; firstly is the potential for identifying high-risk patients that would most benefit from adjuvant treatments and secondly, it potentially provides the clinician with an alternative surrogate marker of response to treatment. Table 1.2 summarises

the results of publishes series to date that investigated the correlation between 18F-FLT uptake and other independent proliferation indices. Although majority of the results support the hypothesis that 18F-FLT may be a useful marker of proliferation, discrepancies in the data warrant a closer consideration.

Type of malignancy (no. of patients)	Proliferation index	Correlation (R value)	Reference
Pulmonary nodules (n=30)	Ki-67	0.87	Buck et al. 2002
NSCLC (n=11)	a)Ki-67; b) SPF	a)0.84; b)0.69	Vesselle et al. 200)
NHL (n=11)	Ki-67	0.95	Wagner et al. 2003
Colorectal carcinoma (n=13)	Ki-67	0.8	Francis et al. 2003a
Melanoma (n=10)	Ki-67	NA	(Cobben et al. 2003)
Soft tissue Sarcoma (n=20)	Mitotic index; Ki-67	0.55-0.75	(Cobben et al. 2004a)
Laryngeal cancer (n=21)	NA	NA	(Cobben et al. 2004b)
Breast cancer (n=14)	Ki-67	0.1-0.14*	(Smyczek-Gargya et al. 2004)
Glioma (n=26)	Ki-67	0.82	(Choi et al. 2005)
Oesophageal (n=10)	Ki-67	0.75	(van Westreenen et al.2005)

Table 1.2: Summary of studies examining the role of 18F-FLT PET in imaging a range of cancers. Their correlation with other indirect measures of cellular proliferation are tabulated. [NSCLC = Non-small cell lung cancer, NHL=Non-Hodgkins lymphoma, SPF=S-phase fraction, *= not significant)

Aside from quantifying proliferation, ^{18}F -FLT has also been proposed to be of clinical value due to its cancer specificity compared to ^{18}F -FDG. While ^{18}F -FDG is a highly sensitive tracer, it lacks specificity as the tracer also accumulates in inflammatory tissue, which also exhibits a high glycolytic activity. It is postulated that as peripheral inflammatory cells are terminally differentiated, they have a relatively lower proliferative activity and thus accumulate significantly less ^{18}F -FLT compared to ^{18}F -FDG. Should ^{18}F -FLT be a more specific tracer, it could allow for a more accurate assessment of local lymph nodes, potentially differentiating between reactive and metastatic lymphadenopathy. Alternatively, it may be of value in conditions where an inflammatory mass may result in false positive ^{18}F -FDG uptake (eg: mass forming pancreatitis vs mass due to pancreatic cancer).

The hypothesis that ^{18}F -FLT is a more cancer specific tracer has been tested by van Waarde et al. (2004) using an animal model of tumour versus inflammation. The biodistribution of ^{18}F -FLT and ^{18}F -FDG were compared in Wistar rats bearing C6 glioma xenografts in the right shoulder as well as an area of sterile inflammation induced by injecting turpentine into the animals' thigh muscle. Within the tumour mass, there was significant accumulation of both tracers, although tumour : normal tissue ratios were higher for ^{18}F -FDG compared to ^{18}F -FLT (13.2 vs 3.8 respectively). On the other hand, ^{18}F -FDG accumulation in the inflamed thigh was 4.8 times higher than the tumour bearing side, compared to 1.3 (+/- 0.4) fold increase for ^{18}F -FLT. A more recent study of ^{18}F -FLT imaging in staging primary squamous cell carcinoma of the head and neck yielded slightly contradictory results. In this study ^{18}F -FLT uptake was demonstrated in both reactive as well as metastatic lymph nodes (Troost et al. 2007). However interestingly, all PET positive lymph nodes

(including those that were reactive in nature) showed an abundance of staining for Ki-67 antigen and iododoxyuridine suggesting yet again that ^{18}F -FLT is a proliferation tracer. As for ^{18}F -FLT's tumour specificity, this requires further validation.

1.7 The role of PET in diagnosis and staging of pancreatic cancer

1.7.1 Background

Worldwide, pancreatic cancer ranks 13th in incidence, yet it is the 8th of commonest cause of cancer death. Over 90% of pancreatic tumours are ductal adenocarcinoma and another 2-5% constitute neuroendocrine and acinar tumours. In the UK, pancreatic adenocarcinoma has an incidence of 9 per 100,000 population. Although pancreatic cancer rates have declined by 17% over the last 3 decades, in women its incidence has remained fairly static, representing the 8th commonest cancer in women. Surgery remains the only potential for long term survival. However, less than 20% of the patients are candidates for a curative resection as the majority present with advanced disease (Li et al. 2004). As early detection of pancreatic cancer is associated with a better outcome, imaging studies that can detect small isolated lesions would be of immense value. Accurate diagnosis and staging allows appropriate clinical decision making and ensures that surgery is performed in patients who benefit most from it. Despite recent advances in the management of pancreatic cancer, its overall 5 year survival rate has remained at around 0.4-4% (Jemal et al. 2003). This perhaps highlights the limitations of our current diagnostic and staging techniques.

1.7.2 Clinical Features of pancreatic cancer

Symptoms of pancreatic malignancy are often non-specific and tend to be ignored by both the patient and the doctor. For this reason patients commonly present with late stage disease. As the disease progresses, the patient develops painless jaundice and an associated weight loss. In over 80 % of patients abdominal pain is a late presenting symptom, which is commonly epigastric and diffuse in nature and thought to occur as

the result of involvement of celiac and superior mesenteric plexus (DiMagno 1999).

Another cardinal symptom is referred pain to the back, which is indicative of retroperitoneal involvement.

Painless jaundice is the principal clinical feature that prompts further investigation.

Physical signs of pancreatic cancer, which often indicate advanced and inoperable disease, may include:

- Presence of an abdominal mass
- Palpable gall bladder (Courvosier's sign)
- Supraclavicular lymphadenopathy (Verchow's node),
- Splenomegaly (as a result of portal or splenic vein obstruction)
- Ascites or Peripheral oedema (due to portal vein involvement or obstruction)

1.7.3 Routine management algorithm of patients with suspected pancreatic cancer

Figure 1.8 summarises the current routine management algorithm for patients in whom pancreatic cancer is suspected. Some of these steps are outlined in more detail in the sections that follow.

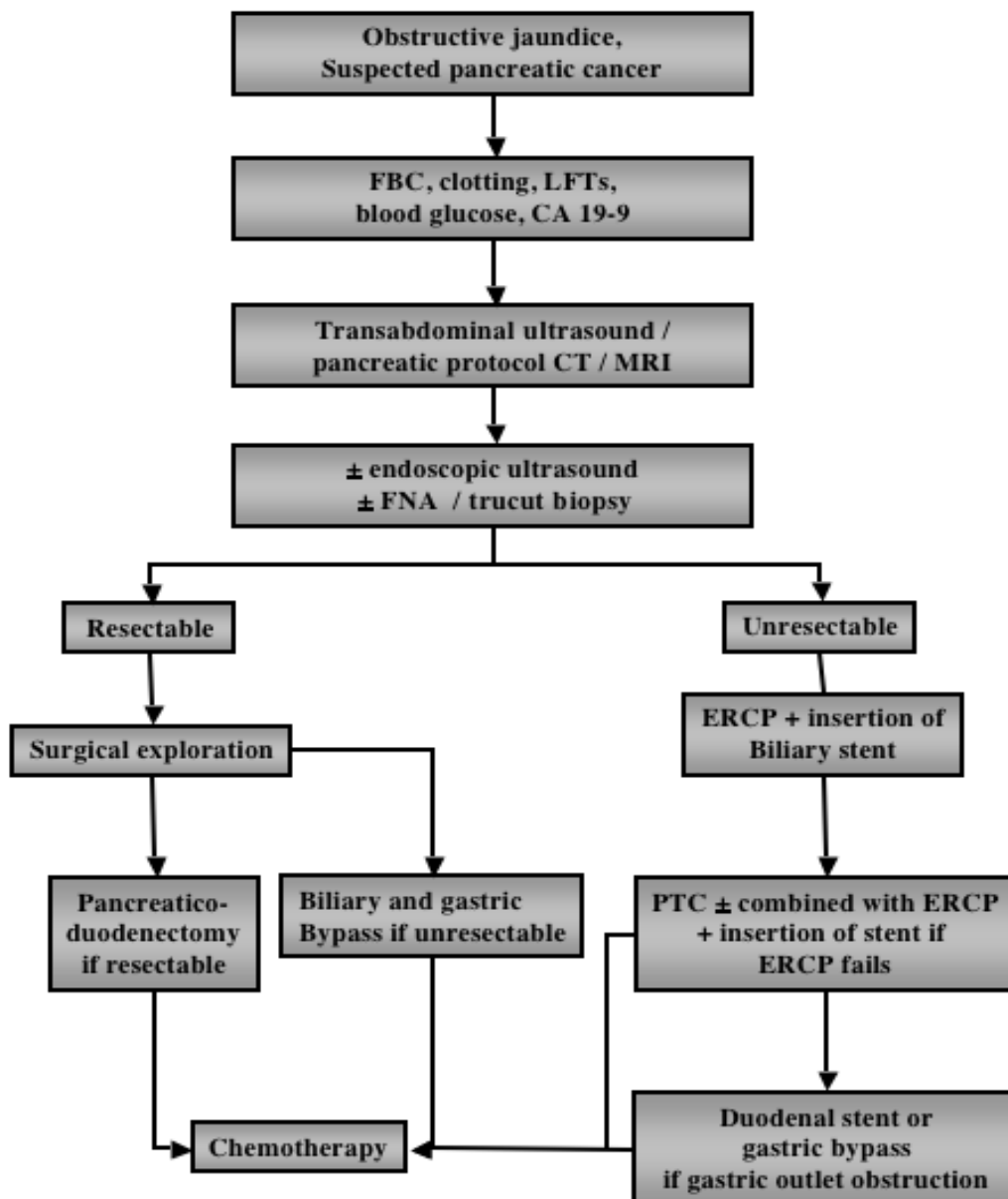


Figure 1.8: The management algorithm of suspected pancreatic cancer (Takhar et al. (2004)).

1.7.3.1 Basic investigations

Haematological and biochemical parameters

Laboratory findings in patients with pancreatic cancer are non-specific. Anaemia and hypoproteinaemia reflect the chronic nature of the condition. Global derangement of liver enzymes is also seen in patients presenting with obstructive jaundice. It has however been suggested that a disproportionately high increase in transaminase may be associated with extensive liver metastases.

Prolonged biliary obstruction also leads to malabsorption of fat-soluble vitamin K and subsequent reduction of vitamin K dependant clotting factor by the liver. Assessment of clotting function is therefore imperative. Pancreatic atrophy also results from prolonged obstruction of the pancreatic duct by the tumour. Frank diabetes or impaired glucose tolerance have has been reported in up to 70% of patients (Saruc and Pour 2003).

Serological markers

Carbohydrate antigen 19-9 (CA 19-9) is the most commonly used serological marker in pancreatic cancer. In detecting pancreatic cancer, CA 19-9 has a sensitivity of about 80% (35;36). Its specificity is also high (60-70%), although raised levels can be detected in other gastrointestinal malignancies as well as benign conditions such pancreatitis (Willett et al. 1996; Yeo et al. 2002; Ozkan et al. 2003). For this reason, CA 19-9 has not been accepted as an independent test for diagnostic purposes. It is however of use as a prognostic tool, in detecting recurrences following surgery and for monitoring response to chemotherapy.

1.7.3.2 Conventional imaging of the pancreas

Ultrasonography (USS)

Transabdominal ultrasound is often the first line screening investigation in patients presenting with jaundice. It can provide information about the size and site of a tumour, diameter of the biliary tree and the site of obstruction. It can also give an accurate assessment of the liver for metastases, where its detection accuracy has been reported to be comparable to CT (Minniti et al. 2003). Use of Doppler ultrasonography can also provide a reasonable indication of vascular patency and vessel infiltration by the tumour and therefore give some indication of local resectability (Clarke et al. 2003). USS however has several limitations. It is operator dependable and its accuracy is significantly affected by the patient's body habitus, presence of ascites or interposed gas filled loops of bowel. Furthermore, its accuracy in correctly identifying pancreatic cancer has been shown to be variable and can range from 57 to 81% (Haycox et al. 1998).

Recently, novel techniques such as echo enhanced Doppler sonography (Rickes et al. 2002) and coded phase inversion harmonic ultrasonography have shown promise (Kitano et al. 2004).. Sensitivity of 95% has been reported in detecting pancreatic tumours of less than 2 cm with the latter. These techniques are not yet routinely available and require further validation.

Contrast enhanced computed tomography (ceCT)

The current modality of choice for diagnosis and staging of pancreatic cancer is fine slice (1-3 mm), contrast enhanced dual phased multidetector CT (ceCT). ceCT provides superior definition than USS and gives accurate assessment of local

infiltration. Current CT criteria for unresectability include the presence of distant metastases (to the liver, lungs or the peritoneum), involvement of adjacent organs such as the stomach or the colon and encasement or occlusion of peri-pancreatic vasculature (Smith and Rajan 2004). With these criteria, CT has been demonstrated to be almost 100% accurate in predicting non-resectability (Fuhrman et al. 1994). However, the positive predictive value of CT for detecting resectable disease is low, so much so that up to 50% of patients deemed to have an operable tumour on CT are found to have inoperable disease at laparotomy (Rickes et al. 2002). Other limitations of CT lie in detection characterisation of small (<2cm) lesions, detection of sub-centimetre liver metastases, accurate differentiation of a malignant lesion from mass forming chronic pancreatitis and finally, the assessment of cystic tumours. The advantage conferred by newer generation multidetector CT scanners is the ability to perform high resolution multiplanar reconstructions of manipulated that can further enhance the accuracy of visualising local anatomy (Smith and Rajan 2004).

Magnetic Resonance Imaging (MRI)

Over the recent years, MRI has been increasingly used for imaging pancreatic tumours. In particular, magnetic resonance cholangiopancreatography (MRCP) has been shown to be able to demonstrate the anatomy of the biliary tree better than CT. It has also been shown to be as sensitive as Endoscopic Retrograde cholangiopancreatography (ERCP) in detecting pancreatic cancer (Adamek et al. 2000). Gadolinium enhancement can also be of value. However, with the advent and success of MDCT, its use in routine practice remains questionable (Hanbidge 2002).

Endoscopic retrograde cholangiopancreatography (ERCP)

ERCP has superseded percutaneous transhepatic cholangiography (PTC) as the modality of choice for imaging the biliary tract. Its advantage over PTC is that it avoids puncturing the liver with its associated risk of bile leak and haemorrhage. It also allows visualization of adjacent organs such as the stomach and duodenum and the ampulla.

Pre-operative duct delineation is usually necessary to verify the exact position of the obstruction and to exclude obstruction at multiple levels, all of which can be accurately performed with ERCP (Conio et al. 2001). When used appropriately, it can lead to a definite diagnosis and can be of additional value in detecting small (<2cm) lesions (Graham et al. 1994).

A principal advantage of ERCP over other imaging techniques is that it confers therapeutic as well diagnostic advantage. Brushings / biopsy specimen can be obtained and stent insertion can be performed, all at the same time.

The main complication resulting from ERCP is acute pancreatitis, which has been reported to occur with a median incidence of 8.7% (range 1.6 – 17.7) (Mariani 2003). While the condition often has a mild natural history following ERCP, severer forms of pancreatitis have been reported (Fung et al. 1997).

Endoscopic ultrasonography (EUS)

This relatively new procedure involves the use of a high frequency ultrasound that has been modified for use endoscopically. By placing the probe in the stomach or duodenum, in close proximity to the pancreas, the whole organ can be visualized.

When compared to CT, EUS has been shown to have a superior sensitivity and specificity, particularly in evaluating tumours <3cm in diameter (Mertz et al. 2000). It is also a highly accurate way of determining local vascular invasion and peri-pancreatic lymph node involvement, although the results in this respect are similar to ceCT.

EUS is set to play a much larger role in the management of pancreatic cancer. However at present, the cost of the equipment and lack of trained endoscopists is limiting its widespread use in the UK.

1.7.3.3 Staging categories of pancreatic cancer

Following the establishment of diagnosis, determining the stage of a pancreatic cancer becomes the most important factor in deciding which treatment pathway is followed. Currently contrast enhanced pancreatic protocol CT is the first line investigation of choice in the staging of pancreatic cancer, while other modalities are used as an adjunct. The universally used staging system for pancreatic cancer is the American Joint Committee on Cancer (AJCC) TNM staging system. Table 1.3 summarises the TNM staging and its equivalent grouping system for pancreatic cancer.

A

Tumour (T)	Description
TX	Primary tumour cannot be assessed
T0	No evidence of primary tumour
Tis	Carcinoma in-situ
T1	Tumour limited to pancreas <2cm in size in any direction
T2	Tumour limited to pancreas >2cm in any direction
T3	Any size tumour, extension beyond the pancreas (duodenum, bile duct) but not coeliac axis or superior mesenteric artery
T4	Tumour involving coeliac axis or superior mesenteric arteries
Regional Lymph nodes (N)	
NX	Regional lymph nodes cannot be assessed
N0	No regional lymph node metastases
N1	Regional lymph node metastases
Distant metastases (M)	
MX	Distant metastases cannot be assessed
M0	No distant metastases
M1	Distant metastases

B

Stage group	Description	Equivalent TNM stage
Stage 0	Carcinoma in-situ	Tis, N0, M0
Stage IA	Tumour confined to pancreas, <2cm, no nodal spread	T1, N0, M0
Stage IB	Tumour confined to pancreas, >2cm, no nodal spread	T2, N0, M0
Stage IIA	Tumour extending beyond pancreas but not into local vessels	T3, N0, M0
Stage IIB	Tumour confined to pancreas or local extension, local lymph node spread	T1-3, N1, M0
Stage III	Local spread beyond pancreas into vessels, +/- nodal spread, no distant spread	T4, Any N, M0
Stage IV	Spread to distant sites	Any T, Any N, M1

Table 1.3: Tabulated summary of (A) the TNM staging system and (B) the stage grouping of pancreatic cancer

1.7.4 18F-FDG PET in diagnosis of primary pancreatic cancer

Anatomical imaging modalities outlined in previous sections, have formed the corner stone of diagnosis and staging of pancreatic cancer. However, many challenges still remain. These in particular include the definitive diagnosis of small tumours and differentiating malignant from benign inflammatory lesions (eg: due to mass forming chronic pancreatitis or secondary to post-treatment fibrosis). The emergence of PET technology has therefore set out to address some of these limitations.

Much of the present evidence supporting the use of PET in pancreatic cancer has been with the use of the tracer 18F-FDG. As normal pancreas has low glucose utilisation, foci of abnormal 18F-FDG uptake can be easily visualised as focal areas of increased tracer activity (Berberat et al. 1999). Suggestions that 18F-FDG would be of value in the diagnosis of malignant pancreatic lesions, have come from early studies that showed quantitative and selective over-expression of GLUT-1 transporters in pancreatic cancer specimens compared to benign tissue (Higashi et al. 1997; Reske et al. 1997). Since then, a number of studies evaluated the clinical role of 18F-FDG PET in primary pancreatic disease. Zimny et al. (1997) examined the accuracy of 18F-FDG PET in determining the diagnosis in 106 suspicious pancreatic masses. In their series, 70% were histologically confirmed to be adenocarcinoma and 30% to be due to chronic pancreatitis. Overall, 18F-FDG PET accurately detected 63/74 of cases with malignancy and 27/32 cases of benign disease, giving it an overall sensitivity and specificity of 85% and 84% respectively.

Compared to conventional imaging, 18F-FDG PET has been shown to be more accurate in making the initial diagnosis of pancreatic cancer. Inokuma et al. (1995) compared 18F-FDG PET with CT, transabdominal US and EUS in 35 patients with

proven carcinoma. While 18F-FDG PET correctly identified 33 (94%) patients with cancer, CT, US and EUS identified 31 (89%), 31 (89%) and 28 (80%) respectively. In another study that compared 18F-FDG PET with CT and MR, the sensitivity of ¹⁸F-FDG PET was found to be lower than CT but better than MR. The specificity of PET however, was superior to both (Koyama et al. 2001).

A major limitation of morphological imaging techniques is their inability to confidently characterise small and cystic lesions. The presence of focal 18F-FDG activity irrespective of lesion morphology therefore provides a significant advantage. One study has suggested 18F-FDG PET to be superior to CT in detecting small lesions less than 2cm in size (Rose et al. 1999). Here, PET's sensitivity was shown to be almost 100% compared to 18% for CT. This finding however, was in a relatively small patient group (n=14) and requires further validation, particularly in the light of recent advances in fine slice CT technology.

More recently, Sperti et al. (2005) examined the usefulness of 18F-FDG PET in differentiating malignant from benign pancreatic cysts. In 50 prospectively recruited patients, 18F-FDG PET was more accurate in detecting a malignant cyst (94% for 18F-FDG PET versus 80% for CT). The limitation of this study was the fact that it represented a small and heterogenous group of malignant cystic lesions. Therefore drawing conclusions regarding 18F-FDG PET's diagnostic accuracy should be done with care. However, the significant finding was that 31 out of 33 (94%) benign lesions demonstrated no 18F-FDG uptake was demonstrated and thus the diagnosis of benign disease was correctly made. This has significant implications for the use of 18F-FDG PET in assessing asymptomatic, high-risk patients.

One of the key strengths of imaging with PET is its quantitative nature, which may be used to further bolster its diagnostic accuracy. Several authors have described tracer semi-quantification with Standardized Uptake Values (SUVs) to improve qualitative assessment of PET detected lesions. Time dependant changes in tracer uptake also have been shown to improve 18F-FDG PET's specificity. Nakamoto et al. (2000) showed that at 2 and 3 hours post-tracer injection, malignant lesions showed a higher 18F-FDG retention index than benign lesions. Combining the tracer retention index with tumour SUV measurements at 2 hours post-injection, improved PET's diagnostic accuracy from 83% to 92%. This interesting finding was demonstrated in one study of 47 patients and thus merits further investigation. Furthermore, the limitation of any quantitative approach in making the correct diagnosis is in defining a precise cut-off value for tracer uptake parameters. Since benign and malignant lesions in the pancreas can exhibit a wide range of tracer uptake, quantitative image analysis is yet to be proven to be absolute. As for this, the routine practice of image interpretation with PET has leant towards qualitative (visual) assessment, where patterns tracer uptake (eg: focal vs diffuse) can be incorporated.

Overall there is considerable evidence to support the usefulness of 18F-FDG PET in imaging the pancreas. A review of published data produced by Gambhir et al. (2001) found that in 387 patient's studied, the overall sensitivity and specificity for 18F-FDG PET was 94% and 90%, as compared to 82% and 75% for CT.

1.7.6 Staging of pancreatic carcinoma with 18F-FDG PET

Local (T) staging

Poor spatial resolution of 18F-FDG PET limits the local (T) staging of pancreatic cancer. Therefore, anatomical imaging modalities particularly with ceCT and EUS, are better suited to demonstrate the relationship between the tumour, adjacent organs and vascular structures. At present there is no data to support the usefulness of dual modality PET/CT in local (T) staging.

Locoregional lymph node (N) staging

In nodal (N) staging of disease, both 18F-FDG PET and ceCT perform poorly. Reported sensitivities and specificities for 18F-FDG PET have varied between 46-71% and 63-100% respectively (Bares et al. 1994; Bares et al. 1996; Diederichs et al. 2000). One possible reason for the apparent low sensitivity of 18F-FDG PET is the close proximity of the peri-pancreatic lymph node basin and the primary tumour, which can obscure and thus hinder detection (Bares et al. 1994; Bares et al. 1996).

Locoregional lymphadenopathy is commonly encountered following biliary instrumentation (ERCP, stent insertion) or following a bout of acute or chronic pancreatitis. However, it must be noted also that in majority of patients with radiological evidence of lymph node disease, the presence of an inoperable tumour ethically prevents extensive sampling of positive nodes. Therefore, the true accuracy of 18F-FDG PET in detecting lymph node disease cannot be reported accurately. Therefore given the non-specific nature of 18F-FDG, histological confirmation of PET positive lymph nodes is essential.

Staging of distant disease (M stage)

The major impact of 18F-FDG PET on staging, is its ability to identify distant metastases (M stage). The liver is the commonest organ to be affected followed by the lungs and the bone marrow. Direct spread into the peritoneum commonly occurs and is often missed on conventional anatomical imaging. Diederichs et al. (2000) showed that in 89 patients with pancreatic malignancy, the sensitivity and specificity of 18F-FDG PET for detecting hepatic metastases to be 70% and 95%, missing one sub-centimetre liver lesion. 18F-FDG PET also detected occult peritoneal metastases in 25% of the cases, once again missing poorly localized and microscopic spread. In a similar study, Frohlich et al. (1999) who looked at the detection of liver metastases with 18F-FDG PET in 168 pre-operative patients, also found 18F-FDG PET to have an overall sensitivity of 68%. In fact, dichotomizing the data into groups with hepatic lesions less than or greater than 1cm, showed PET's sensitivity to be 43% and 97% respectively. In their series overall specificity was high (95%), but significant intrahepatic cholestasis was a cause of false positives.

Table 1.4 summarises some of the published series of 18F-FDG PET in diagnosis and staging of pancreatic cancer.

Author	Year	End-point of study	No. of patients	No of lesions	Sens		Spec		Acc	
					PET	CT	PET	CT	PET	CT
Imdhal et al.	1992	Diagnosis primary disease	48	-	96	81	100	89	-	-
Friess et al.	1995	Diagnosis primary disease	80	-	94	79	88	69	91	74
Inokuma et al.	1995	Diagnosis primary disease	46	-	94	89	82	73	91	85
Stollfuss et al.	1995	Diagnosis primary disease	73	-	95	-	90	-	93	-
				-						
Zimney et al.	1997	Overall diagnosis & staging	106	-	85	-	84	-	85	-
		Lymphnode involvement	26	-	-	-	-	-	46	-
		Metastases	31	-	-	-	-	-	52	-
Delbeke et al.	1999	Diagnosis & staging	65	-	92	65	85	61	91	65
Rose et al.	1999	Diagnosis primary disease	34	-	92	-	91	-	91	-
Nakamoto et al.	1999	Diagnosis 1° lesion & liver mets	NA	51	90	69	91	100	90	82
Frohlich et al.	1999	Staging liver disease	168		68		95		91	
		>1 cm liver lesion		29	97	-	-	-	-	-
		<1 cm liver lesion		37	43	-	-	-	-	-
Martin et al.	2000	Diagnosis and staging	49	-	77	-	74	-	-	-

Table 1.4 Summary of studies comparing the detection accuracy of 18F-FDG PET and conventional imaging with CT in diagnosing and staging of pancreatic cancer

1.7.7 The prognostic significance of 18F-FDG uptake in pancreatic cancer

There are indications that current methods of tumour staging (TNM) for pancreatic cancer are inadequate. For example when compared to other more common cancers, node negative pancreatic cancer still carries a poor outcome. This may be due to the fact that patients are understaged histopathologically or that our current clinical and radiological methods are incomplete. As a result, a number of other factors have been assessed as potential predictors of survival in pancreatic cancer, some of which include; tumour stage and grade (Lim et al. 2003), R0 resection (Wittekind et al. 2002; Lim et al. 2003), levels of the tumour marker CA19-9 (Sperti et al. 1993) and more recently, the detection of circulating tumour cells (Vogel et al. 2002). The ultimate aim is to be able to stratify patients into groups that would most benefit from neoadjuvant and adjuvant treatments.

In addition to its role in staging, quantifying the metabolic activity of the tumour with PET may have significant clinical implications. Nakata et al. (2001) compared the survival of patients with high and low 18F-FDG SUV levels in 14 patients with pancreatic cancer. Using an SUV threshold of 3 (corresponding to the mean 18F-FDG SUV level in the series) they found that mean survival period for those with SUV>3.0 was 5 months, compared to 14 months for those with an SUV of <3.0. In a similar study with a larger patient numbers (N=60), a high SUV (>4.0) was again associated with a shorter survival, with only 7% (2/29) surviving beyond 12 months compared with 32% (10/31) with SUV <4.0 (Sperti et al. 2003). Also, in the subgroup of cancers that were resected, low and high SUV values were associated with mean survival figures of 386 and 224 days respectively. Multivariate analysis revealed that tumour stage and SUV were the only two significant independent predictors of

survival, when compared to factors such as age, tumours grade or type of treatment received.

One small study by Maisey et al. (2000) (n=11) investigated the role of tumour SUVs in predicting survival from 5-fluorouracil (5-FU) based chemotherapy. At 1 month post-treatment, 6 out of 11 patients showed no detectable 18F-FDG activity in the tumour and demonstrated better overall survival. In 4 of the 6 responders, a correlation with symptomatic improvement also was seen.

Measuring proliferation of a tumour is also another potential prognostic indicator. There may be a potential for alternative tracers such as 11C-thymidine or the thymidine analogue 3'-deoxy-3'-[18F]-fluorothymidine (18F-FLT) in prognosticating pancreatic cancer, but at present no published series are available.

1.7.7 18F-FDG PET in detection of recurrent pancreatic cancer

Serial measures of tumour marker levels (CA 19-9) are a sensitive indicator of disease recurrence. However, differentiating recurrent disease from post surgical / radiotherapy changes with CT or MRI is difficult. Molecular imaging on the other hand can detect focal tracer accumulation regardless of morphology. To date few studies have examined the use of 18F-FDG PET in detecting disease recurrence. In their study of suspected pancreatic cancer, Rose et al. (1999) examined 8 patients with rising tumour marker levels and indeterminate ceCT findings. 18F-FDG PET correctly identified recurrent disease in all, with 4 occurring in the surgical bed and 4 as new liver metastases. More recently, Ruf et al. (2005) showed that in 31 patients with suspected recurrent disease, 96% of local recurrences were detected with 18F-

FDG as compared to 23% with CT or MRI In detecting metastatic disease in the liver, CT and MRI was more sensitive, particularly in identifying small lesions. However, 18F-FDG PET additionally helped to detect additional occult disease in non-regional and extra-abdominal sites, thus resulting to a change in management.

There are therefore indications that 18F-FDG PET may be useful in differentiating fibrosis from recurrent disease, in whole body re-staging of the patient and in identifying the focus of recurrence, where there is a rise in tumour marker levels in the face of a negative or equivocal finding by conventional imaging.

1.7.8 The pitfalls of imaging pancreatic disease with 18F-FDG PET

In imaging pancreatic disease with 18F-FDG PET, serum glucose levels are an important consideration, especially when pancreatic insufficiency and diabetes are commonly found in this cohort of patients. High serum glucose levels are believed to compete with 18F-FDG for glucose transporters sites and thus reduce the sensitivity of detecting malignant lesions. In 106 patients with suspected pancreatic carcinoma, Zimny et al. (1997) found that 10 out of 11 false negative 18F-FDG PET results occurred in hyperglycemic patients, thus resulting in a sensitivity of 98% in euglycemic patients as compared to 63% in hyperglycaemic patients.

Lesion size also poses a further challenge. The sensitivity of 18F-FDG PET in detecting sub-centimetre lesions can be low. This problem is not exclusive to that of pancreatic pathology and represents the partial volume effect on a signal from a small lesion. This problem has been partly addressed with the advent of dual modality

PET/CT and density attenuation correction. Future developments in PET detector technology are also set to increase the spatial resolution of PET.

Several benign clinical conditions may also result in focal ¹⁸F-FDG accumulation and thus result in false positive findings. ¹⁸F-FDG despite its exquisite sensitivity is not tumour specific and uptake by inflammatory tissue is often encountered. Although ¹⁸F-FDG PET has been shown to be better than anatomical imaging in differentiating benign from malignant lesions, focal accumulation in areas of active pancreatitis can commonly be seen. In the face of elevated CRP levels, specificity of ¹⁸F-FDG PET has been reported to be as low as 50% (Shreve 1998). It is therefore recommended that CRP levels are routinely checked prior imaging the pancreas with PET. Non-specific ¹⁸F-FDG uptake is also seen following biliary instrumentation (eg: stenting), following haemorrhage into a pancreatic pseudocyst and secondary to portal vein thrombosis or retroperitoneal fibrosis. This is once again another area that PET/CT fusion is set to impact, where the addition of anatomical data can improve the accuracy and certainty of image interpretation.

1.7.9 Pancreatic cancer and image fusion with PET/CT

To date, only two studies have examined the role of PET and CT image fusion in pancreatic cancer. In a study by Lemke et al. (2004), digital image fusion of CT and ¹⁸F-FDG PET was carried out in a prospective series of 104 suspected pancreatic lesions. They showed that image fusion improved the sensitivity of both imaging modalities (CT: 76.%; PET: 84.4% and fused: 89.1%). Sensitivity of detecting infiltration of adjacent tissues also improved over that of CT alone, however this occurred at the expense of reduced specificity. This is a particularly undesirable

situation as over staging the disease can deny a patient a potentially curative resection. Image fusion also resulted in a slight (but statistically insignificant) improvement in sensitivity for detecting lymph node metastases (Sensitivities: PET =25.8%, CT=25.8% and PET/CT fused =32.3%), but the specificities remained unchanged (75%).

More recently, Heinrich et al. (2005) investigated the role and cost-effectiveness of imaging with integrated PET/CT scanners on the management of 59 patients with potentially resectable pancreatic cancer . The important point of note in this study was that PET/CT was acquired with a low dose, unenhanced CT scan according to current routine protocols. Overall, the capability of 18F-FDG PET/CT in detecting pancreatic cancer was found to be in keeping with other studies that used PET in isolation. Furthermore, 5 patients (16%) were found to have CT occult metastases which resulted in avoidance of futile surgery and subsequent cost saving. In fact PET/CT was shown to be cost effective despite patients requiring other investigations (eg: EUS/CT guided biopsies, staging laparoscopy) to confirm the nature of PET detected lesions.

The major challenge of managing pancreatic cancer is its late presentation. Currently there are no established screening programs that would identify the disease early and at present, there is no justification for using 18F-FDG PET as a population wide screening tool. Although a number of above mentioned studies suggest 18F-FDG PET to be of value in earlier diagnosis of pancreatic cancer, these need to be interpreted within the context of the natural history of the disease. In the majority of cases, initiation of investigations occurs following development of clinical signs and

symptoms that may indicate advanced disease. Therefore, by the time the patient undergoes some form of imaging, there is an 80% chance that the disease has become unresectable. It therefore becomes clear that at present, the true impact of 18F-FDG or PET/CT on management appears to occur at initial diagnosis and staging and not as a screening tool.

As compared to CT, a review of published data by Gambhir et al. (2001) suggested PET to result in a change in management of between 36% to 50%. The strength of biological imaging lies in its ability to detect pathology, irrespective of lesion morphology. This property allows 18F-FDG PET to detect small or cystic lesions and to differentiate between benign from malignant disease. In this setting, 18F-FDG PET can alter management by providing a more accurate diagnosis.

1.8 The role of PET in diagnosis and staging of colorectal cancer

1.8.1 Background

Worldwide, an estimated 1 million cases of colorectal cancer (CRC) were diagnosed in 2002. This accounts for more than 9% of all newly diagnosed cancers. In the UK in 2005, there were 36,766 new cases of colorectal cancer registered, two thirds occurring in the colon and remaining one third in the rectum. Over 80% of cases occur in patients over the age of 60 years with it being more common in males than in females (Statistics 2005). Up to 45% of patients with CRC can present with advanced disease (Dukes stages C and D) at initial diagnosis. Of those with earlier disease who receive a curative resection, some 30-40% still go on to develop a local recurrence or metastatic disease (Sugarbaker 1990). Therefore early diagnosis and accurate staging represents the principal determinant of successful management of CRC.

The gold standard in diagnosing primary colorectal cancer is endoscopy. This is followed by computed tomography (CT), which is routinely used for staging, surveillance for metastases and detection of recurrent disease. Other conventional imaging tools such as Ultrasound, Magnetic Resonance Imaging (MRI) and more recently, CT pneumocolonography are routinely applied according to institutional preferences and availability. Overall however, the indications are that conventional imaging modalities seem to play a sub-optimal role in the management of colorectal cancer and hence much attention has been focused on molecular imaging techniques such as Positron Emission Tomography.

PET offers the clinician both an alternative and complementary means of assessing the gastrointestinal tract. While ¹⁸F-FDG has represented the most successful and

widely used PET radiopharmaceutical in oncology, molecular profiling with alternative tracers and the advent of dual modality PET/CT are all re-shaping the way we manage colorectal cancer.

1.8.2 Detection of pre-malignant colonic lesions with PET

Adenomatous polyps are benign neoplasms of colonic mucosa. Amongst asymptomatic patients of average risk, its prevalence is approximately 10% from sigmoidoscopy and 25% from colonoscopy series (Giacosa et al. 2004). World wide however, this figure varies between different countries. Colonic adenomas are well established as precursors of CRC (Fearon and Vogelstein 1990), where the prevalence in these patients is approximately 1%. Barium enema and colonoscopy represent the gold standard of detecting these lesions, the later offering therapeutic as well as diagnostic benefit. More recently CT pneumocolonography has also emerged as an alternative and accurate way of detecting polyps in patients unsuitable for colonoscopy.

Adenomatous polyps exhibit an enhanced glycolytic activity and therefore the incidental detection of polyposis has been frequently reported with 18F-FDG PET (Tatlidil et al. 2002). In a retrospective study by Yasuda et al. (2000), 18F-FDG PET was shown to have a true positive rate of only 24%. This figure did rise to 90%, particularly in polyps greater than 13mm in size suggesting that smaller polyps (<1cm) may not be accumulating enough 18F-FDG to be detected at the resolution limit of PET. Although PET/CT may help in localization of intra-luminal lesions, the size and 18F-FDG avidity of the polyp would remain a limiting factor.

Overall, while 18F-FDG PET or PET/CT are not indicated for routine detection of colonic polyps, focal 18F-FDG accumulation in the colon should be further investigated.

1.8.3 Screening colorectal cancer with PET

To date, the use of 18F-FDG PET in screening for CRC has been reported by one study of 3600 patients (Yasuda et al. 2000). Here, the prevalence of CRC was 2.1% and 18F-FDG PET had a true positive and false negative rate of 54% and 46% respectively. These figures coupled with the cost, availability and radiation exposure risk of 18F-FDG do not justify the routine use of 18F-FDG PET or PET/CT for screening purposes.

1.8.4 Role of 18F-FDG PET in the diagnosis of primary colorectal cancer

The role of 18F-FDG PET in routine preoperative diagnosis of primary CRC has only been reported in small patient numbers. Abdel-Nabi et al. (1998) reported 18F-FDG PET to have a sensitivity and specificity of 100 and 48% (n=48). Similarly Mukai et al. (2000) reported a true positive rate of 98.5% (n=24). False positives often arise due to focal areas of 18F-FDG accumulation in for example diverticulitis or adenomatous polyps. Where physiological tracer uptake in the bowel is encountered, lack of anatomical localization with PET can also lead to diagnostic uncertainty. This has been addressed with PET/CT and although its clinical impact in primary CRC has not yet been conclusively evaluated, early results have shown that PET/CT can improve the certainty of lesion characterisation by 30% and the accuracy of staging by 11% (Cohade et al. 2003a).

Conventional anatomical imaging modalities remain the cornerstone for staging CRC. Local (T-staging) of the tumour cannot be reliably carried out with PET due to its limited resolution and the effect of partial volume averaging of the 18F-FDG signal. Although at present PET/CT imaging protocols limit the diagnostic capability of its CT component, future developments may allow PET/CT to confer advantages over CT or MRI imaging alone.

In terms of lymph node staging (N stage), the sensitivity of 18F-FDG PET has been shown to be similar to that of CT and overall poor (sensitivity of 22-29%) (Abdel-Nabi et al. 1998; Mukai et al. 2000). As the presence of lymph node metastases on CT are detected according to size criteria, image fusion with PET/CT can help further confirm the presence of disease, even in non-enlarged lymph nodes. A pitfall of this however is false positive results where 18F-FDG may accumulate in reactive lymph nodes.

In pre-operative staging, 18F-FDG PET has performed best in detecting hepatic and extra-abdominal metastases. Sensitivities and specificities of 88-91% and 91-100% have been reported, as compared to 38% and 97% for CT (Abdel-Nabi et al. 1998; Kantorova et al. 2003). This can lead to a change in treatment modality and the extent of surgery (Kantorova et al. 2003).

Overall, the indications are that 18F-FDG PET or PET/CT play a limited role in the routine diagnosis and staging of primary CRC. However, in high-risk patients, its accuracy in detecting extra-colonic disease may result in avoidance of futile surgery.

1.8.5 Detecting recurrent and metastatic disease

1.8.5.1 Locoregional recurrence

After apparent curative resection of the primary tumour, the recurrence rate for colorectal cancer is between 30 to 40%, the majority of which occur within the first 3 years after surgery (Scheele et al. 1990; Sugarbaker 1990). Of these, approximately 25% are isolated loco-regional recurrences, which may be amenable to resection. In order to minimize unnecessary morbidity and mortality from surgical treatment, accurately identifying the extent of recurrent disease is vital for appropriate patient selection.

In detecting and staging recurrent disease, ¹⁸F-FDG PET has been shown by several groups to be superior to conventional imaging with CT. Table 1.5 summarises some the results from such studies.

Author	Year	End-point of study	No. of patients	Sens		Spec		Acc		Change in management
				PET	CT	PET	CT	PET	CT	
Schipers et al.	1995	Staging local recurrence or metastases	48	94	85	100	-	98	93	-
Lai et al.	1996	Staging liver metastases	80	100	100	57	15	91	82	-
Vitola et al.	1996	Staging liver metastases	46	90	86	100	58	93	76	-
Delbeke et al.	1997	Staging metastatic disease	73	91	81	96	60	92	78	-
Abdel-Nabi et al.	1998	Detecting primary disease	48	100	-	43	-	-	-	-
		Staging lymphnode disease	14	29	-	85	-	-	-	-
		Staging liver metastases	48	88	38	100	97	98	85	-
Flamen et al.	1999	Staging local recurrence or metastases	106	98	93	100	95	99	94	6
Fong et al.	1999	Staging liver metastases	26	71	-	-	-	-	-	-
Valk et al.	1999	Staging local recurrence or metastases	31	95	84	100	95	97	90	-
Whitford et al.	2000	Staging recurrence or metastases	65	89	71	98	92	95	85	-
Hung et al.	2001	Staging recurrence or metastases	33	100	78	83	61	-	-	-
Topal et al.	2001	Staging liver metastases	91	99	-	-	-	-	-	11
Rydzewski et al.	2002	Staging liver metastases	47	71	55	78	43	73	53	-
Arulampalam et al.	2004	Staging liver metastases	168	100	47	91	91	-	-	20
Traunt et al.	2005	Staging liver metastases	53	80	79	80	25	79	77	8
Huebner et al.	2000	Meta-analysis (recurrent or metastatic)	393	96	-	99	-	98	-	-
Kinkel et al.	2002	Meta-analysis (staging liver metastases)	423	90	72	>85	>85	-	-	-

Table 1.5 Summary of published studies looking at the role of 18F-FDG PET in recurrent and metastatic colorectal cancer

A particular challenge of anatomical imaging modalities has been in differentiating a post surgical scar from local recurrence. The reported accuracy of 18F-FDG PET in detecting pelvic recurrences is 95% as compared to 65% with CT (Schiepers et al. 1995). In particular, Valk et al. (1999) demonstrated the sensitivity and specificity of 18F-FDG PET to be 93% and 98%, where as for CT it was 69% and 96% respectively. In their study, this lead to significant cost saving through avoidance of futile surgical intervention. Image fusion with PET/CT further adds to the diagnostic accuracy of 18F-FDG PET. It is particularly effective in characterising a pre-sacral mass, with quoted sensitivity of 100% and specificity of 96% (Even-Sapir et al. 2004).

Intensive follow-up after curative resection, with regular imaging (US or CT) and tumour marker levels has been shown to correlate with improved survival (Renehan et al. 2002). Measurement of serum carcinoembryonic antigen (CEA) levels is a simple method that can give a first indication of tumour recurrence in approximately 60%, with a mean sensitivity of 80% (range 17-89%). However, up to 30% of patients have been reported not to express the antigen. One of the areas where 18F-FDG PET plays a significant role is in the assessment of patients with rising CEA levels and negative conventional imaging. Flanagan et al. showed 18F-FDG PET to have positive and negative predictive values of 89% and 100% respectively (Flanagan et al. 1998). Flamen et al. (1999) also reported similar findings, but their false positive rate of 21% was of significance. The question remains as to whether all patients with a rising CEA should receive an 18F-FDG PET scan. A pitfall of this approach is the false positive rate of CEA, which occurs in up to 16% of cases. But on the other hand, routine 18F-FDG PET/CT as a first line imaging, followed by further investigation directed by

PET/CT, is also a valid argument (Wahl 2004; Yap et al. 2004). This paradigm requires a more in depth examination.

1.8.5.2 Metastatic disease

The liver is the commonest site for CRC metastases, which can occur in up to 40% of patients after a curative resection of primary disease. Of these, less than 5% are amenable to surgical resection and a median 5 year survival figure of about 30% (range 12-41%) has been quoted (Stehlin et al. 1988; Schlag et al. 1990; Doci et al. 1991; Fegiz et al. 1991; Yamaguchi et al. 1993; Gayowski et al. 1994; Scheele et al. 1995; Jamison et al. 1997; Rees et al. 1997; Fong et al. 1999a; Liu et al. 2002; Kato et al. 2003). Although solitary liver metastases confer a better prognosis, with more aggressive regimes that include pre-operative (neoadjuvant) chemotherapy, two-stage hepatic resections (Adam et al. 2000), intra-operative radiofrequency ablation (Elias et al. 2005) and selective portal vein embolization (Azoulay et al. 2000; Elias et al. 2002), wider indications for surgery and thus improved survival figures are continually achieved. None the less, the accuracy of pre-operative assessment of hepatic and extra-hepatic tumour burden becomes the main determinant of outcome.

Ultrasonography and ceCT currently represent the first line imaging modalities of choice in the assessment of liver metastases. MRI may represent an alternative to the above particularly in assessing indeterminate lesions found on routine imaging. As compared to CT, 18F-FDG PET has been consistently shown to have a superior sensitivity and specificity in detecting liver metastases. Some of the published results to date are again summarised in table 1,.5. A meta-analysis by Huebner et al. (2000)

gave 18F-FDG PET a weighted average sensitivity of 90.86% (86.2% - 95.62%) and specificity of 96.97% (92.5% -100%) for detecting hepatic colorectal metastases

The principal advantage of 18F-FDG PET is the fact that biological signals of disease can be detected before morphological changes become apparent. This can often result in detection of unsuspected metastases which can occur in 13-36% of cases and clinical impact of 14 to 65% (Adson et al. 1984; Beets et al. 1994; Schiepers et al. 1995; Lai et al. 1996; Ogunbiyi et al. 1997; Ruhlmann et al. 1997; Flanagan et al. 1998; Flamen et al. 1999; Imdahl et al. 2000; Staib et al. 2000; Strasberg et al. 2001).

In whole body imaging, Valk et al. (1999) showed the sensitivity of 18F-FDG PET to be higher than CT at all sites, except for the lungs where the two were equivalent. The difference in detection rates were greatest in the abdomen, pelvis and the retroperitoneum where almost 30% of lesions missed on CT were detected with 18F-FDG PET. Lai et al. (1996) also reported similar findings but their study also suggested 18F-FDG PET to be superior in detecting malignant lung deposits.

A point of note however is that the majority of these studies prospectively analysed the 18F-FDG PET data and compared it to retrospectively reviewed CT results. The CT scans were also carried out using different imaging protocols thus resulting in significant heterogeneity of the data. Therefore, although 18F-FDG PET over all demonstrated an exquisitely high detection rate, its comparison with CT data requires a more careful consideration.

More recently, it has been suggested that pre-operative assessment of patients with liver metastases correlates with improved long term survival. By improving patient selection for surgery, 18F-FDG PET has been reported to result in 5-year survival rates of up to 58% as compared to a median of 30% for conventional imaging (Fernandez et al. 2004). The question remains as to whether 18F-FDG PET and PET/CT should be routinely used in pre-operative assessment of liver metastases. One factor that may be of significance is the “clinical risk score” of the patient (Fong et al. 1999a). A recent study by Schussler-Fiorenza et al. (2004) suggested that patients with a clinical risk score of 0 and an isolated hepatic metastasis should only “undergo conventional imaging before surgical exploration”. This is backed-up by other recent papers that have shown 18F-FDG PET and PET/CT to provide similar information regarding liver metastases as for contrast enhanced multidetector CT. However, detection of unrecognised extrahepatic disease and intrahepatic recurrences following prior liver surgery remains the strengths of 18F-FDG PET and PET/CT imaging (Selzner et al. 2004; Truant et al. 2005).

Clearly, the emerging CT technology is continually narrowing the gap between the capability of CT and that of 18F-FDG PET in detecting colorectal liver metastases. Despite this, in characterising lesions less than 1cm, there is no consensus on the best imaging modality that should be used.

1.8.6 The impact of dual modality imaging with PET/CT on the management of colorectal cancer

The incremental value of 18F-FDG PET/CT over 18F-FDG PET alone has been demonstrated in a retrospective study by Cohade et al. (2003a). In 45 patients, 18F-

FDG PET/CT achieved a 50% reduction in the proportion of equivocal and probable lesions, a 25% improvement in lesion localization and 11% increase in accuracy of staging (from 78% to 89%). Interpretation of the CT component of PET/CT alone was also shown by the same group to provide valuable additional information. Similar results were also reported in a larger series of 204 patients with suspicious malignant lesions, of which 34 patients had a GI malignancy.

More recently, a comparison between whole body 18F-FDG PET/CT and MRI (in a range of solid malignancies including CRC) revealed that overall, PET/CT was superior in all staging categories. However interestingly, MRI was superior to 18F-FDG PET/CT in detecting liver and bone metastases (Antoch et al. 2003). Currently the limitation of PET lies in detecting small (<5mm) liver lesions, where high resolution MRI may perform better.

The impact of accurately diagnosing and staging CRC is clear. As larger prospective series emerge, the true clinical value of dual modality imaging will become more apparent. The area where PET/CT shows real promise is in directing the subsequent investigation and treatment of patients. The superior sensitivity of PET, coupled with anatomical information provided by the CT scan, can for example help increase the yield of image guided biopsies (Yap et al. 2004). With the biological boundaries of the tumour volume in mind, surgeons can also perform more precise resections and radiotherapy planning can also be altered, ultimately providing more of a patient specific treatment (Ciernik et al. 2003).

1.8.7 Therapy response monitoring with PET

Measuring tumour response to treatment based on morphological parameters has been a widely debated subject (RECIST & WHO criteria). For this reason, quantitative imaging of tumour metabolism with ¹⁸F-FDG PET confers important advantages. However, the evidence to date for the use of ¹⁸F-FDG PET in treatment response is small.

1.8.7.1 Response to radiotherapy

It has been shown that a reduction in ¹⁸F-FDG uptake correlates better with palliative benefit of radiotherapy than CEA levels (Haberkorn et al. 1991). Early on after radiation treatment, an increase in ¹⁸F-FDG uptake is seen which is attributed to the local inflammatory response induced. Although, a clear time point has not been demonstrated, presence of activity at 6-8 weeks following radiotherapy is often taken as an evidence of residual disease. In locally advanced rectal cancer treated with chemoradiation, Guillem et al. (2004), demonstrated that a reduction in mean ¹⁸F-FDG SUV's at 4-5 weeks post chemo-irradiation to be a predictor of long term outcome. Furthermore, presence of hypermetabolic foci up to 6 months after radiation therapy of rectal tumours, can be a strong indicator of disease recurrence (Moore et al. 2003).

As previously mentioned, one of the specific advantages of PET/CT is in aiding radiotherapy planning. The addition of metabolic boundaries to anatomical data can lead to significant alteration of Gross Tumour Volumes (GTV) estimations, thus subsequently improving the effectiveness of treatment with potential reduction of unwanted side-effects (Yap et al. 2004).

1.8.7.2 Response to chemotherapy

5-fluorouracil (5-FU) has been the most successful and widely used chemotherapeutic agent in colorectal cancer for over 40 years. However overall response rates to it in advanced disease have been poor. Newer agents such as Oxaliplatin or Irinotecan can have reported response rates of up to 70%, but are also associated with debilitating side effects. The need for appropriate patient selection is therefore clear and hence the ability of PET to potentially detect early biological response is significant.

The evidence to date has been encouraging. Findlay et al. (1996) examined ¹⁸F-FDG uptake parameters in 27 liver metastases (tumour : normal liver ratio (T:L) and SUVs) at 1,2 and 4-5 weeks post treatment with 5-FU. A reduction in T:L ratio of 67% and 99% was observed in responders as compared to non-responders respectively ($p < 0.01$). Use of ¹⁸F labelled fluorouracil (¹⁸F-FU) has also yielded interesting results. Early evidence in human studies demonstrated that responsive tumours were associated with a high ¹⁸F-FU uptake than the non-responders (Moehler et al. 1998).

¹⁸F-FDG PET has also been recently used to determine biological response to novel antibody based agents. An example is Bevacizumab, an anti-VEGF monoclonal antibody recently licensed for use in the treatment of advanced colorectal cancer. A reduction in tumour ¹⁸F-FDG uptake has been shown to correspond with reduction in blood supply as measured using dynamic CT and histopathological findings (Goessl and Grozdanovic 2004).

1.8.7.3 Monitoring local ablative therapy

Local ablative therapy of colorectal liver metastases is an increasingly accepted means of treating liver and lung metastases not amenable to resection. Where liver metastases have been treated by radiofrequency ablation, 18F-FDG PET is more accurate than CT for early recognition of incomplete tumour destruction (Donckier et al. 2003; Barker et al. 2005; Veit et al. 2006).

1.8.8 Limitations of imaging with 18F-FDG PET

One of the key limitations of imaging with 18F-FDG PET is lesion size where lesions less than 1cm may be frequently missed due to partial volume effects. This is particularly important in the liver, as there is currently no single imaging modality of choice for detecting such small metastases. False negative findings also commonly occur in mucinous tumours. This has been attributed to the relatively low cellularity of this tumour type and possibly as a result of the abundant mucin (which is rich in poly-mucosaccharides) competing with 18F-FDG for uptake sites (Berger et al. 2000).

Activated macrophages and inflammatory tissue also have a high uptake of 18F-FDG and this may lead to false positive findings. This is of significance in inflammatory bowel disease or in a mass resulting from diverticulitis. Granulomatous diseases such as sarcoidosis and tuberculosis may also produce false positive results that may result in unnecessary invasive investigations in order to confirm them.

Finally, as normal bowel also demonstrates background 18F-FDG uptake, this can occasionally lead to diagnostic uncertainty. Careful clinical assessment, appreciation of the pattern of uptake and correlation with CT findings with PET/CT can all help avoid false interpretations (Delbeke and Martin 2004).

1.9 Chapter overview and aims of thesis

So far, the principals behind molecular imaging and various modalities that are used have been reviewed. The role of conventional imaging and that of ¹⁸F-FDG PET and PET/CT has also been outlined. As a molecular imaging tool, PET has set the scene from which this discipline continues to expand.

In the following chapters, I examine the role of PET and PET/CT in the management of primary pancreatic cancer and advanced colorectal cancer. In the first instance, the routine use of PET/CT using the glucose analogue tracer ¹⁸F-FDG will be examined. Later chapters examine the potential use of the novel thymidine analogue PET tracer ¹⁸F-FLT, in imaging the above two malignancies. In the penultimate chapter, an *in vitro* model of colorectal cancer is also used to investigate the hypothesis that ¹⁸F-FLT can be use to monitor response to cytotoxics, as a tool in monitoring and potentially predicting chemotherapy response.

CHAPTER 2

Materials and Methods

Chapter foreword

To avoid repetition, this chapter serves to outline the basic methodology used both for imaging with PET/CT using the tracers ¹⁸F-FDG and ¹⁸F-FLT, as well as the imaging protocols used in routine contrast enhanced CT scanning. For each subsequent chapter (chapter 3-6), methodology directly relevant to the individual study protocols is outlined in more detail.

In chapter 7, I used an *in vitro* cell line model of colorectal cancer to examine changes in uptake of ¹⁸F-FLT and ¹⁸F-FDG in response to treatment with 5-fluorouracil (5-FU) and Cisplatin. This chapter is regarded as a stand-alone section and therefore the experimental methodology is described separately.

2.1 Patient recruitment

In chapters 3 and 4, the incremental value of 18F-FDG PET/CT over that of routine contrast enhanced multidetector CT was examined. Here, the data was analysed retrospectively from a prospective database of routine referral for PET/CT imaging. Patients were referred for an 18F-FDG PET/CT scan from the each of the respective pancreatic and colorectal multidisciplinary team (MDT) meetings with suspected advanced cancer. A description of inclusion and exclusion criteria is outlined in each of the relevant chapters.

Studies comparing imaging with 18F-FDG and the novel tracer 18F-FLT PET were performed following approval from the joint Local Ethics Committees of University College London (UCL) and University College London Hospital NHS Trust (UCLH) (appendix A). The relevant approval from the Administration of Radioactive Substances Advisory Committee (ARSAC) was also obtained (appendix B). Patients who took part were recruited prospectively from surgical and oncology outpatient clinics. Studies were performed following full informed consent of the patients (Appendix C)

All patient data sets were stored within a departmental computer using Microsoft ExcelTM software. The data were handled in accordance with the Data Protection Act. None of the investigations pertaining to this thesis hindered the routine investigation or treatment of the patients involved.

2.2 Whole body 18F-FDG-PET/CT scans

2.2.1 18F-FDG

The 18F-FDG used for studies in thesis was obtained from P.E.T Net Pharmaceuticals, which utilizes the cyclotron at Mount Vernon Hospital (UK). Prior to patient administration, a written notification from P.E.T Net Pharmaceuticals was obtained to ensure that the tracer had passed quality control. On delivery, documentation regarding the volume of liquid dispensed into the 18F-FDG vials, the time at which the 18F-FDG was measured prior to dispatch and the total assayed activity of the tracer was provided by the cyclotron unit. The routine practice of tracer handling, dose calibration and dispensing followed departmental Standard Operating Procedures (SOP) detailed in appendix D. Using a dose calibrator and a decay chart a dose of up to 400MBq was prepared for patient injection.

2.2.2 Patient preparation

All patients were asked to starve for at least 6 hours prior to the 18F-FDG PET/CT study to achieve normoglycaemia. A patient information sheet was used to record a brief history of the patient as well as the patient's height (cm) and weight (kg) that was subsequently used for quantitative image analysis using standardised uptake values (SUVs). Blood glucose levels (mmol/l) were checked on a commercial glucometer (Glucometer Elite, Bayer Pharmaceuticals, UK). A glucose level of less than 10 mmol/l was accepted as a cut off value. This was in line with the clinical imaging protocols set out by the Institute of Nuclear Medicine (UCLH, London, UK). The injected dose of tracer and the residual activity left in the syringe post injection were also recorded so an accurate administered dose could be calculated.

Prior to injection, venous access was achieved through a 16-gauge cannula in a forearm vein. Unless contraindicated, 5mg of diazepam was routinely administered to all patients to aid relaxation and to reduce the uptake of 18F-FDG in skeletal muscle. Once injected, and in order to further minimize non-specific tracer uptake, the patient was left undisturbed in the darkened patient preparation room for 45-60 minutes. Immediately prior to scanning, the patients were asked to empty their bladder in order to reduce high intensity signal artefacts from the bladder (18F-FDG is renally excreted).

The patient was positioned on the scanning bed with feet facing away from the gantry and with a pillow placed under the knees for comfort. Ideally, patient's arms were placed above their head, out of the way of the thorax and the abdomen. Where this was not possible due to physical difficulty, the arms were placed on either side and strapping was used to help support the arms and to keep them still.

2.2.3 Acquisition of whole body 18F-FDG PET/CT scans

Whole body 18F-FDG PET imaging was performed in 2D mode using the Discovery LSTM dual modality PET/CT scanner (GE medical systems, Milwaukee, USA). The PET emission datasets were attenuation corrected utilising the CT capability of the Discovery LSTM (Visvikis et al. 2003). Spiral CT scans were acquired using a speed of rotation of 0.8 s, couch movement of 22.5 mm per rotation and a slice thickness of 5 mm. The CT images were subsequently converted to maps of PET attenuation coefficients using a bilinear transformation (Visvikis et al. 2003). Transaxial emission images of $4.3 \times 4.3 \times 4.25 \text{mm}^3$ (matrix size $128 \times 128 \times 35$) were reconstructed using

ordered subsets expectation maximisation (OSEM) with two iterations and 28 subsets. These slices were re-orientated to produce whole body coronal and sagittal images.

2.3 Whole body ^{18}F -FLT PET/CT scans

2.3.1 Radiosynthesis of ^{18}F -FLT

The ^{18}F -FLT used for studies in this thesis was obtained from Hammersmith Imanet (Hammersmith Cyclotron Unit, UK). The method of synthesis was a fully automated nucleophilic fluorination with ^{18}F -fluorine, using the commercially available kit, Tracerlab $\text{FX}_{\text{F-N}}$ (GE Medical Systems) (Figure 2.1). The complex radiochemistry leading up to this method of ^{18}F -FLT synthesis is beyond the scope of this thesis. The routine handling of the tracer again followed departmental SOPs detailed in appendix D.

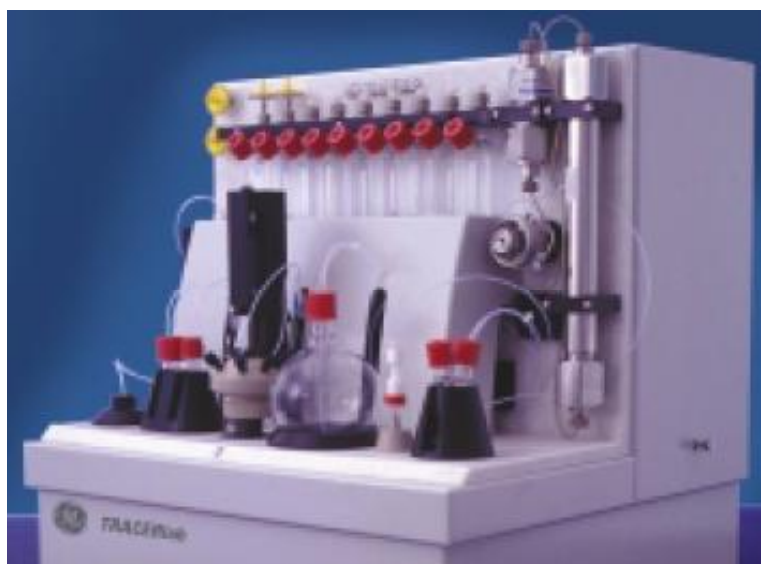


Figure 2.1: Tracerlab $\text{FX}_{\text{F-N}}$ (GE Healthcare) automated fluorination kit

2.3.2 Dose calibration

Prior to dispatch, the ¹⁸F-FLT would undergo quality control testing. The end product had a radiochemical purity of >95% and a specific activity of >300 GBq/mmol. On arrival the ¹⁸F-FLT was assayed using the dose calibrator in an identical manner as described for ¹⁸F-FDG (section 2.2.1).

2.3.3 Patient preparation and dose administration

For ¹⁸F-FLT scanning, patients were not asked to starve, as a glycaemic state has no influence on the rate and the amount of tracer uptake. The rest of the patient preparation was as described for ¹⁸F-FDG in section 2.2.2.

¹⁸F-FLT was injected via a peripheral vein, at a dose of up to 400 MBq. There are currently no established protocols that define the optimal dose of ¹⁸F-FLT suitable for routine clinical use. Radiation dosimetry studies of ¹⁸F-FLT PET imaging have suggested that the effective radiation dose received from a 10mCi (375 MBq) dose of ¹⁸F-FLT is in keeping with acceptable levels of radiation exposure for most nuclear medicine investigations (Vesselle et al. 2003). They also suggested that a tracer activity dose as low as 5 mCi (185 MBq) could provide an adequate image quality at 60 minutes post-injection.

For all ¹⁸F-FLT studies in this thesis, the maximum available dose of tracer was administered. In reality however, week-to-week variations in radiosynthesis meant that we were provided with a wide range of tracer doses. In order to standardise our imaging parameters (which is particularly important for quantitative analysis), the highest available dose was injected into the patient. As a compromise, care was taken

to adhere to strict timing of image acquisition, which was performed at 60 minutes post-injection. As will be outlined in further sections, quantitative analysis was carried out using the SUV method, which gives a measure of tracer uptake corrected for differences in administered dose and patient size. A dose of less than 5 mCi (185 MBq) was deemed too low for acquiring an adequate image as also suggested by previous reports (Vesselle et al. 2003).

2.3.4 Acquisition of whole body ¹⁸F-FLT PET/CT images

The same hardware was utilised to acquire whole body ¹⁸F-FLT images as has been previously described (section 2.2.3). Static 2D images were acquired at 60 minutes post-tracer injection. The datasets were also attenuated corrected in the same manner.

2.4 Image analysis

Tomographic imaging with PET/CT allows reconstruction and analysis of the image sets in three orthogonal planes (axial, coronal and sagittal). In this thesis, all image sets were viewed and analysed using the Xeleris PET/CT workstation (GE Healthcare). Two methods of image analysis were performed; visual (qualitative) and quantitative. These are described in more detail below.

2.4.1 Visual analysis

¹⁸F-FDG and ¹⁸F-FLT PET images were acquired approximately 60 minutes post-injection of tracer, which correspond to the plateau phase of tracer accumulation. Visual analysis of PET images relies on the detection of focal areas of tracer accumulation above that of the surrounding tissue. With ¹⁸F-FDG, high physiological accumulation of tracer uptake is frequently seen in brain and myocardium as these organs normally have high rates of glucose metabolism. More variable levels of physiological tracer uptake are often seen in the liver, spleen, stomach, intestines, bone marrow and skeletal muscle. ¹⁸F-FDG is also renally excreted and therefore accumulation of tracer is seen throughout the urinary tract.

Although visual analysis is a simple technique that is routinely used for image analysis in the clinical setting, it is limited by inter- and intra-observer variability. To account for this, all image sets were analysed by two experienced (consultant grade) nuclear medicine physicians and results were reached by consensus. Where applicable, focal areas of tracer accumulation were graded on a 5-point scale to allow statistical correlation between the results of the two observers (0=definitely negative, 1=probably negative, 2=equivocal, 3=probably positive, 4=definitely positive).

Comparisons between 18F-FDG and 18F-FLT studies were made on whole body image sets on a lesion-by-lesion basis. Comparisons between the detection rate of PET, PET/CT and routine ceCT studies were also made on a patient-by-patient basis.

2.4.2 Quantitative analysis

In addition to obtaining qualitative data, semi-quantitative methods have been developed for measuring tracer uptake. One such method is calculation of standardized uptake value (SUV), which is carried out using the following formula;

$$\text{SUV} = \frac{A \times W}{A_{\text{inj}}}$$

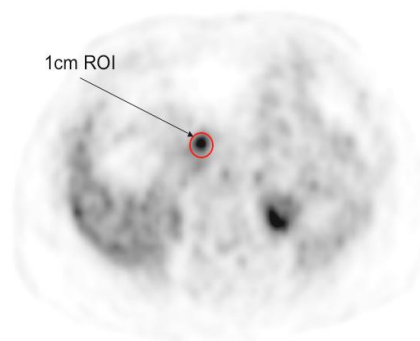
where (A) is the average tumour activity concentration kBq/ml, (W) is the patient's body weight in kg and (A_{inj}) is the injected activity in kBq (Takeuchi et al. 1999; Graham et al. 2000).

The above parameters allow correction of tissue tracer uptake for variations in injected activity and patient's body weight. The resultant SUV value thus represents an index of tracer accumulation within a tissue, which for example can be used to differentiate benign from malignant pathology. Serial measurements can also be used to quantify response to treatment.

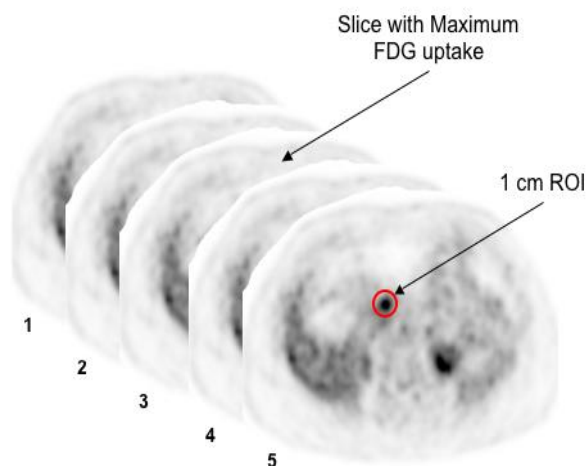
SUV calculations are now automated as they are a standard function incorporated into most PET workstation software. For the purposes of this thesis, SUV measurements were performed using a fixed (1cm) region of interest (ROI). As there are currently no standardised methodologies for SUV determination of a tumour, therefore three

different SUV measurement strategies were used which are detailed below and illustrated in figure 2.1.

- 1) SUV_{Max} – determines the maximum pixel value within the selected 1 cm ROI
- 2) $SUV_{Mean(single\ slice)}$ – determines the average SUV value within a 1cm ROI centred on the slice with the maximal ^{18}F -FDG uptake (ie: the one with the SUV_{Max})
- 3) $SUV_{Mean(multiple\ slices)}$ – determines an average of mean SUV values 2 slices above and below the slice with the maximum SUV



Methods 1 & 2



Method 3

Figure 2.1: Comparison between methodologies for determining tumour SUV

Previous work at our unit (data not presented) had shown methods 2 and 3 to yielded similar results with strong correlation. Maximum pixel values (SUV_{Max}) tended to give a more reproducible measure. Method 3 on the other hand takes an average reading across several adjacent axial image slices, and thus considered to better account for tumour heterogeneity. Therefore two methods of SUV determination were used in this thesis, which is referred to as SUV_{Max} and SUV_{Mean} .

2.5 Computed Tomography imaging protocols

2.5.1 Patient preparation

i) Contrast enhanced CT scan of the thorax, abdomen and the pelvis

Patients were asked not to eat anything for four hours prior to the scan but were allowed to drink non-fizzy drinks up to one hour before the scan. No other special preparations were required. Oral contrast agents were given just prior to scanning of the abdomen and the pelvis.

ii) Pancreatic protocol CT

Patients were asked to fast prior to the scan as for a routine imaging the abdomen and the pelvis detailed above. 200-500 ml of water was given to the patient orally, 30 minutes before the scan; water acted as a negative contrast agent, helping to distend the stomach and the duodenum.

2.5.2 Image acquisition

i) Abdomen, pelvis and liver

Scans of the abdomen and pelvis were acquired using the Siemens Somatom Plus 4, multidetector (4 slice) spiral CT (Siemens AG Medical Engineering Group, Forchheim, Germany). Images were contrast enhanced with 100 ml of intravenous iodinated contrast material (Omnipaque 350, Nycomed Amersham plc, Amersham Place, Little Chalford, Buckinghamshire) infused via a peripheral vein at 4mls/sec. and a delay of 45 seconds. Enhancement of the bowel was also carried out using oral contrast material as outlined above (2.5.1).

The scanning protocol of the abdomen and the pelvis involved imaging at 120 kV, 140-280 mA and 1mm collimation. Bi- or triphasic imaging of the liver was carried out at delays of 20s, 50s, 180s and using a 2.5mm collimation. All images were reconstructed at 3 and 5mm slice thickness.

ii) CT scan of the chest

Standard, non-contrast enhanced scans were performed as detailed above.

iii) Contrast enhanced pancreatic protocol CT

An unenhanced scan of the abdomen was first obtained to determine the upper and the lower boundaries of the pancreas and to detect pancreatic calcification. Using a bolus track technique, the pancreas was imaged at peak arterial phase. Briefly, a region of interest was placed over a representative section of the pancreas. The patient was then given a bolus infusion of 20-50 mls of iv contrast material (Ominopaque 350 at 5mls/sec.), while dynamic CT acquisition was performed over the single slice containing the ROI. Using the software integrated into the CT workstation, the time at which the pancreas achieved maximal enhancement was calculated. Contrast enhanced images of the entire pancreas were then acquired at the peak arterial phase and at 120 keV, 140-280 mAs and 1mm collimation. Images of the pancreas were reconstructed at 1 and 3mm slice thickness. Portal-venous phase images of the liver were also acquired at 60 seconds delay, 2.5 mm collimation and reconstructed at 5mm slice thickness.

2.5.3 Image reconstruction and analysis

All data was processed on the CT scanner Siemens workstation where images were reconstructed accordingly. Images were usually formatted into the transaxial plane, but when necessary coronal and sagittal prints were produced.

A senior radiologist (specialist registrar or consultant grade) evaluated all images. In addition, all CT scans were presented at a weekly CRC MDT meeting where they were re-evaluated by a Radiologist of consultant grade. All films were visually analysed.

2.6 Confirmation of diagnosis and follow-up

All patients studied in this thesis were managed in a multidisciplinary team (MDT) setting, in accordance with Department of Health (DoH) guidelines for optimal cancer management. The MDT consisted of both medical and allied health-care professionals. This included radiologists, nuclear medicine physicians, surgeons, oncologists and cancer specialist nurses. This group made consensus decisions regarding the clinical management of complex cases and therefore formed an ideal forum to present both the PET/CT and the CT data in order to decide management based on the relevant clinical information.

All diagnoses related to this thesis were confirmed by histology and/or following clinical, radiological or surgical follow-up of the patient, within the respective MDT forums of the cancer being studied.

CHAPTER 3

**Does 18F-FDG PET/CT play a role
in the routine management of
pancreatic cancer?**

3.1 Background

Contrast enhanced computed tomography (ceCT) is at present the first line imaging modality of choice for diagnosing and staging pancreatic cancer. Multi-detector spiral CT allows fast image acquisition with thin collimated sections that gives ceCT a positive predictive value for tumour detection of over 90% and an ability to correctly identify non-resectability in almost 100% of the cases (Freeny et al. 1993; Bluemke et al. 1995; Diehl et al. 1998; Freeny 2001). Despite this, ceCT has been shown to have limitations that can potentially result in mis-staging of the disease. A study by Saisho and Yamaguchi (2004) in fact showed ceCT staging to be accurate in 65.7%, while under-staging 25.7% and over-staging 8.6% of the cases.

Several studies to date have suggested PET to be of value in the routine management of pancreatic cancer. ¹⁸F-FDG PET has been demonstrated to be superior to conventional imaging modalities in assessing small pancreatic tumours (<2cm) (Delbeke et al. 1999), differentiating benign from malignant disease (Imdahl et al. 1999) and particularly, in accurately determining the extent of extra-pancreatic disease (Zimny et al. 2000; Jadvar and Fischman 2001; Nakata et al. 2001). What imaging with PET lacks is the anatomical information that would allow precise localisation of PET positive lesions. This limitation has been addressed with the introduction of dual modality PET/CT scanners. However to date, there is little evidence supporting the use of the ¹⁸F-FDG PET/CT in the routine assessment of pancreatic cancer.

3.2 Aims

The aims of this study were:

1. to compare the diagnostic and staging accuracy of ¹⁸F-FDG PET/CT to that of conventional imaging with ceCT.
2. to evaluate the impact of routine PET/CT imaging on the management algorithm of pancreatic cancer.

3.3 Methods

3.3.1 Patient recruitment

This study was a retrospective analysis of consecutive patients referred for an 18F-FDG PET/CT scan between 2003 and 2005. Patients were included in the analyses who meet the following two inclusion criteria:

- 1) A patient with a suspected diagnosis of pancreatic cancer
- 2) The patient having undergone a contrast enhanced pancreatic protocol CT (ceCT) scan within 2 weeks of the 18F-FDG PET/CT study.

The primary outcome measure in this study was the impact of 18F-FDG PET/CT on the management of this cohort of patients. Consequently, the finalised PET/CT reports provided to the referring clinicians were retrospectively compared with the ceCT results. Patient management, as decided by consensus by the hepatobiliary multidisciplinary team was recorded and correlated with clinical, radiological and surgical outcomes. Patients were followed-up for a median duration of 13 months (range of 2-24 months).

3.3.2 Imaging protocols

a) 18F-FDG PET / CT

Imaging protocols for 18F-FDG PET/CT scans are detailed in section 2.2.

Images were acquired at a median of 58 minutes (range 48-65 minutes) post-injection of tracer. A median dose of 378 (range 300-410) MBq of 18F-FDG was administered. Patients were required to drink 200 ml of water, 5 minutes prior to being placed on the scanner bed. This step was only undertaken in acquiring PET/CT images of the

pancreas, with water acting as a negative contrast agent in delineating the duodenum. No intravenous contrast agents were used.

All images were analysed qualitatively (visually) by a senior (consultant grade) nuclear medicine physician. A lesion was deemed positive for malignancy if its ¹⁸F-FDG PET activity was greater than the background. A lesion with activity less than or equal to the background was deemed negative.

b) Contrast Enhanced Pancreatic Protocol CT (ceCT)

Patient preparation and imaging protocols for pancreatic protocol ceCT are described in chapter 2.5. All ceCT scans were reported by a senior (consultant grade) radiologist. Information was provided regarding the presence or absence of a pancreatic mass, degree of suspicion of malignancy, local (eg: vascular) invasion, presence of peri-pancreatic lymphadenopathy and extrapancreatic disease.

3.3.3 Data presentation

Imaging results are classified as true positive (TP), false positive (FP), true negative (TN) and false negative (FN). Sensitivity, specificity, accuracy, positive and negative predictive values were calculated using standard formulae. The difference in detection accuracy of the two imaging modalities were compared using the McNemar's test for correlated proportions. Two tailed *p* values of <0.05 were considered as statistically significant.

3.4 Results

3.4.1 Patient demographics

51 patients were included in this analysis. There were 32 males, 19 females with a median age of 62 years (range 30-82 years). Patient demographics are summarized in table 3.1.

Age (median , range)	62 yrs (30-82)	(%)
		-
Sex (M:F)	1.7 : 1	-
Site of pancreatic mass		
Head	47	(92%)
Body	2	(4%)
Tail	2	(4%)
Histological diagnosis		
Adenocarcinoma	39	(76%)
Benign	9	(18%)
	(1 Tuberculous cyst, 8 mass forming chronic pancreatitis)	
Final stage group (n=39)		
IA/B	7	(18%)
IIA/B	12	(31%)
III	9	(23%)
IV	11	(28%)

Table 3.1: Summary of patient demographics with suspected pancreatic cancer

The final diagnosis was histologically confirmed in 48 patients (94%). Of these, as 39 (76%) were adenocarcinoma and 9 (18%) were found to be benign. In 3 patients (6%) where histological analysis was not performed, pancreatic lesions were later confirmed to be benign by clinical and radiological follow-up for a median duration of 10 months (range 8-19 months).

3.4.2 Diagnosis of the primary pancreatic lesion

Imaging results were compared on a lesion-by-lesion basis for all pancreatic lesions.

Table 3.2 compares the imaging accuracy of 18F-FDG PET/CT and ceCT.

	18F-FDG PET/CT	ceCT
TP	37	38
TN	9	5
FP	3	7
FN	2	1
Total	51	51
Sensitivity(%)	95	97
Specificity (%)	75	42
PPV (%)	93	84
NPV (%)	81	83
Accuracy (%)	90	84

Table 3.2: The detection accuracy of 18F-FDG PET/CT compared to ceCT.

(TP: true positive, TN: True negative, FP: False positive, FN: False negative, PPV: positive predictive value, NPV: negative predictive value)

PET/CT resulted in 2 false negative (both histology showing mucinous adenocarcinoma) and 3 false positive results (one tuberculous cyst of the pancreas, 2 due to chronic pancreatitis). In 9 cases (18%) pancreatic lesions seen on ceCT were reported as equivocal but highly suspicious for malignancy. Of these, 7 lesions showed no focal 18F-FDG accumulation thus suggesting benign disease. Histology confirmed these lesions to be due to chronic pancreatitis, thus correctly corresponding to the diagnosis made by 18F-FDG PET/CT. Figure 3.1 illustrates one such example. As indicated above, the remaining 2 lesions were also falsely positive on 18F-FDG PET/CT. Overall for ceCT therefore, there were 7 false positive and 1 false negative

result (the latter being a subcentimetre primary lesion later found on EUS guided biopsy to be adenocarcinoma).

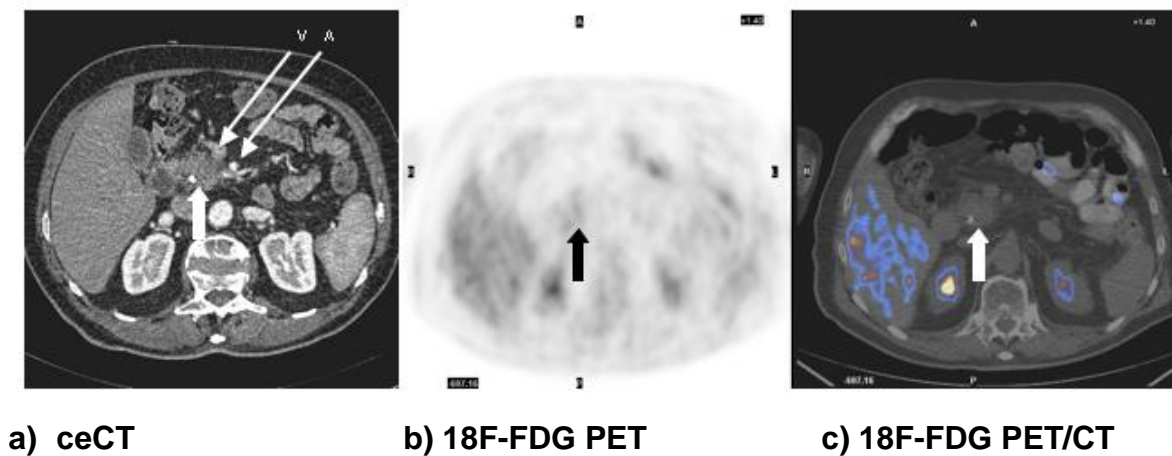


Figure 3.1: Transaxial ceCT image (a) demonstrating a poorly enhancing mass in the uncinate process of the pancreas, with involvement of per-pancreatic vessels (V= Superior mesenteric vein (SMV); A= Superior mesenteric artery (SMA)). No uptake of 18F-FDG was observed in the PET (b) and PET/CT (c) fused images. The mass was later proven on histology to be due to mass forming chronic pancreatitis.

The sensitivity of 18F-FDG PET/CT was similar to ceCT (95% vs 97% respectively; $\chi^2=0$, $p=1.0$; McNemar's test). The specificity of 18F-FDG PET/CT was superior to ceCT, but this difference did not reach statistical significance (75% vs 42% respectively; $\chi^2=2.25$, $p=0.1336$). Overall accuracy of both imaging modalities were also similar (18F-FDG PET/CT=90 vs ceCT=84; $\chi^2=0.80$, $p=0.371$)

3.4.3 Staging accuracy of pancreatic cancer with 18F-FDG PET/CT

3.4.3.1 Local (T) and nodal (N) staging

Of the 39 proven pancreatic cancers, initial staging with ceCT deemed 10 cases (26%) to be locally resectable (T 1-2, stage I). At the time of surgery, 3 cases were found to be inoperable. Thus ceCT underestimated the extent of local disease in 8% of cases. In local staging, 18F-FDG PET/CT did not conclusively provide any additional information to ceCT. This occurred as the combination of PET's limited spatial resolution, the non-diagnostic nature of the CT component of PET/CT and the lack of intravenous contrast enhancement to delineate vascular structures preventing from accurately determining the exact size and local spread of the tumours.

The ceCT criteria for detecting spread to loco-regional lymph nodes routinely use the short axis diameter of the node as marker of abnormal lymphadenopathy. In this study, macroscopically enlarged (> 7 mm) lymph nodes were detected in 5 patients, all of whom were confirmed to have a pancreatic carcinoma. Although in all the above cases, the enlarged nodes were seen on the CT component of PET/CT, they were reported as positive lymph nodes only if focal accumulation of 18F-FDG was demonstrated on the PET/CT scan. As for this, 18F-FDG PET/CT identified loco-regional lymph nodes in 3 of the above 5 patient (60%). As histological sampling of these lymph nodes were not carried out for any of the above 5 patients, it is impossible to determine the accuracy of 18F-FDG PET/CT in correctly staging nodal disease. In fact in two of the 5 patients, there was a biliary stent in situ. Therefore without histological examination, it was impossible to ascertain whether the periportal lymphadenopathy detected on both the ceCT and 18F-FDG PET/CT were reactive or due to malignant spread. In addition to the above, histology from resected

tumour specimen in 3 further patients (6%) showed microscopic peri-pancreatic lymph node spread (N1 disease). None of these were detected by either imaging modality.

3.4.3.2 Detection of distant metastases

The prevalence of metastatic disease (stage IV disease) in this series was 28% (11/39 patients) with histological / radiological follow-up confirming the presence of a total 29 metastatic lesions. Table 3.3 summarises the distribution of extrahepatic lesions detected by the two imaging modalities.

Of the 39 patients with confirmed malignancy, 5 (13%) had indeterminate hepatic lesions, which were highly suspicious for metastases. Of these, 18F-FDG PET/CT correctly interpreted the lesions as benign in 4 cases (10%) and one as a malignant deposit. In one patient, ceCT incorrectly detected liver and lung metastases, whereas 18F-FDG PET/CT showed no tracer uptake in either lesion. Histology was in concordance with the PET/CT findings, resulting in down-staging of the patient from M1 to M0. In 7 patients (18%), 18F-FDG PET/CT detected ceCT occult metastases thus upstaging the patient from M0 to M1 disease. An example is illustrated in figure 3.2. In 3 patients solitary metastases to the liver were noted on the ceCT. In these cases, 18F-FDG PET/CT localized additional metastatic deposits missed by ceCT both in the liver and at extra-abdominal sites. This however did not change the radiological stage of the patients. Therefore overall, 18F-FDG PET/CT resulted in an alteration of staging of 12 out of 39 patients (31%) by down-staging 13% (5 cases, including 4 with equivocal ceCT results) and upstaging 18% of cases. False positive findings with 18F-FDG PET/CT occurred in 3 patients (8%). These were as a result of

18F-FDG uptake in mediastinal granuloma, a reactive hilar lymph node and a vertebral lesion which was found to be negative on bone scintigraphy and bone marrow biopsy. In one patient (3%), a liver metastasis was clearly identified on the ceCT scan but one which did not take up any 18F-FDG. This was later histologically confirmed to be a mucinous adenocarcinoma.

	ceCT detected metastases	18F-FD PET/CT detected metastases
Indeterminate ceCT findings	Indeterminate liver lesion Indeterminate liver lesion Indeterminate liver lesion Indeterminate liver lesion Indeterminate liver lesion (?Haemangioma)	Negative (benign) Negative (benign) Negative (benign) Negative (benign) Liver (segment IV) and lung metastases
Downstaged disease	Liver and lung metastases	Negative
Upstaged disease (ceCT occult metastases)	Negative Negative Negative Negative Negative	Liver (segment IV) Liver (segment VI) Liver (segment VIII) Liver (segment VII), peritoneal deposits Peritoneal deposits
False positives	Negative Negative Negative	Mediastinal lymph node Hilar lymph node Bone lesions (body of T4)
False negatives	Liver metastasis (segment VIII)	Negative (mucinous adenoca)
PET/CT detecting additional metastases	Liver Liver (segment VIII) Liver	Liver/lung/bone/peritoneum Liver (segment I, III, VIII) Liver, bone (scapula & humerus)

Table 3.3: Summary of the distribution of metastatic deposits detected by ceCT and PET/CT

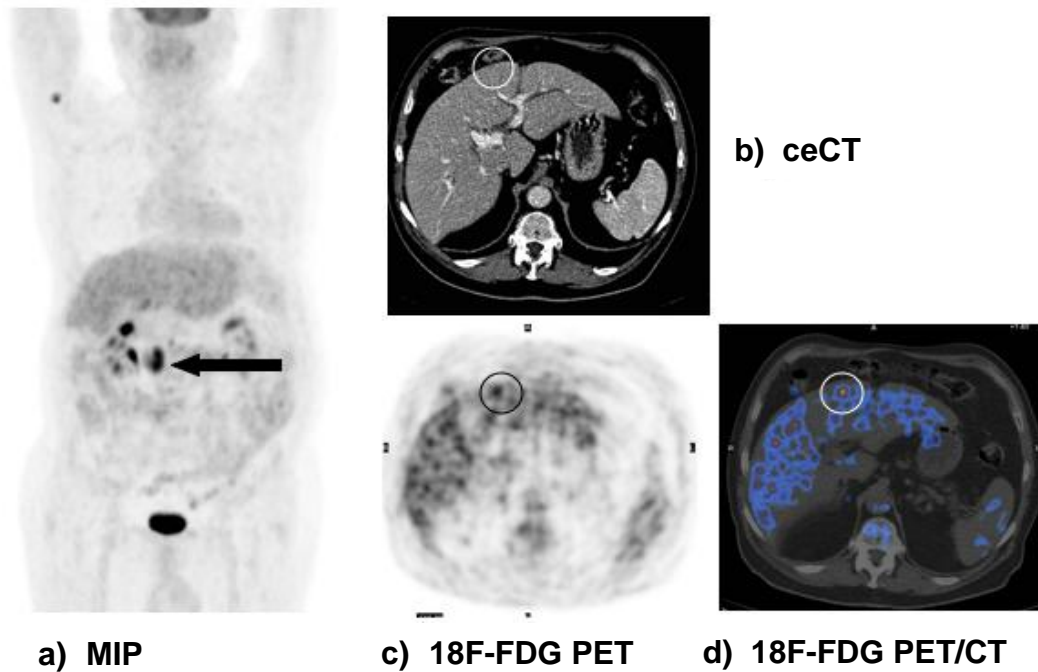


Figure 3.2: Whole body ^{18}F -FDG PET/CT image of a patient with a carcinoma of the head of the pancreas (shown on the Maximum Intensity Projection (MIP) image (a) – thick black arrow). An indeterminate sub-centimetre liver lesion seen on ceCT(b) was found to be ^{18}F -FDG avid, thus representing a metastatic deposit. This is shown on the PET (c) and the PET/CT (d) fused images (lesion circled in each image). ^{18}F -FDG PET/CT also detected a ceCT occult lung metastasis (not shown) thus resulting in upstaging the patient from M0 to M1.

3.4.4 Additional findings

In one patient, focal ^{18}F -FDG accumulation was localised to the ascending colon on the PET/CT. There was however no corresponding abnormality noted on ceCT. Colonoscopic examination revealed a 2cm sessile polyp, which was later found on histology to be a tubulo-villous adenoma with high-grade dysplasia and no evidence of invasiveness (Figure 3.3)

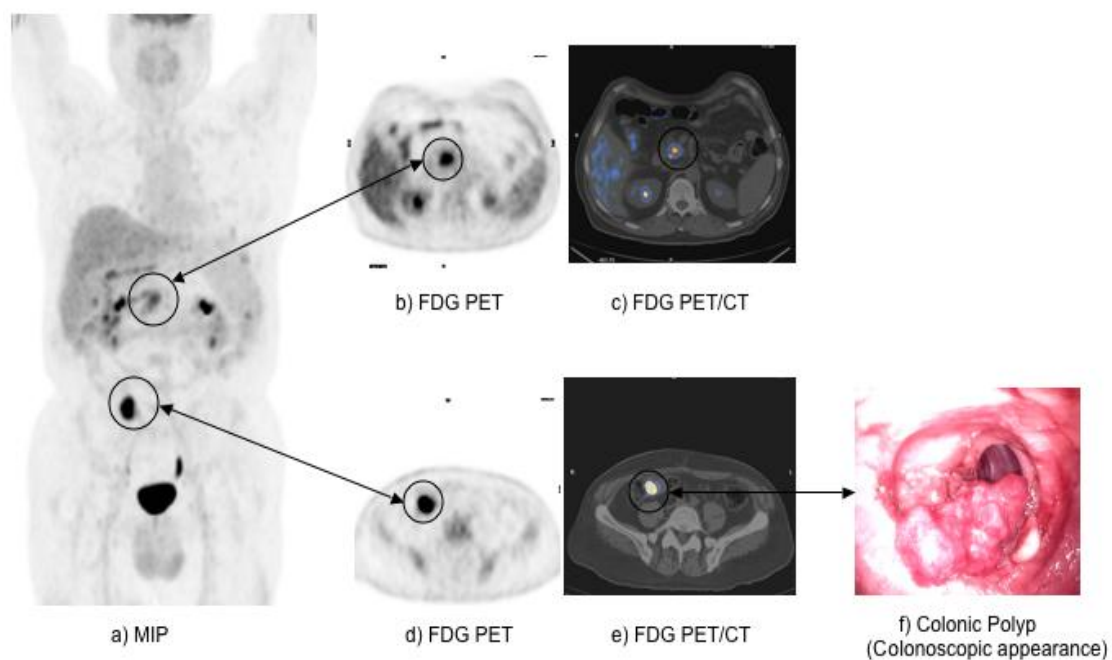


Figure 3.3: Maximum intensity projection (MIP) of ^{18}F -FDG PET (a) and the concurrent ^{18}F -FDG and ^{18}F -FDG PET/CT fused images of the primary pancreatic lesion (b,c). A second area of focal ^{18}F -FDG accumulation was also detected in the right lower quadrant of the abdomen. This was localized on the ^{18}F -FDG PET/CT fused images to a loop of colon (d,e). Colonoscopic examination showed a 2cm sessile polyp (f).

3.4.5 The impact of 18F-FDG PET/CT on clinical management

As presented earlier, in 9 of the 51 patients (18%) the ceCT report indicated an equivocal but highly suspicious mass in the pancreas. In 7 of these cases (14%), 18F-FDG PET/CT correctly characterized these lesions as benign therefore a futile course of treatment for a carcinoma was avoided. Of the 39 patients with confirmed malignancy, 18F-FDG PET/CT changed the clinical stage of the disease in 12 (31%). This however resulted in a change in management of only 2 patients (5%). These were cases with apparently resectable pancreatic tumours on ceCT, but where 18F-FDG PET/CT detected occult metastases. The remaining 10 (26%) patients were found to have a locally advanced and inoperable disease based on the initial ceCT criteria and therefore detection of either ceCT occult metastases or additional extrapancreatic deposits did not change the subsequent management. Overall therefore, 18F-FDG PET/CT directly resulted in a change in management of 9/51 patients (18%).

If the 18F-FDG PET/CT findings were considered alone, false findings would have had a negative impact on the management of 5 patients (10%). 2 patients (4%) with a false negative primary lesion would have been incorrectly treated conservatively, and 3 patients (6%) with false positive distant metastases would have been incorrectly managed palliatively. In the latter 3 patients, the extrapancreatic lesions were histologically confirmed to be benign disease and thus the primary tumours were resected.

3.5 Discussion

In this study, ceCT and 18F-FDG PET/CT showed comparable sensitivities for detecting primary pancreatic lesions (97% and 95% respectively). The lower sensitivity of 18F-FDG PET/CT resulted from two false negative PET/CT findings, both of which were histologically found to be mucinous adenocarcinoma. This low-grade uptake of 18F-FDG in mucinous tumours which has been attributed to the relatively low cellularity of mucinous tumours and the abundance of glycopeptide rich mucin that is thought to compete with 18F-FDG for binding sites (Berger et al. 2000).

While of comparable sensitivity, the specificity of 18F-FDG PET/CT was superior to that of ceCT (78% vs 42% respectively), although this difference did not reach statistical significance. Lesion characterisation with ceCT is limited by the fact that morphological features cannot reliably distinguish benign from malignant pathology. As PET targets biological changes associated with malignancy, focal abnormalities can be detected independent of morphology. In this series, equivocal ceCT findings in 7 patients (14%) with a pancreatic mass were correctly confirmed as benign following a negative 18F-FDG PET/CT result. Conversely, the presence of focal tracer accumulation in small lesions such as those in the liver, were more accurately confirmed with 18F-FDG PET/CT. It is however important to note that the PET/CT findings cannot be considered in isolation due to false positive and false negative results. As previously mentioned, false negative results may be seen in mucinous tumours. More commonly however, false positive findings occur due to the accumulation of 18F-FDG in areas of active or chronic inflammation as macrophages and activated lymphocytes exhibit an enhanced glycolytic rate and thus a higher cellular uptake of 18F-FDG (Ishimori et al. 2002; Kaim et al. 2002). The pattern of

uptake of 18F-FDG in areas of inflammation is often low-grade and diffuse, which together with the clinical history and the presence of pancreatic calcification seen on the CT component of PET/CT, may help in avoiding diagnostic uncertainty. Until such time a more specific PET tracer emerges, focal areas of 18F-FDG uptake in equivocal cases require histological verification.

This study purposefully did not use semi-quantitative analysis of tracer uptake in detecting malignant lesions. The use of Standardised Uptake Values (SUVs) of a lesion has been suggested to improve PETs specificity, where several studies have shown SUV values for inflammatory lesions to be lower than that for malignant ones. Using a cut-off SUV value of 4 for malignant lesions and SUV of 3-4 for chronic pancreatitis, Imdahl et al. (1999) showed 18F-FDG PET to be able to differentiate between cancer and inflammation with a sensitivity of 96% and 100% respectively. In a larger series of patients with a suspected pancreatic cancer (n=86; 65 malignant, 21 benign) Koyama et al. (2001) found that a serum glucose corrected SUV threshold of 2.2 gave the optimal diagnostic accuracy for 18F-FDG PET. Delayed imaging during the glycolytic plateau phase of 18F-FDG uptake has also been suggested to improve specificity but this requires further validation (Nakamoto et al. 2000). The main limitation of using SUVs in the routine assessment of PET images is the as yet undetermined standardized SUV threshold that defines malignancy. Furthermore, there are no standardized protocols that define how an SUV should be measured as this also has a significant bearing on the values obtained. Consequently, as this study mirrored our routine clinical practice of imaging with 18F-FDG PET/CT, quantitative analysis was not employed.

The main determinant of operability of a tumour is its extent of local peri-pancreatic spread and vascular involvement. While ceCT has been shown to be accurate in detecting inoperable lesions, its positive predictive value in detecting resectability can be poor. In our series for example, ceCT underestimated the extent of local disease in 8% (3/39) of all malignant cases, or in other words, 33% (3/10) of all cases deemed operable by ceCT. Despite this shortcoming, ceCT remains the imaging of choice for local (T) staging of disease as 18F-FDG PET/CT did not confer an advantage. The inability of 18F-FDG PET/CT to accurately stage local disease (T staging) is multifactorial. Firstly, the positron-emitting source from a lesion is not a point source and therefore the borders of the tumour cannot be defined according to the boundaries of the 18F-FDG “hot-spot”. Furthermore, the CT component of PET/CT is solely used as a means of lesion localization, which is acquired at a low power and thicker slice width to minimize radiation exposure to the patient. The resultant poor resolution CT images therefore prevent an accurate assessment of local tumour invasion to be made. Lastly, at the time of this study our local imaging protocols did not routinely use intravenous contrast material when acquiring the PET/CT images. This was in large due to anecdotal evidence suggesting that high-density contrast material may result in image artefacts and therefore interfere with the interpretation of 18F-FDG PET data (Cohade et al. 2003b; Visvikis et al. 2003). Once again therefore, an accurate assessment of local vascular involvement (and thus tumour resectability) could not be made with our current PET/CT imaging protocols. There is emerging evidence to suggest that contrast material may be successfully used as part of the routine PET/CT imaging protocol. This however requires formal investigation and validation.

In assessing local lymph node involvement, morphological imaging with ceCT is limited by the fact that lymph node size is a poor predictor of malignant spread. In this respect molecular imaging with PET (theoretically) confers an advantage as it may detect tumour spread to lymph nodes based on their metabolic activity and irrespective of their size. In lung cancer, 18F-FDG PET has been frequently reported to be superior in detecting mediastinal nodal spread (Patz et al. 1995) so much so that it is now become a mandatory investigation in the routine pre-operative assessment of lung tumours. In pancreatic cancer the evidence to date seems to indicate that 18F-FDG PET may be unsuitable for routine staging of loco-regional lymph nodes (Diederichs et al. 2000; Heinrich et al. 2005). Results from our study were severely limited by the fact that routine histological sampling of abnormal looking lymph nodes was not carried out. As a result, the exact sensitivity and specificity for nodal staging could not be reported for either ceCT or PET/CT. Assessment on a patient-by-patient basis revealed 5 cases where suspiciously enlarged loco-regional lymph nodes were seen on the ceCT images. Of those, only 3 cases (60%) demonstrated significant 18F-FDG accumulation to be deemed positive. In further 3 cases that underwent a successful resection, histology confirmed the presence of microscopic lymph node spread (N1 disease), but none of these were detected by either imaging modality.

Despite the limitations of our study, our findings concur with previous reports, suggesting 18F-FDG PET/CT to be of limited value in staging loco-regional lymph node involvement. While theoretically 18F-FDG PET may be useful here, there are several potential factors at play that can limit the accuracy of 18F-FDG PET/CT in detecting lymph node disease. It is generally accepted that the spatial resolution of PET is limited to detecting lesions larger than 1cm, although that quoted by many

manufacturers is between 0.5-0.8cm. This is believed not to be an accurate generalization as lesion detectability with PET is dependent on the metabolic activity of disease and not size. The challenge faced by detecting lymph node disease is therefore likely to be one of the volume of metastatic disease within the node, which is often small, thus accumulating relatively less tracer. Such low-grade tracer uptake is consequently subject to partial volume effects, which can diminish the sensitivity of PET. Furthermore, a weak tracer signal from the loco-regional nodal basin may be obscured by the intense tracer uptake within the primary lesion, thus resulting in positive lymph nodes being missed. It is clear that the sample size of our study and many of those published in the literature are too small to allow this to be adequately assessed. Therefore given the evidence to date, the indications are that 18F-FDG PET/CT plays a limited role in nodal staging of pancreatic cancer. There may however be a role for PET/CT image fusion in assessing lymph node disease where image fusion may augment the accuracy of lymph node staging by combining metabolic and morphological criteria. Future validating studies are required to confirm this.

One of the frequently reported advantages of imaging with 18F-FDG PET has been the whole body evaluation of metastatic spread. Foci of 18F-FDG uptake can be detected with great sensitivity in the liver, lungs and the bones, owing to the high degree of contrast that is achieved between the lesion and the surrounding normal tissues (Nishiyama et al. 2005). In our series, 18F-FDG PET/CT resulted in detection of occult metastases in 7 out of 39 (18%) patients that had histological confirmation of malignancy. Majority of lesions missed on ceCT were hepatic metastases. This shortcoming of ceCT is often due to intrahepatic duct dilatation due to biliary

obstruction making interpretation difficult. This in our series did not interfere with the PET images. Where 18F-FDG PET/CT seemed to be advantageous was also in localizing and differentiating peritoneal deposits from areas of physiological uptake within the abdominal cavity. Due to time constraints of this thesis however, the incremental value of PET/CT over PET alone was not formally examined. Whilst overall 18F-FDG PET/CT resulted in change in radiological stage of the disease in 31% of proven cancers, the impact on management in this group occurred in 2 cases (5%) where the primary disease was deemed to be operable and PET/CT detected occult metastases. The impact of 18F-FDG PET/CT on the management of pancreatic cancer is largely dependent on the therapeutic algorithm that is used. At our institution, a curative pancreaticoduodenectomy is offered to patients with locally resectable tumour (operability determined based on ceCT criteria), and the proof of absence of distant spread. Conversely, patients with inoperable disease are offered palliative chemotherapy and/or a biliary bypass operation. This underlines the vital need for accurate pre-operative assessment of local and metastatic disease burden. Furthermore, unless changes in PET/CT imaging protocol allow for more accurate assessment of local tumour spread, the impact of 18F-FDG PET/CT is only best demonstrated once tumour respectability is fully assessed using ceCT, where it may help to definitively exclude metastatic disease. Overall, 18F-FDG PET/CT changed the management of 18% (9/51) of the whole series, predominantly due to its role as a means of further characterizing primary lesions. In our series, 7 of the 9 suspicious but equivocal lesions in the pancreas seen on ceCT were correctly characterized by 18F-FDG PET/CT as benign lesions, thus resulting in the patients avoiding unnecessary and potentially futile treatment.

3.6 Conclusions

In detecting pancreatic cancer, 18F-FDG PET/CT demonstrated a superior specificity compared to ceCT while the sensitivities of the two imaging modalities were similar. With regard to loco-regional staging, 18F-FDG PET/CT played a limited role in both local (T) and lymph node (N) staging of disease. The indications are therefore that 18F-FDG PET/CT is best applied as a complimentary imaging tool to conventional imaging (ceCT), either as a problem solving tool in assessing equivocal cases or as a means of excluding extrapancreatic disease in patients deemed to have an operable tumour.

CHAPTER 4

**Does ^{18}F -FDG PET/CT provide
additional information to
conventional imaging
in the management of
colorectal liver metastases?**

4.1 Background

Pre-operative selection of patients for liver resection heavily relies on accurate information provided by routine cross-sectional imaging modalities such as CT and MRI. Although the widespread use of contrast enhanced CT (ceCT) has made a significant impact on the management of CLM, pre-operative staging remains a clinical challenge. This is obviated by the fact that up to 20% of patients undergoing liver resection are found to have inoperable disease at laparotomy and up to 60% are reported to develop recurrences within 3 years following a successful resection (Scheele et al. 1995; Fong et al. 1997).

As discussed in chapter 1, a major limitation of imaging with a stand alone PET scanner is its relative lack of anatomical resolution. This is where dual modality imaging with PET/CT confers advantages through the co-registration of anatomical and biological data, which arguably helps to combine the strengths of the two modalities. A number of early studies have consistently suggested ¹⁸F-FDG PET to be superior to CT in detecting and staging liver metastases. More recently however, there are indications that the difference between the two modalities may have been somewhat overestimated. The predominant factor may be due to the widespread use of multidetector, fine slice ceCT that has narrowed the gap between the capabilities of these two modalities (Truant et al. 2005). Overall, ¹⁸F-FDG PET seems to provide specific advantages over routine imaging in advanced CRC and its clinical impact has been shown to occur in up to 29% of cases (Huebner et al. 2000). The question that therefore remains is whether ¹⁸F-FDG PET or PET/CT should be routinely applied in this setting and if not, is there a subgroup of patients that may benefit most from having a PET (or PET/CT) scan incorporated into their management algorithm.

Currently there are no established protocols for the use of 18F-FDG PET in primary or recurrent CRC. Institutional preferences are therefore heavily swayed by the relative cost and availability of PET scanners. One approach to a rational patient selection protocol may be with the use of a clinical scoring tool such the Clinical Risk Score (CRS). CRS was first described by Fong et al. (1999a) as a prognostic tool, allowing patients to be stratified according to their risk of recurrence prior to hepatic surgery for CLM. Multivariate analysis identified five criteria, which are as follows:

- 1) Nodal status of the primary tumour
- 2) Disease free interval from the primary to discovery of the liver metastasis of <12 months
- 3) Number of tumours of >1
- 4) Pre-operative CEA level of >200 ng/ml
- 5) Size of the largest tumour > 5 cm

Since the original work by Fong et al. a number of studies have validate the use of CRS as a reliable predictor of outcome following hepatic surgery for CLM (Mala et al. 2002; Mann et al. 2004). More recently, Schussler-Fiorenza et al. (2004) examined the relationship between CRS and the clinical yield of 18F-FDG PET in patients with hepatic metastases. They demonstrated that patients with a CRS of 1 or more were more likely to have extrahepatic disease detected on PET than those with a low score (<1). In those with a CRS of 0, 18F-FDG PET resulted in a false positive rate of 57%. The authors therefore suggested that patients with an isolated CLM and CRS of 0,

“should undergo conventional imaging alone” (and not a PET scan) before surgical exploration.

4.2 Aims

The aims of this study were:

- 1) to investigate if 18F-FDG PET/CT provides additional information to routine ceCT in the routine pre-operative assessment of patients with CLM.
- 2) to evaluate the clinical impact PET/CT on the management of patients with CLM
- 3) to investigate the incremental value of 18F-FDG PET/CT imaging over that of imaging with PET alone
- 4) to examine the relationship between CRS and the clinical yield of 18F-FDG PET/CT.

4.3 Methods

4.3.1 Patient group

Between October 2003 to October 2005, a database of consecutive patients referred to our unit for assessment of colorectal liver metastases was held. Patient demographics, tumour characteristics (required for clinical risk score determination) and imaging results were recorded and analysed retrospectively. Routine imaging consisted of a contrast enhanced CT scan of the abdomen and the pelvis and where applicable, imaging of the thorax was also performed. Only patients who underwent imaging with ceCT of the thorax, abdomen and the pelvis were compared to whole body 18F-FDG PET/CT scan acquired within 2 weeks of each other were included in the final analysis. Management decisions were decided by consensus in the multidisciplinary team setting. Decision plans were made sequentially, first following the results of the ceCT scan and subsequently following the 18F-FDG PET/CT findings.

4.3.2 Imaging protocols

Most ceCT scans were performed in house using the standard protocol described in chapter 2. If the imaging data from referring institutions was insufficient, (i.e.: of poor quality or greater than 2 weeks old), they were repeated at our centre.

Imaging protocols for the whole body 18F-FDG PET/CT scans are as described in section 2.2. A median dose of 377 MBq of 18F-FDG (range 360 – 400) was administered and scans were acquired at a median time of 62 minutes (range 55-65) post tracer injection. All images were acquired during normoglycaemia. No intravenous or oral contrast agents were used.

4.3.3 Image analysis

All ceCT, PET and PET/CT studies were analysed by senior (consultant grade) radiologists and nuclear medicine physicians. Imaging was used to determine the extent of hepatic and extra-hepatic disease burden. All PET/CT images were analysed qualitatively (visually). A lesion was reported as positive for malignancy if focal 18F-FDG PET accumulation was greater than the background. A lesion with activity less than or equal to the background was deemed negative.

The analysis of results was performed both on a “lesion-by-lesion” and “patient-by-patient” basis. The impact of PET/CT on management was decided by consensus at the specialist (liver) MDT meetings and the outcomes were correlated with the imaging results.

In order to investigate the incremental value of PET/CT over PET alone imaging, the same dataset acquired during the routine PET/CT imaging was used. Here, the standard workstation (Xeleris[®]) could be adjusted to allow the PET images to be viewed separately to the CT and the PET/CT fused images, thus allowing the assessment of PET only data in isolation. For all cases, both the attenuated corrected and uncorrected PET images were viewed simultaneously. The PET only and the PET/CT data were analysed by two independent reporters in order to account for inter-observer variability. Each reporter analysed the PET and the PET/CT data with at least a 2-week intervening gap between the two in order to minimise recall bias.

A 3-point scoring system was used to record the certainty of lesions localization (0=Unknown localization, 1=Probable localization, 2=Definite localization). A 5-

point scoring system was used to record the certainty of lesion characterization (0=Definitely benign, 1=Probably benign, 2=Equivocal lesion, 3=Probably malignant, 4=Definitely malignant).

4.3.4 Clinical Risk Score (CRS)

CRS was determined by adding one point to each of the 5 criteria previously listed (section 4.1). The maximum size of hepatic lesions were determined on the axial slices of the ceCT scans and not on the CT component of PET/CT. The final score for each patient was correlated with the patient / tumour characteristics and the final imaging results.

4.3.5 Data presentation and statistical analysis

The results from the two imaging modalities are presented as true positives, true negatives, false negatives and false positives. Sensitivity, specificity, accuracy, positive and negative predictive values were calculated using standard formulae. The difference in detection accuracy of the two imaging modalities were compared using the McNemar's test for correlated proportions. Comparison between CRS scores were performed using the Fisher's exact test. Two tailed p values of <0.05 were considered significant.

To compare lesion interpretation with PET only imaging against that with PET/CT, the proportion of lesions that were scored as "definite" were compared for each observer. To assess whether PET/CT resulted in a change in inter-observer variability, the Kappa coefficient factor was used.

4.4 Results

4.4.1 Patient demographics

A total of 32 patients (20 men, 12 women) with a median age of 63 years (range 28-82 years) were included in the analysis. The sites of the primary tumour were in the colon in 27 (84%) patients and the rectum in 5 (16%). One patient presented with a synchronous CLM and a carcinoma of the sigmoid colon. One patient had received chemotherapy 2 months prior to being referred for an 18F-FDG PET/CT scan. The patients were followed-up for a median duration of 10 months (range 3-24 months).

4.4.2 18F-FDG PET/CT versus routine ceCT

A total of 55 suspicious lesions were assessed by a combination of clinical, radiological and surgical follow-up of patients. Histological verification was available on 44 (80%) of these, while the true nature of the remaining 11 (20%) lesions was confirmed through radiological follow-up with selective use of repeat ceCT, PET/CT, MRI or bone scans. Of the 55 lesions, 49 (89%) were confirmed to be malignant deposits and 6 (11%) were benign. Analysed on a lesion-by-lesion basis, the detection rates of the two imaging modalities are summarised and compared in table 4.1.

	Hepatic disease		Extrahepatic disease		Overall	
	ceCT	PET/CT	ceCT	PET/CT	ceCT	PET/CT
TP	30	29	6	15	36	44
TN	2	3	1	1	3	4
FP	1	0	2	2	3	2
FN	3	4	10	1	13	5
Total	36	36	19	19	55	55
SENS (%)	91	88	38	94	73	90
SPEC (%)	67	100	33	33	50	67
PPV (%)	97	100	75	88	92	96
NPV (%)	40	43	9	50	6	44
ACC (%)	89	89	31	84	71	87

Table 4.1: Comparison of detection rates between 18F-FDG PET/CT and ceCT, analysed on a lesion-by-lesion basis. [TP = true positive, TN= true negative, FP= false positive, FN= false negative, SENS = sensitivity, SPEC= specificity, PPV= positive predictive value, NPP= negative predictive value, ACC= accuracy]

PET/CT correctly detected 44 of the 55 malignant lesions compared to ceCT, which detected 36 lesions (sensitivity 90% vs 73% respectively; $\chi^2 = 12.07$, $p = 0.0005$, McNemar's test). Overall, 18F-FDG PET/CT was also more specific than ceCT however this difference did not reach statistical significance (specificity 67% vs 50% resp.; $\chi^2 = 0$, $p = \text{NS}$). Region-based analysis showed the main differences between the imaging modalities to occur in detecting extrahepatic disease where the sensitivity of 18F-FDG PET/CT was again superior (94% vs 38%; $\chi^2 = 14.06$, $p = 0.0002$). However, the sensitivity and accuracy of the two imaging modalities for detecting / characterizing hepatic metastases was similar.

On a patient-by-patient analysis, the results of PET/CT were discordant with those of ceCT in 14 patients (44%). A more detailed breakdown of these results is summarised in figure 4.1.

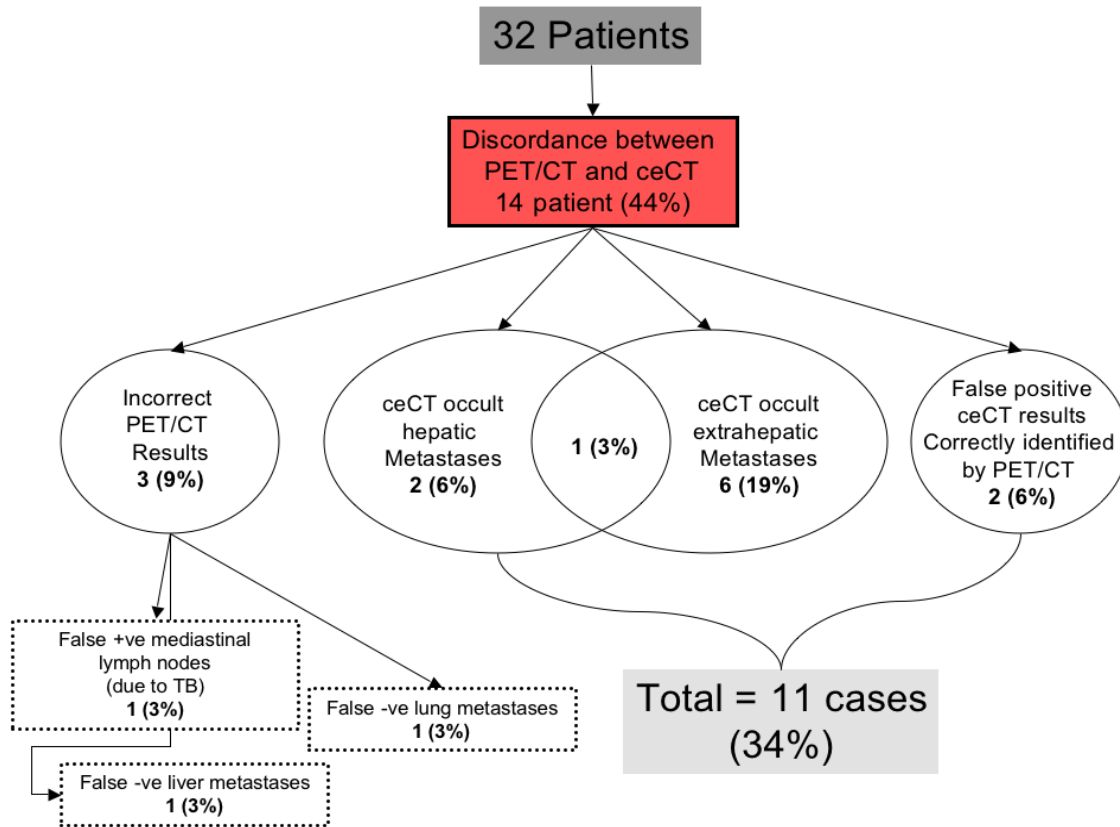


Figure 4.1: The distribution of discordant findings between ^{18}F -FDG PET/CT and ceCT

^{18}F -FDG PET/CT detected occult hepatic and extrahepatic disease in 9 cases (28%). In 2 patients (6%) where ceCT was interpreted as showing solitary liver metastases, the PET/CT correctly confirmed these to be benign lesions. Therefore overall, PET/CT provided additional information to ceCT in 11 patients (34%). The remaining 3 discordant results (9%) occurred due to incorrect (false positive or negative) PET/CT results. In one case, PET/CT detected ^{18}F -FDG avid mediastinal lymph

nodes, which in the presence of a solitary CLM were therefore considered to be metastatic deposits. Histological confirmation using a trans-oesophageal biopsy of one of these lymph nodes confirmed active tuberculosis. The patient therefore underwent a successful hepatic resection following initiation of anti-tuberculous therapy. This case is illustrated in figure 4.2. In the remaining two cases, PET/CT yielded false negative results in detecting liver and lung metastases, both of which were attributed to a lesion size of less than 1cm.

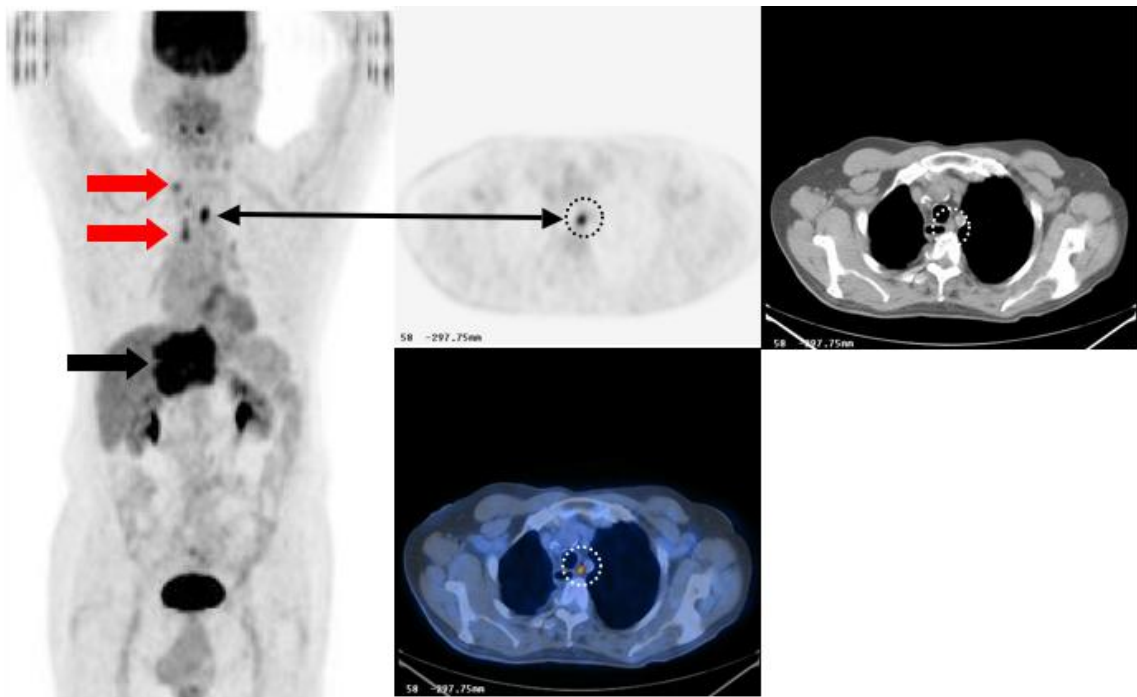


Figure 4.2: *18F-FDG PET/CT study demonstrating the presence of false positive hilar and mediastinal lymph nodes. A large solitary liver metastasis can be seen occupying the right lobe of the liver (Thick black arrow, MIP image). 3 further 18F-FDG avid hot-spots were also seen in the thorax (Thick red and thin black arrows). Axial PET, CT and PET/CT images clearly demonstrating one of these tracer avid lesions to be a para-oesophageal lymph node, which on biopsy was confirmed to be active tuberculosis.*

4.4.3 The impact of 18F-FDG PET/CT on management

18F-FDG PET/CT resulted in a change in the routine management of 11 patients (34%). Of these, the management of 8 patients (25%) were positively impacted as 18F-FDG PET/CT lead to a correct change in diagnosis in one case (a solitary CLM suggested on 18F-FDG PET/CT to be consistent with a hepatocellular carcinoma) and appropriately altered the radiological staging of the remaining 7 patients. Of note is one case where a solitary hepatic lesion seen on ceCT was shown to be negative on 18F-FDG PET/CT. This lead to avoidance of an unnecessary surgery and the patient was radiologically monitored. At the time of writing, the patient had remained disease free over a follow-up period of 19 months. Of the above 11 patients, 18F-FDG PET/CT was also deemed to have a negative impact in 3 cases (9%) due to false negative and false positive results. A summary of the impact of PET/CT on management is detailed in table 4.2.

Management		No. patients
Positive impact		
Upstage disease	Chemotherapy	2
	Chemotherapy + Monoclonal antibody Rx	1
	Radiofrequency ablation	1
	Chemotherapy + Radiofrequency ablation	2
Down staging of disease	No intervention, patient monitored	1
Change of diagnosis	Diagnosis change from CLM to hepatocellular carcinoma	1
TOTAL		8 (25%)
Negative impact		
Incorrect down staging	False negative lung metastases; patient underwent liver resection -> developed progressive lung disease at 10 months	1
	False negative liver metastases -> post chemotherapy => patient assumed to have dormant disease, and monitored without intervention -> disease recurrence at 4 months	1
Incorrect up staging	False positive mediastinal lymph nodes -> patient underwent additional invasive procedure (transoesophageal biopsy); histology confirmed active TB	1
TOTAL		3 (9%)

Table 4.2: *The impact of 18F-FDG PET/CT on management of patients with CLM.*

4.4.4 Correlation between CRS and the clinical yield of 18F-FDG PET/CT

Table 4.3 displays the distribution of clinical risk scores (CRS) for the study group. The median CRS was 2. Using this value, CRS were dichotomised into high and low risk groups.

CRS	n	%
0	6	19
1	8	25
2	11	34
3	4	13
4	2	6
5	1	3

Table 4.3: The distribution of Clinical Risk Scores (CRS) for the study group

Overall, no significant difference was found in the proportion of discordant findings between 18F-FDG PET/CT and ceCT findings in the low and the high CRS groups (CRS < 2 = 12 (48%) vs CRS > 2 = 3 (43%); $p=NS$). However, a high CRS (>2) corresponded to a higher proportion of ceCT occult hepatic and extrahepatic disease being detected with PET/CT. Although at a CRS of >2 PET/CT detected no additional liver metastases (3 vs 0 for PET/CT and ceCT respectively), proportionately more occult extrahepatic disease was detected. None of the above however achieved statistical significance.

In terms of impact on management, 18F-FDG PET/CT resulted in change in management of 48% of cases with a low CRS, compared to 29% for a high CRS. This difference again did not achieve statistical significance. The results are summarised in table 4.4.

18F-FDG PET/CT findings	CRS < 2		CRS >2		Fishers exact test (2 tailed) <i>p</i>
	n	%	n	%	
Discordant findings with ceCT	12	48	3	43	NS
Detected occult disease not seen on conventional imaging (ceCT)	8	32	3	43	NS
Additional liver metastases	3	12	0	0	NS
Additional extrahepatic disease	5	20	3	43	NS
Management change	12	48	2	29	NS

Table 4.4: Break down of results according to dichotomised Clinical Risk Scores (CRS); Low score = <2; High score >2

4.4.5 The incremental value of PET/CT over that of imaging with PET alone

The aim of this section of the study was to test the hypothesis that PET/CT image fusion allows for a more accurate and definite interpretation of abnormal lesions, compared to imaging with PET alone. Interestingly both observers detected a greater number of abnormal 18F-FDG avid foci on the PET only images compared to PET/CT. This was in keeping with the finding that the certainty of lesion localization (ie: the proportion of lesions scored < 2) was also poorer on the PET only scans. For both observers, PET/CT resulted in an improvement in the certainty of lesion interpretation, with an average of 15% improvement in the certainty of lesion localization and 12.5% improvement in the certainty of lesion characterization. These findings are summarized in table 4.5.

	Observer A		Observer B	
	PET Only	PET/CT	PET Only	PET/CT
Total no of lesions	48	44	53	46
Definite localization	85%	98%	78%	94%
Improvement	+13%		+17%	
Definite diagnosis	86%	99%	72%	94%
Improvement	+13%		+22%	

Table 4.5: Tabulated summary of the difference in the certainty of lesion interpretation with PET only imaging compared to that with PET/CT. Results showed PET/CT imaging to improve the certainty of lesion localization and as well as the certainty of lesion characterization (ie: certainty of diagnosis) compared to PET imaging alone.

Next the inter-observer variability between the two observers was assessed using the Kappa coefficient factor. As shown in table 4.6, PET/CT also resulted in an improvement in concordance between the observers, both in terms of lesion localization as well as lesion characterization.

	PET only		PET/CT	
	Kappa coefficient	95% CI	Kappa coefficient	95% CI
Anatomical Localization	0.21 (Poor)	-0.08 - 0.51	0.66 (Good)	0.36 - 1.28
Lesion Characterization	0.62 (Good)	0.57 - 0.87	0.88 (V. good)	0.77 - 1.00

Table 4.6: *The difference in inter-observer variability between PET only scans and PET/CT. PET/CT resulted in a better correlation between the observers in both lesion localization and lesion characterization.*

4.5 Discussion

The role of PET in the routine diagnosis and staging of primary CRC still remains under dispute. However, the strength of PET in assessing the extent of metastatic burden has been a particular focus of attention. The evidence to date has consistently shown 18F-FDG PET to be more sensitive and specific than conventional imaging (CT) in detecting hepatic and extrahepatic disease in colorectal cancer. The meta-analysis by Heubner et al. (2000) gave 18F-FDG PET a weighted average sensitivity and specificity of 96% and 97% respectively for detecting hepatic metastases. It is however important to note that many of the earlier studies compared PET data with CT results that were not homogenous, thus arguably suggesting a bigger difference between the two modalities than may be present. Advances in contrast enhanced, multidetector CT technology, coupled with its widespread use has also lead to a narrowing of the gap between the detection accuracy of CT and PET, so much so that two recently published studies have failed to show any difference in sensitivities between the two modalities in detecting intrahepatic metastases (Selzner et al. 2004; Truant et al. 2005).

Our study population consisted of routine referrals to a tertiary liver unit where management decisions were made in a multidisciplinary setting. During the study period, the multidisciplinary team came to a consensus decision to included 18F-FDG PET/CT as part of the routine diagnostic work-up of patients with suspected CLM. This decision was principally made on the grounds of the availability of a PET/CT scanner at our institution. However, it must be noted that at the time of writing, this did not mirror the situation nationally. None the less, it provided the opportunity to compare the routine application of ceCT and PET/CT.

The primary aim of the study was to compare the diagnostic accuracy of the two imaging modalities. Overall for all lesions analysed, 18F-FDG PET/CT was more sensitive, specific and accurate than ceCT (Sensitivity 90% vs 73%, Specificity= 67% vs 50, Accuracy= 87% vs 71% for 18F-FDG PET/CT and ceCT respectively). Subgroup analysis however showed this difference to be mainly as a result PET/CT's accuracy in detecting extrahepatic disease, whereas the sensitivity of the two imaging modalities in detecting liver metastases was similar. This finding is consistent with that reported by Truant et al. (2005) where the sensitivities for PET and CT were found to be equal (sensitivity of 79% for both). Furthermore similar to our results, their study also demonstrated PET to be overall more specific in detecting liver metastases. It is important to note that neither ceCT nor PET/CT could detect all lesions. With PET/CT in particular, there were 5 false negative lesions, of which 4 were intrahepatic and one extrahepatic (lung) metastasis. Majority of these (5/8 lesions) were also small, sub-centimetre hepatic lesions. Although a size threshold of 5-8 mm is frequently reported as the spatial resolution of 18F-FDG PET, the actual volume of disease is the main determinant of whether a lesion accumulates enough 18F-FDG to be detected. In the lungs, motion artefact can also lead to the partial volume effect, thus resulting in a lesion being missed. Within the liver, the detection of low grade tracer uptake is further hampered by background accumulation of 18F-FDG in hepatocytes, thus resulting in under-detection of hepatic metastases (Beets et al. 1994).

In detecting small hepatic lesions, the CT component of PET/CT did not add to its diagnostic accuracy, as our established PET/CT imaging protocols acquires the CT images at a lower power (80mA), thicker slice width (4.5 mm) and without the use of

the intravenous contrast agents. The use of high-density contrast agents have been suggested to results in image artefacts by affecting the CT attenuation correction of PET images. The use of contrast material has more recently been re-examined (Blodgett et al. 2006; Mawlawi et al. 2006). Mawlawi and colleagues in fact demonstrated that the maximal variation in SUV values occurred where there was maximal accumulation of contrast material (eg: the heart, major vessels). In the remaining tissue compartments, SUV changes were minimal and thus considered clinically insignificant. In the future therefore, it is likely that in selective cases PET/CT may be performed with a CT acquired at full diagnostic capability and with the use of intravenous contrast agents. The feasibility of this approach requires further scrutiny in future studies, with particular focus on the resource implications of adding a full diagnostic CT to the routine dedicated PET/CT protocols.

The strength of ¹⁸F-FDG PET lies in its accuracy of detecting extrahepatic disease. In our series, 9 out of 14 discordant cases (64%) occurred due to PET/CT detecting additional (occult) metastases missed on ceCT. Of these, 6 cases were found to have occult extrahepatic disease, 2 cases with occult liver metastases and 1 case with both. The remaining 2 discordant cases were due to false positive ceCT findings being correctly characterized by PET/CT. Thus excluding the 3 incorrect PET/CT results, PET/CT provided useful additional information to ceCT that impacted the clinical management of patients in over one third of cases (11/32, 34%).

When considering the impact of ¹⁸F-FDG PET/CT on patient management, incorrect results also needed to be taken into account. Overall, PET/CT resulted in a change in the routine management (as planned following the ceCT results) of 11 patients (34%).

Of these, 8 cases (25%) were considered to be positively impacted by PET/CT, as the final PET/CT result changed the clinical management for a more appropriate treatment regimen. Here the accuracy of PET/CT in detecting metastases missed by conventional imaging was its predominant strength, whereby 6 patients were correctly upstaged thus resulting in avoidance of futile surgery. False positive and false negative results on the other hand lead to an adverse clinical impact as additional intervention was undertaken in order to confirm the nature of these findings. It is noteworthy that our study group represents a cohort of patients with suspected CLM who were routinely assessed with both ceCT and PET/CT. In 2 cases where PET/CT yielded false negative results, one patient underwent a hepatectomy but whom on subsequent follow-up was found to have multiple enlarging lung metastases. Incorrect PET/CT findings can be argued to have resulted in an inappropriate management of the patient, with resultant need for additional invasive investigations (e.g: trans-oesophageal biopsy of mediastinal lymph nodes; figure 4.2) and possibly poorer long-term outcomes in the two patients who were incorrectly down staged. While limitations of PET/CT may be subject to further scrutiny, it must be noted that in our series, the 9% negative impact of PET/CT was in face of a 24% positive impact. When compared to the overall sensitivity and specificity of 73% and 50% for ceCT, there still remains a strong argument for the routine use of PET/CT in the routine pre-operative assessment of CLM.

As previously mentioned in the introductory sections, the main limitations of imaging with a stand-alone PET scanners have been their relative lack of anatomical resolution, which when assessing intra-abdominal pathology can lead to diagnostic uncertainty and inaccurate results. Dual modality imaging with PET/CT can

potentially overcome this problem through accurate co-registration of biological (PET) and anatomical (CT) data. In staging primary CRC, Cohade and colleagues have shown this to reduce diagnostic uncertainty in 50% of cases and improve anatomical localisation by up to 30% (Cohade et al. 2003a). Our results were also in agreement with the above. Two aspects of image interpretation were assessed namely that of the certainty of lesion localization and the certainty of lesion characterization. The latter examined the certainty by which the reporting physician would interpret an ^{18}F -FDG avid lesion as malignant or benign. Our results demonstrated that for both observers, PET/CT lead to a more certain anatomical localization of lesions with an average improvement of 15%. There was also an improvement in lesion characterization by an average of 12.5% between the observers with PET/CT compared to PET alone. As is the case with visual assessment of all imaging modalities, there can be subjective differences between reporters. When inter-observer variability was also examined, PET/CT resulted in a better concordance between observers compared to that seen with PET alone. Although the results are from a limited number of patients with a heterogeneous spread of metastatic deposits, overall indication are that PET/CT image fusion can improve the accuracy of image interpretation in the routine clinical setting.

The final aim of this study was to examine if CRS could be useful as a means of selecting patients who would most benefit from having a PET scan. The rationale for this stems from the fact that although PET may provide additional information to conventional imaging, its clinical impact ranges between 20-40%. In other words, up to 80% of cases may not benefit from an additional PET scan in their management algorithm. Given the cost and availability of PET scanners, justification for its routine

use can therefore be made if a tight selection criteria for imaging is made. Here we utilized CRS as means of dichotomizing patients into a low and high risk groups to see if it would help select the most appropriate patients for PET imaging. Unlike the study by Schussler-Fiorenza et al. (2004), the cut-off point in our study was the median CRS for the cohort. Overall no significant difference was seen between the two CRS groups in terms the proportion of discordant findings between ceCT and PET/CT, the detection of occult disease missed on ceCT and the proportion in which PET/CT resulted in a change in management. In terms of the change in management however, there seemed to be a trend towards a low CRS (<2) yielding clinically more relevant PET/CT results, where management change was seen in 48% of cases in the low risk group compared to 29% in the high risk CRS group. This finding further suggests that 18F-FDG PET/CT is unlikely to alter management patient with CLM who are found to have widespread metastatic disease. Given the small sample size of this study, no concrete conclusions can be made from this. However overall indications are that CRS is unlikely to be value in selecting which patients should undergo PET/CT imaging in pre-operative staging of colorectal liver metastases.

4.6 Conclusions

¹⁸F-FDG PET/CT is a powerful adjunct to routine ceCT in the pre-operative staging of patients with CLM. The advantage of PET/CT fusion over PET alone is in improving the certainty of lesion localization and interpretation, thus giving a more robust means of assessing patients in the routine clinical setting.

When compared to ceCT, discordant findings occurred predominantly as a result of ¹⁸F-FDG PET/CT detecting additional metastases at extra-hepatic sites. The sensitivity and accuracy of detecting hepatic lesions were similar for the two techniques. Although PET/CT resulted in a change in the routine management of 34% of cases, false positive and negative results did occur that made a negative impact on patient management. Therefore PET/CT was deemed to be clinically useful in 25% of cases. Finally, CRS was found not to be a clinically useful tool for pre-selecting patients in whom PET/CT would provide the most useful information.

CHAPTER 5

Targeting proliferation in pancreatic cancer using ^{18}F -FLT PET –

A comparative study with ^{18}F -FDG.

5.1 Background

In previous chapters, the role of 18F-FDG PET/CT in the routine management of pancreatic cancer was examined. Targeting glycolysis in cancer inherently gives 18F-FDG its exquisite sensitivity. However, in the presence of an inflammatory process, problems with specificity emerge. While results from chapter 3 demonstrated that a negative 18F-FDG PET/CT scan may be helpful in excluding malignancy, false positive results occurred in two cases of mass forming pancreatitis and in one case of a tuberculous deposit in the pancreas.

As outlined in chapter 1.6.5, 18F-FLT is suggested to be more tumour specific as compared to 18F-FDG. van Waarde et al. (2004) tested this hypothesis *in vivo* in an animal model of malignancy versus inflammation. While 18F-FDG accumulated in both the foci of inflammation and malignancy, 18F-FLT uptake seemed to be confined to the cancer xenograft. At the time of writing, there had been no published reports of imaging pancreatic cancer with 18F-FLT PET. The feasibility of its use has been suggested from an *in vitro* study by Seitz et al. (2002), who showed human pancreatic cancer cell lines to have a higher expression and activity of pyrimidine salvage enzyme TK-1. Consequently, a higher rate of 18F-FLT uptake was demonstrated in pancreatic cancer cell lines compared to normal pancreatic cells and those of chronic pancreatitis. In addition to its tumour specificity, quantifying proliferation with 18F-FLT PET may also have important prognostic implications. This chapter therefore sets out to examine the feasibility of imaging pancreatic cancer using 18F-FLT PET.

5.2 AIMS

The aims of this chapter were:

1. to examine the feasibility of imaging pancreatic cancer with ^{18}F -FLT PET and compare its accuracy to the routine PET tracer ^{18}F -FDG.
2. to investigate whether ^{18}F -FLT uptake *in vivo* correlates with proliferative activity of tumours as measured by Ki-67 immunostaining.
3. to investigate whether ^{18}F -FLT uptake correlates with overall survival.

5.3 Methods

5.3.1 Patient recruitment

Patients were prospectively recruited from routine referrals to the local hepatobiliary unit. Ten patients with clinical and radiological suspicion of pancreatic cancer were included. The diagnosis of pancreatic adenocarcinoma was histologically confirmed in all ten cases. Following routine staging with pancreatic protocol contrast enhanced CT (ceCT), each patient underwent a whole body PET/CT scan using the routine tracer ¹⁸F-FDG and the thymidine analogue tracer ¹⁸F-FLT. The PET/CT studies were performed with a median intervening period of 3 days (range 1-12 days) between the two.

The study was conducted following local hospital ethics committee approval and with full informed consent of the patients as outlined in chapter 2.1.

5.3.2 Imaging protocols

Routine staging with pancreatic protocol ceCT and imaging protocols for whole body ¹⁸F-FDG and ¹⁸F-FLT PET/CT scans are as described in chapter 2.

The median administered doses of tracers were 374 MBq (range 342 – 412) for ¹⁸F-FDG and 313 MBq (range 229 – 435) for ¹⁸F-FLT. The PET images were acquired at a median of 61 minutes post-injection for both tracers. The CT component of PET/CT was acquired without oral or intravenous contrast enhancement.

5.3.3 Image Analysis

The ¹⁸F-FDG and ¹⁸F-FLT PET images were qualitatively (visually) assessed by two experienced (consultant grade) nuclear medicine physicians. Each observer was aware of the presence of a suspicious pancreatic mass, but was blinded to the final

histological diagnosis. The final results were reached by consensus between the two observers.

Lesions were deemed as positive where focal tracer accumulation was above that of the surrounding normal tissues. A 3-point grading system was also used as a visual measure of the intensity of tracer accumulation for each lesion. These were recorded as;

- - = A definite negative lesion
- +/- = A positive but low grade
- + = A definite positive lesion

Tracer uptake was semi-quantified using SUVs (corrected for body weight) and using 1cm circular ROIs. SUV_{Max} and SUV_{Mean} values were determined semi- automatically using the Xeleris[®] workstation. The methodologies used for SUV measurements are detailed in chapter 2.4.2.

Where a lesion was deemed to be “negative” for 18F-FLT uptake, the region of interest was placed over the anatomical area corresponding to the lesion detected on the ceCT and the CT component of PET/CT. These were correlated with the 18F-FDG PET results.

5.3.4 Histological analysis

5.3.4.1 Specimen preparation

All histological specimen were examined by a senior histopathologist, blinded to the results of the PET scans. The specimens were obtained from whole tumour resections in 4 patients and percutaneous core biopsies in the remaining 6. Routine histological examination was performed on 4µm thick Haematoxylin and Eosin (H&E) stained sections. Immunohistochemical analysis was performed on 3µm thick sections cut from paraffin blocks and dried overnight at 60° C. Sections were taken from xylene (2 changes) and ran twice through graded alcohols (100% and 70%) and finally water. Antigen retrieval was performed by pressure cooking for 2 minutes in a conventional 15 lb pressure cooker and the slides were then flushed with running tap water. The slides were then rinsed in 0.05% Tween-20 in Tris buffered saline (TBS-T) in an incubation tray. Endogenous peroxidase activity was blocked for 10 minutes using a commercially available peroxidase blocking solution (DAKO UK Ltd, cat #S2023). The sections were rinsed in TBS-T and then the primary mouse monoclonal antibody MIB-1 (DAKO UK Ltd, cat #M7240) diluted 1/50 in TBS was applied for 60 minutes at room temperature.

The sections were rinsed in TBS-T and secondary antibody (goat anti-rabbit/mouse), (DAKO UK Ltd, cat #K5001) was applied for 30 minutes. The sections were again rinsed in TBS-T and streptavidin-horseradish peroxidase (DAKO, UK Ltd, cat #K5001) was applied for 30 minutes. After rinsing in TBS-T, diaminobenzidine, (DAKO, cat #K5001) was used as a chromogen and applied for 7 minutes. A haematoxylin counter stain was applied for 2mins. The sections were dehydrated

through graded alcohols (70% and 100%), cleared in xylene (2 changes) and mounted with DPX resin.

5.3.4.2 Examination of histological sections

Sections of tumour were first identified on the H&E slides. Twenty high power fields (x40 objective lens) were examined per case and the total number of tumour nuclei were counted. The corresponding area was then examined for positive staining with MIB-1 antibody. Positive nuclear staining was regarded as staining of the entire nucleus. Nuclei with no staining or only nucleolar staining were regarded as negative. A labelling index (LI) was calculated as a percentage of positive staining nuclei out of all nuclei examined.

5.3.5 Statistical analysis

All statistical calculations were performed using the GraphPad statistical Software (V 4.0, California, USA). Correlations between tracer SUVs, and MIB-1 LI were performed by linear regression analysis and Pearson's correlation coefficient. Survival analysis as a function of the SUVs was estimated by the Kaplan-Meier method and compared by the log rank test. p values <0.05 were considered significant.

5.4 Results

5.4.1 Patient demographics and tumour characteristics

Ten patients with a median age of 64 years (range 55-81 years) were included in the study. All pancreatic lesions were histologically confirmed as adenocarcinoma. Patient demographics and tumour characteristics are summarised in table 5.1. Overall, 4 (40%) patients underwent a resection with curative intent. The remaining 6 (60%) patients were deemed to have an inoperable disease on routine imaging (ceCT) and were treated palliatively.

Patient Number	Sex	AGE (y)	Site of tumour	Treatment	Histology	Grade	Conventional Staging	18F-FDG PET	18F-FLT PET	18F-FDG PET		18F-FLT PET		MB 1 U (%)
										SUV _{max}	SUV _{mean}	SUV _{max}	SUV _{mean}	
1	M	59	Head	Chemotherapy	AC	Med-poor	T4N0M0	+	+/-	5.5	4.8	2.8	2.8	41.1
2	M	63	Head	Chemotherapy	AC	Med-poor	T4N0M0	+	-	7.5	5.9	2.8	2.6	37.3
3	M	64	Tail	Resection	AC	Med-poor	T3N0M0	+	+/-	6.2	4.8	2.7	2.1	23.0
4	M	54	Head	Resection	AC	Med-poor	T3N1M0	+	-	3.4	2.5	1.8	1.0	11.6
5	M	57	Head	Resection	AC	Mod	T3N0M0	+	+/-	5.8	5.3	3.0	2.8	43.2
6	F	58	Head	Resection	AC	Mod	T3N1M0	+	+/-	6.7	5.8	2.6	1.5	13.6
7	M	70	Head	Chemotherapy	AC	Med-poor	T4N0M0	+	-	3.2	2.8	2.2	1.9	21.8
8	F	70	Head	Chemotherapy	AC	Mod	T4N0M0	+	+	10.5	7.2	3.9	3.3	27.5
9	F	81	Head	Chemotherapy	AC	Mod	T4N0M0	+	+/-	5.8	4.4	4.8	3.7	50.5
10	F	67	Head	Chemotherapy	AC	Med-poor	T4N0M0	+	+	6.7	5.0	4.9	3.4	37.0

Figure 5.1: The demographics and tumour characteristics of pancreatic cancer patients imaged with 18F-FDG and 18F-FLT PET. [AC=adenocarcinoma; +=definitely positive lesion, +/-=Positive but low grade tracer uptake, -=definitely negative lesion]

5.4.2 Detection of primary pancreatic disease – comparison between 18F-FDG and 18F-FLT PET imaging

18F-FDG PET/CT visualized all 10 pancreatic tumours, whereas 18F-FLT visualized 7 out of 10 (70%). Of these, 2 showed a strong (definitely positive 18F-FLT uptake) and in the remaining 5, 18F-FLT uptake was interpreted as low grade (See table 5.1). In one patient, 18F-FDG PET/CT detected a focal colonic lesion, which was later found to be an adenomatous polyp. This lesion was not visualised on the 18F-FLT PET/CT scan.

In two patients who underwent a pancreatic resection, microscopic peri-pancreatic nodal (N1) spread was detected. No nodal or extra-pancreatic disease was detected by either tracer. This was confirmed on routine imaging, clinical and surgical follow-up of the patient.

Table 5.1 also summarises the SUV measurements for 18F-FDG and 18F-FLT PET detected lesions. On average, pancreatic lesions showed a significantly higher 18F-FDG uptake compared to 18F-FLT (SUV_{Max} : 6.1 vs 3.1 respectively, $p=0.0005$; SUV_{Mean} : 4.9 vs 2.5 respectively, $p=0.0002$; Paired t-test). No correlation was observed between 18F-FDG and 18F-FLT SUVs (figure 5.1)

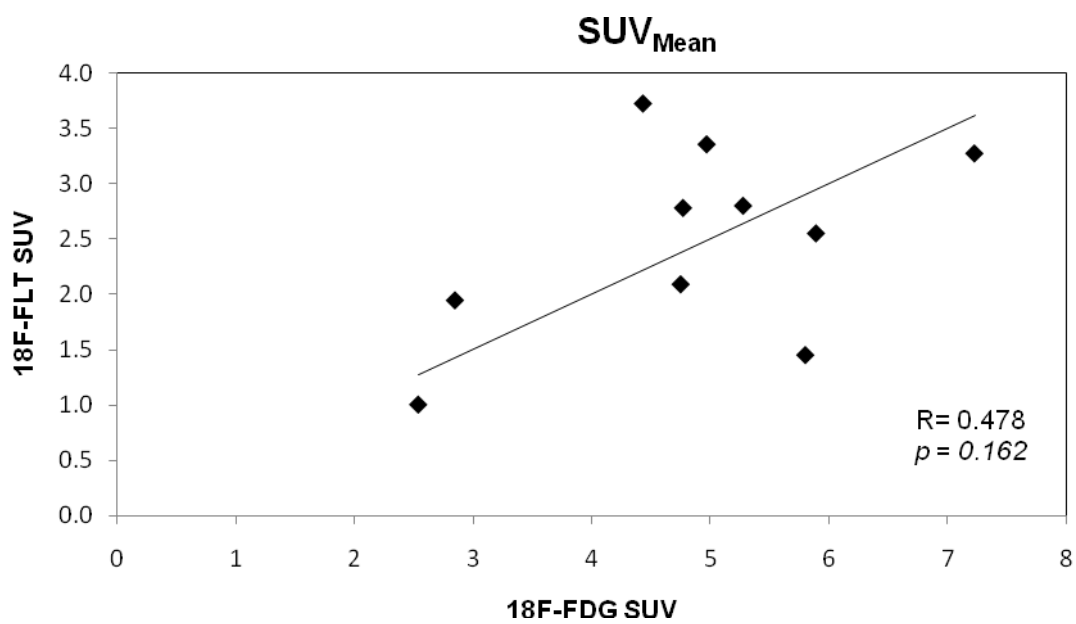
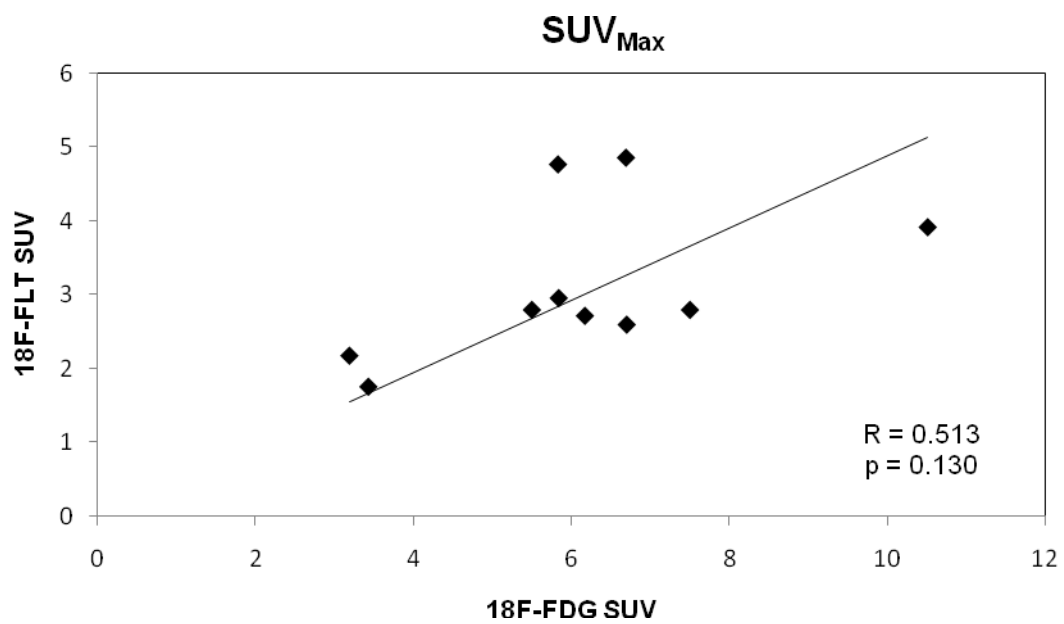
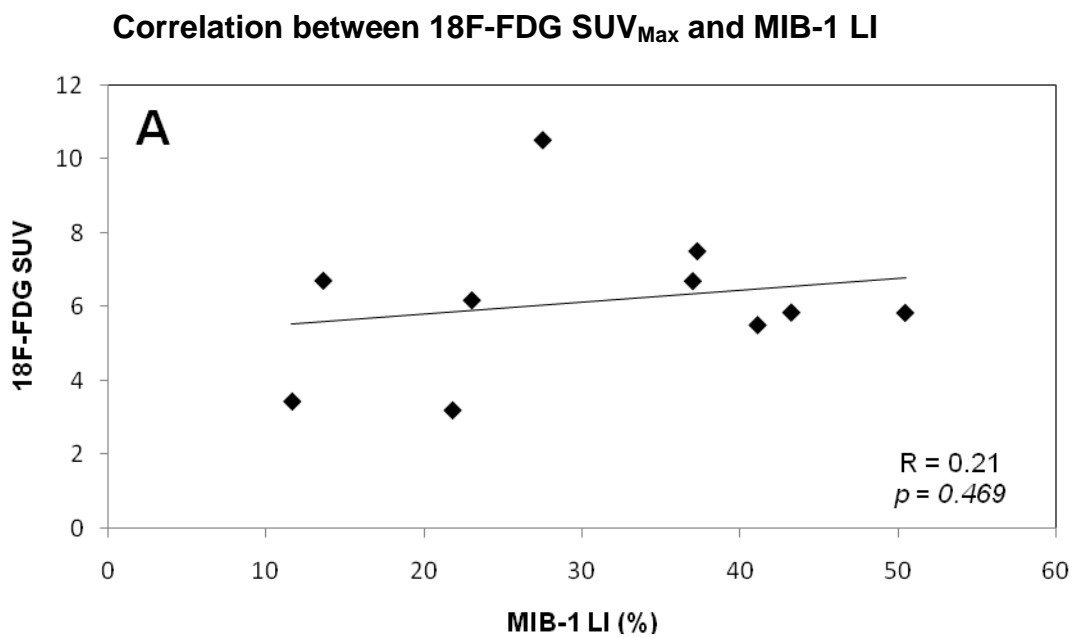


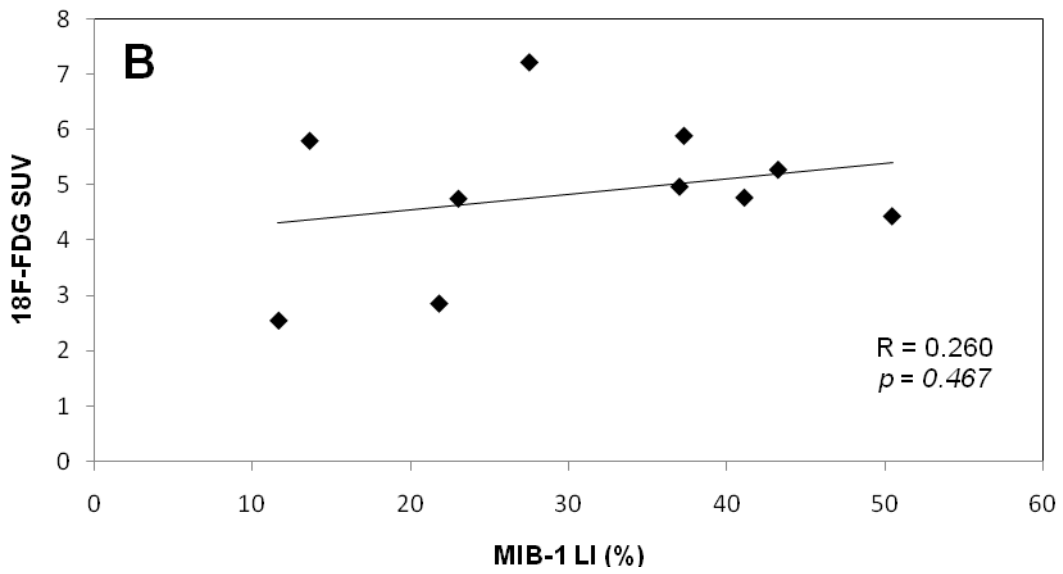
Figure 5.1: Graphs representing the correlation between tumour SUVs for the two tracers (18F-FDG vs 18F-FLT)

5.4.3 Correlation between tracer uptake and proliferative activity

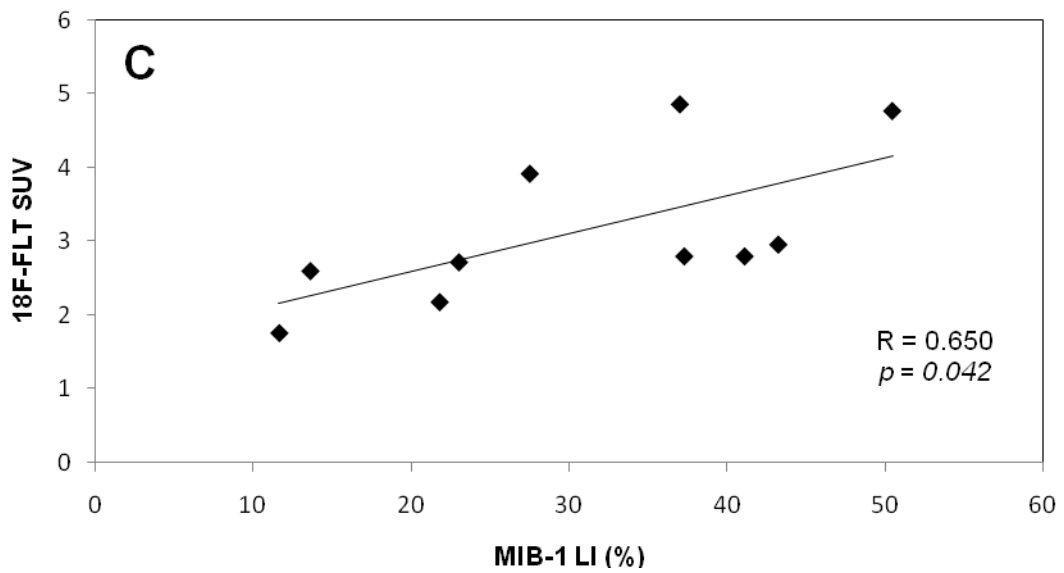
The median MIB-1 LI was 15.2% (range 11.6 - 50.5). As demonstrated by graphs in figure 5.2, no correlation was detected between ^{18}F -FDG SUVs and MIB-1 LI (SUV_{Max} ; $R=0.21$, $p=0.469$; SUV_{Mean} ; $R=0.26$, $p=0.467$). However, ^{18}F -FLT SUVs showed a statistically significant correlation with MIB-1 labelling (SUV_{Max} ; $R=0.65$, $p=0.042$; SUV_{Mean} ; $R=0.86$, $p=0.0012$).



Correlation between 18F-FDG SUV_{Mean} and MIB-1 LI



Correlation between 18F-FLT SUV_{Max} and MIB-1 LI



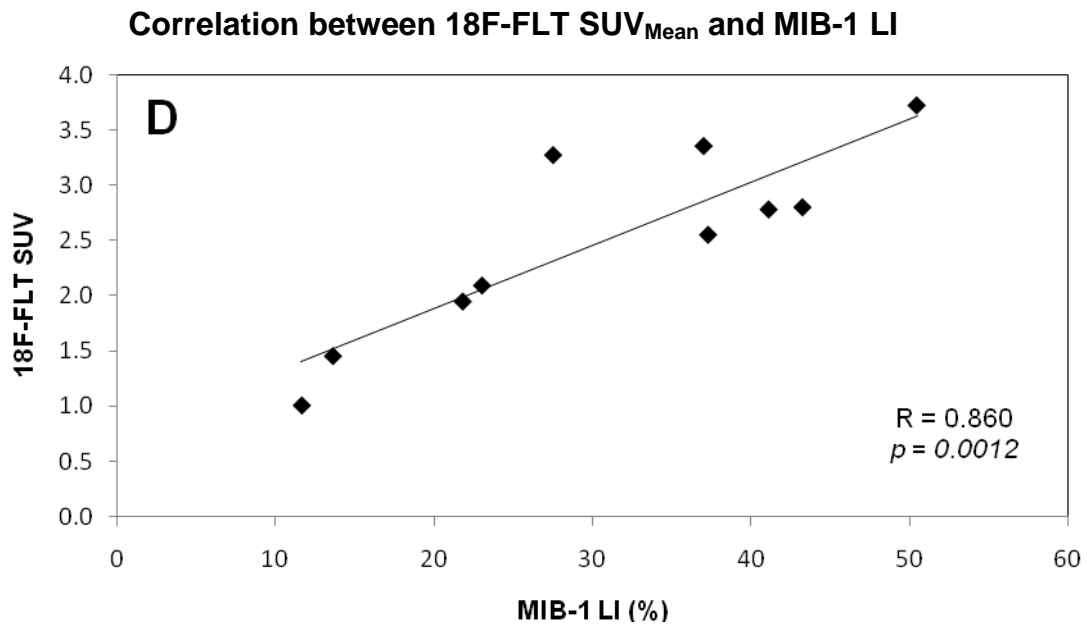


Figure 5.2 (A-D): Graphs illustrating the correlation between 18F-FDG and 18F-FLT SUVs and MIB-1 LI (%). A statistically significant correlation was seen between MIB-1 LI and 18F-FLT SUVs but not 18F-FDG SUVs (A&B).

Figure 5.3 below illustrates the three grades of ^{18}F -FLT uptake in relation to measured SUV_{Mean} and MIB-1 LI.

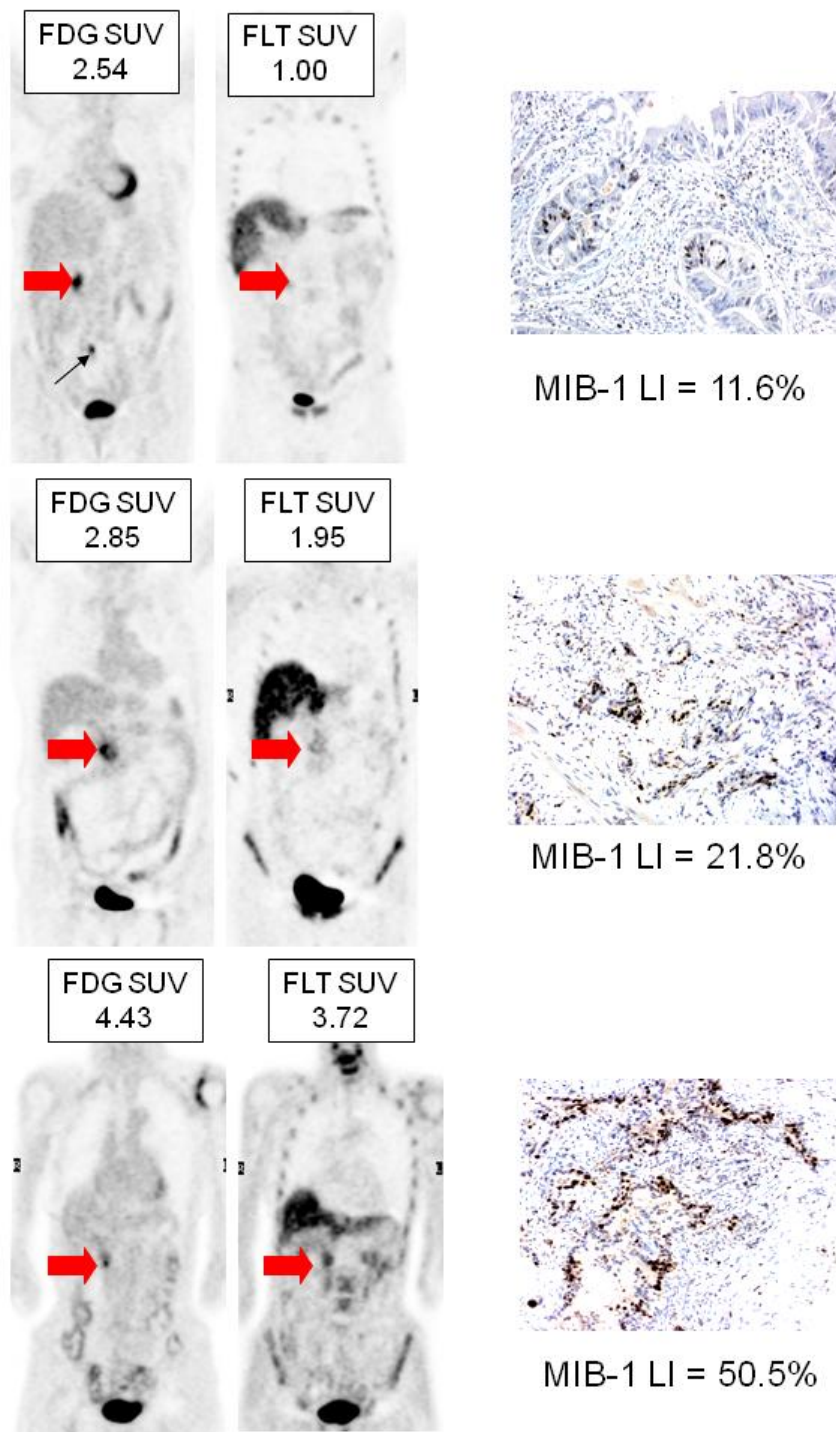
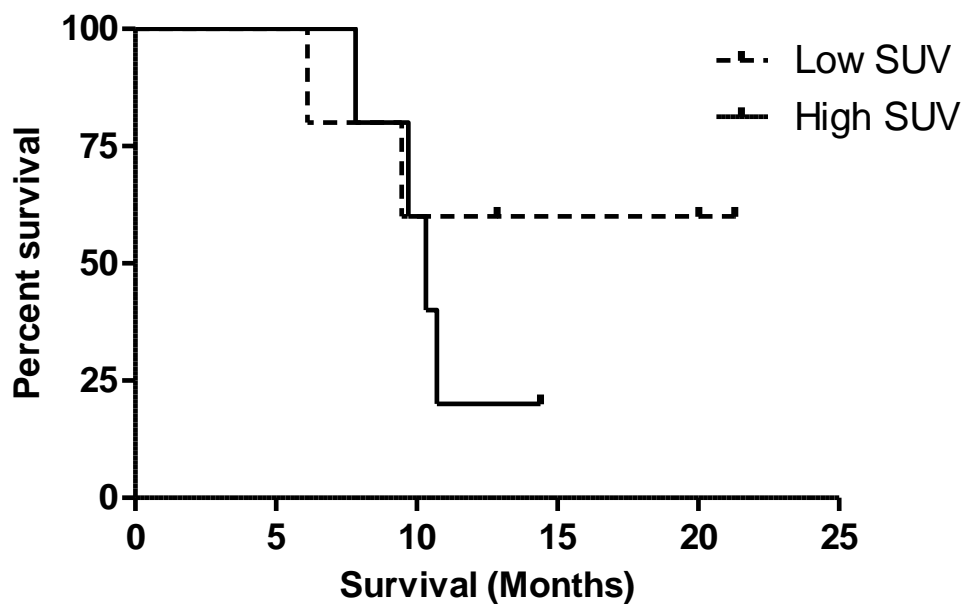


Figure 5.3: Comparative ^{18}F -FDG and ^{18}F -FLT PET images for three patients with pancreatic cancer demonstrating three grades of ^{18}F -FLT uptake and their corresponding MIB-1 LI. (Note: **Red arrows** represent the primary pancreatic lesion; **black arrow** represents tracer excretion in the renal tract).

5.4.4 Correlation tumour SUVs and overall survival

The patients were followed-up for a median duration of 10.52 months (range 7.82 - 21.30). SUV_{Mean} values were dichotomised into “high” and “low” levels using their respective mean values as cut-off points (18F-FDG $SUV=4.85$; 18F-FLT $SUV=2.50$). As seen in figure 5.4 (A-B), there was a divergence of survival curves between high and low tracer SUVs for both 18F-FDG and 18F-FLT. However, differences between groups did not reach statistical significance (18F-FDG SUV_{Mean} : $p=0.420$; 18F-FLT SUV_{Mean} : $p=0.097$; Log rank (Chi squared) test).

A: Survival difference between low & high 18F-FDG SUV_{Mean} (SUV threshold = 4.85)



**B: Survival difference between low & high ^{18}F -FLT SUV_{Mean}
(SUV threshold = 2.50)**

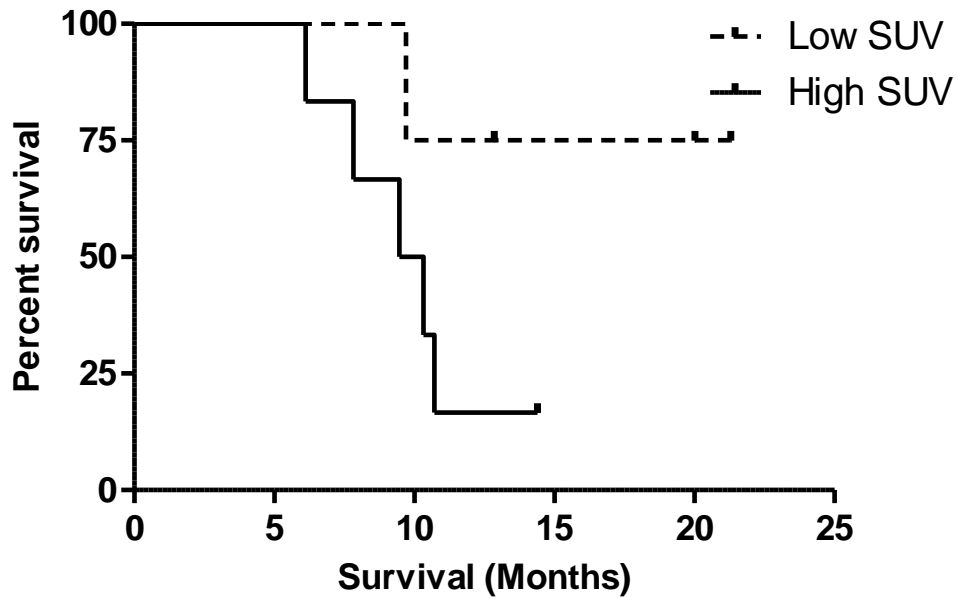


Figure 5.4: Kaplan-Meier survival graphs of patients with high and low tracer SUVs. No statistically significant differences in overall survival was seen between the two SUV thresholds for (A) ^{18}F -FDG SUV_{Mean} and (B) ^{18}F -FLT SUV_{Mean} .

5.5 Discussion

This pilot study examined the use of the novel thymidine analogue tracer ^{18}F -FLT in imaging pancreatic cancer. The aims of this study were three fold. Firstly the accuracy of imaging with the two tracers in visualising pancreatic lesions were compared. Secondly, it tested the hypothesis that tumour ^{18}F -FLT uptake correlates with the proliferation fraction of the tumour and finally, it examined whether tracer SUVs could be used as a prognostic marker in predicting survival.

Overall, pancreatic lesions demonstrated a significantly higher ^{18}F -FDG accumulation compared to ^{18}F -FLT. This resulted in all 10 lesions being correctly identified with ^{18}F -FDG PET (sensitivity of 100%), whereas the lower sensitivity of ^{18}F -FLT PET resulted in visualisation of only 7 lesions (sensitivity of 70%). This difference between the two tracers was also demonstrated semi-quantitatively using tracer SUVs. Overall, SUVs (compared as average SUV_{Max} and SUV_{Mean} measurements) were higher for ^{18}F -FDG compared to ^{18}F -FLT.

It is noteworthy however that 5 out of 7 ^{18}F -FLT avid lesions showed low-grade tracer accumulation, so much so that they were only reliably detected by correlating the PET findings with the CT component of PET/CT. If only the PET images were viewed, the true sensitivity of ^{18}F -FLT PET could have been 20%, where only 2 out of 10 lesions were confidently detected by the PET only images. In the two cases where the primary lesions were found to be highly ^{18}F -FLT avid, maximum SUV (SUV_{Max}) values were found to be greater than 4. This may represent an upper threshold at which ^{18}F -FLT avid pancreatic tumours may become visually detectable. As all 10 lesions were visualized with ^{18}F -FDG and not ^{18}F -FLT PET, tumour blood

supply (and thus tracer delivery) is unlikely to be a limiting factor in 18F-FLT uptake. Therefore mechanisms such as the transport of tracer into cells or the levels of the phosphorylating enzyme TK-1 may be implicated. *In vitro*, Seitz et al. (2002) have shown pancreatic cancer cell lines to have a markedly increased TK-1 activity and thus increased 18F-FLT uptake. In their study, TK-1 mRNA levels in pancreatic cancer specimen were shown to be significantly higher than that for chronic pancreatitis and cells from a normal pancreas. While this may be true for transformed cells *in vitro*, our results suggest that this may not be applicable to whole tumour 18F-FLT uptake *in vivo*. Therefore, future *in vivo* studies correlating 18F-FLT uptake, TK-1 activity and proliferation indices such as Ki-67 expression would provide important additional information to help better understand the difference observed between 18F-FLT and 18F-FDG in pancreatic cancer.

Aside from its use as a diagnostic tool, our results also suggest that 18F-FLT PET is unlikely to be of value as a routine staging tool in pancreatic cancers. As discussed in previous chapters, the spatial resolution of PET does not allow accurate local (T) staging of disease. Given our early results of imaging with 18F-FLT, it is apparent that this would be the case regardless of the type of tracer used. Peri-pancreatic nodal stations may also be missed by both 18F-FDG and 18F-FLT PET, as small volume disease and proximity to the primary tumour can obscure their detection and result in false negatives. This was seen in the above series as both tracers failed to detect microscopic (N1) peri-pancreatic nodal disease later confirmed on histological analysis of resected specimen. Another drawback of imaging with 18F-FLT is the fact that it is catabolized in the liver by glucuronidation, which results in high background hepatic levels (Shields et al. 1998a). Although, this was not formally examined in this

cohort of patients (as none had metastatic disease at presentation), detection of small liver deposits that may exhibit low-grade 18F-FLT uptake may be severely compromised. In fact in a similar study of patients with advanced and metastatic colorectal cancer, Francis et al. (2003a) showed the sensitivity of 18F-FLT PET for detecting liver metastases to be 30% compared to 98% for 18F-FDG PET. Therefore despite suggestion from early *in vitro* studies, our preliminary results suggest that 18F-FLT PET is not a feasible tool for routine diagnosis nor for staging of pancreatic cancer.

The second aim of this study was to examine the correlation between 18F-FLT uptake and cellular proliferation as measured by MIB-1 immunostaining. Both 18F-FLT SUV_{Max} ($r=0.65$) and SUV_{Mean} ($r=0.85$) values correlated strongly with MIB-1 LI. These results are consistent with that of others that examined the role of 18F-FLT PET as surrogate marker of proliferation in a range of solid and haematological cancers (a summary of published data is found in table 1.2). Therefore, our preliminary results support the hypothesis that 18F-FLT is as an *in vivo* marker of proliferation.

In contrast to 18F-FLT, 18F-FDG uptake did not correlate with MIB-1 LI. This has also been shown by other groups. For example, in pancreatic cancer Buck et al. (2001) found no correlation between 18F-FDG uptake and proliferative activity. In colorectal cancer, Francis et al. (2003a) also showed a lack of correlation between 18F-FDG uptake and proliferation. Similar to our findings, their results also did not show a correlation between 18F-FLT and 18F-FDG SUVs. Although it is postulated that a rapidly proliferating cell may need an increased energy supply by glucose

metabolism, metabolic activity is also needed for other cell functions. Furthermore, the enhanced glycolysis exhibited in cancer cells can be regarded as an “exaggerated” consequence of the malignant phenotype, which would occur independent of the DNA turnover. Therefore as suggested by our results and others alike, tumour glycolysis and proliferation seem to be metabolically independent functions.

Finally this study examined the relationship between ^{18}F -FLT uptake and overall survival. There are at present no accepted thresholds for tumour SUVs and therefore the data was dichotomised using an average value of SUV_{Mean} measurements, as an arbitrary cut-off point. Although a divergence in survival curves was observed, neither tracer showed a significant correlation with overall survival. Drawing any firm conclusions from this finding is limited by our small sample size and the heterogeneity of the patient group. However, should a real survival difference exist between high and low ^{18}F -FLT SUVs, there may be important clinical implications in terms of the use of ^{18}F -FLT PET in directing the timing and the choice of neo-adjuvant / adjuvant treatments. This coupled with the use of ^{18}F -FLT PET as a surrogate marker of response to non-surgical treatments, is an avenue that requires further investigation.

When interpreting our results, some of the methodological limitations of our study need to be borne in mind. The small sample size of this study limits the robustness of conclusions as our results are subject to type II errors. None the less, as a pilot project it represents a platform for future avenues of investigation. The additional shortcoming in the study was the fact that histological analysis was performed on core biopsies in 6 out of 10 cases, due to patients’ having inoperable disease at initial

staging. As single tissue specimen cannot account for tumour heterogeneity, the immunohistochemical results may arguably not be representative of the whole tumour. This limitation can be addressed in a larger patient series where only surgically resected tumours can be assessed. As a study, this however would be a much larger undertaking given the relatively low incidence of pancreatic cancer coupled with the fact that majority of patients present with late stage and thus inoperable disease. This was not achievable within the time constraints of this thesis.

5.6 Conclusion

18F-FLT PET is not a feasible tracer for use in the routine diagnosis and staging of pancreatic carcinoma and 18F-FDG seems to remain the PET tracer of choice. A strong association was however observed between 18F-FLT uptake and proliferative activity as measured by Ki-67 antigen expression (MIB-1 labelling index). This finding may have implications for monitoring treatment and prognosticating pancreatic cancer that requires further investigation.

CHAPTER 6

Staging of

advanced colorectal cancer

using 18F-FLT PET –

A comparative study with 18F-FDG.

6.1 Background

¹⁸F-FDG PET is undoubtedly playing an increasing role in the routine management of advanced CRC. The study in chapter 4 illustrated that in the cohort of patients with CLM, ¹⁸F-FDG provided additional information that lead to a change in management of up to 25% of cases. This finding has also been mirrored in a number of other studies of PET imaging in primary and recurrent colorectal cancer.

Despite its superior sensitivity, the limitation posed by imaging with ¹⁸F-FDG remains its lack of specificity. While aerobic glycolysis is a predominant biochemical phenotype of most cancers, glucose metabolism and hence ¹⁸F-FDG uptake is not exclusively seen in cancer cells. Uptake of ¹⁸F-FDG has been frequently reported in inflammatory tissue. This often leads to diagnostic uncertainty where post-treatment inflammatory changes showing ¹⁸F-FDG avidity may be mistaken for tumour recurrence. Peri-tumoural aggregation of inflammatory cells as part of the desmoplastic reaction of a tumour may also lead to aberrant ¹⁸F-FDG accumulation. Thus far, much effort has been focused on developing a more cancer specific PET tracer. An emerging candidate is the thymidine analogue PET tracer, ¹⁸F-FLT.

¹⁸F-FLT has been shown both *in vitro* and *in vivo* to preferentially accumulate in cancer cells. Pre-clinical studies in models of tracer uptake in tumour versus inflammation have also backed up the hypothesis that relative uptake of ¹⁸F-FLT by inflammatory cells is minimal, thus suggesting it to be more tumour specific. In addition to this, ¹⁸F-FLT is shown to correlate well with other markers of proliferative activity, thus introducing itself as a potential surrogate marker of tumour proliferation.

To date, there is only one published study of imaging CRC with ¹⁸F-FLT PET. In their study, Francis et al. (2003b) found ¹⁸F-FLT to be a more specific tracer compared to ¹⁸F-FDG, but its poor sensitivity in detecting hepatic lesions made it a poor candidate as a routine staging tool in the management of CRC. This pilot study therefore aimed at validating these findings in a cohort of patients with advanced CRC. These findings were to be used as stepping stone towards future research examining the use of ¹⁸F-FLT as a prognostic tool as well as a means of monitoring response to medical treatment.

6.2 Aims

The aims of this chapter were:

1. to compare the accuracy of imaging advanced CRC with 18F-FLT PET compared to the gold standard 18F-FDG.
2. to examine the relationship between 18F-FLT and 18F-FDG tumour SUVs

6.3 Material and methods

6.3.1 Patient recruitment

Patients were prospectively recruited from routine referrals to the surgical and oncology outpatients. 10 patients with locally advanced and/or metastatic CRC were included. All patients underwent conventional imaging with contrast enhanced CT (ceCT) of the thorax, abdomen and the pelvis. Each patient also underwent a whole body PET/CT scan using the routine tracer ¹⁸F-FDG and the thymidine analogue tracer ¹⁸F-FLT. The two PET/CT studies were performed with a median intervening period of 2 days between the two (range 2-5 days). The study was conducted following local hospital ethics committee approval and with full informed consent of the patients as outlined in chapter 2.1.

6.3.2 Imaging protocols

Routine staging with ceCT was performed as described in chapter 2.5. The imaging protocol for whole body ¹⁸F-FDG and ¹⁸F-FLT PET/CT scans are also as described earlier. The median administered doses of tracers were 373 MBq (range 342-412) for ¹⁸F-FDG and 313 MBq (range 229 – 435) for ¹⁸F-FLT. The PET images were acquired at a median of 60 (range 58-65) and 61 (range 58-65) minutes post-injection for ¹⁸F-FDG and ¹⁸F-FLT respectively. The CT component of PET/CT was acquired without oral or intravenous contrast enhancement.

6.3.3 Image Analysis

The PET images were qualitatively (visually) assessed by two experienced nuclear medicine physicians, blinded to the results of conventional imaging. To reduce recall bias, 18F-FDG and 18F-FLT images were analysed with at least 2 weeks between each other. Final results were reached by consensus between the two observers. Images were analysed on a lesion-by-lesion basis and grouped according to body region. Lesions were deemed as positive where focal tracer accumulation was above that of the surrounding normal tissues.

Tracer uptake was semi-quantified according to the methods described in chapter 2.4.2. 1cm circular ROIs were used to calculate SUVs (corrected for body weight). SUV_{Max} and SUV_{Mean} values were determined semi-automatically using the Xeleris[®] workstation. Only lesions that were deemed positive with both tracers were included in the analysis.

6.3.4 Statistical analysis

All statistical calculations were performed using the GraphPad statistical Software (V 4.0, California, USA). The correlation between tracer SUVs was tested using the Pearson's correlation coefficient. For statistical analyses, a two-tailed p value of <0.05 was considered as statistically significant.

6.4 Results

6.4.1 Patient demographics

Ten patients with a median age of 67 years (range 45-76 years) were included in the study. These consisted of 6 men and 4 women. A total of 34 abnormal lesions were detected by a combination of routine imaging with ceCT, MRI and 18F-FDG PET/CT. Of these, histological confirmation was obtained for 15 lesions (44%). In the remaining cases (19 lesions, 56%), the colorectal MDT deemed the sampling of lesions inappropriate due to the extent of the patients' tumour burden. As for this, clinical and radiological follow-up of the patients for a median duration of 19 months (range 5-25 months) was used in confirming the diagnoses.

6.4.2 Comparison of 18F-FDG and 18F-FLT PET in detecting malignant lesions

Of the 34 suspicious lesions, final histological / radiological follow-up confirmed 29 (85%) to be consistent with a malignant deposit. Lesions were grouped according to whether they were primary or recurrent/metastatic deposits. Metastatic deposits were further grouped according to body region. Table 6.1 summarises the imaging results for 18F-FDG and 18F-FLT PET according to the number of positive lesions detected.

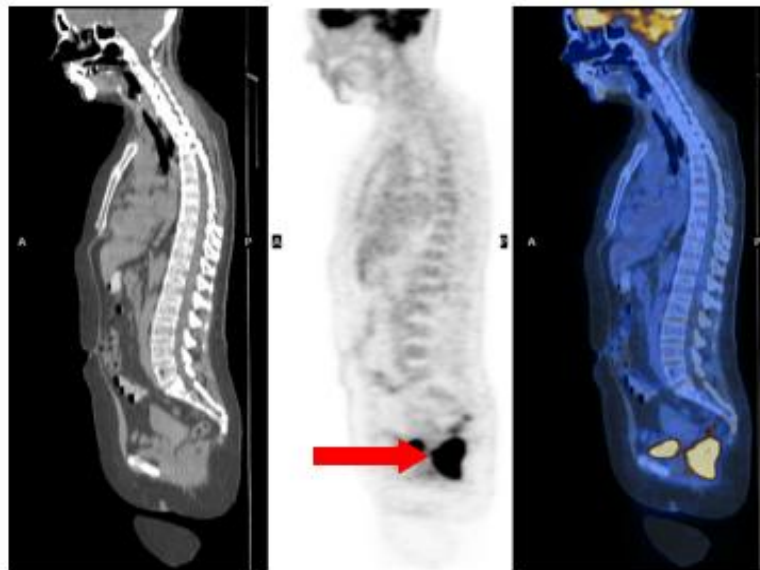
		18F-FDG	18F-FLT	True lesion status on follow-up
Primary	Colon/rectum	2	2	2
Recurrence / metastases	Liver	13	1	14
	Lung	10	5	8
	Peritoneal	4	4	4
	Other abdominal (adrenal)	1	0	1
	TOTAL	30	12	29

Table 6.1: Number of PET positive lesions detected with 18F-FDG compared to 18F-FLT PET scans. Lesions divided according to body region. True lesion status (indicating the presence of a malignant lesion) was determined by subsequent histological and/or radiological follow-up.

In two patients with synchronous primary and metastatic disease, both primary sites were detected by both PET tracers (one primary sigmoid and one primary rectal carcinoma). Although visual analysis of 18F-FLT PET images identified both primary sites, tumour SUVs for 18F-FDG were higher for both lesions compared to that for 18F-FLT. This difference is demonstrated in figure 6.1 for the rectal cancer.

**18F-FDG
PET/CT**

SUV_{Max} = 8.7



**18F-FLT
PET/CT**

SUV_{Max} = 3.4

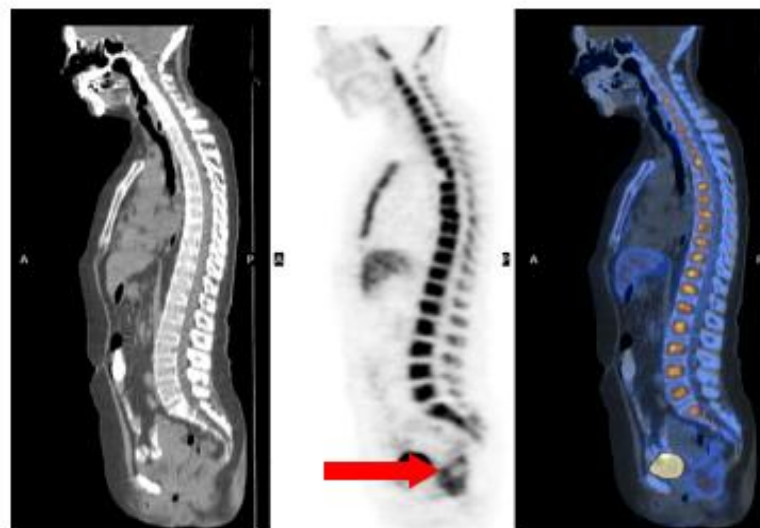


Figure 6.1: Sagittal CT, PET and PET/CT fused images of a rectal cancer imaged with 18F-FDG and 18F-FLT. Images demonstrate relatively lower uptake of 18F-FLT compared to 18F-FDG.

A total of 14 liver metastases were confirmed on subsequent follow-up. Initial staging with ceCT identified 15 liver lesions of which there were 2 false positive and 2 false negative findings. 18F-FDG PET detected 13 (93%) hepatic lesions of which there was one false negative result. This was subsequently found at laparotomy to be a sub-

centimetre lesion on the liver capsule with a concurrent larger lesion in the right lobe of the liver, both of which were resected and histologically confirmed. The two false positive ceCT lesions were correctly characterized as negative on 18F-FDG PET. In comparison to 18F-FDG, only 1 hepatic metastasis was visualized with 18F-FLT (7%). This was a 2cm solitary lesion in the right lobe of the liver (figure 6.2). Both liver lesions that were incorrectly characterised as metastases on ceCT (ie: false positives) were also negative on 18F-FLT PET.

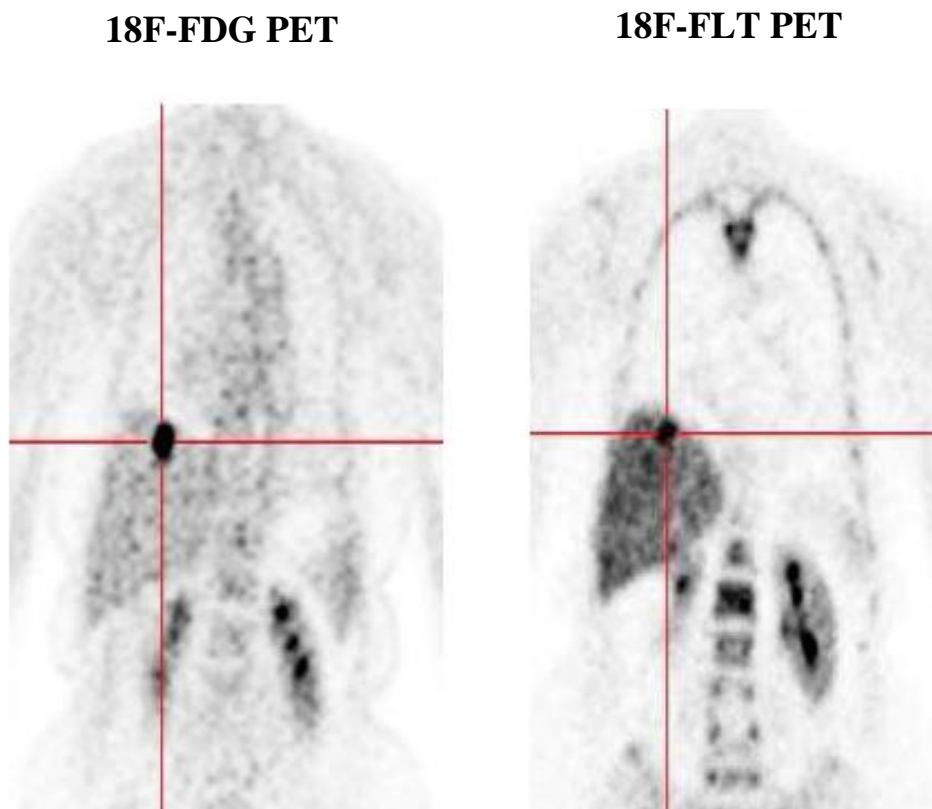


Figure 6.2: Coronal slices of 18F-FDG and 18F-FLT PET scans demonstrating a tracer avid solitary metastasis in the right lobe of the liver.

With regard to metastases to other regions, both 18F-FDG and 18F-FLT PET correctly identified all 4 peritoneal metastases. Of the 10 lung lesions identified on the initial ceCT scans, all 10 showed 18F-FDG avidity but 2 of these lesions were later

confirmed to be false positives as follow-up imaging with ceCT was suggestive of them being of infective aetiology (lesions disappeared on follow-up scans). 18F-FLT PET on the other hand detected 5 lung lesions, all of which were confirmed to be true positive findings. The 2 false positive lesions (infective nodules) seen on the 18F-FDG scans were negative for 18F-FLT. There were also 3 false negative lung lesions missed by the 18F-FLT PET scan.

In one patient with lung and liver metastases, an adrenal mass was also seen on the routine ceCT scan. Assessment with MRI further confirmed this to be highly suggestive of a metastatic deposit. This lesion was visualized on 18F-FDG but was falsely negative on 18F-FLT PET study.

6.4.3 Comparison between 18F-FDG and 18F-FLT SUVs

Of the 29 malignant deposits, 12 lesions were confidently visualized on the 18F-FLT PET/CT scans. SUVs for these were compared to that of 18F-FDG, results of which are presented in table 6.2.

Lesion	Site of lesion	18F-FDG		18F-FLT	
		SUV _{Mean}	SUV _{Max}	SUV _{Mean}	SUV _{Max}
1	Rectum	6.3	8.7	2.2	3.4
2	Colon	6.7	7.3	2.0	6.7
3	Liver	2.6	5.5	1.5	4.5
4	Lung	2.2	3.2	1.0	1.3
5	Lung	3.1	4.0	0.9	2.3
6	Lung	2.9	4.0	1.7	1.2
7	Lung	5.5	7.1	1.5	2.2
8	Lung	3.9	4.5	0.9	2.0
9	Peritoneal	4.4	5.3	1.7	2.3
10	Peritoneal	4.6	6.1	2.1	2.3
11	Peritoneal	3.9	5.5	2.7	4.5
12	Peritoneal	5.5	6.3	1.7	1.9

Table 6.2: Tabulated summary of SUVs measured for 18F-FDG and 18F-FLT avid lesions.

On average, 18F-FDG SUVs were between 1.95 (SUV_{Mean}) to 2.59 (SUV_{Max}) fold higher than 18F-FLT This difference was statistically significant and is represented in figure 6.3.

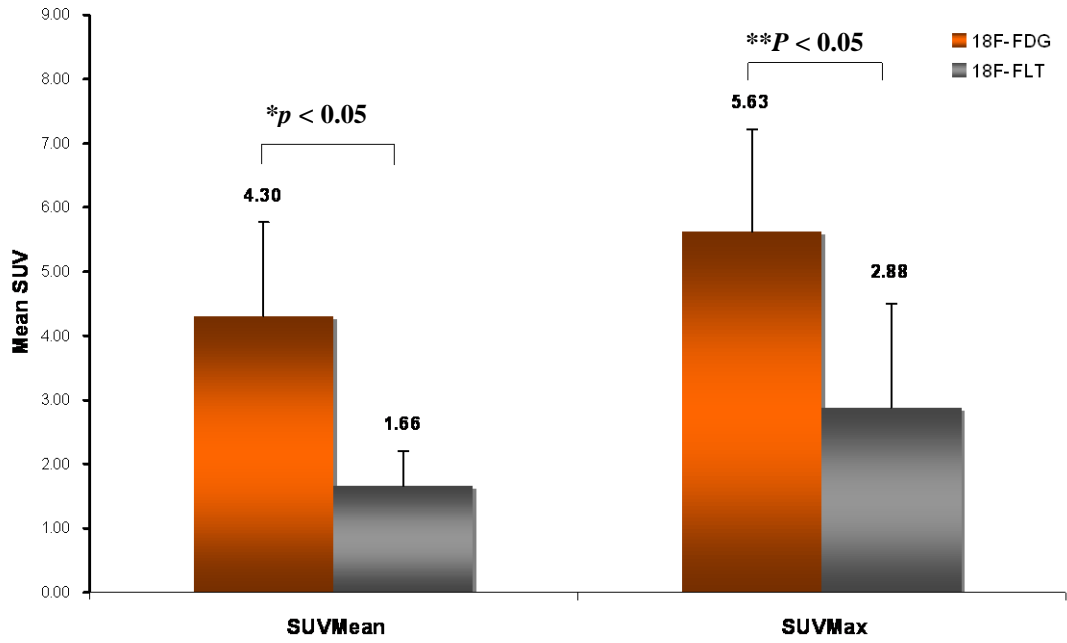


Figure 6.3: Graph demonstrating the difference between the average SUV_{Mean} and SUV_{Max} figures for 18F-FDG and 18F-FLT. The difference between the two reached strong statistical significance (Student's *t*-test).

There was no correlation seen between 18F-FDG and 18F-FLT SUVs as shown in figure 6.4.

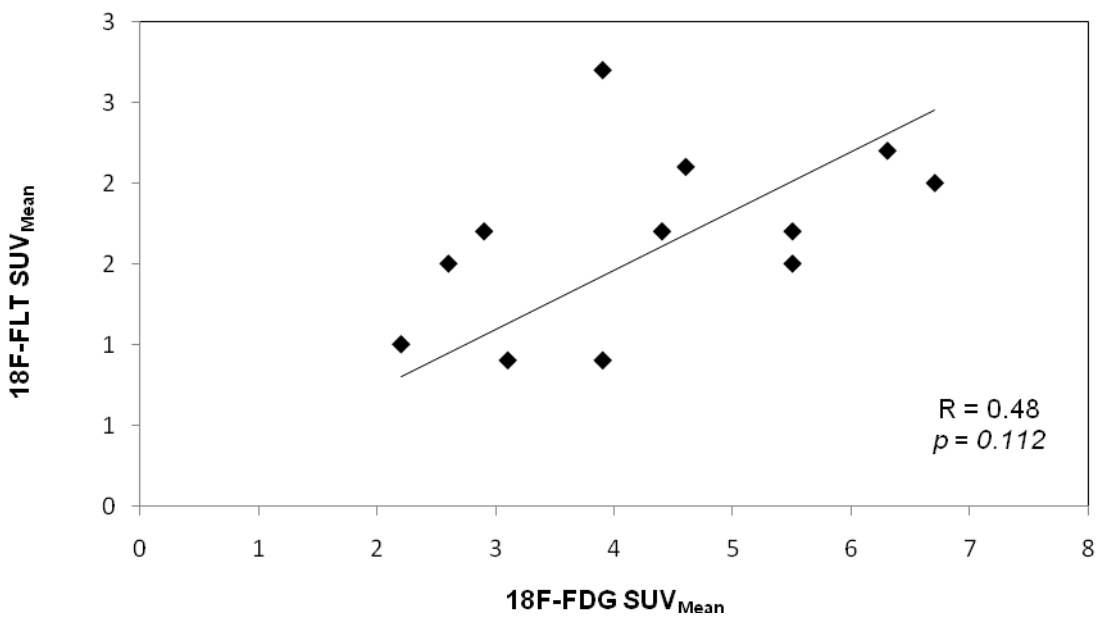
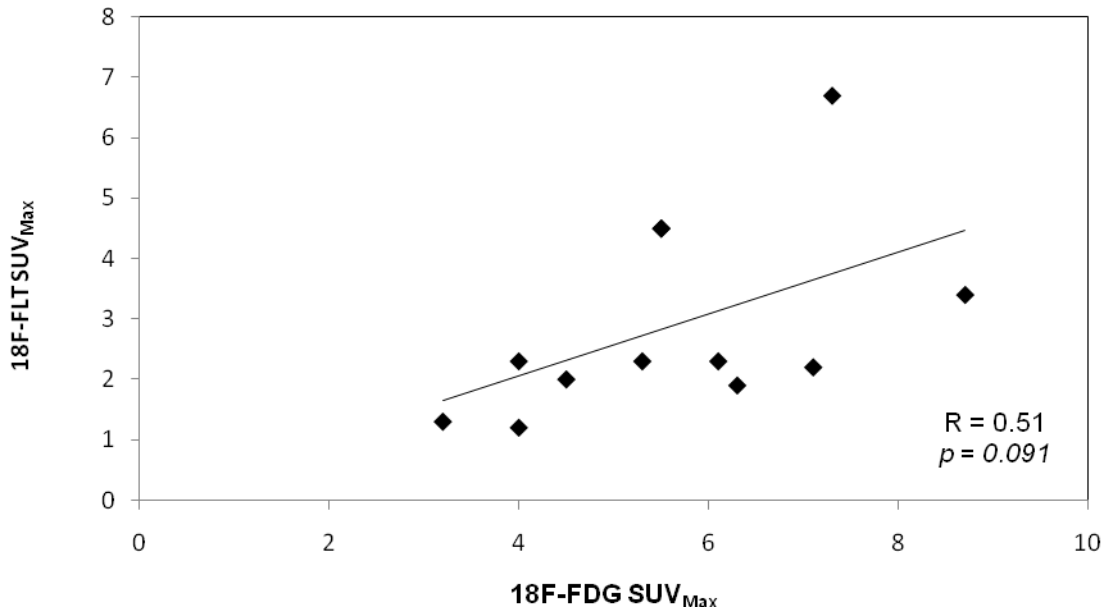


Figure 6.4: Correlation between 18F-FDG and 18F-FLT SUVs for all detected lesion. There was no statistically significant correlation seen between 18F-FDG and 18F-FLT SUV.

6.5 Discussion

The aim of this pilot study was to examine the feasibility of imaging advanced CRC with 18F-FLT PET compared to the routine tracer 18F-FDG. Consistent with several published reports, the overall uptake of 18F-FLT in malignant deposits was lower than for 18F-FDG (Francis et al. 2003b; Cobben et al. 2004b; van Westreenen et al. 2005). Furthermore, the lack of correlation between 18F-FDG and 18F-FLT SUVs supports the hypothesis that tumour glycolysis and cellular proliferation are independent processes in tumorigenesis.

Overall, 18F-FDG PET correctly characterized 26 of the 29 malignant lesions (Sensitivity = 96%), whereas 18F-FLT PET visualized only 12 (sensitivity = 41%). In detecting non-primary foci of disease, 18F-FLT PET identified all peritoneal deposits and 5 out of 8 (63%) lung metastases. In the latter group, 2 lung lesions were found to be falsely positive on the 18F-FDG scan as they were later confirmed to be of infective aetiology. Both these lesions did not show any 18F-FLT avidity, thus correctly characterizing the lesions as non-malignant. This therefore gave 18F-FLT a specificity of 100% compared to 50% for 18F-FDG. Consistent with previously published reports, this suggests 18F-FLT to be a more specific tracer. However, the small proportion of false positive findings in our series makes drawing a firm conclusion from these results difficult. In particular it can be argued that in our series, the negative nature of these two lesions may be related to 18F-FLT's overall poor sensitivity. This argument can only be clarified in a study with a larger sample size, which would allow subgroup analysis of all apparent false positive lesions that are found on conventional imaging and 18F-FDG PET.

In staging the liver, ¹⁸F-FLT also performed poorly, visualizing 1 out of 14 (7%) lesions. The above results are inferior to that reported by Francis et al (2003). In their series of 23 CRC patients, 5 out of 6 (83%) lung and all peritoneal lesions seen with ¹⁸F-FDG PET were also correctly visualized with ¹⁸F-FLT. Their reported sensitivity for detecting liver metastases with ¹⁸F-FLT PET was 34% (11/32 lesions), which was also poor. In the management of CRC, accurate detection and staging of liver metastasis remains a clinical challenge as 30% of patients ultimately develop liver secondaries. Although advances in imaging technology (eg: with the routine use of multidetector CT, MRI and micro-bubble contrast ultrasound scans) have improved the accuracy of detecting disease in the liver, there is still no consensus as to the imaging modality of choice in characterizing small (sub-centimetre) liver lesions. In this respect ¹⁸F-FLT PET does not seem to have an additional advantage.

It must be noted that the apparent success of ¹⁸F-FDG PET in imaging the liver is related to the high degree of contrast achieved between the high ¹⁸F-FDG avidity of CLM and low background accumulation of the tracer in normal liver parenchyma. Our results are consistent with published reports to date that have consistently shown the sensitivity of ¹⁸F-FLT PET in detecting liver metastases to be poor. This finding can in part be attributed to the high background uptake of the tracer in the liver. This phenomenon was first described by Shields et al. (2003) in their original description of imaging with ¹⁸F-FLT using canine models and later in human subjects. The underlying mechanism for this has been explained by examining the hepatic metabolism of AZT, an antiretroviral drug from which FLT was initially developed. Aside from phosphorylation within cells, AZT is metabolised in hepatocytes by glucuronidation, a process that is catalysed by the hepatic enzyme UDP-

glucoronosyltransferase. This makes the compound more water soluble and therefore more easily excreted in urine and bile. As 18F-FLT PET images are on average acquired at about 60 minutes post tracer injection, only excreted tracer is seen to accumulate in the renal tract. There are currently no reports of biliary excretion resulting in image artefact within the gastro-intestinal tract. The problem that arises is due to the high background accumulation of 18F-FLT in hepatocytes, which hinders the detection of small hepatic metastases that are exhibiting relatively low-grade tracer uptake. Previous work at our unit has shown significantly higher normal liver 18F-FLT uptake (median SUV=4.2, range 2.7-5.6) compared to 18F-FDG (median SUV= 2.1, range 1.5-2.4). The above suggests that a minimum threshold for tracer uptake needs to be reached before a hepatic lesion can be clearly visualized. As for this, 18F-FLT PET is unlikely to supersede 18F-FDG as a routine tracer in staging colorectal cancer and colorectal liver metastases.

While the inferior sensitivity of 18F-FLT for detecting liver metastases may be explained by the liver's high background tracer uptake, its relatively poor detection rate of lung lesions may have other explanations. In our series, 50% of lung lesions with avid 18F-FDG uptake were negative for 18F-FLT, although of these 2 were truly negative in the face of false findings with 18F-FDG. In the lungs, background 18F-FLT accumulation is minimal and therefore problems with tumour-to-background contrast are not implicated. However, inaccuracies may arise in small lung lesions where partial volume effect and motion artefacts can reduce 18F-FLT's detection accuracy. In fact coupled with the limitations posed by the spatial resolution of PET, the challenge of visually detecting small volume disease is one that continually limits the overall detection accuracy of PET. Newer generation PET detector units are

reported to have a better spatial resolution, which may help to address this problem. Furthermore, the use of PET/CT image fusion is increasingly allowing a two-pronged approach (metabolic + anatomical imaging) to characterizing small lesions. The latter at present seems to be only clinically relevant if the CT component of PET/CT has full diagnostic capability. Overall however, one cannot disregard the underlying disease biology, which dictates the pharmacokinetics of tracer uptake at cellular level. There is therefore a real need for validating studies that examine the true relationship between what is seen on a PET scan and the biology of the tumour.

There is mounting evidence supporting the hypothesis that 18-FLT uptake is a surrogate marker of proliferation. In CRC, Francis et al. (2003b) showed a strong correlation between 18F-FLT SUV and Ki-67 antigen expression . Table 1.2 (Chapter 1.6.5) also summarised the results of several other published studies that have shown a strong correlation between 18F-FLT accumulation and proliferation in a number of other solid and haematological cancers. Based on this assumption, 18F-FLT negativity may have important prognostic implications. On the one hand, tumours with a lower proliferation index may confer a survival benefit. On the other, they may confer a poorer response to certain cycle dependent chemotherapy regimens. Future avenues of research would therefore need to examine the relationship between 18F-FLT accumulation and the clinical and biological behaviour of colorectal cancer. At present there is growing interest in examining the role of 18F-FLT PET in monitoring response to treatment (eg: radiotherapy, chemotherapy or monoclonal antibody treatment). A potential pitfall that may complicate this line of research is the high false negative rate of imaging with 18F-FLT PET. If lesions exhibit no 18F-FLT accumulation at the outset of the treatment regimen, then the routine morphological

parameters (ie: tumour dimensions) would remain the only mode of monitoring response. As thus, 18F-FLT PET would be of no added value. However as mentioned above, baseline 18F-FLT uptake parameters may have a predictive value, which may potentially influence the selection of the most appropriate treatment regimen, particularly when deciding which chemotherapy agents are used. To the best of my knowledge, this hypothesis has not yet been tested and requires further investigation.

6.6 Conclusion

This study further confirms previous reports that ¹⁸F-FLT PET is a poor candidate as a routine diagnostic and staging tool, in both primary and metastatic CRC. Lack of correlation between ¹⁸F-FDG and ¹⁸F-FLT SUVs supports the hypothesis that there is a poor relationship between glucose metabolism and thymidine turnover. Although not tested in this study, the prognostic implication of ¹⁸F-FLT uptake as a predictor and measure of response to medical treatment warrants further investigation.

CHAPTER 7

**Measuring early adaptive response
to 5-fluorouracil with
18F-FLT -
an *in vitro* study.**

7.1 Background

At present, the mainstay of monitoring response to treatment involves a combination of measuring serial serum tumour marker levels and the visualisation of morphological changes with cross-sectional imaging techniques such as CT or MRI. The limitations of these techniques are their lack of specificity as well as the fact that they represent temporally delayed changes in tumour biology in response to treatment. Being able to detect response early in the course of treatment has the advantage of allowing appropriate and timely changes in treatment regimen, which may ultimately impact overall survival. Attempts at molecular profiling of cancer in monitoring and predicating response to treatment have been largely limited by the need to obtain tissue specimen, which in turn may not always account for tumour heterogeneity. Molecular imaging can be used to address this problem. Assessing whole tumour biology *in vivo* not only provides a non-invasive means of monitoring early response to treatment, but may also aid future investigation into novel molecular targeted treatments.

In previous chapters, the feasibility of imaging with ¹⁸F-FDG and ¹⁸F-FLT PET was investigated in the routine clinical setting of pancreatic and advanced colorectal cancer (CRC). In both cancer types, ¹⁸F-FDG is shown to provide a sensitive means of detecting cancer burden. Its role as a surrogate marker of tumour viability also has the potential to contribute to the paradigm shift, which is the monitoring of therapy response on at a biological level. In the management of CRC for example, a number of studies have examined the role of ¹⁸F-FDG PET in assessing early biological response to radiotherapy (Cascini et al. 2006), chemotherapy (Weber and Wieder 2006) or radiofrequency ablation of liver metastases (Donckier et al. 2003). The

results have consistently indicated a strong correlation between early reduction in ¹⁸F-FDG uptake and a positive response to treatment. Despite ¹⁸F-FDG's widespread use, targeting tumour glycolysis represents one of a number of potential surrogate end points of disease. Therefore, being able to quantify tumour proliferation with the thymidine analogue tracer ¹⁸F-FLT, has recently attracted intense interest.

The challenge of predicting response to chemotherapeutic agents is perhaps best exemplified by the use of 5-fluorouracil (5-FU) in advanced colorectal cancer. Despite its widespread use, overall response rates to 5-FU alone are reportedly no greater than 10-15% (Longley et al. 2003). The mode of action of 5-FU is complex. It exerts its main cytotoxic effect by inhibiting the enzyme Thymidylate Synthase (TS). TS, which is the rate-limiting enzyme of the *de novo* pathway of pyrimidine synthesis, catalyses the reductive methylation of deoxyuridine-5'-monophosphate (dUMP) to deoxy-thymidine-5'-monophosphate (dTMP). This provides the sole *de novo* source of thymidine required for DNA repair and synthesis. Inhibition of TS results in an imbalance of intracellular nucleotide pools (such as deoxyribonucleotide triphosphate (dNTP)) and subsequent lethal DNA damage (Parker and Cheng 1990). More minor and less well understood mechanisms of 5-FU cytotoxicity are also believed to result from the direct incorporation of metabolites of 5-FU into RNA and DNA.

Much effort has been focused on developing predictive biomarkers of 5-FU resistance. However, the mechanisms of resistance to 5-FU are also complex, involving numerous changes that may include; deletions of key activating enzymes, increased expression of catabolising enzymes, lack of reduced folate substrate, gene amplification and alterations in protein expression of TS. Although there are

conflicting reports in the literature, the salvage pathway of nucleotide synthesis has also been implicated as a potential mechanism of 5-FU resistance (Pickard and Kinsella 1996; Kinsella et al. 1997). So far, no one marker has emerged as more specific above others.

The rationale behind this study uses 5-FU as a model for TS inhibition. In response to the imbalance of intracellular dNTP pools outlined earlier, cells acquire exogenous pyrimidines through activation of the salvage pathway (TK-1) (Parker and Cheng 1990; Pickard and Kinsella 1996). This shift from one enzyme system (TS) to the other (TK-1) may potentially be monitored *in vivo* with ¹⁸F-FLT PET. We therefore hypothesized that cellular ¹⁸F-FLT uptake represents a potential tool for monitoring early biological response to 5-FU therapy. This hypothesis was tested in a colorectal cancer cell line model, where early biological effects of 5-FU on cellular uptake of the two tracers ¹⁸F-FDG and ¹⁸F-FLT were compared. Cisplatin, which does not directly influence pyrimidine metabolism, was used as a control drug to 5-FU.

7.2 Aims

The principal aim of this study was to examine *in vitro*, the early changes in uptake of ¹⁸F-FLT compared to ¹⁸F-FDG following treatment with 5-FU. This was carried out in two colorectal cancer cell lines and by determining the response to 5-FU in terms of:

- 1) cell cytotoxicity (ie: tumour viability).
- 2) changes in the cell cycle pattern using flow cytometry.
- 3) changes in Thymidine kinase-1 (TK-1) protein expression.

7.3 Methods

7.3.1 Materials and cell lines

i) Materials: Plastic consumable items were bought from Nunc (VWR, Poole, Dorset, UK), while chemicals were obtained from Cambrex Biowhittaker (Woking, Berks, UK), unless otherwise stated.

ii) Cell lines: Two human colorectal cancer cell lines were used; SW480 is derived from a primary colorectal cancer and SW620 is derived from a colorectal lymph node metastasis. Both cell lines were obtained from the European Collection of Animal Cell Cultures (Porton Down, Wilts, UK).

7.3.2 Routine cell line maintenance

SW480 and SW620 cells were routinely grown in 75cm² flasks in Dulbecco's Modified Eagle's Medium (DMEM) (supplemented with L-glutamine, 10% (v/v) foetal calf serum (FCS), 50 mg/ml Gentamicin) at 37°C. All work described below was carried out within 15 cell passages in order to minimize differences due to phenotypic drift.

To prepare cells for propagating a rolling stock or for carrying out the proposed experiments, the following steps were followed:

- Cells were allowed to grow to near confluence levels (approximately 90%), washed three times; twice in phosphate buffered saline (PBS) followed by one wash with a 0.02% solution of Ethylenediamine tetracetate (EDTA) in PBS. The latter step was necessary to remove FCS (which has an inhibitory effect

on trypsin used for enzymatic disaggregation) and furthermore EDTA chelates membrane bound Ca^{2+} , which aids in the disaggregation process.

- A 1mg/ml solution of trypsin (in EDTA/PBS) was then used for enzymatic disaggregation.
- The disaggregated cells were harvested in medium supplemented with FCS to partially neutralise trypsin, centrifuged (400g, 5min) to separate cells from trypsin containing supernatant and again re-suspended in fully supplemented medium.

Cells were then either (i) passaged into flasks (at 1:3 to 1:10 ratios) and maintained as above for later use, or (ii) counted using a haemocytometer and re-suspended at appropriated dilutions for experiments as described below.

7.3.3 The basic experimental protocol

For all experiments, 2×10^5 cells / well were seeded in six-well plates and kept in a humidified incubator at 5% CO_2 / air. The optimum seeding densities were determined by earlier pilot studies, details of which will not be outlined in this thesis. The reason for using six-well plates (growth area of 9.5 cm^2 per well) for the 5-FU toxicity and radiotracer uptake experiments, was so that at the end of each experiment, harvesting would result in cell numbers sufficient for counting under a light microscope and would give cells suspension volumes large enough (minimum of 2 ml required) for the gamma well counter used for radiotracer uptake measurements.

48 hours after seeding, cells were incubated with 5-FU and assayed for tracer uptake, S-phase fraction (SPF) and TK-1 expression. This will be outlined in more detail in the following sections.

7.3.4 Defining drug dose parameters

5-FU was purchased from Calbiochem (MERK biosciences Ltd, Nottinghamshire, UK) and Cisplatin from Faulding Pharmaceuticals Plc (Warwickshire, UK).

To study the effect of 5-FU on cellular viability, cells were plated for 48 hours (as above) and were exposed to a dose range (1 –250 µg/ml) of 5-FU for 2 hours. Control experiments were drug free, but as 5-FU solutions were made up in fully supplemented culture media, at each corresponding time point the control cells also received a medium change. After 2 hours of drug exposure, the drug was removed and both the treated and untreated cells were washed 3 times with PBS. They were then allowed to recover for 30 minutes, 24 and 48 hours (represented as days 0, 1 and 2 respectively). At each time point following cell recovery, the cells were harvested by trypsinisation and their viability detected by Trypan blue (Sigma, Dorset, UK) exclusion on a haemocytometer. All cytotoxic assays were performed in triplicate.

Both SW480 and SW620 cells showed similar dose response cytotoxicity (Figure 7.1a). Dose response curves were used to determine the optimum cytotoxic dose for 5-FU at which 50% cell killing was observed on day 1. For 5-FU exposure of 2 hours, this dose was found to be 50 µg/ml.

As a control experiment to 5-FU, comparative experiments were carried out using Cisplatin. Earlier pilot studies determined the optimal dose of Cisplatin to be 50

µg/ml (data not shown). The cytotoxic effect of this dose was demonstrated using the cell viability counts on days 0-2 (figure 7.1b).

7.3.5 Tracer uptake experiments:

Radiopharmaceuticals

¹⁸F-FDG and ¹⁸F-FLT were purchased from sources previously detailed in sections 2.2 and 2.3. Radiopharmaceuticals used in each experiment were obtained from the same stock of tracer that was used for clinical studies.

Experimental protocol

Each experiment involved preparing a batch of 5-FU treated and untreated cells, as described in section 7.3.3. Experiments at each respective time point (days 0, 1 and 2) were prepared in separate 6 well plates. Each plate was divided into two halves; 3 wells for the treated group and 3 wells for the untreated group. Cells from one well in each experimental group was used for cell viability counts. This arrangement allowed 2 repeats per experiment and with each experiment being repeated 3 times, it gave 6 repeats per experimental data set.

At 2 hours post 5-FU exposure, the drug was aspirated, cells were washed (PBS x3) and allowed to recover in fresh supplemented medium for 30 minutes. To determine tracer uptake, cells were immediately incubated with fully supplemented culture medium containing 100 KBq total activity of either ¹⁸F-FLT or ¹⁸F-FDG for 90 minutes (incubated at 37°C in 5% CO₂). Following tracer incubation, cells were washed three times with ice cold PBS in order to stop further tracer uptake and to

remove unbound radiotracer. The cells were then harvested by trypsinisation as described before.

Tracer uptake was quantified by measuring the radioactive counts in a gamma well counter (Wallac, Turku, Finland) over 1 minute. Radioactivity measurements were decay corrected. Tracer uptake was calculated as a percentage of total applied radioactivity and corrected for cell numbers.

Using SW480 cells only, ¹⁸F-FLT uptake was also measured following treatment with an increasing dose of 5-FU (dose range 1-250 µg/ml). Control experiments examined the effect of Cisplatin on tracer uptake. The same experimental protocols as that used for 5-FU were again followed.

7.3.6 Cell cycle phase determination

5-FU treated (dose 50 µg/ml) and untreated cells were grown in 6 well plates as described earlier. At each time point (days 0, 1 and 2), the cells were labelled with Bromodeoxyuridine (BrdU) and analysed by flow cytometry as described below. Cells in each experimental group were labelled for 20 minutes with BrdU (10mM) in culture medium, harvested by trypsinisation, fixed in ice cold 70% (v/v) ethanol and stored at 4°C until used. Single cell suspensions were pelleted, washed with 0.5% BSA/PBS, and re-suspended in 0.1M HCL (10 minutes) to unwind DNA. Following three washes with 0.1% Tween-20/PBS (PBS-T), cells were incubated with α-BrdU antibody (Becton Dickinson, CA, USA; 1:20 dilution for 15 min.), washed twice and stained with a fluorescein isothiocyanate (FITC)-conjugated goat α-mouse antibody (Dako, Cambridgeshire, UK; 1:10 dilution for 15 min).

After a final wash (PBS-T), cells were treated with 50 ml of RNase A (Sigma, Dorset, UK; 100 mg/ml for 15 min) and 300 ml of propidium iodide (Sigma, Dorset, UK; 50 mg/ml for 30 min). Samples were analysed on a FACSCalibur (Becton Dickinson, USA). Propidium iodide fluorescence was measured above 670nm and FITC fluorescence between 515 and 545nm. 20,000 events from each sample were recorded and data analysed using the FlowJo software (TreeStar, California, USA).

7.3.7 TK-1 protein expression

Changes in TK-1 expression were investigated in response to 5-FU treatment. Cells were grown in 75cm² flasks to approximately 60% confluence and incubated with 5-FU (as described above). Untreated controls were run in parallel.

7.3.7.1 Protein extraction

At each time point, cells were harvested by trypsinisation as described in section 7.3.4. Protein was extracted by adding an equal volume of distilled water to the cell pellet in order to osmotically lyse cell membranes. The cell suspensions were further lysed by freeze / thawing cycles [6 freeze cycles in liquid nitrogen for 3 minutes followed by thawing in a 30°C water bath for 5 minutes]. The lysed cells were centrifuged at 4°C and 10,000rpm for 10 minutes in order to separate cell debris. The supernatants were then transferred into labelled Eppendorfs™.

7.3.7.2 Protein assay

The concentration of protein lysates were determined by using the Bradford protein assay kit (Biorad Ltd, UK). Serial dilutions of BSA (concentration range of 0 –

2mg/ml) in distilled water were prepared for determination of standard curves (see appendix E).

Samples were prepared by mixing 10 μ l of the lysate to 10 μ l of 0.1M HCL and 80 μ l of water. 3.5 ml of Bradford reagent (diluted 1:5) was then added to the solution, vortexed for 10 seconds and allowed to incubate at room temperature for 5 minutes. The optical density readings were taken at 595nm using a “Perkin Elmer Lambda” photospectrometer. The optical density readings were used to calculate the concentration of protein extracts using the BSA solution as the standards curve.

7.3.7.3 Gel electrophoresis and Western blots

Western blots were performed according to the technique described by Sambrook and Russell (2001), using the protocols detailed in appendix F.

20 μ g aliquots of total protein from cell lysates were mixed with an equal volume of Laemmli sample buffer (Laemmli 1970) and were boiled at 100°C for 3 minutes to denature the proteins (reducing condition). Samples were then loaded onto pre-cast 12% Tris-Glycine polyacrylamide gels (Biorad Ltd, Herts, UK) together with a rainbow molecular weight marker (Color BurstTM, Sigma-Aldrich, Dorset, UK). Electrophoresis was carried out at 150 V for 1 hour.

Proteins were transferred to polyvinylidene difluoride membrane (PVDF) (Hybond-PTM –Amersham, Bucks, UK) at 0.25 amps per mini-gel blot for 20 minutes. The blots were blocked overnight with 1% BSA (in PBS-T) at room temperature. TK-1 was detected with a mouse monoclonal antibody (Abcam, Cambridgeshire, UK). The

membranes were incubated with the α -TK-1 antibody (1:800 dilution in 0.5% BSA/PBS-T) for 2 hours, at room temperature. The blots were then washed with PBS-T and then incubated with a goat α -mouse horse raddish peroxidase (HRP) conjugated secondary antibody (1:600 dilution, 1h; DAKO, Glostrup, Denmark). The membranes were visualized by a calorimetric reaction using 3-3'-diaminobenzidine tetrahydrofluoride (DAB – Sigma Aldrich, Dorset, UK) as a substrate. Lanes were standardized for protein loading by detecting β -tubulin expression (mouse α -tubulin; Sigma-Aldrich UK).

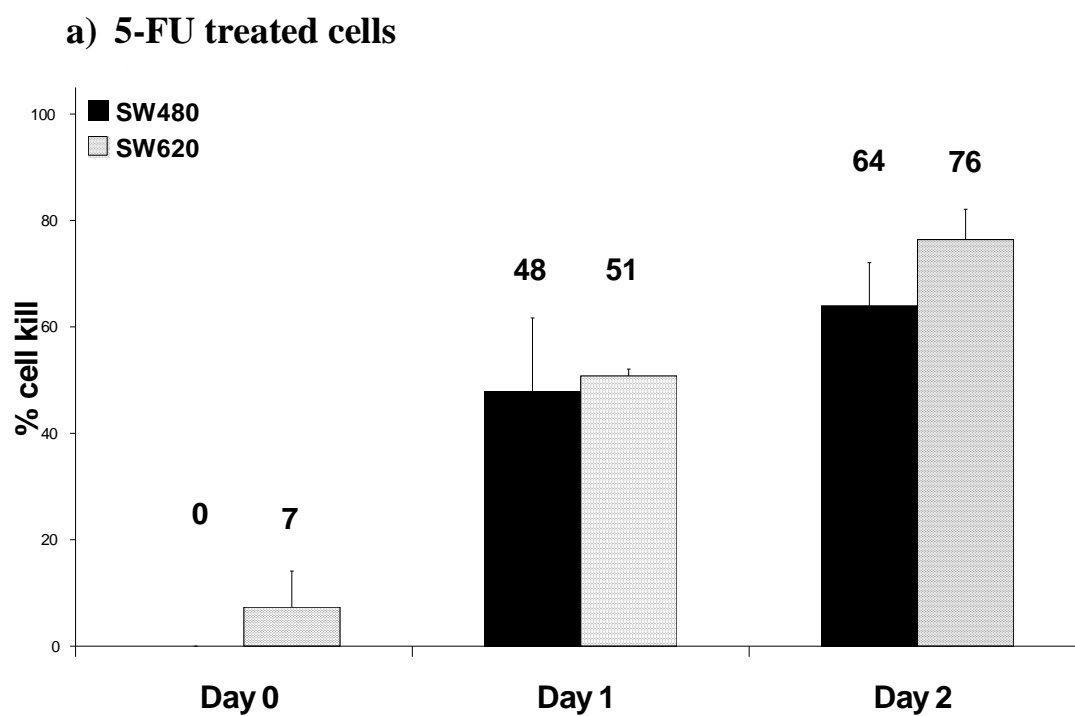
7.3.8 Statistical analysis

Statistical analyses were carried out using the software GraphPad Prism (Version 4.03; California, USA). Analysis of variance was performed using a one-way ANOVA. Differences between paired data were tested for significance using a two-tailed Student's t-test. *p* values of <0.05 were considered to be statistically significant.

7.4 Results

7.4.1 Cytotoxic effects of 5-FU and Cisplatin

Figure 7.1 (a and b) demonstrate the percentage cell killing by 5-FU (50 $\mu\text{g/ml}$) and Cisplatin (50 $\mu\text{g/ml}$) for SW480 and SW620 cells. Both cell lines exhibited a similar cytotoxic response to the drugs, with minimal cell killing observed on day 0 (5-FU: 0-7%); Cisplatin: 0-13%). However, on subsequent days (days 1 and 2), the cytotoxic effect of both drugs are seen to increase. For all subsequent experiments, only the above 5-FU and Cisplatin doses were used.



b) Cisplatin treated cells

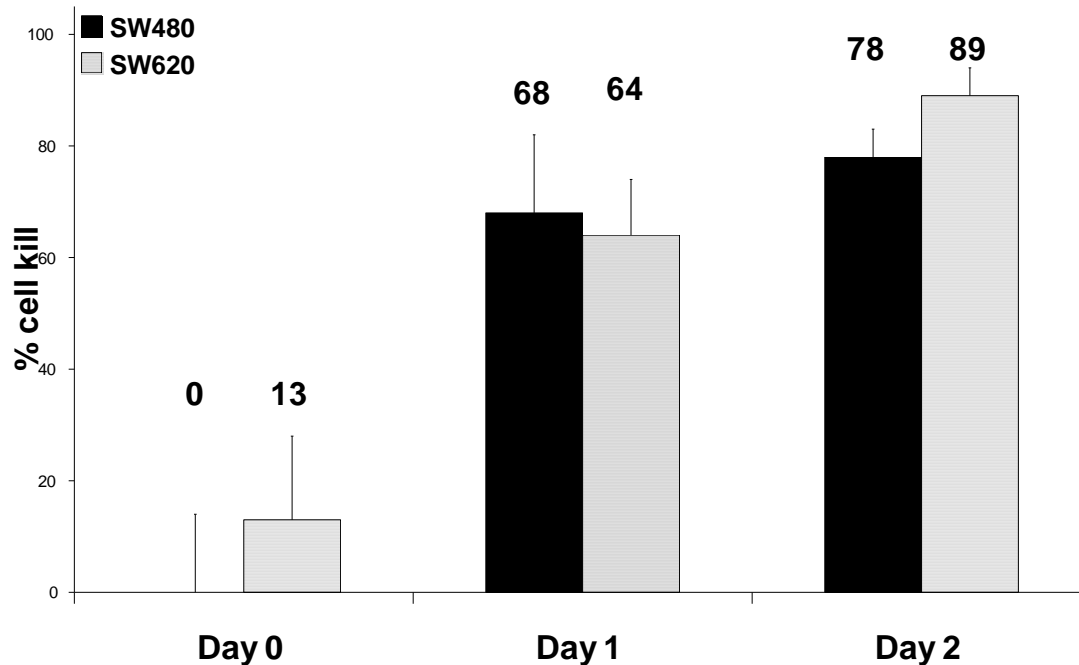
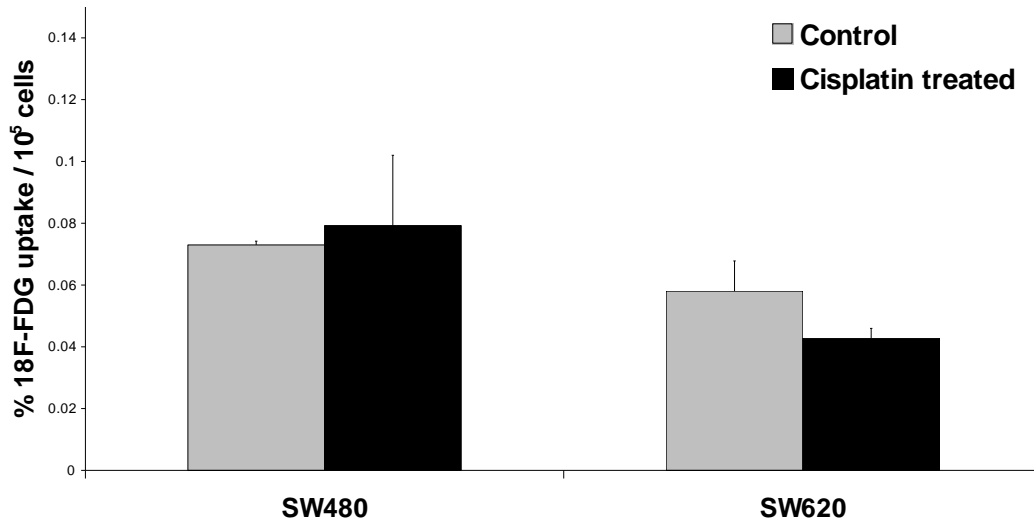


Figure 7.1 (a and b): Cytotoxic effect of 5-FU (50 $\mu\text{g/ml}$ for 2 hours) and Cisplatin (50 $\mu\text{g/ml}$ for 2 hours) on cell numbers. Minimal cell kill was observed on day 0 (ie: at 2 hours post drug exposure) for both drugs. The increasing cytotoxic effect of the drugs on subsequent days post-treatment (day 1 & 2) are demonstrated.

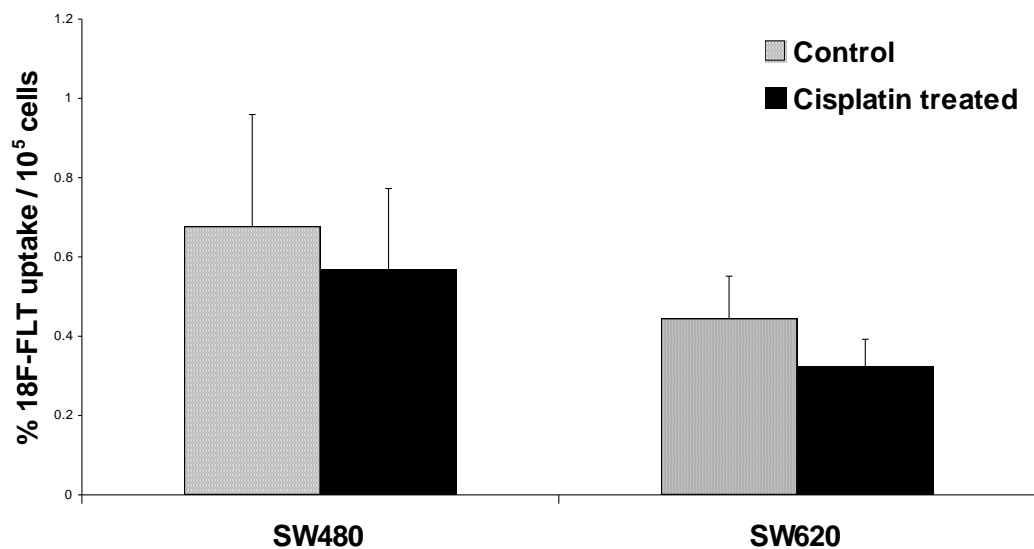
7.4.2 18F-FLT vs 18F-FDG uptake following 5-FU treatment

Figure 7.2 (a-d) graphically represents changes in tracer uptake (18F-FLT vs 18F-FDG) on day 0, in response to treatment with 5-FU and Cisplatin.

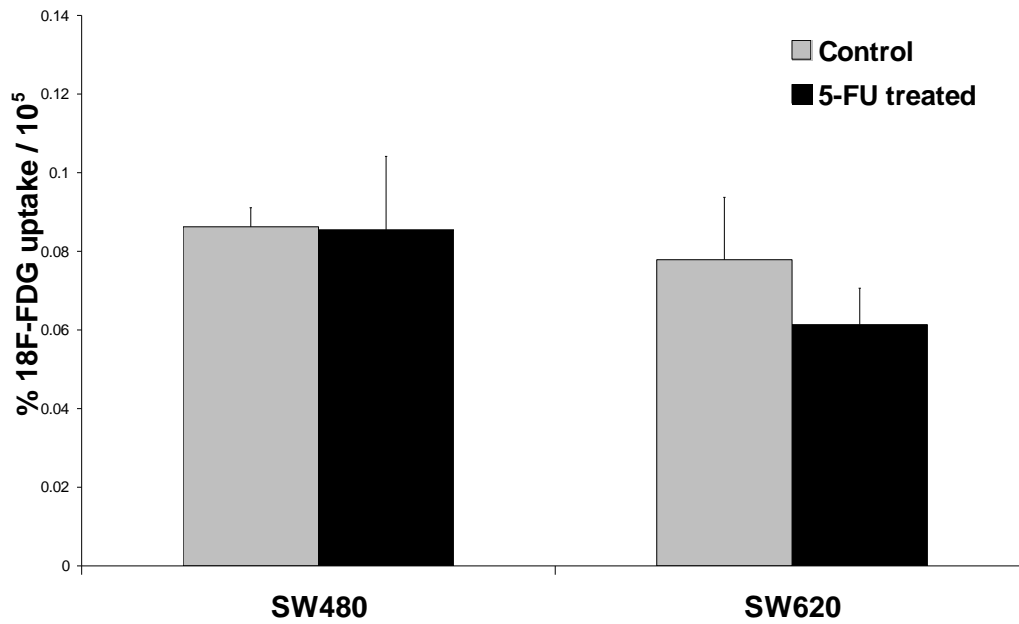
(a) 18F-FDG uptake in Cisplatin treated cells



(b) 18F-FLT uptake in Cisplatin treated cells



(c) 18F-FDG uptake in 5-FU treated cells



(d) 18F-FLT uptake in 5-FU treated cells

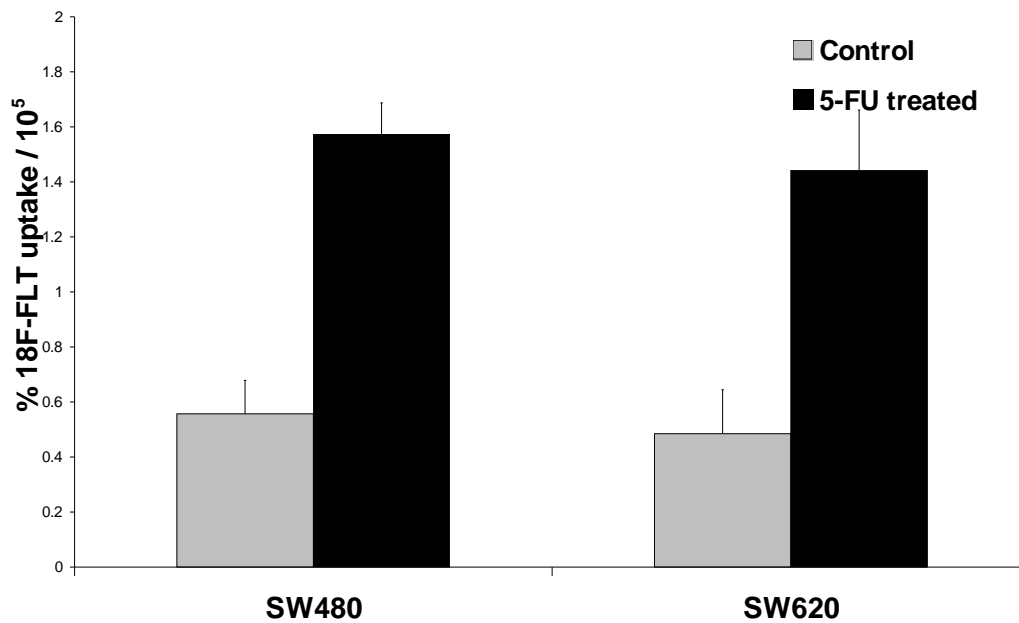


Figure 7.2: Changes in uptake of 18F-FDG (a & c) and 18F-FLT (b & d) on day 0, in response to treatment with 5-FU (50 $\mu\text{g/ml}$ for 2 hours) and Cisplatin (50 $\mu\text{g/ml}$ for 2 hours).

After a two hours pulse treatment with 5-FU, there was a mean 2.8 fold increase in 18F-FLT uptake SW480 ($p < 0.0001$) and 2.9 fold for SW620 cells ($p = 0.0004$).

Cisplatin treatment under identical conditions resulted in a minor reduction in mean ¹⁸F-FLT uptake, but this did not reach statistical significance (SW480: $p=0.55$; SW620: $p=0.19$; t-test). In comparison to ¹⁸F-FLT, ¹⁸F-FDG uptake changed little for SW480 cells (5-FU: $p=0.92$; Cisplatin: $p=0.81$; t-test). SW620 cells on the other hand, showed a reduction in tracer uptake in response to both cytotoxics but this difference again did not reach statistical significance (5-FU: $p=0.05$, Cisplatin: $p=0.05$; t-test).

In order to determine if changes in ¹⁸F-FLT uptake following 5-FU treatment were dose dependent, a parallel experiment on SW480 cells was carried out on day 0. Across 5-FU dose of range of 1-250 $\mu\text{g/ml}$, a statistically significant dose dependent increase in ¹⁸F-FLT uptake was seen ($p = 0.005$; one way ANOVA) (figure 7.3).

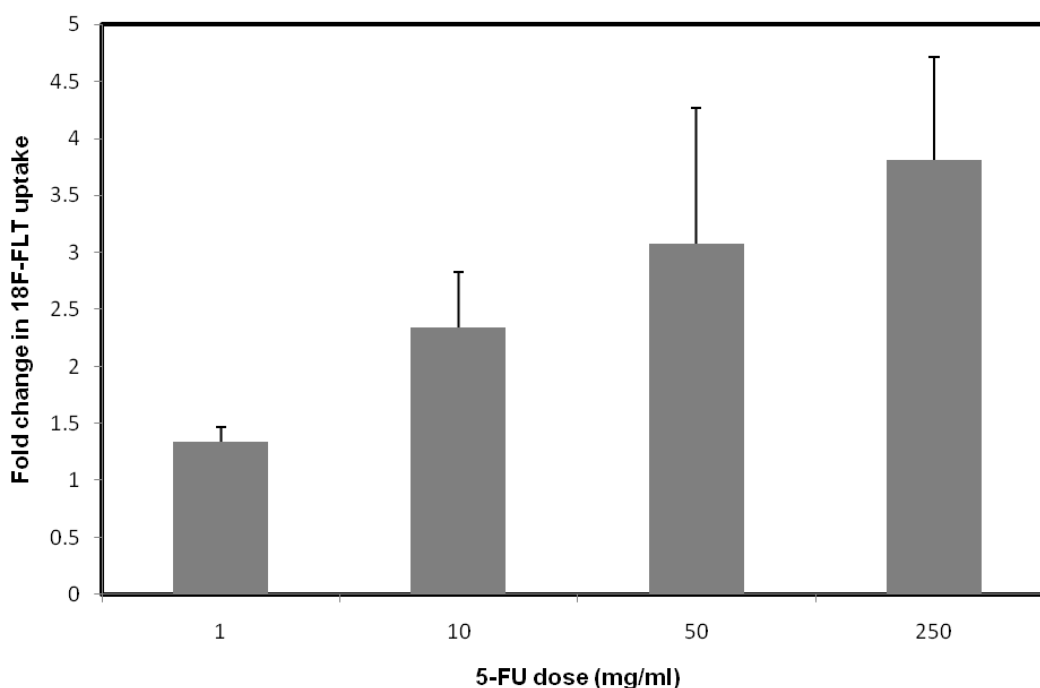


Figure 7.3: Dose dependent increase in ¹⁸F-FLT uptake in SW480 cells, across a range of 5-FU doses. A statistically significant difference between the groups was observed ($n=6$, $p=0.005$; one way ANOVA).

7.4.3 Cell cycle changes in 5-FU treated cells

Flow-cytometric analysis of BrdU incorporation was used to detect changes in the SPF at three time points following 5-FU treatment (days 0-2). The distribution of S-phase cells at each time point is summarised in table 7.1.

		% S-phase cells				<i>p</i>
		Treated		Untreated		
		Mean	<i>SD</i>	Mean	<i>SD</i>	
SW620	Day 0	52.4	11.0	47.0	8.1	NS
	Day 1	77.7	14.0	28.7	11.5	0.002
	Day 2	46.0	19.5	34.7	0.1	NS
SW480	Day 0	57.6	4.5	49.4	4.0	NS
	Day 1	61.1	3.1	35.8	6.6	0.004
	Day 2	32.5	23.6	21.8	4.4	NS

Table 7.1 : The distribution of S-phase cells at different time points in the 5-FU treated and untreated groups.

On day 0, no significant change in SPF was observed between the treated and control (untreated) cells. This is better demonstrated by the representative scatter plots in figure 7.4 (a-d).

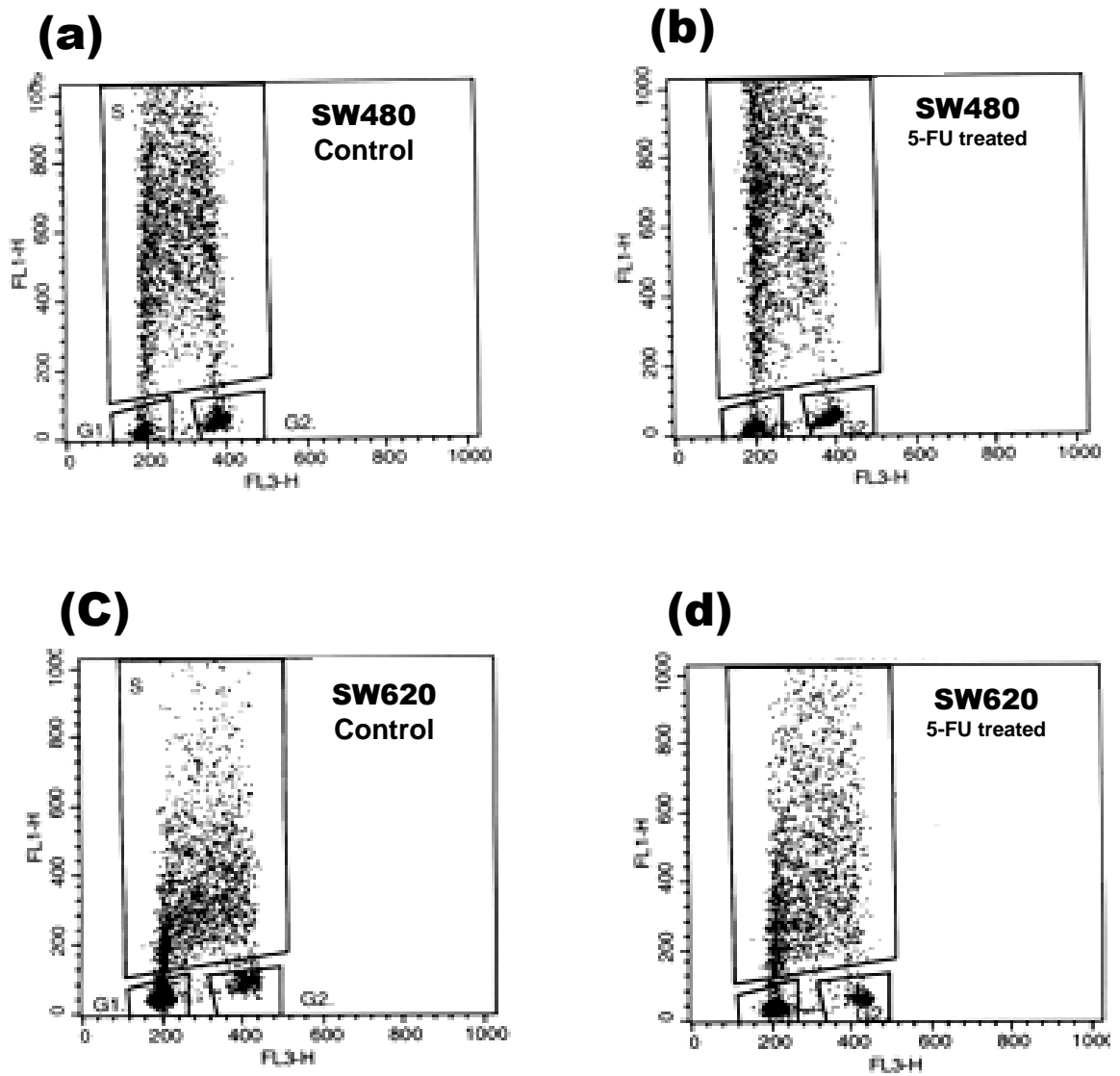


Figure 7.4 (a-d): Scatter plots representing the distribution of S-phase cells on day 0 following 5-FU treatment [SW480 cells: a) Control cell, b) 5-FU treated cells; SW620 cells: c) Control cells, d) 5-FU treated cells].

On subsequent days, there appeared to be a cell cycle phase shift in response to 5-FU treatment. On day 1 both cells lines showed a statistically significant increase in S-phase accumulation (Fold change in SPF: SW480 = 1.76 ± 0.43 ($p=0.002$); SW620= 2.88 ± 0.69 ($p=0.004$)), with SW620 cells demonstrating a higher fold change in SPF as compared to SW480 cells (figure 7.6). By day 2, the proportion of S-phase cells seemed to decrease again. This corresponded to the cell viability changes observed earlier. At this time point, there was again no statistical difference seen in the proportion of S-phase cells in 5-FU treated and untreated group (Mean fold change in SPF: SW480 = 1.41 ± 0.81 ($p = 0.48$); SW620 = 1.32 ± 0.56 ($p = 0.50$)).

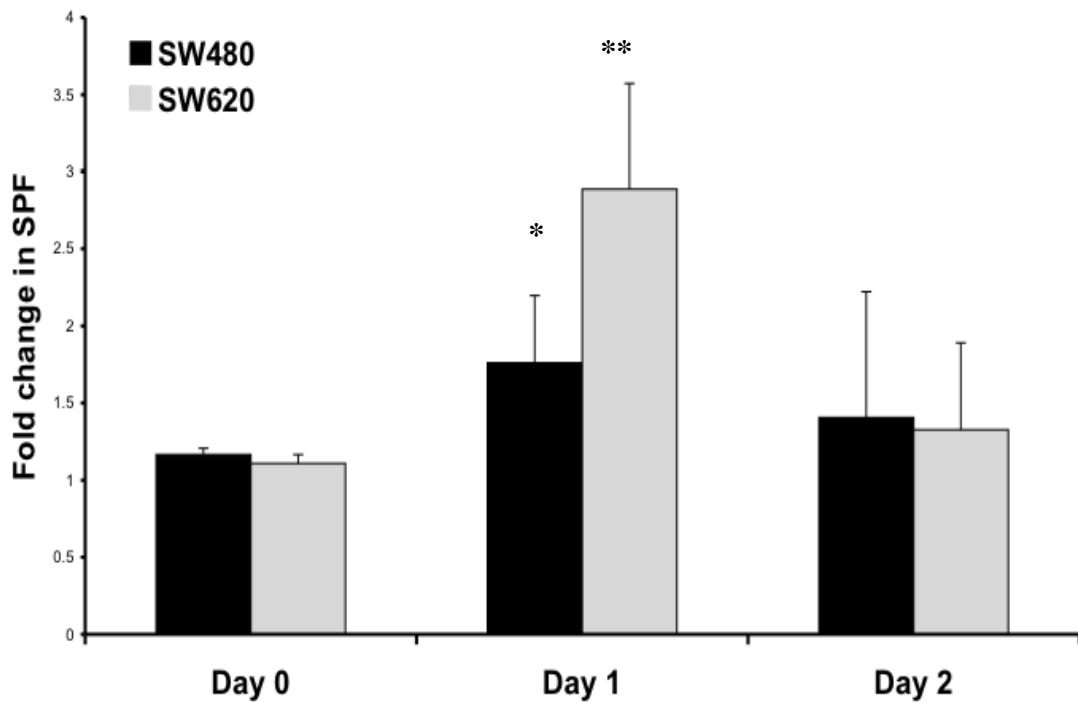
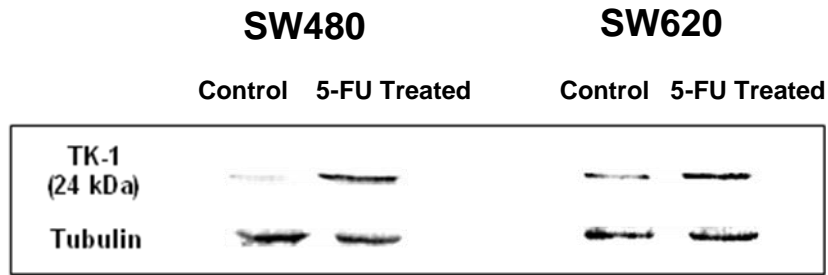


Figure 7.5: Fold change in SPF of cells on days 0 to 2 following treatment with 5-FU. On day 0, there was no significant change in SPF, whereas a significant increase in S-phase cells was seen on day 1 [Mean fold change (SD) on day 1: *SW480 = 1.76 ± 0.43 ($p=0.002$), **SW620 = 2.88 ± 0.69 ($p=0.004$)].

7.4.4 Changes in TK-1 expression

Protein separations were carried out under reducing conditions and therefore the expression of TK-1 in its monomeric form (24 kDa) was detected. The level of β -tubulin in each sample was used as an internal standard to ensure equal protein loading. As demonstrated in Figure 7.7, for both cell lines 5-FU treatment was associated with an increase in TK-1 protein expression. This was also in line with the observed increase in ^{18}F -FLT uptake seen in 5-FU treated cells. Analysis of bands by densitometry (corrected for protein loading) showed this difference to be statistically significant (SW480: $p=0.012$, SW620: $p=0.013$; Student's t-test).

a)



b)

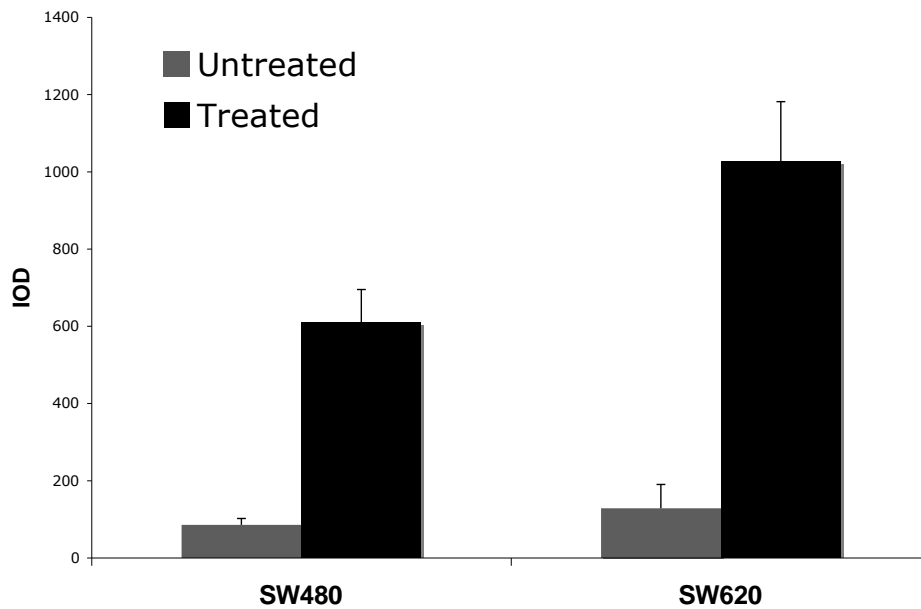


Figure 7.6: (a) Western blot analysis for TK-1 (24 kDa) expression (representative result of 3 independent experiments). (b) Densitometric analysis of bands (expressed as Integrated Optical Density (IOD)). For both cell lines, a statistically significant increase in expression of TK-1 was observed in 5-FU treated cells compared to the untreated controls ($p < 0.05$),

7.5 Discussion

This study examined the early effects of TS inhibition with 5-FU, on uptake of the two PET tracers ¹⁸F-FDG and ¹⁸F-FLT. The time point at which the experiments were carried out was of particular importance as at 2 hours after drug exposure (day 0), there were no changes observed in either cell numbers, nor the cell cycle phase of the drug exposed cell lines (shown in figures 7.1 and 7.2). The chosen drug doses were however demonstrated to be cytotoxic as a reduction in cell viability was observed on days 1 and 2 post-treatment with both 5-FU and Cisplatin. This setting therefore represented a time point when biological response to 5-FU could be assessed before changes in morphology were apparent.

On day 0, no significant change in ¹⁸F-FDG uptake was seen in response to 5-FU. This correlated with the unchanged cellular viability. Conversely, 5-FU treatment resulted in a dose dependent increase in ¹⁸F-FLT uptake as compared to the untreated controls. Treatment with Cisplatin (which exerts its cytotoxic effect by causing DNA chain termination and not directly through altering pyrimidine (thymidine) metabolism) did not result in the same increase in uptake of ¹⁸F-FLT, thus suggesting that the observed increase in ¹⁸F-FLT uptake may be a specific response to 5-FU. These findings were consistent with that of Dittmann et al. (2002) where in a human oesophageal cancer cells line (OSC-1), a 5-10 fold increase in ¹⁸F-FLT uptake was seen within 24 hours of cells being exposed to antimetabolites 5-FU, methotrexate and Gemcitabine, but once again not Cisplatin. Also in a very similar study to ours, Yau et al. (2006) also demonstrated an increase in uptake of ¹¹C-thymidine at 2 and 6 hours following pulse treatment with 5-FU and Nolatrexate (AG337), the latter being a novel selective TS inhibitor.

In our *in vitro* model, 5-FU treatment was shown to result in an increased expression of TK-1. This finding was consistent with our initial proposed hypothesis that treatment with 5-FU may result in activation of the salvage pathway of pyrimidine synthesis. However, it must be noted that the increase in TK-1 protein expression, may only represent one arm of the mechanism involved in thymidine salvage. Earlier work in a bladder cancer cell line showed TS inhibition to result in an increased expression of both nucleoside transporters (NT) as well as TK-1 activity (Pressacco et al. 1995). Their study suggested a common regulatory pathway for the TK-1 and NT expression, which may be dependent on intracellular thymidine pools, a function that is affected by TS inhibition. More recently, Perumal et al. (2006) re-examined the cellular response mechanisms to 5-FU in a mouse model bearing a RIF-1 tumour xenograft. Consistent with our results and other earlier studies, once again a 1.8 fold increase in tumour uptake of ¹⁸F-FLT was observed within 1 hour following treatment with 5-FU. Their study went on to assay tumour and plasma deoxyuridine, TK-1, ATP and type-1 equilibrative nucleoside transporter (ENT) levels. Tumour and plasma deoxyuridine levels increased significantly whereas contrary to our findings, TK-1 (and ATP levels) were unchanged. Furthermore, they observed an increase in ENT binding sites, but no changes in transporter affinity was observed. This lead them to suggest that early changes observed in ¹⁸F-FLT uptake may be related to changes in re-distribution of nucleoside transporters to plasma membrane and not changes in TK-1 expression. It can be argued that a significant upregulation of TK-1 expression to 5-FU treatment may take a longer while than the 2 hour time limit of our experiments would allow. In this scenario, an enhanced re-distribution of membrane nucleoside transporters would be a more plausible mechanism for the increased ¹⁸F-FLT uptake that is seen. Currently there are no published studies that

have quantified the amount of time it takes for TK-1 gene translation/transcription. While our finding of increased TK-1 expression may be in keeping with our original hypothesis, this finding requires further validation in light of the above recent findings. A correlative study that compares TK-1 gene and protein expression would be of great value.

Following on from the above, in considering TK-1 protein as the principal target for why cellular uptake of 18F-FLT increases, there are other consideration that need to be made. Much of our understanding of TK-1's biological activity stems from mechanistic studies carried out *in vitro*. It is understood that TK-1 undergoes a complex array of transcriptional and translational modifications that regulate its cell cycle control (Coppock and Pardee 1987; Ito and Conrad 1990; Chang and Huang 1993; Frederiksen et al. 2004). As such, alteration in dimer-tetramer transformations of the protein or post-transcriptional mechanisms of protein induction that may alter TK-1's enzymatic activity, may be also be highly relevant to drug induced effects on 18F-FLT uptake. In our study, the protein samples from cell lysates were prepared in reducing conditions, and thus the predominant form of TK-1 detected by the Western blot technique was its monomeric form at 24 kDa. It would therefore be of value to examine TK-1 in its native, non-reduced form in order to further assess the effect of 5-FU on its function as well as its sub-unit configuration.

Interestingly, our results suggest that TK-1 expression and SPF do not directly correlate. As previously mentioned, TK-1 is believed to be tightly regulated by the cell cycle. It is maximally expressed during S/G2 phase of the cell cycle, after which its levels decline to background levels by the end of the M phase (Sherley and Kelly

1988). A possible explanation for our results may lie in the fact that the maximal requirement for nucleotides during DNA synthesis is the principal reason for the inherent S-phase specificity of TK-1. Activation of the salvage pathway shortly after 5-FU treatment may therefore represent a fail-safe mechanism to counteract the deleterious effects of 5-FU on intracellular thymidine pools. The fact that 18F-FLT uptake shows a dose dependent pattern, further suggests that the pyrimidine salvage mechanism may represent an adaptive and not simply an “on-off” response. This assumption requires further investigation and future experiments should aim at correlating TK-1 activity / enzyme expression with changes in intracellular thymidine pools following 5-FU treatment.

A pitfall of our experimental model is related to the complex mode of action of 5-FU. Although TS inhibition is believed to be the principal mechanisms of 5-FU cytotoxicity, it has also been shown to have deleterious effect through direct incorporation into DNA and RNA. Future studies should therefore aim at defining the relative effects of the various metabolites of 5-FU on 18F-FLT uptake. Furthermore, as suggested by recent studies such as that of Prumal et al. (2006) and Yeu et al. (2006) (mentioned above), 18F-FLT may in fact be a more appropriate tracer for monitoring the effects of selective TS inhibitors such as Nolatrexate and not 5-FU.

18F-FLT at present is the second most commonly available PET radiopharmaceutical after 18F-FDG. The feasibility of using 18F-FLT PET in monitoring response to therapy has been shown in a number of *in vivo* animal models (Barthel et al. 2003; Oyama et al. 2004; Leyton et al. 2005; Waldherr et al. 2005). Early results in human subjects have also been reported in a small series of breast cancer patients (Kenny et

al. 2007). At one-week post treatment with FEC (5-fluorouracil, Epirubicin, Cyclophosphamide) chemotherapy, a reduction in 18F-FLT uptake was seen in responders ahead of changes in tumour size. Serial imaging also demonstrated a reduction in 18F-FLT uptake, corresponding to a change in tumour proliferation. The main focus of all these studies has been to monitor the anti-proliferative effects of cytotoxics with 18F-FLT PET. Our experimental model however, takes the application of 18F-FLT one step further back to a time point when 5-FU has not had any effect on cellular viability and / or proliferation. The observed paradoxical increase in 18F-FLT at this early time point may represent a surrogate marker of TS inhibition, thus raising the possibility of its application as a means of differentiating between tumours that may be sensitive to TS inhibitors from those which may not be. If these early changes in 18F-FLT uptake can be mirrored in the clinical setting, then potentially 18F-FLT PET can be used to determine 5-FU responsiveness after a small test dose, before the full treatment regimen has begun.

7.6 Conclusions

In an *in vitro* cell line model we have demonstrated an early, dose dependent biological response to TS inhibition with 5-FU, which is measurable with the thymidine analogue PET tracer ¹⁸F-FLT and not the routine glucose analogue ¹⁸F-FDG. Quantifying such changes in the salvage pathway of pyrimidine synthesis with ¹⁸F-FLT PET, may therefore provide a potential tool for predicting response to TS inhibition, before changes in tumour morphology and volume become apparent.

Chapter 8

Summary of results and overall conclusions

8.1 Summary of results

The modern management of cancer increasingly utilizes patient specific characteristics to provide patient centred care. Within this framework, cross-sectional imaging has played a predominant role in dictating the course of treatment. More recently however, our enhanced understanding of the molecular biology of disease is shifting the focus in cancer management to a more tumour specific one. This for example has led to the emergence of targeted biological treatments such as that with monoclonal antibodies. This concept shift in disease management has also paved the way for molecular imaging to develop as a discipline, which once a concept has become a clinical mainstay of imaging with the use of dedicated PET scanners.

The routine application of PET in cancer management can be considered with a two-pronged approach. In the first instance, molecular imaging may be used as an alternative tool to conventional cross-sectional imaging to improve diagnosis and staging of disease. With PET, this has largely been as a result of the success of ¹⁸F-FDG as a universally sensitive probe in targeting glycolysis, a process that is common to most cancers. The alternative approach is the application of PET imaging as a quantitative and a functional imaging tool. In this respect, a specific molecular probe may be applied both globally and individually to provide *in vivo* measures of disease biology. This paradigm can then be used not only to prognosticate, but also to monitor temporal changes in disease behaviour in response to treatment that can be measured at an earlier time point than what is achievable using morphological criteria.

This thesis aimed to examine the above two facades of molecular imaging with PET. To do this, two solid gastrointestinal cancers were chosen, each providing a model for

the routine use of PET that was able to highlight many of the strengths and weaknesses of this imaging modality. In chapters 3 and 4, the role of multimodality imaging with PET/CT using 18F-FDG was examined when applied routinely to the multidisciplinary management of pancreatic cancer and as tool to decision making in managing colorectal liver metastases. The main question raised was: “Does 18F-FDG PET/CT provide additional (clinically useful) information to routine imaging with CT?”

In the routine management of pancreatic cancer, 18F-FDG PET/CT was more sensitive and specific than routine ceCT in detecting the disease at the primary site. Although more specific than ceCT, false positive results with 18-FDG PET/CT occurred where there was tracer accumulation in focal areas of inflammation, namely in that of mass forming chronic pancreatitis. None the less, PET/CT was particularly useful where ceCT results were equivocal but suspicious, where the lack of tracer accumulation within a pancreatic mass was correctly interpreted as benign disease. The role of 18F-FDG PET/CT in staging locoregional disease was also limited. Poor spatial resolution of PET and the suboptimal (non-diagnostic) nature of the CT component of PET/CT did not allow for an accurate assessment of local (T) stage of a tumour. As for this, decisions about resectability of malignant lesions could not be made with PET/CT alone. Our results also indicated that accurate detection of locoregional lymph node involvement with 18F-FDG PET/CT may also not be superior to ceCT and overall poor. Therefore ultimately, the advantage conferred by 18F-FDG PET/CT was in determining / excluding the extent metastatic disease in patient who were deemed to have an operable tumour based on convention ceCT criteria.

In advanced colorectal cancer, it was similarly demonstrated that 18F-FDG PET/CT was more accurate than CT in detecting the extent of extrahepatic disease and provided a means of characterising equivocal liver lesions seen on CT. The sensitivity of 18F-FDG PET/CT and ceCT for detecting hepatic lesions were similar. Once again, the impact of 18F-FDG PET/CT on clinical management was through its accuracy in assessing the extent of metastatic disease both above and below the diaphragm. This potentially lead to a better patient selection for resection of liver metastases. Due to the small sample size of the study and limited time frame of follow-up, this impact of PET/CT on overall survival could not be assessed. However, similar studies previously published have shown pre-operative staging of CLM with 18F-FDG PET to correlate with an improved 5-year survival when compared with conventional CT (Fernandez et al. 2004).

One of the challenges faced by the routine use of PET/CT technology remains its relative high costs and the availability of PET/CT scanners particularly in the UK. An approach to tackling this is to define precise criteria based on parameters that predict which patient would most benefit from imaging with 18F-FDG PET/CT. One such potential selection criteria is the Clinical Risk Score, (CRS) originally described as a means of predicting the probability of recurrence in patient undergoing hepatic resection for CLM. We hypothesized that the CRS could identify patients in whom the clinical yield of 18F-FDG PET/CT would be the greatest. Our results however failed to show a significant correlation between CRS and the clinical yield of 18F-FDG PET/CT. It is likely that the study's small sample size may have resulted in such a trend not to become statistically apparent. On the other hand it can be argued that

¹⁸F-FDG PET could provide additional information regardless of prognostic scores of disease, thus justifying the routine application of ¹⁸F-FDG PET/CT. None the less, this hypothesis requires further examination in larger patient series and possibly with the use of alternative prognostic scoring systems.

Despite its high sensitivity, one of the drawbacks of the imaging with ¹⁸F-FDG PET has been its lack of tumour specificity. In the routine setting, false positive results often resulted in patients undergoing additional invasive diagnostic procedures. Should ¹⁸F-FDG PET become the mainstay of routine imaging in cancer, false positive results could result in considerable wasted resources, as patients may need to undergo unnecessary investigations, treatments and/or be refused curative therapies. Therefore in interpreting ¹⁸F-FDG PET studies, a clear knowledge of disease behaviour and understanding of tracer uptake patterns are paramount, in order so that truly malignant and benign lesions are not misinterpreted. Furthermore, alternative strategies to improve the specificity of PET, with for example the use of multimodality PET/CT scanners or the use of alternative radiopharmaceuticals (such as ¹⁸F-FLT) need to be further investigated.

Following on from the above, two pilot studies also examined the potential role of ¹⁸F-FLT PET in our two gastrointestinal cancer models. Consistent with the results of other published studies, the relative amount of ¹⁸F-FLT uptake within lesions was lower than that for ¹⁸F-FDG, thus resulting in poorer detection rates of malignant foci. In fact, any advantage conferred from ¹⁸F-FLT being a more cancer specific tracer was counteracted by its overall high false negative rate. Despite our two studies lacking adequate sample size and thus statistical power, the results strongly indicated

that ¹⁸F-FLT PET would be an unlikely candidate to supersede ¹⁸F-FDG as a routine PET tracer.

Access to tissue specimen in the cohort of pancreatic cancer patients allowed us to test the hypothesis of whether ¹⁸F-FLT uptake was a surrogate measure of cellular proliferation. The strong correlation between tumour ¹⁸F-FLT SUVs and Ki-67 antigen expression was again in keeping with other similar studies supporting the role of ¹⁸F-FLT as a marker of proliferation. Survival analysis although did not reveal statistically significant results, did show a divergence of survival curves between high and low ¹⁸F-FLT SUV thresholds. Unfortunately due to a lack of tissue specimen, the above hypothesis could not be tested for our group of patients with advanced colorectal cancer. However, earlier work in our unit has shown a similar positive correlation between ¹⁸F-FLT SUV and MIB-1 labelling in colorectal primary and metastatic lesions (Francis et al. 2003b). The results from this thesis and that of previously published data therefore support the role of ¹⁸F-FLT PET as a means quantifying the proliferation index of lesions and potentially as a means of obtaining prognostic information. However future larger scale studies are required to further ascertain the clinical relevance ¹⁸F-FLT, particularly in directing decision making prior to the start of neoadjuvant and adjuvant therapies.

Finally, the last chapter in this thesis examined a potential role for ¹⁸F-FLT to monitor response to chemotherapy using an *in vitro* cell line model of CRC. An increase in uptake of ¹⁸F-FLT was seen with 5-FU treatment and not Cisplatin. Furthermore, this response was also not seen with ¹⁸F-FDG uptake. The dose dependant response of ¹⁸F-FLT occurred at a time point before any changes in cell

number and cell cycle phase were observed thus supporting the notion that PET can potentially quantify biological changes, before changes in morphology become apparent. Interestingly, the increase in uptake of ¹⁸F-FLT with 5-FU treatment corresponded to an increase in expression of the phosphorylating (and trapping) enzyme, TK-1. The time constraints of this thesis did not allow for examination of any changes in TK-1 activity nor gene expression. Moreover, the recent study by Perumal et al. (2006) attributed a similar pattern of increased ¹⁸F-FLT uptake to redistribution of nucleoside transporters to the plasma membrane and not to an increase expression of TK-1. Therefore, despite our findings supporting our original working hypothesis, the mechanism underlying the observed thymidine / ¹⁸F-FLT uptake in response to TS inhibition requires further validation. Future studies are also required to examine whether 5-FU resistant cell lines would exhibit a higher or lower ¹⁸F-FLT uptake response. This can potentially be used in the clinical setting to predict good responders early in the course of treatment (ie: within hours), negating the need to undergo a futile course of chemotherapy before traditional measures of morphological response declare the treatment a success or not.

8.2 Overall conclusions

In conclusion, there are clear indications that molecular imaging with PET has emerged as a powerful adjunct to our conventional cross-sectional imaging techniques. Its routine application at present however seems to be best directed towards the assessment of overall disease / metastatic burden but, as our primary mode of curative treatment is still surgery, there remains a heavy reliance on accurate anatomical information that current PET and PET/CT imaging protocols fail to fulfil. Despite this, there is a real potential for a one-stop approach to diagnosing and staging cancer using ¹⁸F-FDG PET/CT. However, there are practical, logistical and cost implications that need to be addressed. At present ¹⁸F-FDG remains the gold standard tracer for PET imaging, which despite its limitations, is overall the most sensitive and specific tracer available for the routine clinical application of PET in oncology. Where alternative tracers such as ¹⁸F-FLT may be of value is in providing additional prognostic information which when used selectively, could in turn provide specific information required to treat cancer on an individualized basis.

References

- Abdel-Nabi, H., R. J. Doerr, et al. (1998). "Staging of primary colorectal carcinomas with fluorine-18 fluorodeoxyglucose whole-body PET: correlation with histopathologic and CT findings." *Radiology* 206(3): 755-60.
- Adam, R., A. Laurent, et al. (2000). "Two-stage hepatectomy: A planned strategy to treat irresectable liver tumors." *Ann Surg* 232(6): 777-85.
- Adamek, H. E., J. Albert, et al. (2000). "Pancreatic cancer detection with magnetic resonance cholangiopancreatography and endoscopic retrograde cholangiopancreatography: a prospective controlled study." *Lancet* 356(9225): 190-3.
- Adson, M. A., J. A. van Heerden, et al. (1984). "Resection of hepatic metastases from colorectal cancer." *Arch Surg* 119(6): 647-51.
- Akhurst, T. and S. M. Larson (1999). "Positron emission tomography imaging of colorectal cancer." *Semin Oncol* 26(5): 577-83.
- Antoch, G., F. M. Vogt, et al. (2003). "Whole-body dual-modality PET/CT and whole-body MRI for tumor staging in oncology." *Jama* 290(24): 3199-206.
- Arulampalam, T. H., D. L. Francis, et al. (2004). "FDG-PET for the pre-operative evaluation of colorectal liver metastases." *Eur J Surg Oncol* 30(3): 286-91.
- Azoulay, D., D. Castaing, et al. (2000). "Resection of nonresectable liver metastases from colorectal cancer after percutaneous portal vein embolization." *Ann Surg* 231(4): 480-6.
- Bares, R., B. M. Dohmen, et al. (1996). "[Results of positron emission tomography with fluorine-18 labeled fluorodeoxyglucose in differential diagnosis and staging of pancreatic carcinoma]." *Radiologe* 36(5): 435-40.
- Bares, R., P. Klever, et al. (1994). "F-18 fluorodeoxyglucose PET in vivo evaluation of pancreatic glucose metabolism for detection of pancreatic cancer." *Radiology* 192(1): 79-86.

Barker, D. W., R. J. Zagoria, et al. (2005). "Evaluation of liver metastases after radiofrequency ablation: utility of 18F-FDG PET and PET/CT." *AJR Am J Roentgenol* 184(4): 1096-102.

Barnard, N. J., P. A. Hall, et al. (1987). "Proliferative index in breast carcinoma determined in situ by Ki67 immunostaining and its relationship to clinical and pathological variables." *J Pathol* 152(4): 287-95.

Barthel, H., M. C. Cleij, et al. (2003). "3'-deoxy-3'-[18F]fluorothymidine as a new marker for monitoring tumor response to antiproliferative therapy in vivo with positron emission tomography." *Cancer Res* 63(13): 3791-8.

Barthel, H., M. Perumal, et al. (2005). "The uptake of 3'-deoxy-3'-[18F]fluorothymidine into L5178Y tumours in vivo is dependent on thymidine kinase 1 protein levels." *Eur J Nucl Med Mol Imaging* 32(3): 257-63.

Beets, G., F. Penninckx, et al. (1994). "Clinical value of whole-body positron emission tomography with [18F]fluorodeoxyglucose in recurrent colorectal cancer." *Br J Surg* 81(11): 1666-70.

Belt, J. A., N. M. Marina, et al. (1993). "Nucleoside transport in normal and neoplastic cells." *Adv Enzyme Regul* 33: 235-52.

Berberat, P., H. Friess, et al. (1999). "Diagnosis and staging of pancreatic cancer by positron emission tomography." *World J Surg* 23(9): 882-7.

Berger, K. L., S. A. Nicholson, et al. (2000). "FDG PET evaluation of mucinous neoplasms: correlation of FDG uptake with histopathologic features." *AJR Am J Roentgenol* 174(4): 1005-8.

Bergers, E., J. P. Baak, et al. (1997a). "Prognostic implications of different cell cycle analysis models of flow cytometric DNA histograms of 1,301 breast cancer patients: results from the Multicenter Morphometric Mammary Carcinoma Project (MMMCP)." *Int J Cancer* 74(3): 260-9.

Bergers, E., I. Jannink, et al. (1997b). "The influence of fixation delay on mitotic activity and flow cytometric cell cycle variables." *Hum Pathol* 28(1): 95-100.

Bergers, E., P. J. van Diest, et al. (1997c). "Comparison of five cell cycle analysis models applied to 1414 flow cytometric DNA histograms of fresh frozen breast cancer." *Cytometry* 30(1): 54-60.

Blodgett, T. M., B. M. McCook, et al. (2006). "Positron emission tomography/computed tomography: protocol issues and options." *Semin Nucl Med* 36(2): 157-68.

Bluemke, D. A., J. L. Cameron, et al. (1995). "Potentially resectable pancreatic adenocarcinoma: spiral CT assessment with surgical and pathologic correlation." *Radiology* 197(2): 381-5.

Boothman, D. A., T. W. Davis, et al. (1994). "Enhanced expression of thymidine kinase in human cells following ionizing radiation." *Int J Radiat Oncol Biol Phys* 30(2): 391-8.

Buck, A. C., H. H. Schirrmeister, et al. (2001). "Ki-67 immunostaining in pancreatic cancer and chronic active pancreatitis: does in vivo FDG uptake correlate with proliferative activity?" *J Nucl Med* 42(5): 721-5.

Buck, A. K., H. Schirrmeister, et al. (2002). "3-deoxy-3-[(18)F]fluorothymidine-positron emission tomography for noninvasive assessment of proliferation in pulmonary nodules." *Cancer Res* 62(12): 3331-4.

Cascini, G. L., A. Avallone, et al. (2006). "18F-FDG PET is an early predictor of pathologic tumor response to preoperative radiochemotherapy in locally advanced rectal cancer." *J Nucl Med* 47(8): 1241-8.

Cattoretti, G., M. H. Becker, et al. (1992). "Monoclonal antibodies against recombinant parts of the Ki-67 antigen (MIB 1 and MIB 3) detect proliferating cells in microwave-processed formalin-fixed paraffin sections." *J Pathol* 168(4): 357-63.

Chang, Z. F. and D. Y. Huang (1993). "The regulation of thymidine kinase in HL-60 human promyeloleukemia cells." *J Biol Chem* 268(2): 1266-71.

Choi, S. J., J. S. Kim, et al. (2005). "[18F]3'-deoxy-3'-fluorothymidine PET for the diagnosis and grading of brain tumors." *Eur J Nucl Med Mol Imaging* 32(6): 653-9.

- Ciernik, I. F., E. Dizendorf, et al. (2003). "Radiation treatment planning with an integrated positron emission and computer tomography (PET/CT): a feasibility study." *Int J Radiat Oncol Biol Phys* 57(3): 853-63.
- Clarke, D. L., S. R. Thomson, et al. (2003). "Preoperative imaging of pancreatic cancer: a management-oriented approach." *J Am Coll Surg* 196(1): 119-29.
- Cobben, D. C., P. H. Elsinga, et al. (2004a). "Detection and grading of soft tissue sarcomas of the extremities with (18)F-3'-fluoro-3'-deoxy-L-thymidine." *Clin Cancer Res* 10(5): 1685-90.
- Cobben, D. C., P. L. Jager, et al. (2003). "3'-18F-fluoro-3'-deoxy-L-thymidine: a new tracer for staging metastatic melanoma?" *J Nucl Med* 44(12): 1927-32.
- Cobben, D. C., B. F. van der Laan, et al. (2004b). "18F-FLT PET for visualization of laryngeal cancer: comparison with 18F-FDG PET." *J Nucl Med* 45(2): 226-31.
- Cohade, C., M. Osman, et al. (2003a). "Direct comparison of (18)F-FDG PET and PET/CT in patients with colorectal carcinoma." *J Nucl Med* 44(11): 1797-803.
- Cohade, C., M. Osman, et al. (2003b). "Initial experience with oral contrast in PET/CT: phantom and clinical studies." *J Nucl Med* 44(3): 412-6.
- Conio, M., J. F. Demarquay, et al. (2001). "Endoscopic treatment of pancreaticobiliary malignancies." *Crit Rev Oncol Hematol* 37(2): 127-35.
- Coppock, D. L. and A. B. Pardee (1987). "Control of thymidine kinase mRNA during the cell cycle." *Mol Cell Biol* 7(8): 2925-32.
- Czernin, J. and M. E. Phelps (2002). "Positron emission tomography scanning: current and future applications." *Annu Rev Med* 53: 89-112.
- Delbeke, D. and W. H. Martin (2004). "PET and PET-CT for evaluation of colorectal carcinoma." *Semin Nucl Med* 34(3): 209-23.
- Delbeke, D., D. M. Rose, et al. (1999). "Optimal interpretation of FDG PET in the diagnosis, staging and management of pancreatic carcinoma." *J Nucl Med* 40(11): 1784-91.

Delbeke, D., J. V. Vitola, et al. (1997). "Staging recurrent metastatic colorectal carcinoma with PET." *J Nucl Med* 38(8): 1196-201.

Di Chiro, G. (1987). "Positron emission tomography using [18F] fluorodeoxyglucose in brain tumors. A powerful diagnostic and prognostic tool." *Invest Radiol* 22(5): 360-71.

Di Stefano, D., P. L. Mingazzini, et al. (1991). "A comparative study of histopathology, hormone receptors, peanut lectin binding, Ki-67 immunostaining, and nucleolar organizer region-associated proteins in human breast cancer." *Cancer* 67(2): 463-71.

Diederichs, C. G., L. Staib, et al. (2000). "Values and limitations of 18F-fluorodeoxyglucose-positron-emission tomography with preoperative evaluation of patients with pancreatic masses." *Pancreas* 20(2): 109-16.

Diehl, S. J., K. J. Lehmann, et al. (1998). "Pancreatic cancer: value of dual-phase helical CT in assessing resectability." *Radiology* 206(2): 373-8.

DiMagno, E. P. (1999). "Pancreatic cancer: clinical presentation, pitfalls and early clues." *Ann Oncol* 10 Suppl 4: 140-2.

Dittmann, H., B. M. Dohmen, et al. (2002). "Early changes in [18F]FLT uptake after chemotherapy: an experimental study." *Eur J Nucl Med Mol Imaging* 29(11): 1462-9.

Dittmann, H., B. M. Dohmen, et al. (2003). "[18F]FLT PET for diagnosis and staging of thoracic tumours." *Eur J Nucl Med Mol Imaging* 30(10): 1407-12.

Doci, R., L. Gennari, et al. (1991). "One hundred patients with hepatic metastases from colorectal cancer treated by resection: analysis of prognostic determinants." *Br J Surg* 78(7): 797-801.

Donckier, V., J. L. Van Laethem, et al. (2003). "[F-18] fluorodeoxyglucose positron emission tomography as a tool for early recognition of incomplete tumor destruction after radiofrequency ablation for liver metastases." *J Surg Oncol* 84(4): 215-23.

Donhuijsen, K., U. Schmidt, et al. (1990). "Changes in mitotic rate and cell cycle fractions caused by delayed fixation." *Hum Pathol* 21(7): 709-14.

Eary, J. F., D. A. Mankoff, et al. (1999). "2-[C-11]thymidine imaging of malignant brain tumors." *Cancer Res* 59(3): 615-21.

Elias, D., O. Baton, et al. (2005). "Hepatectomy plus intraoperative radiofrequency ablation and chemotherapy to treat technically unresectable multiple colorectal liver metastases." *J Surg Oncol* 90(1): 36-42.

Elias, D., J. F. Ouellet, et al. (2002). "Preoperative selective portal vein embolization before hepatectomy for liver metastases: long-term results and impact on survival." *Surgery* 131(3): 294-9.

Even-Sapir, E., Y. Parag, et al. (2004). "Detection of recurrence in patients with rectal cancer: PET/CT after abdominoperineal or anterior resection." *Radiology* 232(3): 815-22.

Falk, P. M., N. C. Gupta, et al. (1994). "Positron emission tomography for preoperative staging of colorectal carcinoma." *Dis Colon Rectum* 37(2): 153-6.

Fearon, E. R. and B. Vogelstein (1990). "A genetic model for colorectal tumorigenesis." *Cell* 61(5): 759-67.

Fegiz, G., G. Ramacciato, et al. (1991). "Patient selection and factors affecting results following resection for hepatic metastases from colorectal carcinoma." *Int Surg* 76(1): 58-63.

Fernandez, F. G., J. A. Drebin, et al. (2004). "Five-year survival after resection of hepatic metastases from colorectal cancer in patients screened by positron emission tomography with F-18 fluorodeoxyglucose (FDG-PET)." *Ann Surg* 240(3): 438-47; *discussion* 447-50.

Findlay, M., H. Young, et al. (1996). "Noninvasive monitoring of tumor metabolism using fluorodeoxyglucose and positron emission tomography in colorectal cancer liver metastases: correlation with tumor response to fluorouracil." *J Clin Oncol* 14(3): 700-8.

Flamen, P., S. Stroobants, et al. (1999). "Additional value of whole-body positron emission tomography with fluorine-18-2-fluoro-2-deoxy-D-glucose in recurrent colorectal cancer." *J Clin Oncol* 17(3): 894-901.

Flanagan, F. L., F. Dehdashti, et al. (1998). "Utility of FDG-PET for investigating unexplained plasma CEA elevation in patients with colorectal cancer." *Ann Surg* 227(3): 319-23.

Flexner, C., C. van der Horst, et al. (1994). "Relationship between plasma concentrations of 3'-deoxy-3'-fluorothymidine (alovudine) and antiretroviral activity in two concentration-controlled trials." *J Infect Dis* 170(6): 1394-403.

Fong, Y., A. M. Cohen, et al. (1997). "Liver resection for colorectal metastases." *J Clin Oncol* 15(3): 938-46.

Fong, Y., J. Fortner, et al. (1999a). "Clinical score for predicting recurrence after hepatic resection for metastatic colorectal cancer: analysis of 1001 consecutive cases." *Ann Surg* 230(3): 309-18; *discussion* 318-21.

Fong, Y., P. F. Saldinger, et al. (1999b). "Utility of 18F-FDG positron emission tomography scanning on selection of patients for resection of hepatic colorectal metastases." *Am J Surg* 178(4): 282-7.

Francis, D. L., A. Freeman, et al. (2003a). "In vivo imaging of cellular proliferation in colorectal cancer using positron emission tomography." *Gut* 52(11): 1602-6.

Francis, D. L., D. Visvikis, et al. (2003b). "Potential impact of [18F]3'-deoxy-3'-fluorothymidine versus [18F]fluoro-2-deoxy-D-glucose in positron emission tomography for colorectal cancer." *Eur J Nucl Med Mol Imaging* 30(7): 988-94.

Frederiksen, H., D. Berenstein, et al. (2004). "Effect of valine 106 on structure-function relation of cytosolic human thymidine kinase. Kinetic properties and oligomerization pattern of nine substitution mutants of V106." *Eur J Biochem* 271(11): 2248-56.

Freeny, P. C. (2001). "Pancreatic carcinoma: imaging update 2001." *Dig Dis* 19(1): 37-46.

- Freeny, P. C., L. W. Traverso, et al. (1993). "Diagnosis and staging of pancreatic adenocarcinoma with dynamic computed tomography." *Am J Surg* 165(5): 600-6.
- Friess, H., J. Langhans, et al. (1995). "Diagnosis of pancreatic cancer by 2[18F]-fluoro-2-deoxy-D-glucose positron emission tomography." *Gut* 36(5): 771-7.
- Frohlich, A., C. G. Diederichs, et al. (1999). "Detection of liver metastases from pancreatic cancer using FDG PET." *J Nucl Med* 40(2): 250-5.
- Fuhrman, G. M., C. Charnsangavej, et al. (1994). "Thin-section contrast-enhanced computed tomography accurately predicts the resectability of malignant pancreatic neoplasms." *Am J Surg* 167(1): 104-11; discussion 111-3.
- Fung, A. S., G. G. Tsiotos, et al. (1997). "ERCP-induced acute necrotizing pancreatitis: is it a more severe disease?" *Pancreas* 15(3): 217-21.
- Gambhir, S. S. (2002). "Molecular imaging of cancer with positron emission tomography." *Nat Rev Cancer* 2(9): 683-93.
- Gambhir, S. S., J. Czernin, et al. (2001). "A tabulated summary of the FDG PET literature." *J Nucl Med* 42(5 Suppl): 1S-93S.
- Gayowski, T. J., S. Iwatsuki, et al. (1994). "Experience in hepatic resection for metastatic colorectal cancer: analysis of clinical and pathologic risk factors." *Surgery* 116(4): 703-10; discussion 710-1.
- Giacosa, A., F. Frascio, et al. (2004). "Epidemiology of colorectal polyps." *Tech Coloproctol* 8 Suppl 2: s243-7.
- Goessl, C. and Z. Grozdanovic (2004). "PET concerns in bevacizumab treatment." *Nat Med* 10(6): 561; author reply 561.
- Graham, M. M., L. M. Peterson, et al. (2000). "Comparison of simplified quantitative analyses of FDG uptake." *Nucl Med Biol* 27(7): 647-55.
- Graham, R. A., M. Bankoff, et al. (1994). "Fine-needle aspiration biopsy of pancreatic ductal adenocarcinoma: loss of diagnostic accuracy with small tumors." *J Surg Oncol* 55(2): 92-4.

Grierson, J. R., J. L. Schwartz, et al. (2004). "Metabolism of 3'-deoxy-3'-[F-18]fluorothymidine in proliferating A549 cells: validations for positron emission tomography." *Nucl Med Biol* 31(7): 829-37.

Grierson, J. R. and A. F. Shields (2000). "Radiosynthesis of 3'-deoxy-3'-[(18)F]fluorothymidine: [(18)F]FLT for imaging of cellular proliferation in vivo." *Nucl Med Biol* 27(2): 143-56.

Guillem, J. G., H. G. Moore, et al. (2004). "Sequential preoperative fluorodeoxyglucose-positron emission tomography assessment of response to preoperative chemoradiation: a means for determining longterm outcomes of rectal cancer." *J Am Coll Surg* 199(1): 1-7.

Gupta, N. C., P. M. Falk, et al. (1993). "Pre-operative staging of colorectal carcinoma using positron emission tomography." *Nebr Med J* 78(2): 30-5.

Haberkorn, U., L. G. Strauss, et al. (1991). "PET studies of fluorodeoxyglucose metabolism in patients with recurrent colorectal tumors receiving radiotherapy." *J Nucl Med* 32(8): 1485-90.

Hanbidge, A. E. (2002). "Cancer of the pancreas: the best image for early detection--CT, MRI, PET or US?" *Can J Gastroenterol* 16(2): 101-5.

Haycox, A., M. Lombard, et al. (1998). "Review article: current treatment and optimal patient management in pancreatic cancer." *Aliment Pharmacol Ther* 12(10): 949-64.

Heinrich, S., G. W. Goerres, et al. (2005). "Positron emission tomography/computed tomography influences on the management of resectable pancreatic cancer and its cost-effectiveness." *Ann Surg* 242(2): 235-43.

Higashi, T., N. Tamaki, et al. (1997). "Expression of glucose transporters in human pancreatic tumors compared with increased FDG accumulation in PET study." *J Nucl Med* 38(9): 1337-44.

Howard, A. and S. Pelc (1951). "Nuclear incorporation of P32 as demonstrated by autoradiographs." *Exp Cell Res* 2: 178-187.

Huebner, R. H., K. C. Park, et al. (2000). "A meta-analysis of the literature for whole-body FDG PET detection of recurrent colorectal cancer." *J Nucl Med* 41(7): 1177-89.

Hung, G. U., Y. C. Shiau, et al. (2001). "Value of 18F-fluoro-2-deoxyglucose positron emission tomography in the evaluation of recurrent colorectal cancer." *Anticancer Res* 21(2B): 1375-8.

Imbriaco, M., T. Akhurst, et al. (2000). "Whole-Body FDG-PET in Patients with Recurrent Colorectal Carcinoma. A Comparative Study with CT." *Clin Positron Imaging* 3(3): 107-114.

Imdahl, A., E. Nitzsche, et al. (1999). "Evaluation of positron emission tomography with 2-[18F]fluoro-2-deoxy-D-glucose for the differentiation of chronic pancreatitis and pancreatic cancer." *Br J Surg* 86(2): 194-9.

Imdahl, A., M. J. Reinhardt, et al. (2000). "Impact of 18F-FDG-positron emission tomography for decision making in colorectal cancer recurrences." *Langenbecks Arch Surg* 385(2): 129-34.

Inokuma, T., N. Tamaki, et al. (1995). "Evaluation of pancreatic tumors with positron emission tomography and F-18 fluorodeoxyglucose: comparison with CT and US." *Radiology* 195(2): 345-52.

Ishimori, T., T. Saga, et al. (2002). "Increased (18)F-FDG uptake in a model of inflammation: concanavalin A-mediated lymphocyte activation." *J Nucl Med* 43(5): 658-63.

Isola, J. J., H. J. Helin, et al. (1990). "Evaluation of cell proliferation in breast carcinoma. Comparison of Ki-67 immunohistochemical study, DNA flow cytometric analysis, and mitotic count." *Cancer* 65(5): 1180-4.

Ito, K., T. Kato, et al. (1992). "Recurrent rectal cancer and scar: differentiation with PET and MR imaging." *Radiology* 182(2): 549-52.

Ito, M. and S. E. Conrad (1990). "Independent regulation of thymidine kinase mRNA and enzyme levels in serum-stimulated cells." *J Biol Chem* 265(12): 6954-60.

- Jadvar, H. and A. J. Fischman (2001). "Evaluation of pancreatic carcinoma with FDG PET." *Abdom Imaging* 26(3): 254-9.
- Jaffer, F. A. and R. Weissleder (2005). "Molecular imaging in the clinical arena." *Jama* 293(7): 855-62.
- Jamison, R. L., J. H. Donohue, et al. (1997). "Hepatic resection for metastatic colorectal cancer results in cure for some patients." *Arch Surg* 132(5): 505-10; *discussion* 511.
- Jemal, A., T. Murray, et al. (2003). "Cancer statistics, 2003." *CA Cancer J Clin* 53(1): 5-26.
- Kaim, A. H., B. Weber, et al. (2002). "Autoradiographic quantification of 18F-FDG uptake in experimental soft-tissue abscesses in rats." *Radiology* 223(2): 446-51.
- Kantorova, I., L. Lipska, et al. (2003). "Routine (18)F-FDG PET preoperative staging of colorectal cancer: comparison with conventional staging and its impact on treatment decision making." *J Nucl Med* 44(11): 1784-8.
- Kato, T., K. Yasui, et al. (2003). "Therapeutic results for hepatic metastasis of colorectal cancer with special reference to effectiveness of hepatectomy: analysis of prognostic factors for 763 cases recorded at 18 institutions." *Dis Colon Rectum* 46(10 *Suppl*): S22-31.
- Kenny, L., R. C. Coombes, et al. (2007). "Imaging early changes in proliferation at 1 week post chemotherapy: a pilot study in breast cancer patients with 3'-deoxy-3'-[18F]fluorothymidine positron emission tomography." *Eur J Nucl Med Mol Imaging* 34(9): 1339-47.
- Kim, E. E., S. K. Chung, et al. (1992). "Differentiation of residual or recurrent tumors from post-treatment changes with F-18 FDG PET." *Radiographics* 12(2): 269-79.
- Kinkel, K., Y. Lu, et al. (2002). "Detection of hepatic metastases from cancers of the gastrointestinal tract by using noninvasive imaging methods (US, CT, MR imaging, PET): a meta-analysis." *Radiology* 224(3): 748-56.

Kinsella, A. R., D. Smith, et al. (1997). "Resistance to chemotherapeutic antimetabolites: a function of salvage pathway involvement and cellular response to DNA damage." *Br J Cancer* 75(7): 935-45.

Kitano, M., M. Kudo, et al. (2004). "Dynamic imaging of pancreatic diseases by contrast enhanced coded phase inversion harmonic ultrasonography." *Gut* 53(6): 854-9.

Koyama, K., T. Okamura, et al. (2001). "Diagnostic usefulness of FDG PET for pancreatic mass lesions." *Ann Nucl Med* 15(3): 217-24.

Laemmli, U. K. (1970). "Cleavage of structural proteins during the assembly of the head of bacteriophage T4." *Nature* 227(5259): 680-5.

Lai, D. T., M. Fulham, et al. (1996). "The role of whole-body positron emission tomography with [18F]fluorodeoxyglucose in identifying operable colorectal cancer metastases to the liver." *Arch Surg* 131(7): 703-7.

Lee, A. K., B. Wiley, et al. (1992). "Quantitative DNA analysis and proliferation in breast carcinomas. A comparison between image analysis and flow cytometry." *Pathol Res Pract* 188(4-5): 428-32.

Leyton, J., J. R. Latigo, et al. (2005). "Early detection of tumor response to chemotherapy by 3'-deoxy-3'-[18F]fluorothymidine positron emission tomography: the effect of cisplatin on a fibrosarcoma tumor model in vivo." *Cancer Res* 65(10): 4202-10.

Li, D., K. Xie, et al. (2004). "Pancreatic cancer." *Lancet* 363(9414): 1049-57.

Lim, J. E., M. W. Chien, et al. (2003). "Prognostic factors following curative resection for pancreatic adenocarcinoma: a population-based, linked database analysis of 396 patients." *Ann Surg* 237(1): 74-85.

Liu, C. L., S. T. Fan, et al. (2002). "Hepatic resection for colorectal liver metastases: prospective study." *Hong Kong Med J* 8(5): 329-33.

Longley, D. B., D. P. Harkin, et al. (2003). "5-fluorouracil: mechanisms of action and clinical strategies." *Nat Rev Cancer* 3(5): 330-8.

- Machulla, H., A. Blocher, et al. (2000). "Simplified labeling approach for synthesizing 3'-deoxy-3-[18F]fluorothymidine ([18F]FLT)." *J Radioanal Nucl Chem* 243: 843-846.
- Maisey, N. R., A. Webb, et al. (2000). "FDG-PET in the prediction of survival of patients with cancer of the pancreas: a pilot study." *Br J Cancer* 83(3): 287-93.
- Mala, T., G. Bohler, et al. (2002). "Hepatic resection for colorectal metastases: can preoperative scoring predict patient outcome?" *World J Surg* 26(11): 1348-53.
- Mankoff, D. A., A. F. Shields, et al. (1998). "Kinetic analysis of 2-[carbon-11]thymidine PET imaging studies: compartmental model and mathematical analysis." *J Nucl Med* 39(6): 1043-55.
- Mann, C. D., M. S. Metcalfe, et al. (2004). "The clinical risk score: emerging as a reliable preoperative prognostic index in hepatectomy for colorectal metastases." *Arch Surg* 139(11): 1168-72.
- Marchetti, E., P. Querzoli, et al. (1990). "Assessment of proliferative rate of breast cancer by Ki-67 monoclonal antibody." *Mod Pathol* 3(1): 31-5.
- Mariani, A. (2003). "Pharmacological prevention of post-ERCP pancreatitis: which therapy is best?" *Jop* 4(1): 68-74.
- Masih, P. J., D. Kunnev, et al. (2008). "Mismatch Repair proteins are recruited to replicating DNA through interaction with Proliferating Cell Nuclear Antigen (PCNA)." *Nucleic Acids Res* 36(1): 67-75.
- Mawlawi, O., J. J. Erasmus, et al. (2006). "Quantifying the effect of IV contrast media on integrated PET/CT: clinical evaluation." *AJR Am J Roentgenol* 186(2): 308-19.
- McCormick, D., H. Chong, et al. (1993). "Detection of the Ki-67 antigen in fixed and wax-embedded sections with the monoclonal antibody MIB1." *Histopathology* 22(4): 355-60.
- Mertz, H. R., P. Sechopoulos, et al. (2000). "EUS, PET, and CT scanning for evaluation of pancreatic adenocarcinoma." *Gastrointest Endosc* 52(3): 367-71.

Mier, W., U. Haberkorn, et al. (2002). "[18F]FLT; portrait of a proliferation marker." *Eur J Nucl Med Mol Imaging* 29(2): 165-9.

Minniti, S., C. Bruno, et al. (2003). "Sonography versus helical CT in identification and staging of pancreatic ductal adenocarcinoma." *J Clin Ultrasound* 31(4): 175-82.

Moehler, M., A. Dimitrakopoulou-Strauss, et al. (1998). "18F-labeled fluorouracil positron emission tomography and the prognoses of colorectal carcinoma patients with metastases to the liver treated with 5-fluorouracil." *Cancer* 83(2): 245-53.

Moore, H. G., T. Akhurst, et al. (2003). "A case-controlled study of 18-fluorodeoxyglucose positron emission tomography in the detection of pelvic recurrence in previously irradiated rectal cancer patients." *J Am Coll Surg* 197(1): 22-8.

Mukai, M., S. Sadahiro, et al. (2000). "Preoperative evaluation by whole-body 18F-fluorodeoxyglucose positron emission tomography in patients with primary colorectal cancer." *Oncol Rep* 7(1): 85-7.

Munch-Petersen, B., L. Cloos, et al. (1995). "Human thymidine kinase 1. Regulation in normal and malignant cells." *Adv Enzyme Regul* 35: 69-89.

Murray, A. W. and M. W. Kirschner (1989). "Dominoes and clocks: the union of two views of the cell cycle." *Science* 246(4930): 614-21.

Nakamoto, Y., T. Higashi, et al. (2000). "Delayed (18)F-fluoro-2-deoxy-D-glucose positron emission tomography scan for differentiation between malignant and benign lesions in the pancreas." *Cancer* 89(12): 2547-54.

Nakata, B., S. Nishimura, et al. (2001). "Prognostic predictive value of 18F-fluorodeoxyglucose positron emission tomography for patients with pancreatic cancer." *Int J Oncol* 19(1): 53-8.

Nishiyama, Y., Y. Yamamoto, et al. (2005). "Contribution of whole body FDG-PET to the detection of distant metastasis in pancreatic cancer." *Ann Nucl Med* 19(6): 491-7.

Ogunbiyi, O. A., F. L. Flanagan, et al. (1997). "Detection of recurrent and metastatic colorectal cancer: comparison of positron emission tomography and computed tomography." *Ann Surg Oncol* 4(8): 613-20.

Oyama, N., D. E. Ponde, et al. (2004). "Monitoring of therapy in androgen-dependent prostate tumor model by measuring tumor proliferation." *J Nucl Med* 45(3): 519-25.

Ozkan, H., M. Kaya, et al. (2003). "Comparison of tumor marker CA 242 with CA 19-9 and carcinoembryonic antigen (CEA) in pancreatic cancer." *Hepatogastroenterology* 50(53): 1669-74.

Pardee, A. B. (1989). "G1 events and regulation of cell proliferation." *Science* 246(4930): 603-8.

Parker, W. B. and Y. C. Cheng (1990). "Metabolism and mechanism of action of 5-fluorouracil." *Pharmacol Ther* 48(3): 381-95.

Patz, E. F., Jr., V. J. Lowe, et al. (1995). "Thoracic nodal staging with PET imaging with 18FDG in patients with bronchogenic carcinoma." *Chest* 108(6): 1617-21.

Perumal, M., R. G. Pillai, et al. (2006). "Redistribution of nucleoside transporters to the cell membrane provides a novel approach for imaging thymidylate synthase inhibition by positron emission tomography." *Cancer Res* 66(17): 8558-64.

Pickard, M. and A. Kinsella (1996). "Influence of both salvage and DNA damage response pathways on resistance to chemotherapeutic antimetabolites." *Biochem Pharmacol* 52(3): 425-31.

Pressacco, J., B. Mitrovski, et al. (1995). "Effects of thymidylate synthase inhibition on thymidine kinase activity and nucleoside transporter expression." *Cancer Res* 55(7): 1505-8.

Rasey, J. S., J. R. Grierson, et al. (2002). "Validation of FLT uptake as a measure of thymidine kinase-1 activity in A549 carcinoma cells." *J Nucl Med* 43(9): 1210-7.

Rees, M., G. Plant, et al. (1997). "Late results justify resection for multiple hepatic metastases from colorectal cancer." *Br J Surg* 84(8): 1136-40.

Renehan, A. G., M. Egger, et al. (2002). "Impact on survival of intensive follow up after curative resection for colorectal cancer: systematic review and meta-analysis of randomised trials." *Bmj* 324(7341): 813.

Reske, S. N., K. G. Grillenberger, et al. (1997). "Overexpression of glucose transporter 1 and increased FDG uptake in pancreatic carcinoma." *J Nucl Med* 38(9): 1344-8.

Rickes, S., K. Unkrodt, et al. (2002). "Differentiation of pancreatic tumours by conventional ultrasound, unenhanced and echo-enhanced power Doppler sonography." *Scand J Gastroenterol* 37(11): 1313-20.

Rose, D. M., D. Delbeke, et al. (1999). "18Fluorodeoxyglucose-positron emission tomography in the management of patients with suspected pancreatic cancer." *Ann Surg* 229(5): 729-37; *discussion* 737-8.

Ruf, J., E. Lopez Hanninen, et al. (2005). "Detection of recurrent pancreatic cancer: comparison of FDG-PET with CT/MRI." *Pancreatology* 5(2-3): 266-72.

Ruhlmann, J., A. Schomburg, et al. (1997). "Fluorodeoxyglucose whole-body positron emission tomography in colorectal cancer patients studied in routine daily practice." *Dis Colon Rectum* 40(10): 1195-204.

Rydzewski, B., F. Dehdashti, et al. (2002). "Usefulness of intraoperative sonography for revealing hepatic metastases from colorectal cancer in patients selected for surgery after undergoing FDG PET." *AJR Am J Roentgenol* 178(2): 353-8.

Sahin, A. A., J. Ro, et al. (1991). "Ki-67 immunostaining in node-negative stage I/II breast carcinoma. Significant correlation with prognosis." *Cancer* 68(3): 549-57.

Saisho, H. and T. Yamaguchi (2004). "Diagnostic imaging for pancreatic cancer: computed tomography, magnetic resonance imaging, and positron emission tomography." *Pancreas* 28(3): 273-8.

Sambrook, J. and D. W. Russell (2001). *Molecular Cloning: A Laboratory Manual*. Cold Spring Harbor, NY, USA, Cold Spring Harbor Laboratory Press.

Saruc, M. and P. M. Pour (2003). "Diabetes and its relationship to pancreatic carcinoma." *Pancreas* 26(4): 381-7.

Scheele, J., R. Stang, et al. (1995). "Resection of colorectal liver metastases." *World J Surg* 19(1): 59-71.

Scheele, J., R. Stangl, et al. (1990). "Hepatic metastases from colorectal carcinoma: impact of surgical resection on the natural history." *Br J Surg* 77(11): 1241-6.

Schiepers, C., F. Penninckx, et al. (1995). "Contribution of PET in the diagnosis of recurrent colorectal cancer: comparison with conventional imaging." *Eur J Surg Oncol* 21(5): 517-22.

Schlag, P., P. Hohenberger, et al. (1990). "Resection of liver metastases in colorectal cancer--competitive analysis of treatment results in synchronous versus metachronous metastases." *Eur J Surg Oncol* 16(4): 360-5.

Schussler-Fiorenza, C. M., D. M. Mahvi, et al. (2004). "Clinical risk score correlates with yield of PET scan in patients with colorectal hepatic metastases." *J Gastrointest Surg* 8(2): 150-7; *discussion* 157-8.

Schwartz, J. L., Y. Tamura, et al. (2003). "Monitoring tumor cell proliferation by targeting DNA synthetic processes with thymidine and thymidine analogs." *J Nucl Med* 44(12): 2027-32.

Scwartz, J. L., J. R. Gierson, et al. (2001). "Rates of accumulation and retention of 3-deoxy-3-fluorothymidine (FLT) in different cell lines." *J Nucl Med* 42 (Suppl): 283P.

Seitz, U., M. Wagner, et al. (2002). "Evaluation of pyrimidine metabolising enzymes and in vitro uptake of 3'-[(18)F]fluoro-3'-deoxythymidine ([18)F]FLT) in pancreatic cancer cell lines." *Eur J Nucl Med Mol Imaging* 29(9): 1174-81.

Selzner, M., T. F. Hany, et al. (2004). "Does the novel PET/CT imaging modality impact on the treatment of patients with metastatic colorectal cancer of the liver?" *Ann Surg* 240(6): 1027-34; *discussion* 1035-6.

Sherley, J. L. and T. J. Kelly (1988). "Regulation of human thymidine kinase during the cell cycle." *J Biol Chem* 263(17): 8350-8.

Shields, A. F. (2006). "Positron emission tomography measurement of tumor metabolism and growth: its expanding role in oncology." *Mol Imaging Biol* 8(3): 141-50.

Shields, A. F., D. A. Briston, et al. (2005). "A simplified analysis of [18F]3'-deoxy-3'-fluorothymidine metabolism and retention." *Eur J Nucl Med Mol Imaging* 32(11): 1269-75.

Shields, A. F., J. R. Grierson, et al. (1998a). "Imaging proliferation in vivo with [F-18]FLT and positron emission tomography." *Nat Med* 4(11): 1334-6.

Shields, A. F., D. A. Mankoff, et al. (1998b). "Carbon-11-thymidine and FDG to measure therapy response." *J Nucl Med* 39(10): 1757-62.

Shreve, P. D. (1998). "Focal fluorine-18 fluorodeoxyglucose accumulation in inflammatory pancreatic disease." *Eur J Nucl Med* 25(3): 259-64.

Siitonen, S. M., O. P. Kallioniemi, et al. (1993). "Proliferating cell nuclear antigen immunohistochemistry using monoclonal antibody 19A2 and a new antigen retrieval technique has prognostic impact in archival paraffin-embedded node-negative breast cancer." *Am J Pathol* 142(4): 1081-9.

Smith, S. L. and P. S. Rajan (2004). "Imaging of pancreatic adenocarcinoma with emphasis on multidetector CT." *Clin Radiol* 59(1): 26-38.

Smyczek-Gargya, B., N. Fersis, et al. (2004). "PET with [18F]fluorothymidine for imaging of primary breast cancer: a pilot study." *Eur J Nucl Med Mol Imaging* 31(5): 720-4.

Sperti, C., C. Pasquali, et al. (1993). "CA 19-9 as a prognostic index after resection for pancreatic cancer." *J Surg Oncol* 52(3): 137-41.

Sperti, C., C. Pasquali, et al. (2003). "18-Fluorodeoxyglucose positron emission tomography in predicting survival of patients with pancreatic carcinoma." *J Gastrointest Surg* 7(8): 953-9; *discussion* 959-60.

Staib, L., H. Schirrmeister, et al. (2000). "Is (18)F-fluorodeoxyglucose positron emission tomography in recurrent colorectal cancer a contribution to surgical decision making?" *Am J Surg* 180(1): 1-5.

Statistics, O. f. N. (2005). Cancer statistics registration: Registrations of cancer diagnosed in 2005, England.

Stehlin, J. S., Jr., P. D. de Ipolyi, et al. (1988). "Treatment of cancer of the liver. Twenty years' experience with infusion and resection in 414 patients." *Ann Surg* 208(1): 23-35.

Stolfuss, J., G. Glatting, et al. (1995). "2-(fluorine-18)-fluoro-2-deoxy-D-glucose PET in detection of pancreatic cancer" value of quantitative image interpretation." *Radiology* 195(2): 339-44.

Strasberg, S. M., F. Dehdashti, et al. (2001). "Survival of patients evaluated by FDG-PET before hepatic resection for metastatic colorectal carcinoma: a prospective database study." *Ann Surg* 233(3): 293-9.

Strauss, L. G., J. H. Clorius, et al. (1989). "Recurrence of colorectal tumors: PET evaluation." *Radiology* 170(2): 329-32.

Sugarbaker, P. H. (1990). "Surgical decision making for large bowel cancer metastatic to the liver." *Radiology* 174(3 Pt 1): 621-6.

Takeuchi, O., N. Saito, et al. (1999). "Clinical assessment of positron emission tomography for the diagnosis of local recurrence in colorectal cancer." *Br J Surg* 86(7): 932-7.

Takhar, A. S., P. Palaniappan, et al. (2004). "Recent developments in diagnosis of pancreatic cancer." *Bmj* 329(7467): 668-73.

Tatlidil, R., H. Jadvar, et al. (2002). "Incidental colonic fluorodeoxyglucose uptake: correlation with colonoscopic and histopathologic findings." *Radiology* 224(3): 783-7.

Topal, B., P. Flamen, et al. (2001). "Clinical value of whole-body emission tomography in potentially curable colorectal liver metastases." *Eur J Surg Oncol* 27(2): 175-9.

Toyohara, J., A. Waki, et al. (2002). "Basis of FLT as a cell proliferation marker: comparative uptake studies with [3H]thymidine and [3H]arabinothymidine, and cell-analysis in 22 asynchronously growing tumor cell lines." *Nucl Med Biol* 29(3): 281-7.

Troost, E. G., W. V. Vogel, et al. (2007). "18F-FLT PET does not discriminate between reactive and metastatic lymph nodes in primary head and neck cancer patients." *J Nucl Med* 48(5): 726-35.

Truant, S., D. Huglo, et al. (2005). "Prospective evaluation of the impact of [18F]fluoro-2-deoxy-D-glucose positron emission tomography of resectable colorectal liver metastases." *Br J Surg* 92(3): 362-9.

Tubiana, M. and A. Courdi (1989). "Cell proliferation kinetics in human solid tumors: relation to probability of metastatic dissemination and long-term survival." *Radiother Oncol* 15(1): 1-18.

Tubiana, M., M. H. Pejovic, et al. (1984). "The long-term prognostic significance of the thymidine labelling index in breast cancer." *Int J Cancer* 33(4): 441-5.

Valk, P. E., E. Abella-Columna, et al. (1999). "Whole-body PET imaging with [18F]fluorodeoxyglucose in management of recurrent colorectal cancer." *Arch Surg* 134(5): 503-11; *discussion* 511-3.

van Diest, P. J., G. Brugal, et al. (1998). "Proliferation markers in tumours: interpretation and clinical value." *J Clin Pathol* 51(10): 716-24.

van Eijkeren, M. E., A. De Schryver, et al. (1992). "Measurement of short-term 11C-thymidine activity in human head and neck tumours using positron emission tomography (PET)." *Acta Oncol* 31(5): 539-43.

van Waarde, A., D. C. Cobben, et al. (2004). "Selectivity of 18F-FLT and 18F-FDG for differentiating tumor from inflammation in a rodent model." *J Nucl Med* 45(4): 695-700.

van Westreenen, H. L., D. C. Cobben, et al. (2005). "Comparison of 18F-FLT PET and 18F-FDG PET in esophageal cancer." *J Nucl Med* 46(3): 400-4.

Veit, P., G. Antoch, et al. (2006). "Detection of residual tumor after radiofrequency ablation of liver metastasis with dual-modality PET/CT: initial results." *Eur Radiol* 16(1): 80-7.

Vesselle, H., J. Grierson, et al. (2002). "In vivo validation of 3'deoxy-3'-[(18)F]fluorothymidine ([18)F]FLT) as a proliferation imaging tracer in humans: correlation of [18)F]FLT uptake by positron emission tomography with Ki-67 immunohistochemistry and flow cytometry in human lung tumors." *Clin Cancer Res* 8(11): 3315-23.

Vesselle, H., J. Grierson, et al. (2003). "18F-Fluorothymidine radiation dosimetry in human PET imaging studies." *J Nucl Med* 44(9): 1482-8.

Vijayalakshmi, D. and J. A. Belt (1988). "Sodium-dependent nucleoside transport in mouse intestinal epithelial cells. Two transport systems with differing substrate specificities." *J Biol Chem* 263(36): 19419-23.

Visscher, D. W., S. Wykes, et al. (1992). "Comparison of PCNA/cyclin immunohistochemistry with flow cytometric S-phase fraction in breast cancer." *Breast Cancer Res Treat* 22(2): 111-8.

Visvikis, D., D. C. Costa, et al. (2003). "CT-based attenuation correction in the calculation of semi-quantitative indices of [18F]FDG uptake in PET." *Eur J Nucl Med Mol Imaging* 30(3): 344-53.

Vitola, J. V., D. Delbeke, et al. (1996). "Positron emission tomography to stage suspected metastatic colorectal carcinoma to the liver." *Am J Surg* 171(1): 21-6.

Vogel, I., H. Kalthoff, et al. (2002). "Detection and prognostic impact of disseminated tumor cells in pancreatic carcinoma." *Pancreatology* 2(2): 79-88.

Vogel, S. B., W. E. Drane, et al. (1994). "Prediction of surgical resectability in patients with hepatic colorectal metastases." *Ann Surg* 219(5): 508-14; discussion 514-6.

Wagner, M., U. Seitz, et al. (2003). "3'-[18F]fluoro-3'-deoxythymidine ([18F]-FLT) as positron emission tomography tracer for imaging proliferation in a murine B-Cell lymphoma model and in the human disease." *Cancer Res* 63(10): 2681-7.

Wahl, R. L. (2004). "Why nearly all PET of abdominal and pelvic cancers will be performed as PET/CT." *J Nucl Med* 45 *Suppl 1*: 82S-95S.

Waldherr, C., I. K. Mellingerhoff, et al. (2005). "Monitoring antiproliferative responses to kinase inhibitor therapy in mice with 3'-deoxy-3'-18F-fluorothymidine PET." *J Nucl Med* 46(1): 114-20.

Weber, W. A. and H. Wieder (2006). "Monitoring chemotherapy and radiotherapy of solid tumors." *Eur J Nucl Med Mol Imaging* 33 *Suppl 13*: 27-37.

Weidner, N., D. H. Moore, 2nd, et al. (1993). "Correlation of bromodeoxyuridine (BRDU) labeling of breast carcinoma cells with mitotic figure content and tumor grade." *Am J Surg Pathol* 17(10): 987-94.

Weissleder, R., C. H. Tung, et al. (1999). "In vivo imaging of tumors with protease-activated near-infrared fluorescent probes." *Nat Biotechnol* 17(4): 375-8.

Wells, P., R. N. Gunn, et al. (2002). "Assessment of proliferation in vivo using 2-[(11)C]thymidine positron emission tomography in advanced intra-abdominal malignancies." *Cancer Res* 62(20): 5698-702.

Whiteford, M. H., H. M. Whiteford, et al. (2000). "Usefulness of FDG-PET scan in the assessment of suspected metastatic or recurrent adenocarcinoma of the colon and rectum." *Dis Colon Rectum* 43(6): 759-67; *discussion* 767-70.

Willett, C. G., W. J. Daly, et al. (1996). "CA 19-9 is an index of response to neoadjuvant chemoradiation therapy in pancreatic cancer." *Am J Surg* 172(4): 350-2.

Wilson, I. K., S. Chatterjee, et al. (1991). "Synthesis of 3'-fluoro-3'-deoxythymidine and studies of its 18F-radiolabeling, as a tracer for the non invasive monitoring of the biodistribution of drugs against AIDS." *Journal of Fluorine chemistry* 55: 283-289.

Wittekind, C., C. C. Compton, et al. (2002). "TNM residual tumor classification revisited." *Cancer* 94(9): 2511-6.

Yamaguchi, A., Y. Kurosaka, et al. (1993). "Analysis of hepatic recurrence of colorectal cancer after resection of hepatic metastases." *Int Surg* 78(1): 16-9.

Yap, J. T., J. P. Carney, et al. (2004). "Image-guided cancer therapy using PET/CT." *Cancer J* 10(4): 221-33.

Yasuda, S., M. Ide, et al. (2000). "Application of positron emission tomography imaging to cancer screening." *Br J Cancer* 83(12): 1607-11.

Yau, K., P. Price, et al. (2006). "Elevation of radiolabelled thymidine uptake in RIF-1 fibrosarcoma and HT29 colon adenocarcinoma cells after treatment with thymidylate synthase inhibitors." *Eur J Nucl Med Mol Imaging* 33(9): 981-7.

Yeo, T. P., R. H. Hruban, et al. (2002). "Pancreatic cancer." *Curr Probl Cancer* 26(4): 176-275.

Yonekura, Y., R. S. Benua, et al. (1982). "Increased accumulation of 2-deoxy-2-[18F]Fluoro-D-glucose in liver metastases from colon carcinoma." *J Nucl Med* 23(12): 1133-7.

Zimny, M., R. Bares, et al. (1997). "Fluorine-18 fluorodeoxyglucose positron emission tomography in the differential diagnosis of pancreatic carcinoma: a report of 106 cases." *Eur J Nucl Med* 24(6): 678-82.

Zimny, M., J. Fass, et al. (2000). "Fluorodeoxyglucose positron emission tomography and the prognosis of pancreatic carcinoma." *Scand J Gastroenterol* 35(8): 883-8.

Appendix A

**(¹⁸F-FLT PET study
Ethics committee approval)**

The Joint UCL/UCLH Committees on the Ethics of
Human Research: Committee Alpha

Chairman:
Professor André McLean

Professor PJ Ell
Institute of Nuclear Medicine
The Middlesex Hospital
Mortimer Street
London
W1N 8AA

Please address all correspondence to:

Iwona Nowicka
Research & Development Directorate
UCLH NHS Trust
1st floor, Vezey Strong Wing
112 Hampstead Road, LONDON NW1 2LT
Tel. 020 7380 9579 Fax 020 7380 9937
e-mail: iwona.nowicka@uclh.org

06 February 2002

Dear Professor Ell

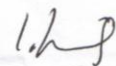
Study No: 02/0013 (Please quote in all correspondence)
Title: Comparison of F-18-3-deoxy-3-fluoro-thymidine (FLT) and F-18-fluorodeoxyglucose (FDG) PET imaging in patients with metastatic or locally advanced cancer: A phase I pilot study.

Thank you for letting us see the above application which was reviewed by the Chairman and agreed by Chairman's Action. There are no objections on ethical grounds to this study going ahead on condition that the radiation dose is explained in the patient information sheet. Please supply a copy of an amended information sheet for completeness of our records.

Please ensure that you have obtained final approval from the Trust (via the R&D office) before proceeding with your research.

Please note that it is important that you notify the Committee of any adverse events or changes (name of investigator etc) relating to this project. You should also notify the Committee on completion of the project, or indeed if the project is abandoned. **Please remember to quote the above number in any correspondence.**

Yours sincerely

pp. 

**Professor André McLean, BM BCh PhD FRC Path
Chairman**

/comalpha/am/ijn/06/02/02



UCL Hospitals is an NHS Trust incorporating the Eastman Dental Hospital, Elizabeth Garrett Anderson and Obstetric Hospital, Hospital for Tropical Diseases, The Middlesex Hospital, National Hospital for Neurology & Neurosurgery and University College Hospital.

Appendix B
(ARSAC licence
&
MHRA approval letter)

CERTIFICATE

FOR THE

ADMINISTRATION OF RADIOACTIVE MEDICINAL PRODUCTS

Certificate Reference Number RPC 141-259 (16269)

It is hereby certified for the purposes of the Medicines (Administration of Radioactive Substances) Regulations 1978, amended by the Medicines (Administration of Radioactive Substances) Amendment Regulations 1995, that

Jamshed BOMANJI
The Middlesex Hospital
Institute of Nuclear Medicine
Mortimer Street
London
W1T 3AA

may administer until 31 Jan 2006 the radioactive medicinal products specified in the Schedule to this certificate for the purpose(s) there specified.

for The Secretary of State for Health



.....

Health Care Directorate
Specialist Clinical Services Division
Department of Health

14-Jan-2004

Jamshed BOMANJI
The Middlesex Hospital
Institute of Nuclear Medicine
Mortimer Street
London
W1T 3AA

Date of
Certificate 1.02.02

Schedule to Research Certificate Number RPC 141-259 (16269)

Research Project

A comparison between FDG and FLT for PET imaging of patients with metastatic and locally advanced disease.

Serial*	Nuclide	Chemical Form
9a211	18F	FDG
9a37	18F	flurothymidine (FLT)

*As listed in Appendix I of the Notes for Guidance.
Unlisted Serial numbers are included for ease of
identification by the ARSAC Secretariat.



**Medicines and Healthcare products
Regulatory Agency**

Market Towers
1 Nine Elms Lane, London SW8 5NQ

Telephone 020 7273 0328
Facsimile 020 7273 0443

Dr J. Bomanji
Institute of Nuclear Medicine
UCL Medical School
Middlesex Hospital
Mortimer Street
London W1T 3AA

Our Ref: MF8000/11475

19 September 2003

Dear Dr Bomanji

**THE MEDICINES (EXEMPTION FROM LICENCES) (SPECIAL CASES AND
MISCELLANEOUS PROVISIONS) ORDER 1972
PRODUCT: (F-18) Fluorothymidine**

I am writing in connection with your notification dated 16 September 2003 under the Medicines (Exemption from Licences) (Special Cases and Miscellaneous Provisions) Order 1972 which relates to a proposed trial using **(F-18) Fluorothymidine** supplied by **Imaging Research Solutions Ltd.**

We note that the study is ongoing and it needs to be continued for a further 18 month period. The Licensing Authority agrees that this is acceptable.

We shall be pleased to see a copy of any report which is produced as a result of this trial.

Yours sincerely

Mrs S. Syed
CLINICAL TRIALS UNIT
ddxappro

Appendix C

**(Patient information sheet
and
consent form)**



CONFIDENTIAL
Patient Information Sheet

Comparison of F-18-3-deoxy-fluoro-thymidine (FLT) (a new tracer) and F-18-fluorodeoxyglucose (FDG) PET imaging in patients with metastatic or locally advanced cancer

You are invited to take part in a research study. Before you decide it is important for you to understand why the research is being done and what it will involve. Please take time to read the following information carefully and discuss it with others if you wish. Ask us if there is anything that is not clear or if you would like more information. Take time to decide whether or not you wish to take part.

Purpose of the study

1. This study aims to establish if positron emission tomography (PET) scans using an alternative radioactive tracer, FLT, is more accurate than the conventional radioactive tracer, FDG for imaging different cancers.
2. It has been shown that FDG-PET is an accurate and safe means of imaging patients with cancers. This allows the most appropriate treatment to deal with an individual patient's cancer to be chosen. The information, therefore, influences the extent of surgery performed and possibly the use of other treatments such as chemotherapy or radiotherapy.
3. The accuracy of FDG-PET, although extremely good, is not perfect. One method of improving this situation is to use an alternative radioactive substance to pinpoint the site of cancer cells in the body. FLT is such an alternative and it can be safely substituted for FDG for PET scanning. We hope that this research will allow detection of quite small tumours, which would not otherwise be detected.

Why have I been chosen?

You have been chosen for this study, as your doctors feel that your type of cancer may be advanced and have therefore referred you for a conventional FDG PET scan. By performing two types of PET scan which includes the new tracer chemical FLT, we would then be in a position to compare the two scans, in order so that we can decide which one may be more accurate and which may give us additional information which may possible help in your management and others in the future.

Director and Head of Department
Professor Peter Josef Ell MD, MSc, PD, FRCP, FRCR, FMedSci
Tel: +44 (0)20 7380 9424 • +44 (0)20 7631 1066
Fax: +44 (0)20 7436 0603
Email: p.ell@nucmed.ucl.ac.uk

Version: 2
Project ID: 02/0013
Date: 21st July 2005

Consultant/Honorary Senior Lecturer
Dr Jamshed Bomanji
+44 (0)20 7380 9425
j.bomanji@nucmed.ucl.ac.uk

Chair of Medical Physics in Nuclear Medicine and
Molecular Imaging Science
Professor Dr Brian Hutton
+44 (0)20 7380 9392
b.hutton@nucmed.ucl.ac.uk

Consultant/Honorary Senior Lecturer
Dr Liz Prvulovich
+44 (0)20 7380 9387
l.prvulovich@nucmed.ucl.ac.uk

Royal Free and University College Medical School
UNIVERSITY COLLEGE LONDON



INSTITUTE OF NUCLEAR MEDICINE

Middlesex Hospital
Mortimer Street
London W1T 3AA

Do I have to take part?

Its up to you to decide whether or not to take part. If you decide to take part you will be given this information sheet to keep and be asked to sign a consent form. If you decide to take part you are still free to withdraw at any time and without giving a reason. A decision to withdraw at any time, or a decision not to take part, will not affect the standard of care you receive.

What is involved in the study?

In addition to a routine FDG-PET scan that patients with cancer undergo at this hospital, you will have an FLT-PET scan.

PET scans take place in the Institute of Nuclear Medicine at the Middlesex hospital, usually on separate days. The procedure will entail you having to fast for a period of four hours (so that glucose that you consume in your diet will not interfere with the FDG-PET scan). Once you are in the Institute of Nuclear Medicine you will be given an injection of FDG (chemically similar to glucose, but which has been labelled with a radioactive substance) through a cannula (plastic tube) in a vein. The radioactivity lasts approximately 90 minutes, therefore you do not have to wait for the scan. You will have to lie on a platform that moves you into the scanner.

The scan itself takes one hour and you will need to lie still with minimum interaction with staff, as this interferes with the scan quality. The whole process takes between 2 to 4 hours.

The procedure for the FLT scan is similar to that described above, but you will receive an injection of FLT instead of FDG. A comparison will be made between both types of PET scans to see if there is any difference in the information gained. Both scan findings will be compared to conventional X-ray, CT or MRI scans which you may have already undergone as part of your routine work-up. This all helps to increase the accuracy of the scan report we give to the doctors looking after you.

What are the possible benefits of taking part?

We hope that this study will directly help in your management. However, this cannot be guaranteed. The information we get from this study may allow us make better decisions about the treatment of your type of cancer in the future.

Director and Head of Department
Professor Peter Josef Ell MD, MSc, PD, FRCP, FRCR, FMedSci
Tel: +44 (0)20 7380 9424 • +44 (0)20 7631 1066
Fax: +44 (0)20 7436 0603
Email: p.ell@nucmed.ucl.ac.uk

Version: 2
Project ID: 02/0013
Date: 21st July 2005

Consultant/Honorary Senior Lecturer
Dr Jamshed Bomanji
+44 (0)20 7380 9425
j.bomanji@nucmed.ucl.ac.uk

**Chair of Medical Physics in Nuclear Medicine and
Molecular Imaging Science**
Professor Dr Brian Hutton
+44 (0)20 7380 9392
b.hutton@nucmed.ucl.ac.uk

Consultant/Honorary Senior Lecturer
Dr Liz Prvulovich
+44 (0)20 7380 9387
l.prvulovich@nucmed.ucl.ac.uk



What are the known risks/side effects of any treatment?

The main risk of the study is that of radiation exposure from the tracer chemicals but the amount of radiation you will receive, in comparison to natural radiation we all receive, is very small. In order to put things into perspective, the following table summarizes the risk from a nuclear medicine scan compared to other everyday activities:

Activity	Risk of:	Cases per million
Nuclear Medicine scan	genetic damage	4
Travel 1000 miles by air	fatal accident	3
Nuclear Medicine scan	fatal cancer or leukaemia	13
Travel 1000 miles by car	fatal accident	20
Travel 1000 miles by motorcycle	fatal accident	400
Working 10 years in a typical factory	fatal accident	300
1 glass of wine a day for 10 years	cirrhosis	1,000
1 cigarette a day for 10 years	Heart attack or lung cancer	2,500
Living for 1 year at age 30	death from all causes	1,000
Living for 1 year at age 55	death from all causes	10,000

Table shown risk from a nuclear medicine scan compared to other every day activities.

Once you have been injected with the tracer chemical, your body that has absorbed it will be emitting radioactivity to others. However, this radioactivity does not last long (it halves every 2 hours). We therefore advise not to be in very close contact with children or pregnant mothers until the following day. Pregnant women are excluded from this study.

The information held about you

All information which is collected about you during the course of the research will be kept strictly confidential. Any information about you, which leaves the hospital will have your name and address, date of birth and all identifiable information (including hospital/NHS number) removed so that you cannot be recognised from it.

Director and Head of Department
Professor Peter Josef El MD, MSc, PD, FRCP, FRCR, FMedSci
Tel: +44 (0)20 7380 9424 • +44 (0)20 7631 1066
Fax: +44 (0)20 7436 0603
Email: p.el@nucmed.ucl.ac.uk

Version: 2
Project ID: 02/0013
Date: 21st July 2005

Consultant/Honorary Senior Lecturer
Dr Jamshed Bomanji
+44 (0)20 7380 9425
j.bomanji@nucmed.ucl.ac.uk

**Chair of Medical Physics in Nuclear Medicine and
Molecular Imaging Science**
Professor Dr Brian Hutton
+44 (0)20 7380 9392
b.hutton@nucmed.ucl.ac.uk

Consultant/Honorary Senior Lecturer
Dr Liz Prvulovich
+44 (0)20 7380 9387
l.prvulovich@nucmed.ucl.ac.uk



What if something goes wrong?

What happens to the results of research study?

Once enough data has been gathered, the results will be carefully analysed so that conclusions about the findings can be made. Once the data has been studied, the results may be shared with the scientific forum. As pointed out before, all information about will be kept strictly confidential through out.

Who is organising and funding the research?

This research study is internally funded by the University College London.

Withdrawal from the project

Your participation in this trial is entirely voluntary. You are free to decline to enter or withdraw from the study any time with out having to give a reason. If you choose not to enter the trial, or withdraw once entered, this will in no way affect your future medical care. All information regarding your medical records will be treated as strictly confidential and will only be used for medical reasons. Your medical records may be inspected by competent medical authorities and properly authorized persons, but if any information is released this will be done in a code form so that confidentiality is strictly maintained. Participation in this study will in no way affect your legal rights.

All proposals for research using human subjects are reviewed by an ethics committee before they can proceed. This proposal was reviewed by the joint UCL/UCLH Committees on Ethics of Human Research.

Director and Head of Department
Professor Peter Josef Ell MD, MSc, PD, FRCP, FRCR, FMedSci
Tel: +44 (0)20 7380 9424 • +44 (0)20 7631 1066
Fax: +44 (0)20 7436 0603
Email: p.ell@nucmed.ucl.ac.uk

Chair of Medical Physics in Nuclear Medicine and
Molecular Imaging Science
Professor Dr Brian Hutton
+44 (0)20 7380 9392
b.hutton@nucmed.ucl.ac.uk

Consultant/Honorary Senior Lecturer
Dr Jamshed Bomanji
+44 (0)20 7380 9425
j.bomanji@nucmed.ucl.ac.uk

Version: 2
Project ID: 02/0013
Date: 21st July 2005

Consultant/Honorary Senior Lecturer
Dr Liz Prvulovich
+44 (0)20 7380 9387
l.prvulovich@nucmed.ucl.ac.uk

Royal Free and University College Medical School
UNIVERSITY COLLEGE LONDON



INSTITUTE OF NUCLEAR MEDICINE
UCL Hospitals NHS Trust
Nuclear Medicine Service

Middlesex Hospital
Mortimer Street
London W1T 3AA

Telephone: +44 (0)20 7380 9421
Fax: +44 (0)20 7637 0578

CONFIDENTIAL

**Comparison of F-18-3-deoxy-fluoro-thymidine (FLT)
(a new tracer) and F-18-fluorodeoxyglucose (FDG) PET imaging in
patients with metastatic or locally advanced cancer**

Principal Investigator:

Professor P.J. Ell,
Institute of Nuclear Medicine,
Mortimer Street,
London W1N 8AA

Other Investigators:

Dr. JB Bomanji	The Institute of Nuclear Medicine
Dr. S McKinnon	Department of Haematology
Dr. MN Gaze	Myerstein Institute of Oncology
Dr. A Cassoni	Myerstein Institute of Oncology
Dr. JA Lederman	Myerstein Institute of Oncology

If you have any queries regarding this information sheet, please contact **Mr. Farrokh Pakzad** at the department of surgery and the Institute of Nuclear Medicine on **07980 690842**

Version 1.1
16/07/2005

Director and Head of Department
Professor Peter Josef Ell MD, MSc, PD, FRCP, FRCR, FMedSci

Royal Free and University College Medical School
UNIVERSITY COLLEGE LONDON



INSTITUTE OF NUCLEAR MEDICINE
UCL Hospitals NHS Trust
Nuclear Medicine Service

Middlesex Hospital
Mortimer Street
London W1T 3AA

CONSENT FORM

CONFIDENTIAL

Telephone: +44 (0)20 7380 9421
Fax: +44 (0)20 7637 0578

Comparison of the novel tracer F-18-3-deoxy-3-Fluoro-thymidine (FLT) (a new tracer) and F-18-fluorodeoxyglucose (FDG) PET imaging in patients with metastatic or locally advanced cancer.

PATIENT NAME:

HOSPITAL NUMBER:

WARD/ ADDRESS:

By signing this form I agree that:

1. I have read the patients information sheet and the procedure has been fully explained to me.
2. I have had the opportunity to ask questions and I did receive satisfactory answers.
3. I have been given a copy of the information sheet and the consent form to keep.
4. I understand that I am participating in a research study and I understand the risks and benefits involved. I freely give my consent to participate in the research study outlined in the patient information sheet.
5. I understand that I may withdraw from this research study at any time without giving a reason for withdrawing and such a decision would not affect the standard of care that I receive in any way.

Signature of participant.....Date...../...../.....

Name of participant (Block Capitals).....

Investigator Statement

I have carefully explained to the above named patient the nature of the research protocol. I hereby certify that to the best of my knowledge the subject signing this form understands the nature, demands, risks and benefits involved in participating in this study.

Signature of investigator..... Name of investigator (Block Capitals).....
Date...../...../.....

Principal investigator : Prof. P.J. Ell (tel: **020-7380-9421**)

Version 1.1
16/07/2005

Director and Head of Department
Professor Peter Josef Ell MD, MSc, PD, FRCP, FRCR, FMedSci

Appendix D

(Departmental SOPs for PET imaging)

SOP:	PET_7	TITLE:	Measuring FDG upon arrival in the PET Suite		
Rev:	1.0	Date:	22/10/2001	Review:	Oct 2002
Group:	PET	Author:	CET / WW	Authorised:	PJE

OVERVIEW

This SOP addresses the checks which must be performed on each consignment of 18F-FDG *before* it may be used to dispense patient dose preparations that day.

RELEVANT STAFF

INM practitioners and operators working in the PET Suite.

BACKGROUND

The PET Unit obtains 18-F FDG from three centres :

- Addenbrooke's Hospital, Cambridge (Wolfson Brain Imaging Centre)
- Hammersmith Hospital (MRC Cyclotron Unit)
- St Thomas' Hospital (PET Centre)

Before any FDG may be injected into a patient there must be notification from the producing cyclotron that it has passed its QC.

- Cambridge dispatches the FDG and will then fax to confirm if the consignment has passed the QC. The fax will be sent to the fax machine in the PET Suite.
- St Thomas' Hospital do the same.
- Hammersmith Hospital perform QC testing before the FDG leaves them, and confirmation that the FDG has passed its QC is on the delivery note.

PROCEDURE

Pre-Dispensing Checks to be done daily :

- Daily QC testing must be performed on the Dose Calibrator before the FDG consignment can be assayed. Refer to the SOP for Dose Calibrator QC in PET.
- The FDG will arrive in a lead shielded container. (Take care when lifting it, as it is heavy.)
- Display a sign at the door of the dispensing lab - 'Please do not enter: Dose dispensing in progress. Radioactive sources in use'. Ensure that you are wearing a white coat, film badge, and finger dose TLDs.
- Take a new Radiopharmaceutical Holding Record Sheet. (See Appendix). Indicate on the record sheet that you have received confirmation that the consignment of FDG has passed its QC. From the delivery note mark the volume of liquid dispensed into the FDG vial, the time at which the FDG was measured prior to despatch, and the assayed activity.
- Remove the glass vial containing the FDG from the lead shielded container using the tongs provided; check that it has a label on saying FDG. Place in the dose calibrator.
- Check that the dose calibrator is set to the correct radioisotope setting (18-F). Measure the activity and note this, together with the time at it was measured.
- Using the 18F decay chart displayed on the wall, check that the activity that was dispatched matches the activity that has arrived to within $\pm 10\%$. If it does circle the appropriate box on the sheet, and initial this.
- Put the FDG vial in the lead shielded dispensing station and screw on the top.
- File the delivery notes and the QC confirmation notes in the file in the dispensing suite.

GLOSSARY

APPENDIX

INM PET Facility - Record Sheet of Current Radiopharmaceutical Holdings

Date : _____ Radiopharmaceutical Form : _____ Radiopharmaceutical QA Status (circle and initial) : Pass Fail

Consignor (tick) : _____ University of Cambridge UMDS (Guy's and St. Thomas') MRC Cyclotron Unit, Hammersmith

Activity Assay - Entire Shipment

	Stock Volume (mls)	Time of Assay	Assayed Activity (MBq)	Two Assays in Agreement ?
Consignor Activity Assay	_____	_____	_____	(i.e. both agree within $\pm 10\%$)
Decay-Corrected Consignor Assay	_____	_____	_____	circle below as appropriate
INM PET Unit Activity Assay	_____	_____	_____	Yes / No

Activity Assay - Sub-dispensed Preparations

Time of Assay	Operator Initials	Stock Volume Diluted ?	Volume Removed (mls)	Assayed Activity (MBq)	Volume Remaining (mls)	Activity Remaining	Purpose

Consignment of Current Holdings to Waste

Time	Operator Initials	Volume Remaining (mls)	Estimated Max. Remaining Activity (MBq)	Purpose
				WASTE
				WASTE

SOP:	PET_11	TITLE:	Whole Body FDG PET-CT		
Rev:	1.0	Date:	Oct 2004	Review:	Oct 2005
Group:	Diagnostic	Author:	CET/JCD	Authorised:	

OVERVIEW

The PET CT exam is a combined imaging study where both CT and PET images are acquired over the same area of the patient. The PET images provide a functional image of the radiopharmaceutical distribution in the patient, while the CT images provide an image of the anatomy which is used for localizing the radiopharmaceutical uptake and for attenuation correction of the PET images

REQUEST

Valid reasons for examination:

- Staging of disease
- Recurrence of disease
- Post treatment

Valid referrers:

See SOP V_2

Persons who may vet:

All Consultant staff

Vetting:

See SOP P_1

Booking:

- Patient is asked to arrive 60 minutes before the due time for injection. This is to allow time for them to have valium and relax.
- Patient or ward is sent an appointment letter. This letter asks the patient to starve, eating and drinking nothing but water for 6hours prior to the study.
- Letter also asks them to contact us if they are diabetic.
- Tells patient that they will be given valium so not to drive.
- If the patient is a private patient refer to SOP for private patients/ FDG. Patient's bill should be settled prior to scan starting.

PATIENT PREPARATION

- Patients should starve for 6 hours prior to the scan.
- They may drink water only.
- Patients on TPN should have this discontinued for 4-6 hours.
- Patients on glucose drips should have this discontinued for 4-6 hours.
- The appointment letter asks patients to contact the department if they are diabetic. Patients who are insulin dependent diabetics should speak with the duty practitioner about scheduling their scan. SOP-
- The weight limit for the PET scanner is 180kgs. If it is know in advance that the patient approaches this weight ask them to come to the department prior to giving them an appointment to see if they will fit the scanner's aperture.
- Children under 10 should be asked to arrive 60-90minutes before the appointment time to have emla cream.

RADIOPHARMACEUTICAL AND ADMINISTRATION

Radiopharmaceutical:	18FDG
ARSAC Serial No:	
DRL: (Maximum usual activity)	400MBq
ED:	
Minimum dose for paediatrics:	6MBq/Kg minimum dose of 100MBq
Advice re breastfeeding:	ARSAC
Persons who may administer:	
Procedure:	See below
Route of administration: (IV etc)	IV
Advice after administration:	Patient should lie still for the 45-60 minutes after the injection and before the scan. This reduces the uptake of FDG in muscles of the

PROCEDURE*Daily Checks*

1. Blank scan acquisition, reconstruction and correction. PET_05
2. Tube Warm-up and CT Fast Calibration CT_01
3. QC of dose calibrator to be done before measuring first FDG/ Fluoride dose of the day. PET_09
4. No injection is to be done before the QC for the dose has been received from the dispensing hospital.

Weekly Checks

1. Volumetric QC
2. Water phantom QC

Patient Preparation

1. Check the patient's name and DoB. INM_EP09
2. Check that the patient is not pregnant or breastfeeding. INM_EP03
3. If the patient needs to be accompanied by a nurse or parent and this person is a female make sure that they are not pregnant. Make sure that this person keeps as far as is reasonably possible from the patient.
4. Take the height of the patient in centimetres, mark on the clerking sheet.
5. Take the weight of the patient in kilograms, mark on the clerking sheet. These are used for SUV calculations on the Discovery.
6. Take a brief history from the patient.
7. Ask patient to lie on the patient trolley, make sure that they are comfortable. Explain the procedure to them.

Administration

8. Cannulate the patient, using a pink or blue venflon. Attach a 3-way tap and check that the line is patent with a saline flush.
9. Leave the patient to relax for 30 minutes. Show them the red pull cord which when pulled will alert the technologist. Put up the sign saying the patient 'Patient examination in progress'.
10. Draw up the FDG using a 5ml syringe in the lead syringe holder. Note the time the dose is calibrated, from the clock in the dispensing bay. This clock should be set with the Discovery, and checked regularly to make sure that they are in synch.
11. Note the activity in MBq and the volume (all on the clerking sheet).
12. Before giving the patient the FDG check that they do not wish to go to the toilet.
13. Explain the procedure one more time make sure that they do not have any questions. Give the patient the injection; note the time (from the same clock in the dispensing bay). Assay the syringe and needle again after the injection, note the activity and time on the clerking sheet.
14. The injector should sign the clerking sheet.
15. The technologist as the operator will sign the patient's request card.
16. Make sure the patient is warm enough.
17. Turn the lights off above their head and leave them alone. Make sure the red pull cord is within their reach. Change the sign 'Patient post injection present'.

Imaging

18. After 1 hour take the venflon out of the patient's arm, cover the site with cotton wool. Change the cotton wool for a clean piece just prior to the scan.
19. Ask patient to empty their bladder.
20. Take the patient into the scanning room
21. Ask patient to change into a gown, check for other metal objects.
22. Place sign on door to read 'Do not enter. Clinical Scan in progress'.

ACQUISITION TECHNIQUE

Patient Positioning

1. Ask the patient to go to the toilet prior to positioning on the bed.
2. If oral contrast is being given ask the patient to have a couple of mouthfuls before lying on the bed. See SOP for Oral Contrast.
3. Position the patient on the bed with the feet facing away from the gantry.
4. Put a pillow under the patient's knees for comfort.
5. Make sure the patient is warm and comfortable.
6. If possible, ask the patients to place their arms above their heads, occasionally patients may to have their arms by their side. Raise the bed up slightly to ensure that the bed will fit in the bore of the scanner.
7. Tell patient to lie still.
8. Make patient aware of the voice intercom between them and the control room.
9. If the patient cannot speak give them the hand held alarm.

Acquisition Preparation

10. On the Scan monitor, click the New Patient icon. Enter the patient's details. Patient ID is the INM database number. Patient Name enter as SMITH John.
11. Enter the rest of the details.
12. The scan protocols are classified in two main groups adults and infants. If the patient is a child, click on the infant icon.
13. Under Protocol Selection, the PET-CT protocol for whole body scan is defined in the Routine Chest selection No 5. Click on the chest, select protocol 5.13 INMPET_CTBody_Head_In.
14. Check the CT parameters. Ask patient to close their eyes.
15. On the gantry control press *Laser Lights*.
16. Move the bed inside the gantry until the laser lights is level with the midbrain.
17. On the gantry control press the internal landmark button.
18. Remind the patient to lie still.

Acquiring the Image

19. Check all staff are clear of the scanning room before the CT starts.
20. Confirm CT prescription, and press *Move to Scan*
21. Press *Start* to start scout view. The bed will then move.
22. At the end of the scout view, select *Next Series*. The scout will be displayed on the Image Monitor with the PET FOVs overlaid. Select as many FOV as necessary to cover midbrain to upper femora. Click *Confirm*.
23. Check CT parameters are correct and then acquire CT by pressing *Start Scan*.
24. Click *PET series*.
25. The PET screen is displayed on the PETOWS / Scan Monitor. The patient name and scan details will have been transferred from the CT system. Add the FDG data under additional tracer info. Click Prospective Recon, and select *PROSP_NO_AC* and *PROSP_WB_AC*, this will enable prospective reconstruction to occur.
26. Click *Accept Setup*. Press *Move to Scan*, and then press *Start Scan*
27. Following the completion of the acquisition the system will automatically store the data and clean up the acquisition processor (final message displayed should be acquisition completed successfully). Under *Options, Quit* screen.
28. Under options, click *Options/Quit Screen* to close the PET acquisition window.
29. Then on the image monitor, click on *Exam RX* to bring up the CT window. Click *End Exam*, to complete the whole examination.

ADVICE TO PATIENT ON DISCHARGE

Do not allow the patient to leave the hospital through the INM. If relations or transport comes to collect the patient get them to come to the PET suite and leave from there.

Make sure the patient knows how they will obtain the results of the study.

DATA ANALYSIS

Reformatting Images

1. From *Screens* select *Display*, then from the Display window select *Reformat*.
2. From the displayed list select *Orthogonal (MIP)*, and then on the resulting screen, click *Load*.
3. Select the required patient name and under then the “WB Emission CTAC” image reconstructed above.
4. Click the *Re-slice* control button.
5. Adjust the number of sagittal and coronal slices to cover the patient.
6. Change the slice thickness to 11.72mm. Click *Re-slice*.
7. Review images prior to patient departure. Ensure there is no need for further acquisitions. If a further acquisition is needed, remember to contact a Doctor to get it justified.
8. Under *Options*, select *Save/Coronal*. Name the slices ‘Generated Coronals, WB+CTAC 11.72 mm’

Transferring the data to the Xeleris

1. From *Screens*, select *Network*. Source should be set to ‘INMPET01’, destination should be ‘ews_DICOM’, and Sort by ‘Date Time’.
2. Select the patient, and select Coronals, WB emission CTAC and No AC recon. Click on *Select*, and click *Transfer Items*. Ensure that the images are transferred successfully.

DATA DISPLAY

On the Entegra.

1. Select the patient and ‘Generated Coronals’.
2. Click on the *Templates* tab. Choose Generated FDG Coronals, and click *Start Review Template*. This will display 5 x 3 coronal images. Ensure that the slices cover the whole body and are centred on the review pane from front to back.
3. Alter black and white intensity to 30,000 Bq/ml.
4. Check that the images look OK, and print one copy to the ‘Codonics’ and one copy to the ‘Windows Printer’.

REPORTING

Persons who may report: All consultant staff.

Reporting procedure:

DATA ARCHIVE

Raw data is archived twice onto DAT tapes. One tape is called TAPE_{xx}, the other is called WEEK_{xx}. The current tape called TAPE_{xx} will be kept in the fireproof safe in the PET scanning room. The older ones will be kept in the basement storeroom. Archive the raw data, the 2D Whole body Emission, 5 mins/step and corresponding CTAC client.

On the Xeleris, archive the CT slices, Generated Coronals, WB Emission CTAC, and No AC Recon to Optical disk and PETARC. Also upload the same data to Xel_Sem (reporting Xeleris to PET). Details of Xeleris archiving are given in General Nuclear Medicine SOPs.

Detailed procedure for DAT tape archiving:

From *Screens* select *Archive*.

Place the current raw data DAT tape in the tape drive.

Once the light on the tape deck stops flashing click *Ready* on the Archive screen. If Ready is not displayed the program has already started running.

Depending on the amount of data already archived on the tape this may take up to 10 minutes. During this period the Archive screen is blank.

After the reading of the tape is completed a list of the datasets in the tape will be displayed.

From *Data type* select *Raw*.

Select *Archive*. A list of the system image database will appear.

Select the patient name.

Click *Start*. A dialogue box will be displayed containing all the raw data files contained under the patient’s

folder and will ask for confirmation of the start archiving command. Click *ok*.

During the process of archiving none of the buttons in the Archive screen can be pressed. A bar with the process progress will be displayed. The number appearing under the bar is the percentage of the process completed.

Following completion of the raw data archive click Remove tape. This will rewind the tape and it will also eject the tape from the tape drive. On the database book tick under the raw data archive column.

The procedure should be repeated for the image data archive using the current image DAT tape and selecting *Image* in the *Data type*.

Warning: Never start the archive process of a particular patient data if any other process currently uses data from this particular patient.

ADDITIONAL COMMENTS

Once the emission scan has been acquired reconstruct and reformat it. Show the duty doctor in case there is a need to acquire a single slice.

SOP:	PET_21	TITLE:	Whole Body FLT PET-CT		
Rev:	1.0	Date:	Oct 2004	Review:	Oct 2005
Group:	Diagnostic	Author:	CET/JCD	Authorised:	

OVERVIEW

FLT is a novel radiopharmaceutical that potentially allows imaging of proliferation (cellular growth potential) with PET. Currently, FLT is being used as part of comparative research study protocols, comparing it to the routine FDG PET. The aims of these studies are to determine whether imaging with FLT PET provides better images or additional information that would be relevant to treatment of patients with cancer.

REQUEST

Valid reasons for examination:

Current running research protocols include:

- Comparison of FLT and FDG PET in locally advanced and metastatic colorectal cancer
- Comparison of FLT and FDG PET in locally advanced & metastatic cancer (includes: breast cancer, head & neck cancer, melanoma, connective tissue tumours, prostate cancer, thyroid cancer, Ovarian / gynaecological malignancies, lymphoma, pancreatic cancer, lung cancer, hepatocellular carcinoma, brain tumours, renal cancer and neuroendocrine tumours)
- Comparison of FLT and FDG in monitoring response to radiation therapy of head and neck cancers

Valid referrers:

See SOP V_2

Persons who may vet:

All Consultant staff

Vetting:

See SOP P_1

Booking:

- Patient is asked to arrive 60 minutes before the due time for injection. This is to allow time for them to have valium and relax.
- Patient or ward is sent an appointment letter. This letter asks the patient to starve, eating and drinking nothing but water for 6hours prior to the study.

PATIENT PREPARATION

- Patients should starve for 6 hours prior to the scan.
- They may drink water only.
- Patients on TPN should have this discontinued for 4-6 hours.
- Patients on glucose drips should have this discontinued for 4-6 hours.
- The weight limit for the PET scanner is 180kgs. If it is know in advance that the patient approaches this weight ask them to come to the department prior to giving them an appointment to see if they will fit the scanner's aperture.

RADIOPHARMACEUTICAL AND ADMINISTRATION

Radiopharmaceutical:	18FLT
ARSAC Serial No:	
DRL: (Maximum usual activity)	400MBq
ED:	
Minimum dose for paediatrics:	6MBq/Kg minimum dose of 100MBq
Advice re breastfeeding:	ARSAC
Persons who may administer:	
Route of administration: (IV etc)	IV
Advice after administration:	Patient should lie still for the 45-60 minutes after the injection and before the scan.

PROCEDURE

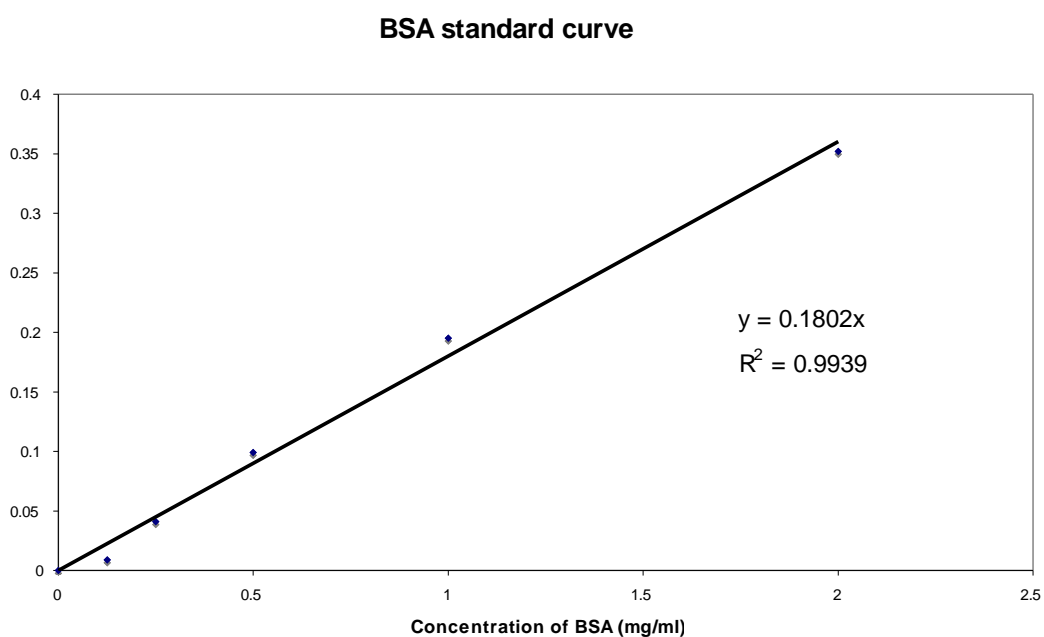
For the remaining procedural SOP's for whole body FLT PET/CT imaging, please refer to SOP_11 (Whole Body FDG PET/CT protocol).

Appendix E

(Protein assay and standard curve estimations)

In order to determine the concentration of the protein lysate, first a standard concentration curve using serial dilutions (concentration range of 0-2 mg/ml) of Bovine Serum Albumin (BSA) was made. Using the method described earlier (section 7.3.7.2) the Bradford protein assay kit was used to give corresponding light absorbance values using a photospectrometer. Linear regression analysis allows a best fit line to be applied to the BSA standard curve values, thus giving rise to graph similar to that below. Using the formula for the best fit line (ie: $y = 0.1802x$ in the example shown), the concentration of protein lysates was extrapolated by determining the corresponding light absorbance values using the photospectrometer and the Bradford assay kit. Table below illustrates an example of concentration values obtained.

BSA standard curve						
Concentration (mg/ml)	0	0.125	0.25	0.5	1	2
Absorbance (nm)	0	0.009	0.041	0.099	0.195	0.352



		Day 0	Day 1	Day 2
5-FU untreated cells (SW480)	Absorbance (595 nm)	0.009	0.063	0.06
	Concentration (mg/ml)	0.05	0.35	0.33
5-FU treated cells (SW480)	Absorbance (595 nm)	0.004	0.034	0.005
	Concentration (mg/ml)	0.02	0.19	0.03

Example of protein concentration of cell lysates, extrapolated from the above standard curve.

Appendix F

**(Protocol for gel electrophoresis
and Western blots)**

General recipes:

Reducing sample buffer

1.51g Tris
dissolve in 25ml distilled water
pH to 7.5 with conc. HCL

then add-

40ml of 10% SDS solution
10ml mercaptoethanol
0.002g bromophenol blue
10g sucrose or 20ml glycerol

Make up to 100 ml with distilled water
Divide into 1ml aliquots and store frozen

Running buffer

(x5 concentrated stock solution)

70g glycine
15g Tris
5g SDS
Make up to 500ml in distilled water
For use dilute 1/5 in distilled water.
Store in dry cool place

Blotting buffer for semi-dry electroblotting

Anode buffer I

9.24g Tris
500ml of 20% methanol in distilled water

Anode buffer II

1.52g Tris
500ml of 20% methanol

Cathode buffer

1.52g Tris
2.62g aminocaproic acid
500ml of 20% methanol

Recipe for making aliquots of DAB

- 1) Dilute 1g DAB in 200ml of distilled water
- 2) Put 1ml aliquots into 200 tubes (as quickly as possible as oxidises at room temperature)
- 3) Cap tube and store frozen

Preparation of samples

- 1) Sample should be as clean as possible -> centrifuge/filter to remove solid particles/de-lipidise by chloroform/methanol precipitation
- 2) Protein should be at a concentration of 1-10mg in distilled water or 0.1% SDS solution (Laemmli sample buffer)
- 3) Add equal volume of protein solution to reducing or non-reducing sample buffer. Vortex to mix.
- 4) If reducing conditions are required, boil sample in water bath for 30 sec-2 minutes. Allow to cool.
- 5) Samples are ready to load onto gels

Loading and running gels

- 1) Insert prepared gels into electrophoresis chamber (can load two gels)
- 2) Fill upper and lower buffer reservoirs up to the indicator marks
- 3) Load samples (15-30 μ l depending on gel size)
- 4) Attach leads to power pack
- 5) Run at 150-180 volts for 1-1.5 hours, until bromophenol blue marker reaches the end of gel.

After the run:-

- 6) Turn the voltage down slowly to zero, remove lid from electrophoresis chamber
- 7) Wear gloves -> remove adhesive tape around plates and ease plates apart. Trim off stacking segment and carefully remove gel.

Transfer to:

- Coomassie blue or silver stain (for total protein)
- Blot

Instructions for semi-dry electroblotting (Western blot)

Wear gloves!

- 1) Soak 1 sheet of filter paper in Anode buffer I
- 2) Soak 2 sheets of filter paper in Anode buffer II
- 3) Soak 3 sheets of filter paper in cathode buffer
- 4) Soak a sheet of nitrocellulose/PVDF sheet in distilled water
- 5) Position Anode buffer I paper on anode -> roll flat to exclude air bubbles
- 6) Position Anode buffer II paper on top-> roll flat as above
- 7) Position the PVDF sheet on top -> roll
- 8) Position the gel on top
- 9) Cut all layers to size of gel-> replace on anode
- 10) Position the cathode buffer paper on top. Trim to size and roll
- 11) Lower cathode (lid) into place and secure gently
- 12) Blot at 0.25 amps per mini-gel for 30 minutes

After blotting:-

- 1) Slowly decrease power to zero
- 2) gently remove PVDF sheets from sandwich
- 3) Stain with Ponceau red to assess transfer (destain in distilled water until pink bands show on white background. Destain completely in distilled water.)
- 4) Immunostain

Instructions for Immunostaining

- 1) Block blots (to avoid background binding) with 1% BSA in PBS-T overnight at room temperature
- 2) Apply primary and secondary antibodies according to pre-determined concentration / incubation time protocols
- 3) Wash blots with TBS-T 5 times and with TBS alone 5 times
- 4) For colorimetric analysis use DAB -> an aliquot of DAB made up to 10ml with TBS. 2ml of 30% H₂O₂ is then added to the solution and immediately poured over blot. Keep blot in DAB for 15 minutes (or until desired staining achieved), remove and wash with distilled water.
- 5) Store developed blots in a dry, dark place.

LIST OF PUBLICATIONS

Book Chapters

Clinical Molecular Anatomic Imaging: PET, PET/CT and SPECT/CT.

Editor: von Schulthes GK (2006 Edition)

Publisher: Lippincott Williams & Wilkins

Chapter 45: “PET/CT of Colorectal and Anal carcinoma.” **Pakzad F**, Bomanji JB, Ell PJ.

Index Medicus Journals

Pakzad F, Groves Am, Ell PJ. The Role of Positron Emission Tomography in the management of pancreatic cancer. [Review] *Sem Nuc Med.* 2006 Jul;36(3): 248 -56.

Pakzad F, Ell PJ, Cario I. Molecular imaging in animal models of disease – every little detail counts. (Mier et al.) – *EJNM* 2005; 32(8): 899-900

Non-index Medicus Journals

Pakzad F, Francis DL. “The role of PET and PET/CT in the management of colorectal cancer”, *Oncology news.* Aug-Sept 2007; 2(2): 12-14.

LIST OF PRESENTATIONS

International

- May 2006 “ **Does ¹⁸F-FDG PET/CT alter management of patients with colorectal liver metastases?**” – Oral; ASGBI annual meeting (Edinburgh)
- “**Does Clinical Risk Score (CRS) influence the diagnostic yield of ¹⁸F-FDG PET/CT in the assessment of patients with Colorectal liver metastases?**” – Poster; ASGBI annual meeting (Edinburgh)
- July 2005 “**Incremental value of dual Modality FDG PET/CT over PET only imaging, in the management of advanced colorectal cancer.**” –Oral; Association of Coloproctology of Great Britain and Ireland, Tripartite Meeting (Dublin)
- May. 2005 “**Activation of thymidine salvage pathway measured with FLT PET, as a potential indicator of response to 5FU in colorectal cancer**” – Poster ; American Society of Clinical Oncology (ASCO) – Orlando.
- Apr. 2005 “**Measuring early adaptive response to 5-FU therapy using FLT-PET**” – Oral; Selected for representation as 6 of the Best SARS papers at ASGBI (Glasgow)
- Jan. 2005 “**Measuring early adaptive response to 5-FU therapy using FLT-PET**” – Oral (Patey Prize section); Society of Academic and Research Surgery (Newcastle)
- Sep. 2004 “**Does FDG PET/CT have an impact on the management of pancreatobiliary pathology – a retrospective study**” – Poster - European Association of Nuclear Medicine (Helsinki)
- June 2004 “**Does ¹⁸F-FDG PET/CT as compared to dedicated CT alter management of pancreatobiliary tumours?**” – Oral - Society of Nuclear Medicine (Philadelphia)
- April 2003 “**Role of FDG PET/CT in the management of pancreatobiliary pathology**” – Oral presentation (Best of the six upper GI papers) at the Association of Surgeons of Great Britain and Ireland (ASGBI)(Harrogate)

LIST OF PRESENTATIONS

National

- May 2006 **“Comparison of diagnostic accuracy and clinical impact of integrated ^{18}F -FDG PET/CT relative to ^{18}F -FDG PET alone in advanced colorectal cancer”** – Oral (2nd author) UK radiological congress (Manchester)
- Nov. 2004 **“Can FDG PET/CT play a role in the management algorithm of patients with pancreatobiliary malignancy?”** – Oral – British Association of Surgical Oncology (London)
- April 2004 **“ ^{18}F -FDG PET/CT - does it have a role in the management algorithm of pancreatobiliary tumours?”** – Oral – Association of Upper GI surgeons (Cambridge)